UC Berkeley

UC Berkeley Electronic Theses and Dissertations

Title

Tandem Catalytic Processes Involving Olefins

Permalink

https://escholarship.org/uc/item/57w9r0b8

Author

Hanna, Steven George

Publication Date

2021

Peer reviewed|Thesis/dissertation

eScholarship.org Powered by the California Digital Library
University of California

Tandem Catalytic Processes Involving Olefins

By

Steven G. Hanna

A dissertation submitted in partial satisfaction of the

requirements for the degree of

Doctor of Philosophy

in

Chemistry

in the

Graduate Division

of the

University of California, Berkeley

Committee in charge:
Professor John F. Hartwig, Chair
Professor K. Peter C. Vollhardt
Professor Alexis T. Bell

Summer 2021

Abstract

Tandem Catalytic Processes Involving Olefins

by

Steven George Hanna

Doctor of Philosophy in Chemistry

University of California, Berkeley

Professor John F. Hartwig, Chair

The following dissertation discusses the development of tandem catalytic processes involving olefins. These processes include the hydroaminomethylation of α-olefins, the contra-thermodynamic isomerization of internal olefins to terminal olefins, and the chemical recycling of polyolefins by dehydrogenation in concert with isomerizing ethenolysis.

Chapter 1 surveys the chemistry of olefins and the tandem catalytic processes that involve olefins.

Chapter 2 describes the development of a multi-catalytic approach to the hydroaminomethylation of α-olefins. We report an approach to conducting the hydroaminomethylation of diverse α-olefins with a wide range of alkyl, aryl, and heteroarylamines at low temperatures (70-80 °C) and pressures (1.0-3.4 bar) of synthesis gas. This approach is based on simultaneously using two distinct catalysts that are mutually compatible. The hydroformylation step is catalyzed by a rhodium diphosphine complex, and the reductive amination step, which is conducted as a transfer hydrogenation with aqueous, buffered sodium formate as the reducing agent, is catalyzed by a cyclometallated iridium complex. By adjusting the ratio of CO to H_2, we conducted the reaction at one atmosphere of gas with little change in yield. A diverse array of olefins and amines, including hetreroarylamines that do not react under more conventional conditions with a single catalyst, underwent hydroaminomethylation with this new system, and the pharmaceutical ibutilide was prepared in higher yield and under milder conditions than those reported with a single catalyst.

Chapter 3 describes the development of a contra-thermodynamic, positional isomerization of internal olefins to terminal olefins by chain-walking hydrosilylation in concert with dehydrosilylation. We report a contra-thermodynamic isomerization of internal olefins to terminal olefins driven by redox reactions and formation of Si–F bonds. This process involves chain-walking hydrosilylation of internal olefins and subsequent formal retro-hydrosilylation. The process rests upon the high activities of platinum hydrosilylation catalysts for isomerization of metal alkyl intermediates and a new, metal-free process for the conversion of alkylsilanes to alkenes. By this approach, 1,2-disubstituted and trisubstituted olefins are converted to terminal olefins.

Chapter 4 describes the development of a contra-thermodynamic, positional isomerization of internal olefins to terminal olefins by chain-walking hydrosilylation in concert with a catalytic dehydrosilylation. We report a newly developed, palladium-catalyzed dehydrosilylation of terminal alkylsilanes that combines with chain-walking hydrosilylation to create a one-pot isomerization of internal olefins to terminal olefins. This catalytic dehydrosilylation is one of the few examples of thermal catalytic functionalizations of unactivated alkylsilanes. The reaction involves transmetalation of an alkylsilane, β-hydride elimination, release of the terminal olefin, and reoxidation of the palladium catalyst. A variety of linear internal olefins underwent the overall isomerization to terminal olefins in good yields and in good regioselectivities. Particularly noteworthy, isomerizations occurring over seven carbon units proceeded in yields that are comparable to those of isomerizations occurring over one carbon unit.

Chapter 5 describes the development of a contra-thermodynamic, positional isomerization of internal olefins to terminal olefins by chain-walking hydroboration in concert with dehydroboration. We report a newly developed dehydroboration reaction that can be coupled to chain-walking hydroboration to create a one-pot, contra-thermodynamic isomerization of internal olefins to terminal olefins. This dehydroboration reaction is the first dehydroboration of unactivated boronic esters. The reaction involves activation of the boronic acid, followed by iodination and base-promoted elimination. A variety of linear and branched internal olefins underwent the isomerization in good yields and with excellent regioselectivities.

Chapter 6 describes the chemical recycling of polyethylene by dehydrogenation and isomerizing ethenolysis. We converted polyethylene to olefins by either catalytic cracking or dehydrogenation, and we converted these olefins to propene by a highly selective isomerizing ethenolysis. Up to 33% yield of propene was obtained from dehydrogenated polyethylene and up to 72% yield of propene was obtained from octadecene, a model long-chain alkene.

Table of Contents

Chapter 1 **1**

1.1 The chemistry of olefins 2

1.1.1 The C–C π bond 2

1.1.2 Binding of olefins to metals 2

1.1.3 Reactions of olefins 3

1.2 Tandem catalytic processes involving olefins 9

1.2.1 Tandem catalytic processes involving addition & isomerization reactions 10

1.2.2 Tandem catalytic processes involving addition & metathesis reactions 11

1.2.3 Tandem catalytic processes involving hydrofunctionalization or difunctionalization and other subsequent transformations 11

1.2.4 Tandem catalytic processes involving isomerization and metathesis 12

1.2.5 Tandem catalytic processes involving dehydrogenation 14

1.3 The present dissertation 15

1.4 References 16

Chapter 2 **22**

2.1 Introduction 23

2.2 Results and discussion 25

2.3 Conclusion 29

2.4 Experimental 30

2.4.1 General methods and materials 30

2.4.2 Synthesis of Xiao's catalyst 30

2.4.3 General procedures for hydroaminomethylations 31

2.4.4 Impact of CO on the DRA of undecanal 33

2.4.5 Control experiments 34

2.4.6 Catalytic hydroaminomethylations 35

2.4.7 Application to the synthesis of Ibutilide 66

2.4.8 Procedure for hydroaminomethylation on a 6 mmol scale 68

2.4.9 Procedure for hydroaminomethylation at 1 atm syngas 69

2.4.10 Spectra of novel compounds 70

2.5 References 132

Chapter 3 **134**
3.1 Introduction 135
3.2 Results and discussion 138
3.3 Conclusion 141
3.4 Experimental 142
3.4.1 General information 142
3.4.2 Synthesis of substrates 142
3.4.3 General procedure for contra-thermodynamic olefin isomerizations 143
3.4.4 Products of olefin isomerization 144
3.4.6 ^{1}H NMR and ^{13}C NMR Spectra 147
3.4 References 158
Chapter 4 **160**
4.1 Introduction 161
4.2 Results and Discussion 163
4.3 Conclusion 167
4.4 Experimental 168
4.4.1 General information 168
4.5.2 Development of conditions for oxidative dehydrosilylation (Table 1) 169
4.5.3 Procedure for contra-thermodynamic olefin isomerizations (Table 2) 170
4.5.4 ^{1}H NMR spectra (Table 2) 171
4.4 References 180
Chapter 5 **183**
5.1 Introduction 184
5.2 Results and discussion 185
5.3 Conclusion 190
5.4 Experimental 191
5.4.1 General methods and materials 191
5.4.2 Preparation of Potassium Methoxide 191
5.4.3 Synthesis of Catalyst C1 192
5.4.4 Synthesis of Catalyst C2 194
5.4.5 Synthesis of olefins 199
5.4.6 General procedures for olefin isomerizations 203

5.4.7 Isomerization of olefins 204
5.4.8 NMR spectra of olefin isomerizations 207
5.5 References 217
Chapter 6 **220**
6.1 Introduction 221
6.2 Results and discussion 224
6.3 Conclusion 228
6.4 Experimental 229
6.4.1 General methods and materials 229
6.4.2 Dehydrogenations 230
6.4.3 Isomerizing ethenolyses 235
6.5 References 237

Acknowledgements

It is an honor to be receiving my PhD from UC Berkeley, and I would like to thank everyone who has helped me realize this tremendous achievement. First, I would like to thank my mom and dad, Leonard and Xeni Hanna, for raising me to value kindness and the pursuit of knowledge and for unconditionally loving and supporting me throughout my life. I would also like to thank my brother, Nicholas Hanna, my grandparents, George and Athena Sarris, my great grandmother, Lucille Piperides, my aunt and uncle, Richard and Stacy Sapp, and my cousins, Erin Sapp and Dr. Christie Savas, who have all been loving and supportive. I am also grateful to Sallie Oliver, my girlfriend, for her love and encouragement over the past years.

I would like to thank my principal advisor, Professor John F. Hartwig, for the opportunity to work in his laboratory and for being an incredible teacher, mentor, and role model. It has been an honor and a privilege to work with John. I will always appreciate John's diligence, intelect, and unwavering enthusiasm for chemistry. I will also appreciate the way that John challenged me to think critically in a way that I had never quite been challenged. I am confident that working with John has shaped me into the scholar that I am today and instilled in me a deep appreciation for logical scientific inquiry and clear communication. I am also immensely grateful to John for granting me, and indeed and all of his students, the freedom to pursue diverse research directions that we found interesting, all while supporting us through the ups and downs of our projects. Furthermore, I am grateful to John for the opporunity to serve as the graduate student instructor for his Organometallics class. This position was one of my favorite experiences during my PhD program and was tremendously educational.

I would like to thank the many educators, scholars, and mentors who helped mold me into the scholar that I am today. I would like to thank Abigail Freiberger, my high school chemistry teacher, for her patience and for inspiring me to succeed in science. I would also like to thank Dr. Brett McLarney, my undergraduate research mentor, and Professor Stefan France, my undergraduate research advisor, for setting me up for success in graudate school, for teaching me how to conduct academic research, for patiently answering all of my questions, and for helping me apply to graduate schools. I am also grateful to Dr. Pamela Pollet and Professor Seth Marder for teaching me undergraduate organic chemistry and for helping me apply to graduate schools and to Professors Kent Barefield and Joseph Sadighi for introducing me to organometallics and for inspiring me to pursue this field in my graduate studies.

Many people at Berkeley provided me with vital support and friendship throughought graduate school. The community of chemists at Berkeley is truly one of a kind. In particular, I would like to thank Dr. Trevor Butcher for his friendship and intellectual support over the past five years – I literally could not imagine what graduate school would have been like without him. I would also like to thank Brandon Bloomer, Jonathan Yang, Dr. Shelby McCowen, Dr. Melissa Hardy, Melessio Perea, Fernando Alvarez, Jessica Burch, Danny Thatch, Dr. Thomas O'Connor, and Dr. Haoquan Li for their friendship and support. I would also like to thank all of my coworkers in 705 Latimer, past and present: Dr. Sophie Arlow, Dr. Justin Wang, Dr. Haoquan Li, Dr. Bo Su, Dr. Liye Chen, Yehao Qiu, Jake Shi, and Nico Ciccia. I would also like to Dr. Miao Zhang and Dr. Chithra Asokan, who have managed the CSD catalysis facility, Dr. Hasan Celik, who managed the NMR Facility, and Anneke Runtupalit, John's administrative assistant, for their support over the past years. A special thanks to Professors K. Peter C. Vollhardt, Matthew Francis, T. Don Tilley, and Alexis T. Bell for serving on my qualifying exam committee and to Professors John F. Hartwig, K. Peter C. Vollhardt, and Alexis T. Bell for serving on my dissertation committee. I am also very grateful to Dr. Sophie Arlow, Dr. Chris Hill, Dr. Matt Peacock, and Dr. Yumeng Xi for helpful scientific discussions.

Several individuals direcly contributed to the work in this dissertation, and I would like to thank them all for their intellectual and experimental contributions. Thanks to Dr. Jeffrey Holder and Dr. Thomas O'Connor for their progress on developing a multicatalytic approach to the hydroaminomethylation of α-olefins prior to my arrival at Berkeley. Thanks to Dr. Trevor Butcher, Tyler Wills, Brandon Bloomer, and Nico Ciccia for their contributions to the development of long-range, contra-thermodynamic, positional olefin isomerizations. Thanks to Richard Conk, Dr. Liang Qi, Nico Ciccia, Brandon Bloomer, Dr. Ji Su, Jake Shi, and Professor Alexis T. Bell for their contributions to the development of a method for the chemical recycling of polyethylene through dehydrogneation and isomerizing ethenolysis. I am also grateful to Alvin Hsu, Tyler Wills, Whitney Zhao, and Golsa Ghebei, whom I had the privilege of mentoring during their undergraduate careers at UC Berkeley. These students are exceptionally talented and are destined for great things. I would also like to thank the organizations responsible for funding the research in this dissertation: the US Department of Energy, Lawrence Berkeley National Laboratory, and Chevron USA, Inc.

Chapter 1

The Chemistry of Olefins, the Nature of Tandem Catalytic Processes, and the Development of Tandem Catalytic Processes Involving Olefins

1.1 The chemistry of olefins

Olefins are compounds that contain carbon–carbon double bonds, which consist of one σ bond and one π bond. The word olefin is derived from the Latin words *oleum*, which means oil, and *facere*, which means "to make," because olefins form oily compounds upon reaction with halogens. The overall strength of a carbon–carbon double bond is 146 kcal/mol, and the strength of a carbon–carbon single bond is 83 kcal/mol. Thus, the strength of a carbon–carbon π bond can be approximated as 63 kcal/mol.[1]

1.1.1 The C–C π bond

The behavior and properties of π bonds are central to the reactivity of olefins because the frontier molecular orbitals of monoenes bearing no functional groups contain significant contributions from the carbon *p* orbitals that form π bonds. For such molecules, the molecular orbital corresponding to the π bond is the HOMO, and the molecular orbital corresponding to the π* antibonding orbital is the LUMO. Thus, the reactivity of olefins with electrophiles and electrophilic radicals is controlled by interactions between the unfilled or partially filled orbitals of the electrophile and the π bonds of the olefin, and the reactivity of nucleophiles and nucleophilic radicals with olefins is controlled by interactions between the filled or partially filled orbitals of the nucleophile and the π* antibonding orbitals of the olefin.

Given the central role of π bonds in the chemistry of olefins, it is not surprising that the installation of substituents around a π bond can significantly alter said chemistry. In any stable conformation, alkyl substituents possess a filled orbital with the correct symmetry to mix with both the π and π* orbitals of an olefin.[2] Mixing of the filled π-bonding orbital with the filled π-symmetric orbital of the alkyl substituent raises the energy of the π bond, increasing the nucleophilicity of the olefin and slightly destabilizing the molecule relative to an unsubstituted alkene. Mixing of the unoccupied π* antibonding orbital of the alkene with the filled π-symmetric orbital of the alkyl substituent stabilizes the molecule relative to an unsubstituted alkene.[2]

1.1.2 Binding of olefins to metals

Just as frontier orbitals influence the reactivity, properties, and relative stabilities of olefins, they control interactions of olefins with metals. Metals bind olefins according to the Dewar-Chatt-Duncanson model.[3] According to this model, olefins both donate electron density to metal centers through mixing of filled π orbitals with empty *d* orbitals of appropriate symmetry and accept electron density from metal centers through mixing of unfilled π* orbitals with filled *d* orbitals of appropriate symmetry. The former form of orbital mixing is referred to as forward donation, and the latter form is referred to as back donation. The contributions of each type of donation to the strength of the interaction between the olefin and the metal depend on the properties of the metal complex and of the olefin, and the magnitudes of each contribution have consequences for the properties and reactivity of the overall complex.

1.1.3 Reactions of olefins

Olefins undergo a variety of reactions, virtually all of which involve the π and π* orbitals. Most industrially relevant reactions of monounsaturated olefins can be categorized as addition reactions, isomerizations, or metatheses. Examples of each type of reaction are given in Figure 1.

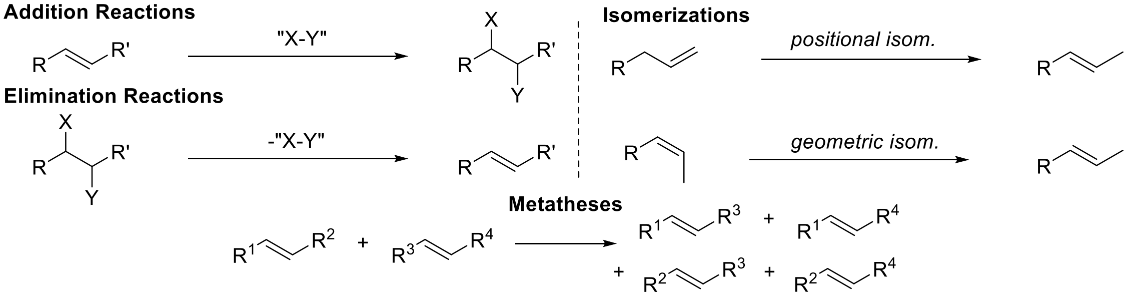
Addition Reactions
"X-Y"
R
R'
X
Y
Elimination Reactions
-"X-Y"
Isomerizations
positional isom.
geometric isom.
Metatheses
R1 R2 + R3 R4
R1 R3 + R1 R4
+ R2 R3 + R2 R4

Figure 1. Fundamental reactions of olefins

1.1.3.1 Addition reactions

Addition reactions involve the combination of an olefin with a second molecule to form a larger molecule (Figure 2). In such reactions, the π-bond of the olefin breaks, and σ-bonds between each carbon atom and the reagent(s) used for the addition form. A σ bond in the reagent used for the addition is often broken as well. Since such reactions often involve the formation of two σ bonds and the breaking of one π bond and one σ bond, they are typically exergonic.

Addition reactions of olefins can be broadly categorized as hydrogenations, hydrofunctionalizations, difunctionalizations, or cycloadditions, depending on the substituents that are added across the carbon–carbon double bond (Figure 2). For a reaction to classified as a hydrogenation, hydrofunctionalization, or difunctionalization, reagents need not be directly added across the double bond. That is, the atoms of the "H–H," "H–X," and "X–Y" reagents of Figure 2 need not be bound together at any time before or during an addition reaction. Cycloadditions involve the combination of multiple unsaturated molecules to form a cyclic adduct; cycloadditions are beyond the scope of this dissertation.

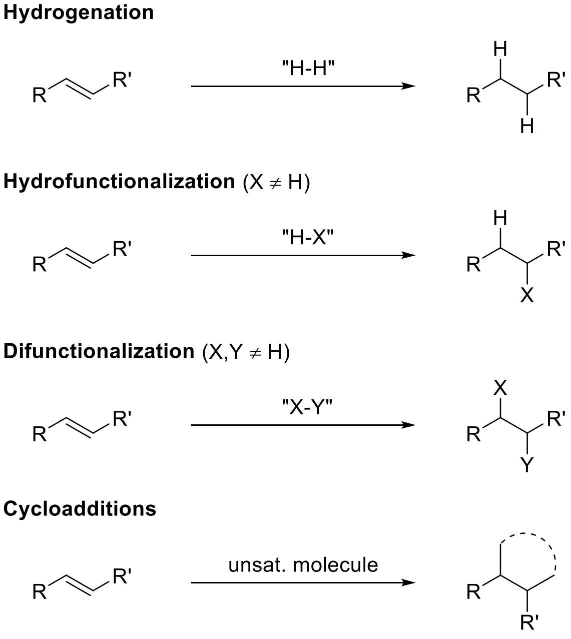
Hydrogenation
"H-H"
Hydrofunctionalization (X ≠ H)
"H-X"
Difunctionalization (X,Y ≠ H)
"X-Y"
Cycloadditions
unsat. molecule
R
R'
H
X
Y

Figure 2. Addition reactions

Hydrogenations involve the addition of two hydrogen atoms across the double bond, and hydrofunctionalizations involve the addition of a hydrogen atom and an atom, labeled X in the figure, other than hydrogen across the double bond. Examples of hydrofunctionalizations include hydration,[4] hydrohalogenation,[4] hydrocyanation,[5] hydroboration,[6] hydrosilylation,[7] hydroamination,[8] hydroformylation,[9] hydroaminomethylation,[10] methoxycarbonylation,[11] and the ene reaction.[2] Hydrofunctionalizations of internal olefins can proceed with regioselectivities in which the functional group is added to the terminus of a carbon chain.[12] These hydrofunctionalizations are known as chain-walking hydrofunctionalizations. Difunctionalizations of olefins are addition reactions in which both olefinic carbons form bonds to elements other than hydrogen. Classically, difunctionalizations are thought to involve the formation of bonds from each olefinic carbon to separate atoms. Examples of such reactions include dihydroxylation, dihalogenation, halohydration, diboration, disilylation, silaboration, homopolymerization, carbodifunctonalizations, and copolymerization.[3-4]

1.1.3.2 Elimination reactions

The reverses of addition reactions are elimination reactions. These reactions form olefins from saturated starting materials. Dehydrogenations remove an equivalent of H_2 from a saturated compound.[13] Dehydrogenations can be categorized as acceptorless dehydrogenations,[13g,13h,13n,13p-s] which proceed at elevated temperatures to directly eliminate H_2, transfer dehydrogenations,[13e] which involve transfer of an equivalent of H_2 to an acceptor olefin, and polar dehydrogenations,[13t] which involve the transfer of H^+ and H^- equivalents to an acceptor compound. Dehydrofunctionalizations remove a hydrogen atom and a functional group from a saturated compound. Examples include dehydrohalogenation,[4] dehydration,[4] Hoffman eliminations,[4] dehydroformylation,[14] dehydrocyanation,[15] dehydroboration,[16] and dealkoxycarbonylation.[17] Functional groups can also be removed from two vicinal carbon atoms to form an alkene. Examples of this reaction include the Peterson olefination,[18] the Corey-Winter olefination,[19] de-epoxidation,[20] and retro-cylopropanation.[21]

1.1.3.3 Isomerization reactions

Isomerizations can be categorized as either positional or geometric.[22] Positional isomerizations involve changes in the connectivity of substituents about a double bond. The favorability of positional isomerizations is typically determined by the electronic properties of the substituents attached to the double bond. Isomers with more donating substituents about the double bond are generally more stable than those with less donating substituents about the double bond, although a notable exception involves the stability of α,β-unsaturated carbonyl compounds relative to unconjugated, unsaturated carbonyl compounds. The enhanced stability of conjugated α,β-unsaturated carbonyl compounds relative to nonconjugated α,β-unsaturated carbonyl compounds originates from favorable mixing of the π-orbital of the alkene moiety with the π* orbital of the carbonyl moiety. The enhanced stability of alkyl-substituted olefins relative to unsubstituted isomers originates from the favorable mixing of filled orbitals on donating substituents and the empty π* orbital of the olefin moiety.[2] Since alkyl substituents are more donating than hydrogen, alkenes bearing more alkyl substituents are generally more stable than their unsubstituted isomers. Thus, for monoenes bearing no functional groups, positional isomerizations that increase the number of substituents about the double bond are thermodynamically favorable. This trend can be quantified with heats of formation. Monosubstituted olefins are less stable than disubstituted olefins by about 1–2 kcal/mol, less stable than trisubstituted olefins by about 5 kcal/mol, and less stable than tetrasubstituted olefins by about 6 kcal/mol (Figure 3).[23] The trend in exothermicities of hydrogenations parallels the trend in exergonicities of isomerizations.[4] Since olefins bearing more alkyl substituents are more stable than olefins bearing fewer substituents, hydrogenations of olefins bearing more substituents are less exothermic than those of olefins bearing fewer substituents.

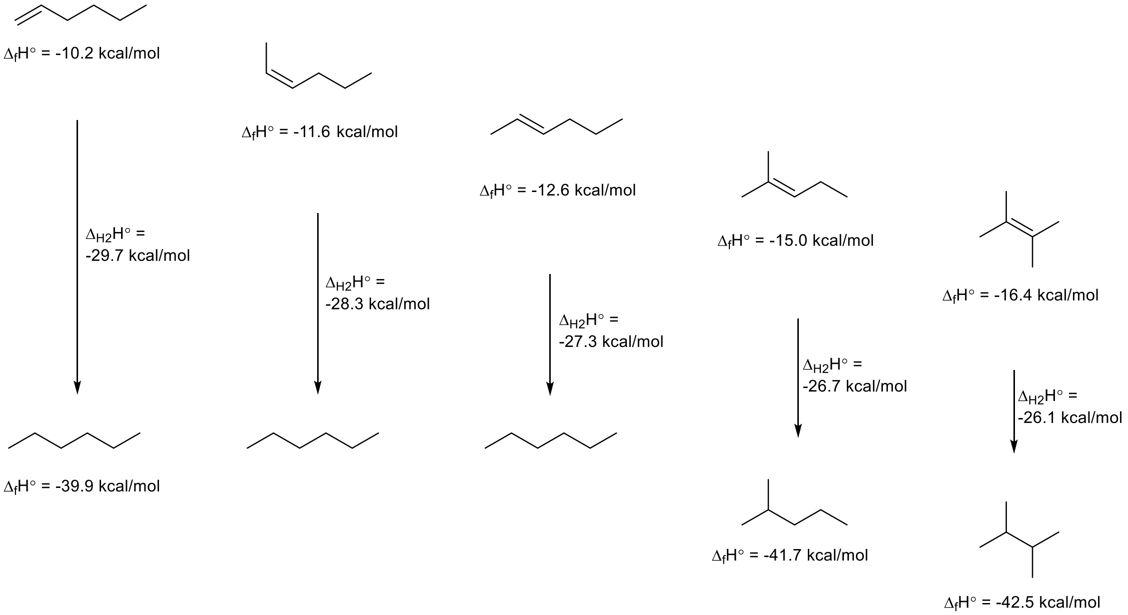

Figure 3. Relative stabilities of olefin isomers with different substitution patterns, adapted from Yale Organic Chemistry Study Aids[23]

Both thermodynamic, i.e., net-exergonic, and contra-thermodynamic, i.e., net-endergonic, isomerizations have been reported (Figure 4). Thermodynamic isomerizations are exergonic reactions in which relatively unstable molecules react to form relatively stable molecules. Classes of thermodynamic isomerizations include positional isomerizations of alkenes with less donating substituents about the double bond to alkenes with more donating substituents about the double bond as well as geometric isomerizations of more sterically strained alkenes to less sterically strained alkenes. While positional isomerizations alter the connectivity of olefins, geometric isomerizations alter only the configuration of olefins. Contra-thermodynamic olefin isomerizations involve the conversion of relatively stable olefins into relatively unstable olefins. Such conversions are endergonic; therefore, they do not occur spontaneously unless coupled to additional, sufficiently exergonic processes. Classes of contra-thermodynamic isomerizations include positional isomerizations of alkenes with more donating substituents about the double bond to alkenes with fewer donating substituents about the double bond as well as geometric isomerizations of alkenes with less steric crowding about the double bond to alkenes with more steric crowding about the double bond.

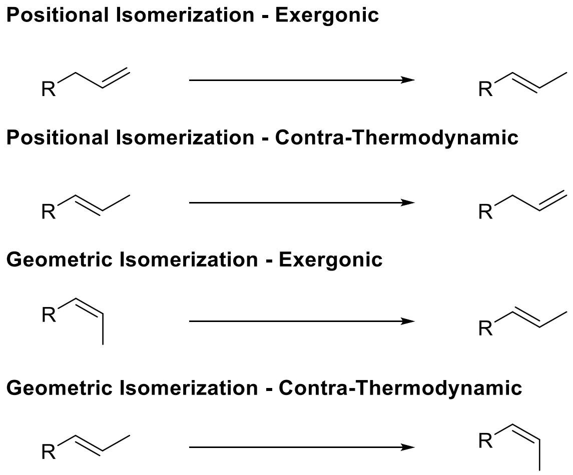
Positional Isomerization - Exergonic
Positional Isomerization - Contra-Thermodynamic
Geometric Isomerization - Exergonic
Geometric Isomerization - Contra-Thermodynamic
R

Figure 4. Classes of olefin isomerizations

Because positional, thermodynamic olefin isomerizations are exergonic, many methods to conduct them have been reported (Figure 5).[22,24] The most common methods are acid- and base-catalyzed tautomerizations. Acid-catalyzed thermodynamic isomerizations involve initial protonation of a double bond to form a carbocation, followed by deprotonation of the carbon α to the cationic carbon. Base-catalyzed thermodynamic isomerizations involve deprotonation of the carbon α to the double bond to form a carbanion followed by protonation of the carbon β to the anionic carbon. Transition-metal hydrides also catalyze positional, thermodynamic olefin isomerizations.[24g] These reactions can proceed through either insertion/elimination,[24g] oxidative addition/reductive elimination,[24f,24j] or hydrogen-atom transfer mechanisms.[24h]

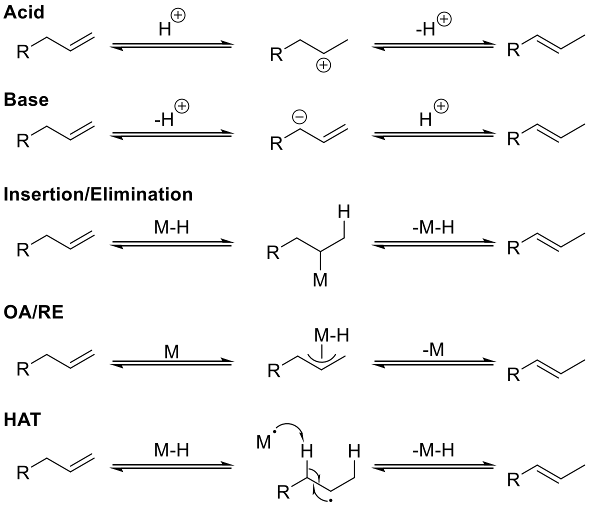
Acid
H⊕
-H⊕
Base
-H⊕
H⊕
Insertion/Elimination
M-H
-M-H
H
M
OA/RE
M
M-H
-M
HAT
M-H
M•
H
H
-M-H
R

Figure 5. Strategies for thermodynamic, positional isomerization of olefins

Positional, contra-thermodynamic olefin isomerizations are considerably rarer than positional, thermodynamic olefin isomerizations (Figure 6). These reactions typically proceed by allylic functionalization followed by defunctionalization with allylic transposition or by photodeconjugation.[25] These strategies for positional, contra-thermodynamic olefin isomerization allow for translocation of the double bond through a maximum of only one carbon unit. An alternative strategy involves chain-walking hydrofunctionalization followed by dehydrofunctionalization, which is the subject of chapters 3, 4, and 5 of this dissertation.[16g,16m-o,26]

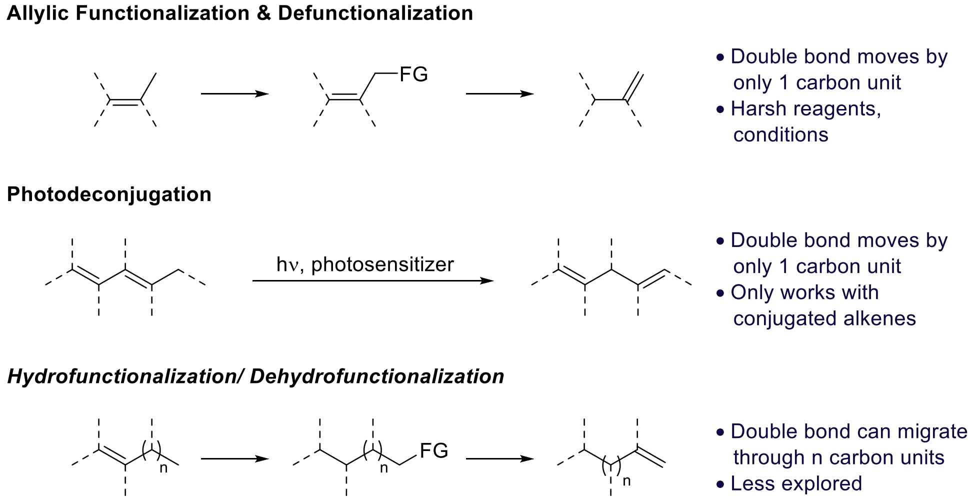
Allylic Functionalization & Defunctionalization
FG
• Double bond moves by only 1 carbon unit
• Harsh reagents, conditions
Photodeconjugation
hν, photosensitizer
• Double bond moves by only 1 carbon unit
• Only works with conjugated alkenes
Hydrofunctionalization/ Dehydrofunctionalization
n
n
FG
n
• Double bond can migrate through n carbon units
• Less explored

Figure 6. Contra-thermodynamic, positional olefin isomerizations

While positional isomerizations involve changes in the connectivity of substituents about a double bond, geometric isomerizations involve changes in the configuration of the substituents about a double bond.[22] The substituents can be arranged in either an *E* or *Z* fashion. For acyclic olefins, the *E* isomer is generally more stable than the *Z* isomer due to steric clashes between the two substituents on the same side of the double bond. The barrier for rotation about a double bond of olefins is roughly equal to the strength of the π bond because the transition state for rotation involves a perpendicular arrangement of the two carbon *p* orbitals in which the *p* orbitals have no overlap, i.e., the π bond is broken.[2,4]

1.1.3.4 Metatheses

Olefin metathesis is a substitution reaction of olefins that involves the redistribution of the substituents about the double bonds of two olefins (Figure 7). Olefin metatheses can be both intra- and intermolecular and can occur as self-metatheses (SM), which involve recombination of two identical olefins, or as cross metatheses (CM), which involve recombination of two distinct olefins. Examples of olefin metathesis include ring-opening metathesis (ROM), ring-closing metathesis (RCM), ring-opening metathesis polymerization (ROMP), and ethenolysis (Figure 7).

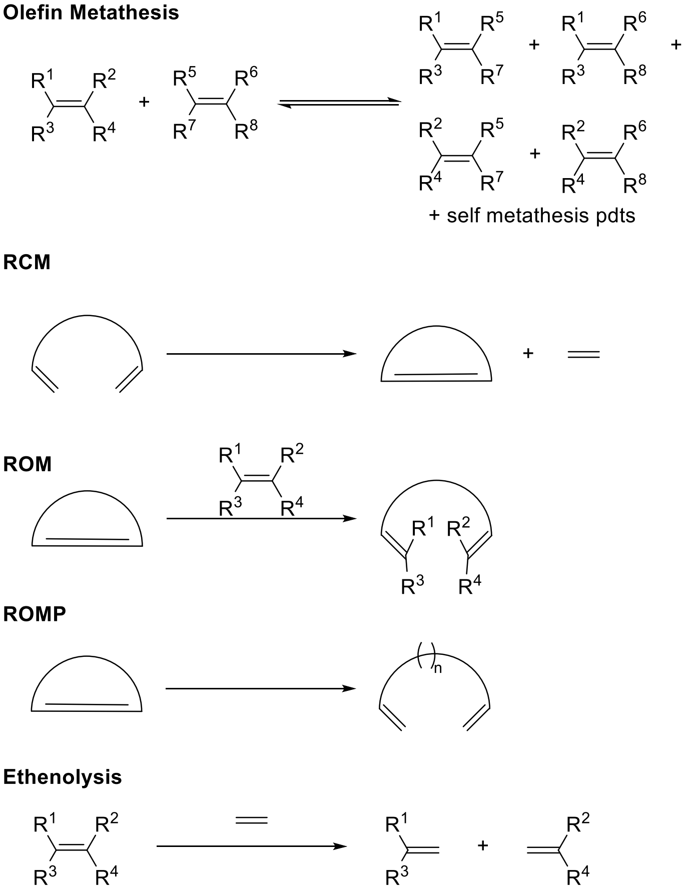

Figure 7. Examples of olefin metathesis

The first widely accepted mechanism of olefin metathesis was proposed by Chauvin in 1971 (Figure 8). This mechanism involves cycloaddition of an olefin to a metal alkylidene to form a metallacyclobutane, which, upon cycloelimination, releases the metathesis product and generates a second alkylidene with substituents distinct from those of the original alkylidene (Figure 8). Olefin metatheses of hydrocarbons are often close to thermoneutral. In these cases, all steps of the catalytic cycle are reversible, and degenerate metatheses occur concurrently with non-degenerate, i.e., productive, metatheses. For metatheses that are thermoneutral under standard conditions, selectivity for a given product is typically achieved through addition of excess reactants or removal of products.

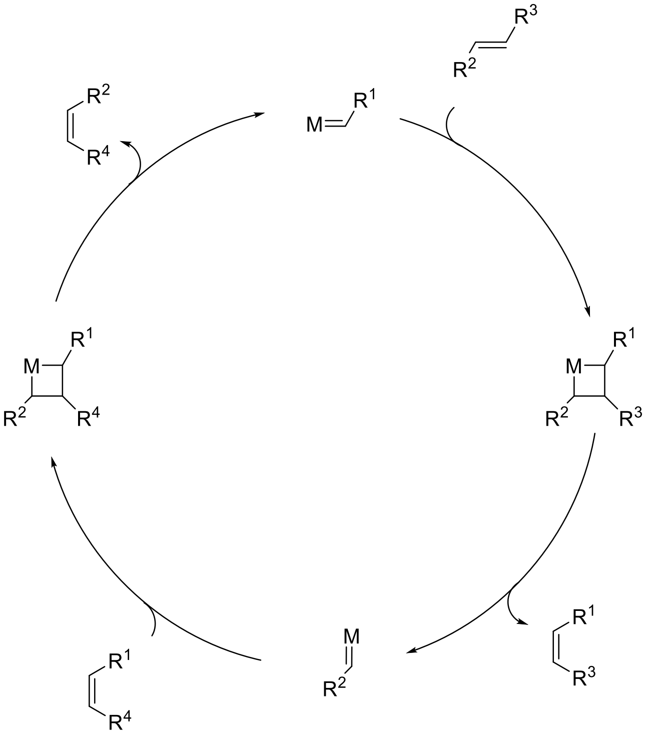
M=R¹
R²–CH=CH–R³
M–R¹ / R² R³ metallacyclobutane
R¹=R³
M=R²
R¹=R⁴
M–R¹ / R² R⁴ metallacyclobutane
R²=R⁴

Figure 8. Mechanism of olefin metathesis

1.2 Tandem catalytic processes involving olefins

A variety of tandem catalytic processes involving olefins have been developed (Figure 9). Olefins can be the starting materials, intermediates, or products of a tandem catalytic processes. Virtually all such processes involve additions, eliminations, isomerizations, or metatheses. Tandem catalytic processes involving olefins can be classified orthogonal-tandem or one-pot sequential processes.[27]

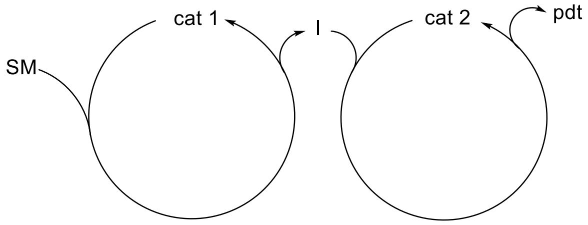

Figure 9. Tandem catalysis

Concurrent tandem catalysis involves conducting multiple processes in the same reaction vessel at the same time, and one-pot sequential catalysis involves conducting multiple processes in the same reaction vessel at different times. Advantages of concurrent tandem catalysis include the ability to minimize the concentration of the intermediate, I, which might undergo unproductive side reactions, and the ability to automate cascades that involve multiple iterations of the same sequence of steps. Challenges associated with concurrent tandem catalysis include the selection of mutually compatible catalysts with non-interfering cycles and the identification of a single set of reaction conditions under which both catalysts can operate. One-pot sequential catalysis enables chemists to conduct multiple reactions in the same pot without isolation of intermediates while select catalysts that need not necessarily be mutually compatible at the same time. However, isolation of the intermediate can only be avoided if catalysts in the second and subsequent transformations can still operate in the presence of reagents, solvents, and the deactivated forms of catalysts used for prior transformations. Thus, the development of one-pot, sequential catalytic reactions often involves more engineering challenges than the development of single-step catalytic transformations.

1.2.1 Tandem catalytic processes involving addition & isomerization reactions

Many hydrofunctionalizations can proceed in tandem with isomerization (Figure 10).[12] These hydrofunctionalizations are referred to as chain-walking hydrofunctionalizations. The isomerization step can involve isomerization of an olefin to generate a statistical mixture of constitutional isomers followed by selective hydrofunctionalization of the terminal olefin or isomerization of a metal alkyl to the terminal position followed by direct installation of a functional group at the terminal position.[12,28] The main advantage of chain-walking hydrofunctionalization is that it enables installation of functional groups at positions that are remote from the initial position of the double bond. Thus, terminally functionalized products can be obtained without starting from the internal olefin. However, chain-walking hydrofunctionalizations typically proceed in lower *n*:*iso* ratios than analogous hydrofunctionalizations of terminal olefins because the secondary metal alkyl intermediates or internal olefins formed during the isomerization process can react to form internally hydrofunctionalized products. In addition, chain-walking hydrofunctionalizations often proceed in lower conversion than analogous hydrofunctionalizations of terminal olefins because insertion of internal olefins into metal hydrides is typically slower than insertion of terminal olefins into metal hydrides.

Examples of hydrofunctionalizations that can follow isomerization include hydroformylation,[29] hydroaminomethylation,[30] hydrocyanation,[5a,5b] hydrosilylation,[31] hydroboration,[6] hydroarylation,[28] and methoxycarbonylation.[11] Several chain-walking hydrofunctionalizations involve isomerization through methine units to form the terminally hydrofunctionalized product in high regioselectivity; examples of such chain-walking hydrofunctionalizations include hydrosilylation,[31a] hydroboration,[6e,6f] and methoxycarbonylation.[11d-f]

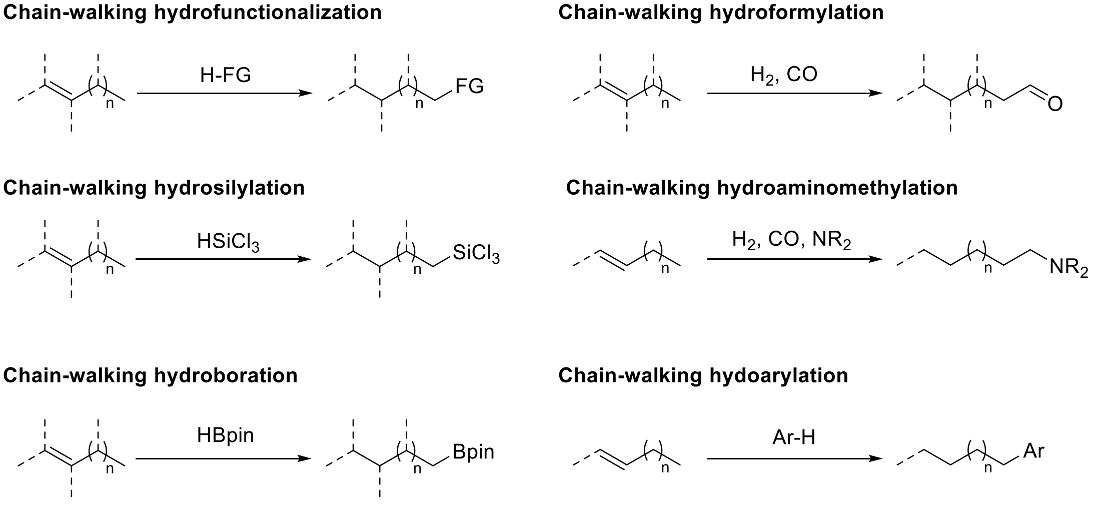
Chain-walking hydrofunctionalization
H-FG
FG
n
Chain-walking hydroformylation
H2, CO
O
Chain-walking hydrosilylation
HSiCl3
SiCl3
Chain-walking hydroaminomethylation
H2, CO, NR2
NR2
Chain-walking hydroboration
HBpin
Bpin
Chain-walking hydoarylation
Ar-H
Ar

Figure 10. Chain-walking hydrofunctionalizations

1.2.2 Tandem catalytic processes involving addition & metathesis reactions

Metathesis can precede addition reactions.[32] Examples include hydrogenation,[33] hydroarylation,[34] and dihydroxylation.[35]

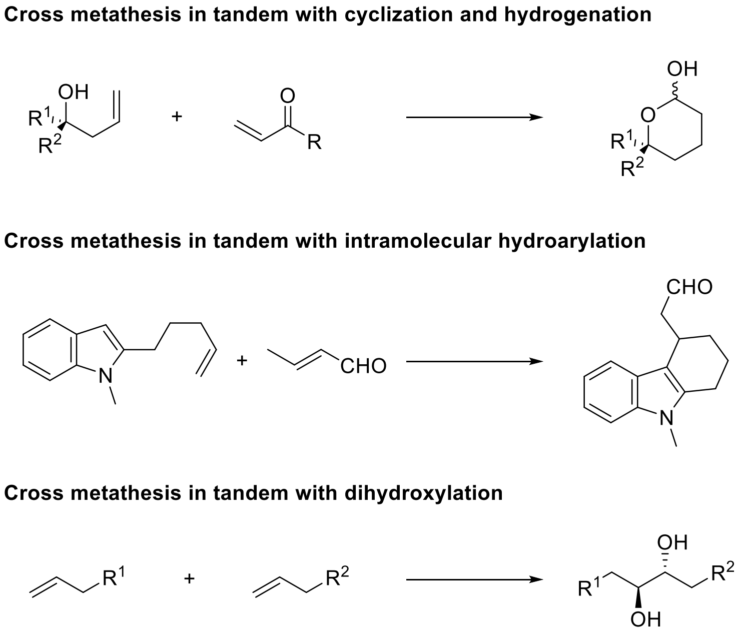
Cross metathesis in tandem with cyclization and hydrogenation

Cross metathesis in tandem with intramolecular hydroarylation

Cross metathesis in tandem with dihydroxylation

Figure 11. Tandem catalytic processes involving olefin metathesis and addition reactions

1.2.3 Tandem catalytic processes involving hydrofunctionalization or difunctionalization and other subsequent transformations

Hydrofunctionalizations can also occur in tandem with transformations other than isomerization. For example, hydroaminomethylation involves hydroformylation in tandem with reductive amination.[10,36] Similarly, hydroformylation can occur in tandem with aldehyde hydrogenation.[36-37] Hydroformylation can also occur in tandem with aldehyde condensation[36] or Wittig olefination[36] but the latter two transformations are typically not conducted with catalysts. Hydroboration and diboration can precede Suzuki couplings.[38] Additionally, hydroboration and diboration can precede oxidation[4] and ammoxidation,[39] although the latter two transformations are typically not conducted with catalysts. The nitrile products of hydrocyanation can be reduced, and this process is used in the synthesis of nylon-6 polymers.[5c] Similarly, the products of methoxycarbonylation can be reduced.[40]

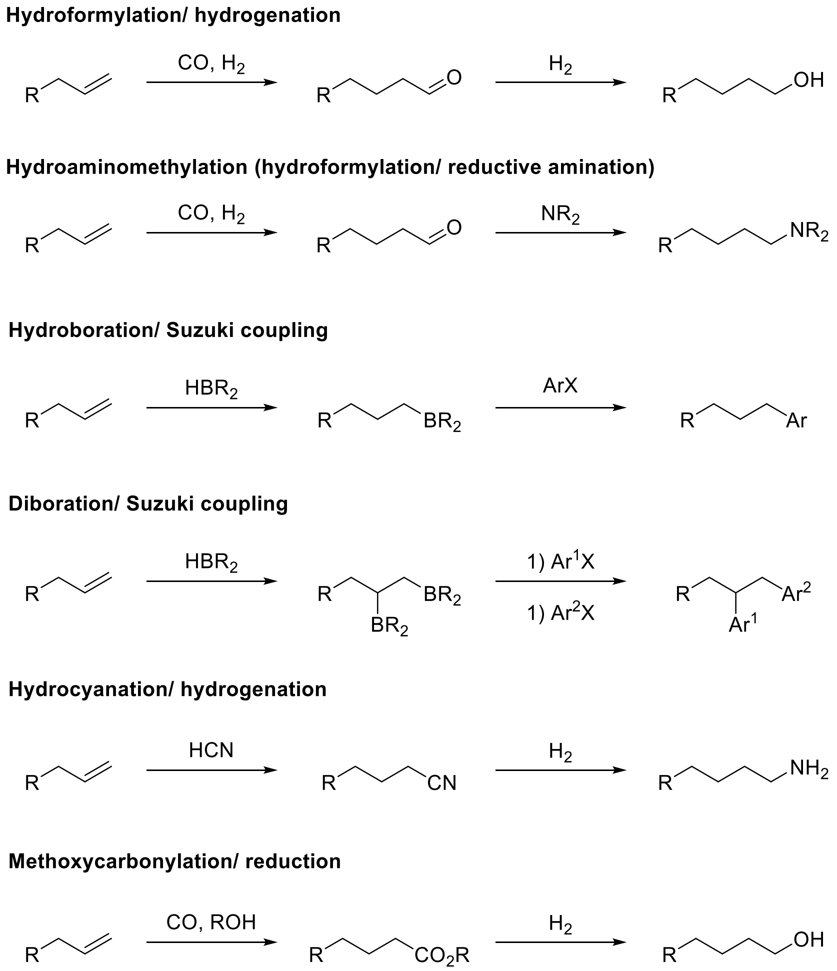
Hydroformylation/ hydrogenation
R
CO, H2
R
O
H2
R
OH
Hydroaminomethylation (hydroformylation/ reductive amination)
R
CO, H2
R
O
NR2
R
NR2
Hydroboration/ Suzuki coupling
R
HBR2
R
BR2
ArX
R
Ar
Diboration/ Suzuki coupling
R
HBR2
R
BR2
BR2
1) Ar1X
1) Ar2X
R
Ar2
Ar1
Hydrocyanation/ hydrogenation
R
HCN
R
CN
H2
R
NH2
Methoxycarbonylation/ reduction
R
CO, ROH
R
CO2R
H2
R
OH

Figure 12. Tandem catalytic processes involving hydrofunctionalization or difunctionalization and subsequent transformations

1.2.4 Tandem catalytic processes involving isomerization and metathesis

In addition to occurring in concert with hydrofunctionalization, isomerization can occur in concert with olefin metathesis.[41] These transformations are referred to as isomerizing metatheses (ISOMET). The isomerization step can occur before or after the metathesis step. Additionally, the metathesis step can involve cross metathesis (isomerizing cross-metathesis) or self-metathesis (isomerizing self-metathesis). In theory, all ISOMET reactions can precede hydrofunctionalizations.

Varying degrees of selectivity can be achieved in ISOMET processes. Often, distributions of alkene products form. Schrock developed a seminal product-specific ISOMET reaction involving initial isomerization of an internal olefin to a statistical mixture of olefins followed by self-metathesis of the terminal olefin to generate a higher molecular-weight internal olefin.[41j] Selectivity for (*Z*)-5-decene from (*E*)-3-hexene was achieved by selecting an isomerization catalyst that selectively isomerizes *E* but not *Z* olefins and a metathesis catalyst with high selectivity for self-metathesis of terminal olefins and with high selectivity for the formation of (*Z*)-metathesis products, which do not undergo subsequent isomerization under the reaction conditions.

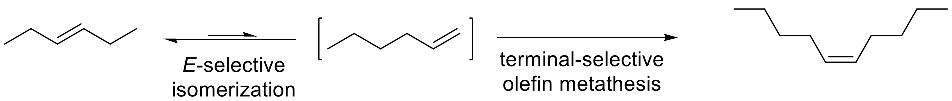

Figure 13. Product-selective self-metathesis of (*E*)-3-hexene

In other examples of ISOMET processes, distributions of alkenes form. For example, Consorti and Dupont reported an isomerizing self-metathesis of 3-hexene which produced a nearly statistical distribution of alkenes with lengths ranging from C_2–C_{17}.[41c] Gooßen and co-workers later reported an isomerizing cross-metathesis of 3-hexene and 1-octadecne that produced a product distribution with a mean chain length equal to stoichiometry-weighted average of the chain-lengths of the starting olefins. That is, the mean chain length, L, can be calculated from the chain lengths, L_1 and L_2, and stoichiometries, x_1 and x_2, of the two starting olefins according to the formula $L = (x_1L_1 + x_2L_2)/(x_1 + x_2)$.[41d] This strategy has been used by Gooßen to modify the physical properties of biodiesel.

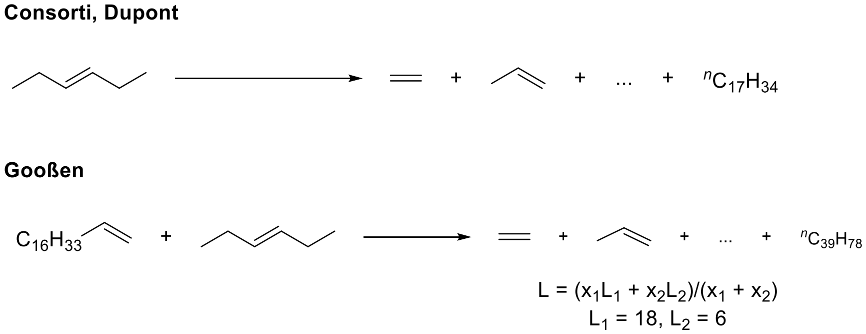

Figure 14. Isomerizing self- and cross-metatheses that lead to mixtures of olefins with statistical distributions of chain lengths

Isomerizing cross metatheses in which one of the starting olefins is ethylene are referred to as isomerizing ethenolyses. These reactions, known as isomerizing ethenolyses, decrease the molecular weight of the starting olefin. Isomerizing ethenolysis has been applied in the synthesis of vinylarenes from allylarenes (Figure 15)[41e] and in the conversion of fatty-acid esters to defined distributions of olefin products, as in Figure 14.[41d]

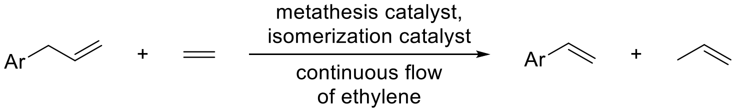

Figure 15. Isomerizing ethenolysis applied in the synthesis of vinylarenes from allylarenes

The Shell Higher Olefins Process (SHOP) involves addition, isomerization, and metathesis reactions (Figure 16).[42] This process involves initial oligomerization of ethylene to a Flory-Schultz mixture of linear α-olefins (LAOs) with even numbers of carbon atoms ranging from C_4 to C_{40}. These olefins then undergo isomerization to linear internal olefins (LIOs) over a heterogeneous catalyst, typically MgO or K/Al_2O_3. The resulting statistical mixture of LIOs is passed over a Mo/Al_2O_3 catalyst; the resulting cross metathesis generates a mixture of LIOs with odd and even numbers of carbons. These LIOs are subsequently ethenolyzed to shorter LAOs, which undergo hydroformylation, hydrogenation, and subsequent transformations to produce detergents.

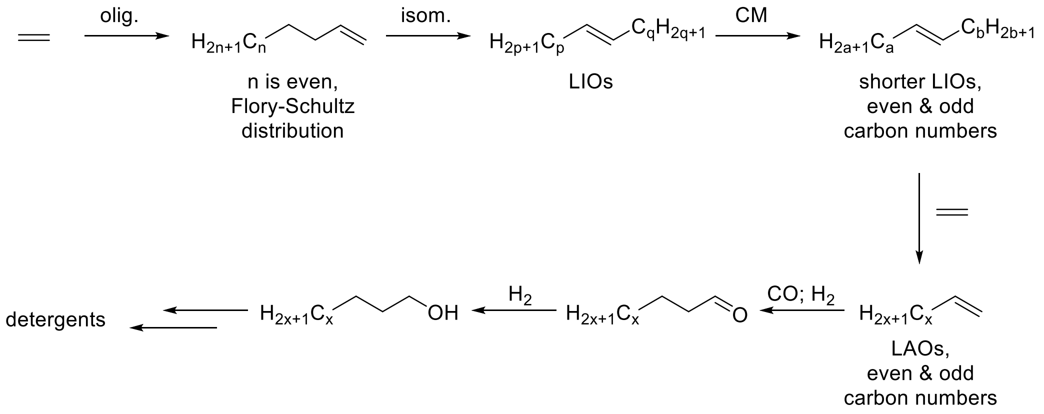

olig.
$H_{2n+1}C_n$
n is even,
Flory-Schultz
distribution
isom.
$H_{2p+1}C_p$
C_qH_{2q+1}
LIOs
CM
$H_{2a+1}C_a$
C_bH_{2b+1}
shorter LIOs,
even & odd
carbon numbers
CO; H_2
$H_{2x+1}C_x$
LAOs,
even & odd
carbon numbers
O
H_2
OH
detergents

Figure 16. Shell Higher Olefins Process (SHOP)

1.2.5 Tandem catalytic processes involving dehydrogenation

Dehydrogenation can occur in concert with olefin metathesis. This reaction is known as alkane metathesis.[43] In this case, the olefin is an intermediate, rather than a starting material or product. Alkane starting materials undergo initial dehydrogenation to alkenes, which undergo olefin metathesis. Typically, the cross-metathesis products are desired. The products of olefin metathesis undergo hydrogenation under the reaction conditions. This final hydrogenation is coupled to the thermodynamically unfavorable loss of hydrogen by the alkane starting materials to make spontaneous the overall alkane metathesis. Typically, an iridium pincer catalyst conducts dehydrogenation, and a heterogeneous Re/Al_2O_3 catalyst conducts metathesis. This reaction has been applied in the degradation of polyethylene to light alkanes.[44]

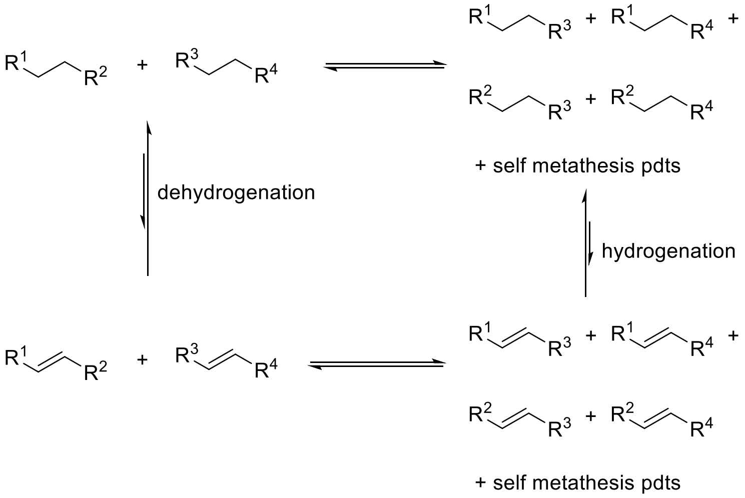

R^1
R^2
+
R^3
R^4
R^1 R^3 + R^1 R^4 +
R^2 R^3 + R^2 R^4
+ self metathesis pdts
dehydrogenation
hydrogenation

Figure 17. Alkane metathesis

In the previous example of alkane metathesis, the thermodynamically unfavorable dehydrogenation step was coupled to transfer hydrogenation of the alkenes formed after cross-metathesis. Dehydrogenation also can be coupled to other thermodynamically favorable addition reactions. Zheng Huang showed that dehydrogenation can be coupled to chain-walking hydrofunctionalization.[7b] This reaction involves initial dehydrogenation of an alkane to generate an internal olefin, which is the more thermodynamically stable alkene formed under the harsh conditions of the reaction, followed by chain-walking hydrosilylation or chain-walking hydroboration to produce terminal alkylsilicon or alkylboron species.

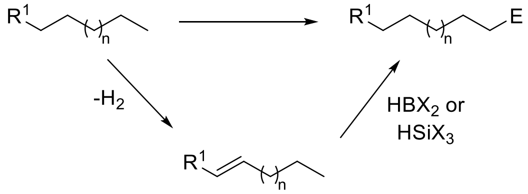

Figure 18. Dehydrogenation in concert with chain-walking hydrofunctionalization

1.3 The present dissertation

The present dissertation discusses the development of novel tandem catalytic processes involving olefins. These processes involve hydrofunctionalizations, isomerizations, dehydrofunctionalizations, dehydrogenations, and metatheses. Through this work, we have shown that the various reactions of olefins can be combined in simple ways to enable processes that are challenging or indeed impossible to accomplish in a single step. These processes are the multicatalytic hydroaminomethylation of α-olefins at low pressures, several contra-thermodynamic isomerization of internal olefins to terminal olefins that involve chain-walking hydrofunctionalization in concert with dehydrofunctionalization, and the depolymerization of polyethylene to propene through dehydrogenation and isomerizing ethenolysis.

1.4 References

1. (a) Chemical Bonds in Organic Compounds. In *Physical Chemistry*, Sanderson, R. T., Ed. Elsevier: 1976; Vol. 21, pp 177. (b) James Speight, P. D., *Lange's Handbook of Chemistry, Sixteenth Edition*. 16th ed.; McGraw-Hill Education: New York, 2005.

2. Eric V. Anslyn; Dougherty, D. A., *Modern Physical Organic Chemistry*. University Science Books: Sausalito, CA, 2005.

3. Hartwig, J. F., *Organotransition Metal Chemistry: From Bonding to Catalysis*. 1 ed.; University Science Books: Mill Valley, California, 2009.

4. T. W. Graham Solomons, C. F., Scott Snyder, *Organic Chemistry*. 11th ed.; Wiley: 2012.

5. (a) Gao, J.; Ni, J.; Yu, R.; Cheng, G.-J.; Fang, X. Ni-Catalyzed Isomerization–Hydrocyanation Tandem Reactions: Access to Linear Nitriles from Aliphatic Internal Olefins. *Org. Lett.* **2021**, *23*, 486. (b) Arthur, P.; England, D. C.; Pratt, B. C.; Whitman, G. M. Addition of Hydrogen Cyanide to Unsaturated Compounds. *J. Am. Chem. Soc.* **1954**, *76*, 5364. (c) Tolman, C. A.; McKinney, R. J.; Seidel, W. C.; Druliner, J. D.; Stevens, W. R., Homogeneous Nickel-Catalyzed Olefin Hydrocyanation. In *Advances in Catalysis*, Eley, D. D.; Pines, H.; Weisz, P. B., Eds. Academic Press: 1985; Vol. 33, pp 1.

6. (a) Hu, M.; Ge, S. Versatile cobalt-catalyzed regioselective chain-walking double hydroboration of 1,n-dienes to access gem-bis(boryl)alkanes. *Nat. Commun.* **2020**, *11*, 765. (b) Léonard, N. G.; Palmer, W. N.; Friedfeld, M. R.; Bezdek, M. J.; Chirik, P. J. Remote, Diastereoselective Cobalt-Catalyzed Alkene Isomerization–Hydroboration: Access to Stereodefined 1,3-Difunctionalized Indanes. *ACS Catal.* **2019**, *9*, 9034. (c) Ogawa, T.; Ruddy, A. J.; Sydora, O. L.; Stradiotto, M.; Turculet, L. Cobalt- and Iron-Catalyzed Isomerization–Hydroboration of Branched Alkenes: Terminal Hydroboration with Pinacolborane and 1,3,2-Diazaborolanes. *Organometallics* **2017**, *36*, 417. (d) Scheuermann, M. L.; Johnson, E. J.; Chirik, P. J. Alkene Isomerization–Hydroboration Promoted by Phosphine-Ligated Cobalt Catalysts. *Org. Lett.* **2015**, *17*, 2716. (e) Palmer, W. N.; Diao, T.; Pappas, I.; Chirik, P. J. High-Activity Cobalt Catalysts for Alkene Hydroboration with Electronically Responsive Terpyridine and α-Diimine Ligands. *ACS Catal.* **2015**, *5*, 622. (f) Obligacion, J. V.; Chirik, P. J. Bis(imino)pyridine Cobalt-Catalyzed Alkene Isomerization–Hydroboration: A Strategy for Remote Hydrofunctionalization with Terminal Selectivity. *J. Am. Chem. Soc.* **2013**, *135*, 19107. (g) Lata, C. J.; Crudden, C. M. Dramatic Effect of Lewis Acids on the Rhodium-Catalyzed Hydroboration of Olefins. *J. Am. Chem. Soc.* **2010**, *132*, 131. (h) Ghebreyessus, K. Y.; Angelici, R. J. Isomerizing-Hydroboration of the Monounsaturated Fatty Acid Ester Methyl Oleate. *Organometallics* **2006**, *25*, 3040. (i) Cipot, J.; Vogels, C. M.; McDonald, R.; Westcott, S. A.; Stradiotto, M. Catalytic Alkene Hydroboration Mediated by Cationic and Formally Zwitterionic Rhodium(I) and Iridium(I) Derivatives of a P,N-Substituted Indene. *Organometallics* **2006**, *25*, 5965. (j) Edwards, D. R.; Crudden, C. M.; Yam, K. One-Pot Carbon Monoxide-Free Hydroformylation of Internal Olefins to Terminal Aldehydes. *Adv. Synth. Catal.* **2005**, *347*, 50. (k) Cipot, J.; McDonald, R.; Stradiotto, M. New bidentate cationic and zwitterionic relatives of Crabtree's hydrogenation catalyst. *Chem. Commun.* **2005**, 4932. (l) Pereira, S.; Srebnik, M. Transition Metal-Catalyzed Hydroboration of and CCl_4 Addition to Alkenes. *J. Am. Chem. Soc.* **1996**, *118*, 909. (m) Pereira, S.; Srebnik, M. A study of hydroboration of alkenes and alkynes with pinacolborane catalyzed by transition metals. *Tetrahedron Lett.* **1996**, *37*, 3283.

7. (a) Du, X.; Huang, Z. Advances in Base-Metal-Catalyzed Alkene Hydrosilylation. *ACS Catal.* **2017**, *7*, 1227. (b) Jia, X.; Huang, Z. Conversion of alkanes to linear alkylsilanes using an iridium–iron-catalysed tandem dehydrogenation–isomerization–hydrosilylation. *Nat. Chem.* **2016**, *8*, 157. (c) Du, X.; Zhang, Y.; Peng, D.; Huang, Z. Base–Metal-Catalyzed Regiodivergent Alkene Hydrosilylations. *Angew. Chem. Int. Ed.* **2016**, *55*, 6671. (d) Zuo, Z.; Zhang, L.; Leng, X.; Huang, Z. Iron-catalyzed asymmetric hydrosilylation of ketones. *Chem. Commun.* **2015**, *51*, 5073. (e) Obligacion, J. V.; Chirik, P. J. Earth-abundant transition metal catalysts for alkene hydrosilylation and hydroboration. *Nat. Rev. Chem.* **2018**, *2*, 15. (f) Schuster, C. H.; Diao, T.; Pappas, I.; Chirik, P. J. Bench-Stable, Substrate-Activated Cobalt Carboxylate Pre-Catalysts for Alkene Hydrosilylation with Tertiary Silanes. *ACS Catal.* **2016**, *6*, 2632. (g) Sakaki, S.; Takayama, T.; Sumimoto, M.; Sugimoto, M. Theoretical Study of the Cp_2Zr-Catalyzed Hydrosilylation of Ethylene. Reaction Mechanism Including New σ-Bond Activation. *J. Am. Chem. Soc.* **2004**, *126*, 3332. (h) Sakaki, S.; Mizoe, N.; Sugimoto, M. Theoretical Study of Platinum(0)-Catalyzed Hydrosilylation of Ethylene. Chalk−Harrod Mechanism or Modified Chalk−Harrod Mechanism. *Organometallics* **1998**, *17*, 2510. (i) Trichlorosilane. In *Encyclopedia of Reagents for Organic Synthesis*, 2006.

8. (a) Muller, T. E.; Beller, M. Metal-initiated amination of alkenes and alkynes. *Chem. Rev.* **1998**, *98*, 675. (b) Strom, A. E.; Hartwig, J. F. One-Pot Anti-Markovnikov Hydroamination of Unactivated Alkenes by Hydrozirconation and Amination. *J. Org. Chem.* **2013**, *78*, 8909. (c) Huang, L.; Arndt, M.; Gooßen, K.; Heydt, H.; Gooßen, L. J. Late Transition Metal-Catalyzed Hydroamination and Hydroamidation. *Chem. Rev.* **2015**, *115*, 2596. (d) Musacchio, A. J.; Lainhart, B. C.; Zhang, X.; Naguib, S. G.; Sherwood, T. C.; Knowles, R. R. Catalytic intermolecular hydroaminations of unactivated olefins with secondary alkyl amines. *Science* **2017**, *355*, 727. (e) Xi,

Y.; Butcher, T. W.; Zhang, J.; Hartwig, J. F. Regioselective, Asymmetric Formal Hydroamination of Unactivated Internal Alkenes. *Angew. Chem. Int. Ed.* **2016**, *55*, 776.

9. (a) Börner, A. F., R., Front Matter. In *Hydroformylation: Fundamentals, Processes, and Applications in Organic Synthesis*, Wiley-VCH Verlag GmbH & Co. KGaA: 2016; pp I. (b) Whiteker, G. T.; Cobley, C. J. Applications of Rhodium-Catalyzed Hydroformylation in the Pharmaceutical, Agrochemical, and Fragrance Industries. *ChemInform* **2013**, *44*. (c) Yu, S.; Zhang, X.; Yan, Y.; Cai, C.; Dai, L.; Zhang, X. Synthesis and Application of Tetraphosphane Ligands in Rhodium-Catalyzed Hydroformylation of Terminal Olefins: High Regioselectivity at High Temperature. *Chem. Eur. J.* **2010**, *16*, 4938. (d) Yan, Y.; Zhang, X.; Zhang, X. Retaining catalyst performance at high temperature: The use of a tetraphosphine ligand in the highly regioselective hydroformylation of terminal olefins. *Adv. Synth. Catal.* **2007**, *349*, 1582. (e) Kim, J. J.; Alper, H. Ionic diamine rhodium(I) complexes - highly active catalysts for the hydroformylation of olefins. *Chem. Commun.* **2005**, 3059. (f) Chen, A. C.; Ren, L.; Decken, A.; Crudden, C. M. Rhodium carbene complexes: Highly selective catalysts for the hydroformylation of styrene derivatives. *Organometallics* **2000**, *19*, 3459. (g) Cuny, G. D.; Buchwald, S. L. Practical, high-yield, regioselective, rhodium-catalyzed hydroformylation of functionalized alpha-olefins. *J. Am. Chem. Soc.* **1993**, *115*, 2066.

10. (a) Kalck, P.; Urrutigoïty, M. Tandem Hydroaminomethylation Reaction to Synthesize Amines from Alkenes. *Chem. Rev.* **2018**, *118*, 3833. (b) Vanbésien, T.; Le Nôtre, J.; Monflier, E.; Hapiot, F. Hydroaminomethylation of oleochemicals: A comprehensive overview. *Eur. J. Lipid Sci. Technol.* **2017**, 1700190. (c) Chen, C. D., X.-Q.; Zhang, X. Recent progress in rhodium-catalyzed hydroaminomethylation. *Org. Chem. Front.* **2016**, *3*, 1359. (d) Raoufmoghaddam, S. Recent advances in catalytic C-N bond formation: a comparison of cascade hydroaminomethylation and reductive amination reactions with the corresponding hydroamidomethylation and reductive amidation reactions. *Organic & Biomolecular Chemistry* **2014**, *12*, 7179. (e) Raoufmoghaddam, S. Recent advances in catalytic C–N bond formation: a comparison of cascade hydroaminomethylation and reductive amination reactions with the corresponding hydroamidomethylation and reductive amidation reactions. **2014**. (f) Crozet, D.; Urrutigoity, M.; Kalck, P. Recent Advances in Amine Synthesis by Catalytic Hydroaminomethylation of Alkenes. *ChemCatChem* **2011**, *3*, 1102. (g) Eilbracht, P.; Schmidt, A., Synthetic Applications of Tandem Reaction Sequences Involving Hydroformylation. In *Catalytic Carbonylation Reactions*, Beller, M., Ed. 2006; Vol. 18, pp 65. (h) Teuma, E.; Loy, M.; Le Berre, C.; Etienne, M.; Daran, J. C.; Kalck, P. Tandem carbonylation reactions: Hydroformylation and hydroaminomethylation of alkenes catalyzed by cationic $[(H_2C(3,5\text{-}Me_2pz)_2)Rh(CO)L]^+$ complexes. *Organometallics* **2003**, *22*, 5261. (i) Eilbracht, P.; Barfacker, L.; Buss, C.; Hollmann, C.; Kitsos-Rzychon, B. E.; Kranemann, C. L.; Rische, T.; Roggenbuck, R.; Schmidt, A. Tandem reaction sequences under hydroformylation conditions: New synthetic applications of transition metal catalysis. *Chem. Rev.* **1999**, *99*, 3329.

11. (a) Mgaya, J. E.; Bartlett, S. A.; Mubofu, E. B.; Mgani, Q. A.; Slawin, A. M. Z.; Pogorzelec, P. J.; Cole-Hamilton, D. J. Synthesis of Bifunctional Monomers by the Palladium-Catalyzed Carbonylation of Cardanol and its Derivatives. *ChemCatChem* **2016**, *8*, 751. (b) Jiménez-Rodriguez, C.; Eastham, G. R.; Cole-Hamilton, D. J. Dicarboxylic Acid Esters from the Carbonylation of Unsaturated Esters Under Mild Conditions. *Inorg. Chem. Commun.* **2005**, *8*, 878. (c) Jimenez Rodriguez, C.; Foster, D. F.; Eastham, G. R.; Cole-Hamilton, D. J. Highly Selective Formation of Linear Esters from Terminal and Internal Alkenes Catalysed by Palladium Complexes of Bis-(di-*tert*-Butylphosphinomethyl)benzene. *Chem. Commun.* **2004**, 1720. (d) Sang, R.; Kucmierczyk, P.; Dong, K.; Franke, R.; Neumann, H.; Jackstell, R.; Beller, M. Palladium-Catalyzed Selective Generation of CO from Formic Acid for Carbonylation of Alkenes. *J. Am. Chem. Soc.* **2018**. (e) Dong, K.; Sang, R.; Fang, X.; Franke, R.; Spannenberg, A.; Neumann, H.; Jackstell, R.; Beller, M. Efficient Palladium-Catalyzed Alkoxycarbonylation of Bulk Industrial Olefins Using Ferrocenyl Phosphine Ligands. *Angew. Chem. Int. Ed.* **2017**, *56*, 5267. (f) Dong, K.; Fang, X.; Gülak, S.; Franke, R.; Spannenberg, A.; Neumann, H.; Jackstell, R.; Beller, M. Highly Active and Efficient Catalysts for Alkoxycarbonylation of Alkenes. *Nat. Commun.* **2017**, *8*, 14117.

12. Sommer, H.; Juliá-Hernández, F.; Martin, R.; Marek, I. Walking Metals for Remote Functionalization. *ACS Cent. Sci.* **2018**, *4*, 153.

13. (a) Das, K.; Kumar, A., Chapter One - Alkane dehydrogenation reactions catalyzed by pincer-metal complexes. In *Adv. Organomet. Chem.*, Pérez, P. J., Ed. Academic Press: 2019; Vol. 72, pp 1. (b) Fang, H.; Liu, G.; Huang, Z., Chapter 18 - Pincer Iridium and Ruthenium Complexes for Alkane Dehydrogenation. In *Pincer Compounds*, Morales-Morales, D., Ed. Elsevier: 2018; pp 383. (c) Sattler, J. J. H. B.; Ruiz-Martinez, J.; Santillan-Jimenez, E.; Weckhuysen, B. M. Catalytic Dehydrogenation of Light Alkanes on Metals and Metal Oxides. *Chem. Rev.* **2014**, *114*, 10613. (d) Choi, J.; MacArthur, A. H. R.; Brookhart, M.; Goldman, A. S. Dehydrogenation and Related Reactions Catalyzed by Iridium Pincer Complexes. *Chem. Rev.* **2011**, *111*, 1761. (e) Kumar, A.; Bhatti, T. M.; Goldman, A. S. Dehydrogenation of Alkanes and Aliphatic Groups by Pincer-Ligated Metal Complexes. *Chem. Rev.* **2017**, *117*, 12357. (f) Kumar, A.; Zhou, T.; Emge, T. J.; Mironov, O.; Saxton, R. J.; Krogh-Jespersen, K.;

Goldman, A. S. Dehydrogenation of n-Alkanes by Solid-Phase Molecular Pincer-Iridium Catalysts. High Yields of α-Olefin Product. *J. Am. Chem. Soc.* **2015**, *137*, 9894. (g) Chowdhury, A. D.; Julis, J.; Grabow, K.; Hannebauer, B.; Bentrup, U.; Adam, M.; Franke, R.; Jackstell, R.; Beller, M. Photocatalytic Acceptorless Alkane Dehydrogenation: Scope, Mechanism, and Conquering Deactivation with Carbon Dioxide. *ChemSusChem* **2015**, *8*, 323. (h) Chianese, A. R.; Drance, M. J.; Jensen, K. H.; McCollom, S. P.; Yusufova, N.; Shaner, S. E.; Shopov, D. Y.; Tendler, J. A. Acceptorless Alkane Dehydrogenation Catalyzed by Iridium CCC-Pincer Complexes. *Organometallics* **2014**, *33*, 457. (i) Punji, B.; Emge, T. J.; Goldman, A. S. A Highly Stable Adamantyl-Substituted Pincer-Ligated Iridium Catalyst for Alkane Dehydrogenation. *Organometallics* **2010**, *29*, 2702. (j) Huang, Z.; Rolfe, E.; Carson, E. C.; Brookhart, M.; Goldman, A. S.; El-Khalafy, S. H.; MacArthur, A. H. R. Efficient Heterogeneous Dual Catalyst Systems for Alkane Metathesis. *Adv. Synth. Catal.* **2010**, *352*, 125. (k) Ray, A.; Zhu, K.; Kissin, Y. V.; Cherian, A. E.; Coates, G. W.; Goldman, A. S. Dehydrogenation of aliphatic polyolefins catalyzed by pincer-ligated iridium complexes. *Chem. Commun.* **2005**, 3388. (l) Zhu, K.; Achord, P. D.; Zhang, X.; Krogh-Jespersen, K.; Goldman, A. S. Highly Effective Pincer-Ligated Iridium Catalysts for Alkane Dehydrogenation. DFT Calculations of Relevant Thermodynamic, Kinetic, and Spectroscopic Properties. *J. Am. Chem. Soc.* **2004**, *126*, 13044. (m) Liu, F.; S. Goldman, A. Efficient thermochemical alkane dehydrogenation and isomerization catalyzed by an iridium pincer complex. *Chem. Commun.* **1999**, 655. (n) Nakaya, Y.; Miyazaki, M.; Yamazoe, S.; Shimizu, K.-i.; Furukawa, S. Active, Selective, and Durable Catalyst for Alkane Dehydrogenation Based on a Well-Designed Trimetallic Alloy. *ACS Catal.* **2020**, 5163. (o) Abdulrhman S. Al-Awadi, S. M. A.-Z., Ahmed Mohamed El-Toni, and; Abasaeed, A. E. Dehydrogenation of Ethane to Ethylene by CO_2 over Highly Dispersed Cr on Large-Pore Mesoporous Silica Catalysts. *Catalysts* **2020**, *10*, 97. (p) He, S.; Castello, D.; Krishnamurthy, K. R.; Al-Fatesh, A. S.; Winkelman, J. G. M.; Seshan, K.; Fakeeha, A. H.; Kersten, S. R. A.; Heeres, H. J. Kinetics of long chain n-paraffin dehydrogenation over a commercial Pt-Sn-K-Mg/γ-Al2O3 catalyst: Model studies using n-dodecane. *Appl. Catal., A* **2019**, *579*, 130. (q) He, S.; Krishnamurthy, K. R.; Seshan, K., Dehydrogenation of long chain n-paraffins to olefins – a perspective. In *Catalysis: Volume 29*, The Royal Society of Chemistry: 2017; Vol. 29, pp 282. (r) He, S.; Wang, B.; Dai, X.; Sun, C.; Bai, Z.; Wang, X.; Guo, Q. Industrial development of long chain paraffin (n-C_{100}–C_{130}) dehydrogenation catalysts and the deactivation characterization. *Chem. Eng. J.* **2015**, *275*, 298. (s) Siri, G. J.; Casella, M. L.; Santori, G. F.; Ferretti, O. A. Tin/Platinum on Alumina as Catalyst for Dehydrogenation of Isobutane. Influence of the Preparation Procedure and of the Addition of Lithium on the Catalytic Properties. *Ind. Eng. Chem.* **1997**, *36*, 4821. (t) Shada, A. D. R.; Miller, A. J. M.; Emge, T. J.; Goldman, A. S. Catalytic Dehydrogenation of Alkanes by PCP–Pincer Iridium Complexes Using Proton and Electron Acceptors. *ACS Catal.* **2021**, *11*, 3009. (u) Sun, X.; Han, P.; Li, B.; Mao, S.; Liu, T.; Ali, S.; Lian, Z.; Su, D. Oxidative dehydrogenation reaction of short alkanes on nanostructured carbon catalysts: a computational account. *Chem. Commun.* **2018**, *54*, 864. (v) Kustov, L. M.; Kucherov, A. V.; Finashina, E. D. Oxidative dehydrogenation of C2–C4 alkanes into alkenes: Conventional catalytic systems and microwave catalysis. *Russ. J. Phys. Chem. A* **2013**, *87*, 345.

14. (a) Murphy, S. K.; Park, J.-W.; Cruz, F. A.; Dong, V. M. Rh-Catalyzed C–C Bond Cleavage by Transfer Hydroformylation. *Science* **2015**, *347*, 56. (b) Kusumoto, S.; Tatsuki, T.; Nozaki, K. The Retro-Hydroformylation Reaction. *Angew. Chem. Int. Ed.* **2015**, *54*, 8458.

15. (a) Bhawal, B. N.; Reisenbauer, J. C.; Ehinger, C.; Morandi, B. Overcoming Selectivity Issues in Reversible Catalysis: A Transfer Hydrocyanation Exhibiting High Kinetic Control. *J. Am. Chem. Soc.* **2020**, *142*, 10914. (b) Fang, X.; Yu, P.; Morandi, B. Catalytic Reversible Alkene-Nitrile Interconversion Through Controllable Transfer Hydrocyanation. *Science* **2016**, *351*, 832. (c) Bhawal, B. N.; Morandi, B. Catalytic Transfer Functionalization through Shuttle Catalysis. *ACS Catal.* **2016**, *6*, 7528.

16. (a) Cornils, B., Dehydroboration. In *Catalysis from A to Z* [Online] Wiley: 2020. https://onlinelibrary.wiley.com/doi/10.1002/9783527809080.cataz04896. (b) Murray, S. A.; Luc, E. C. M.; Meek, S. J. Synthesis of Alkenyl Boronates from Epoxides with Di-[B(pin)]-methane via Pd-Catalyzed Dehydroboration. *Org. Lett.* **2018**, *20*, 469. (c) Sakamoto, Y.; Amaya, T.; Suzuki, T.; Hirao, T. Palladium(II)-Catalyzed Dehydroboration via Generation of Boron Enolates. *Chem. Eur. J.* **2016**, *22*, 18686. (d) Weliange, N. M.; McGuinness, D. S.; Patel, J. Thermal Dehydroboration: Experimental and Theoretical Studies of Olefin Elimination from Trialkylboranes and Its Relationship to Alkylborane Isomerization and Transalkylation. *Organometallics* **2014**, *33*, 4251. (e) Knochel, P.; Boudier, A.; Bromm, L. O.; Hupe, E.; Varela, J. A.; Rodriguez, A.; Koradin, C.; Bunlaksananusorn, T.; Laaziri, H.; Lhermitte, F. Selective transformations mediated by main-group organometallics. *Pure Appl. Chem.* **2000**, *72*, 1699. (f) Laaziri, H.; Bromm, L. O.; Lhermitte, F.; Gschwind, R. M.; Knochel, P. A New Highly Stereoselective Rearrangement of Acyclic Tertiary Organoboranes: An Example of Highly Stereoselective Remote C−H Activation. *J. Am. Chem. Soc.* **1999**, *121*, 6940. (g) Brown, H. C.; Joshi, N. N. Hydroboration of terpenes. 9. A simple improved procedure for upgrading the optical purity of commercially available alpha- and beta-pinenes. Conversion of (+)-alpha-pinene to (+)-beta-pinene via hydroboration-

isomerization. *J. Org. Chem.* **1988**, *53*, 4059. (h) Midland, M. M.; Petre, J. E.; Zderic, S. A.; Kazubski, A. Thermal reactions of B-alkyl-9-borabicyclo[3.3.1]nonane (9-BBN). Evidence for unusually facile dehydroboration with B-pinanyl-9-BBN. *J. Am. Chem. Soc.* **1982**, *104*, 528. (i) Midland, M. M.; Tramontano, A.; Zderic, S. A. The reaction of B-alkyl-9-borabicyclo[3.3.1]nonanes with aldehydes and ketones. A facile elimination of the alkyl group by aldehydes. *J. Organomet. Chem.* **1978**, *156*, 203. (j) Chiu, K.-W.; Negishi, E.-I.; S. Plante, M.; Silveria, A. An unusually facile dehydroboration of triorganoboranes formed by treatment of alkenyltrialkylborates with hydrochloric acid. *J. Organomet. Chem.* **1976**, *112*, C3. (k) Holliday, A. K.; Ottley, R. P. Reactions of trivinylborane with diboron tetrahalides: properties of some dihalogenoboryl(vinylboryl)ethanes. *J. Chem. Soc. A.* **1971**, 886. (l) Knights, E. F.; Brown, H. C. Cyclic hydroboration of 1,5-cyclooctadiene. A simple synthesis of 9-borabicyclo[3.3.1]nonane, an unusually stable dialkylborane. *J. Am. Chem. Soc.* **1968**, *90*, 5280. (m) Brown, H. C.; Bhatt, M. V.; Munekata, T.; Zweifel, G. Organoboranes. VII. The Displacement Reaction with Organoboranes Derived from the Hydroboration of Cyclic and Bicyclic Olefins. Conversion of Endocyclic to Exocyclic Double Bonds. *J. Am. Chem. Soc.* **1967**, *89*, 567. (n) Brown, H. C.; Bhatt, M. V. Organoboranes. IV. The Displacement Reaction with Organoboranes Derived from the Hydroboration of Branched-Chain Olefins. A Contrathermodynamic Isomerization of Olefins. *J. Am. Chem. Soc.* **1966**, *88*, 1440. (o) Brown, H. Isomerization of internal olefins to terminal olefins. US3173967A, 1965. (p) Köster, R. Transformations of Organoboranes at Elevated Temperatures. *Angew. Chem., Int. Ed. Engl.* **1964**, *3*, 174.

17. (a) Fieser, M. E.; Schimler, S. D.; Mitchell, L. A.; Wilborn, E. G.; John, A.; Hogan, L. T.; Benson, B.; LaPointe, A. M.; Tolman, W. B. Dual-catalytic decarbonylation of fatty acid methyl esters to form olefins. *Chem. Commun.* **2018**, *54*, 7669. (b) Liu, Y.; Virgil, S. C.; Grubbs, R. H.; Stoltz, B. M. Palladium-Catalyzed Decarbonylative Dehydration for the Synthesis of α-Vinyl Carbonyl Compounds and Total Synthesis of (−)-Aspewentins A, B, and C. *Angew. Chem. Int. Ed.* **2015**, *54*, 11800. (c) Liu, Y.; Kim, K. E.; Herbert, M. B.; Fedorov, A.; Grubbs, R. H.; Stoltz, B. M. Palladium-Catalyzed Decarbonylative Dehydration of Fatty Acids for the Production of Linear Alpha Olefins. *Adv. Synth. Catal.* **2014**, *356*, 130. (d) Gooßen, L. J.; Paetzold, J. Pd-Catalyzed Decarbonylative Olefination of Aryl Esters: Towards a Waste-Free Heck Reaction. *Angew. Chem. Int. Ed.* **2002**, *41*, 1237.

18. Ager, D. J. The Peterson Reaction. *Synthesis* **1984**, *1984*, 384.

19. Corey, E. J.; Winter, R. A. E. A New, Stereospecific Olefin Synthesis from 1,2-Diols. *J. Am. Chem. Soc.* **1963**, *85*, 2677.

20. Maulbetsch, T.; Jürgens, E.; Kunz, D. Deoxygenation of Epoxides with` Carbon Monoxide. *Chem. Eur. J.* **2020**, *26*, 10634.

21. Asako, S.; Kobashi, T.; Takai, K. Use of Cyclopropane as C1 Synthetic Unit by Directed Retro-Cyclopropanation with Ethylene Release. *J. Am. Chem. Soc.* **2018**, *140*, 15425.

22. Molloy, J. J.; Morack, T.; Gilmour, R. Positional and Geometrical Isomerisation of Alkenes: The Pinnacle of Atom Economy. *Angew. Chem. Int. Ed.* **2019**, *58*, 13654.

23. Ziegler, F. E. Heats of Formation and Hydrogenation of Alkenes. http://ursula.chem.yale.edu/~chem220/chem220js/STUDYAIDS/thermo/HfAlkenes.html.

24. (a) Scaringi, S.; Mazet, C. Kinetically Controlled Stereoselective Access to Branched 1,3-Dienes by Ru-Catalyzed Remote Conjugative Isomerization. *ACS Catal.* **2021**, 7970. (b) Zhang, S.; Bedi, D.; Cheng, L.; Unruh, D. K.; Li, G.; Findlater, M. Cobalt(II)-Catalyzed Stereoselective Olefin Isomerization: Facile Access to Acyclic Trisubstituted Alkenes. *J. Am. Chem. Soc.* **2020**, *142*, 8910. (c) Ren, W.; Sun, F.; Chu, J.; Shi, Y. A Pd-Catalyzed Site-Controlled Isomerization of Terminal Olefins. *Org. Lett.* **2020**, *22*, 1868. (d) Liu, X.; Li, B.; Liu, Q. Base-Metal-Catalyzed Olefin Isomerization Reactions. *Synthesis* **2019**, *51*, 1293. (e) Kochi, T.; Kanno, S.; Kakiuchi, F. Nondissociative chain walking as a strategy in catalytic organic synthesis. *Tetrahedron Lett.* **2019**, *60*, 150938. (f) Kapat, A.; Sperger, T.; Guven, S.; Schoenebeck, F. Olefins through intramolecular radical relocation. *Science* **2019**, *363*, 391. (g) Larionov, E.; Li, H.; Mazet, C. Well-Defined Transition Metal Hydrides in Catalytic Isomerization. *Chem. Commun.* **2014**, *50*, 9816. (h) Crossley, S. W. M.; Barabé, F.; Shenvi, R. A. Simple, Chemoselective, Catalytic Olefin Isomerization. *J. Am. Chem. Soc.* **2014**, *136*, 16788. (i) Larsen, C. R.; Grotjahn, D. B. Stereoselective Alkene Isomerization over One Position. *J. Am. Chem. Soc.* **2012**, *134*, 10357. (j) Biswas, S.; Huang, Z.; Choliy, Y.; Wang, D. Y.; Brookhart, M.; Krogh-Jespersen, K.; Goldman, A. S. Olefin Isomerization by Iridium Pincer Catalysts. Experimental Evidence for an η^3-Allyl Pathway and an Unconventional Mechanism Predicted by DFT Calculations. *J. Am. Chem. Soc.* **2012**, *134*, 13276.

25. (a) Andrianome, M.; Häberle, K.; Delmond, B. Allyl-and benzylstannanes, new reagents in terpenic synthesis. *Tetrahedron* **1989**, *45*, 1079. (b) Araki, S.; Hatano, M.; Butsugan, Y. Regioselective conversion of allylic alcohols to 1-propenes via organoiron complexes. *J. Org. Chem.* **1986**, *51*, 2126. (c) Arnold, D. R.; Mines, S. A. Radical ions in photochemistry. 21. The photosensitized (electron transfer) tautomerization of alkenes; the phenyl

alkene system. *Can. J. Chem.* **1989**, *67*, 689. (d) Eng, S. L.; Ricard, R.; Wan, C. S. K.; Weedon, A. C. Photochemical Deconjugation of α,β-Unsaturated Ketones. *J. Chem. Soc., Chem. Commun.* **1983**, 236. (e) Guignard, R. F.; Petit, L.; Zard, S. Z. A Method for the Net Contra-thermodynamic Isomerization of Cyclic Trisubstituted Alkenes. *Org. Lett.* **2013**, *15*, 4178. (f) Harwood, L. M.; Julia, M. A Convenient Synthesis of (+)-β-Pinene from (+)-α-Pinene. *Synthesis* **1980**, *1980*, 456. (g) Mangion, D.; Kendall, J.; Arnold, D. R. Photosensitized (Electron-Transfer) Deconjugation of 1-Arylcyclohexenes. *Org. Lett.* **2001**, *3*, 45. (h) Min, Y.-F.; Zhang, B.-W.; Cao, Y. A New Synthesis of (-)-β-Pinene from (-)-α-Pinene. *Synthesis* **1982**, *1982*, 875.

26. (a) Hanna, S.; Butcher, T. W.; Hartwig, J. F. Contra-thermodynamic Olefin Isomerization by Chain-Walking Hydrofunctionalization and Formal Retro-hydrofunctionalization. *Org. Lett.* **2019**, *21*, 7129. (b) Hanna, S.; Wills, T.; Butcher, T. W.; Hartwig, J. F. Palladium-Catalyzed Oxidative Dehydrosilylation for Contra-Thermodynamic Olefin Isomerization. *ACS Catal.* **2020**, *10*, 8736. (c) Robert H. Allen, R. W. L., Andrew D. Overstreet Continuous Process for Preparing Aluminm 1-Alkyls and Linear 1-Olefins from Internal Olefins. US005274153A 1993. (d) de Klerk, A.; Hadebe, S. W.; Govender, J. R.; Jaganyi, D.; Mzinyati, A. B.; Robinson, R. S.; Xaba, N. Linear α-Olefins from Linear Internal Olefins by a Boron-Based Continuous Double-Bond Isomerization Process. *Ind. Eng. Chem. Res.* **2007**, *46*, 400.

27. (a) Fogg, D. E.; dos Santos, E. N. Tandem catalysis: a taxonomy and illustrative review. *Coord. Chem. Rev.* **2004**, *248*, 2365. (b) Galván, A.; Fañanás, F. J.; Rodríguez, F. Multicomponent and Multicatalytic Reactions – A Synthetic Strategy Inspired by Nature. *Eur. J. Inorg. Chem.* **2016**, *2016*, 1306. (c) Sancheti, S. P.; Urvashi; Shah, M. P.; Patil, N. T. Ternary Catalysis: A Stepping Stone toward Multicatalysis. *ACS Catal.* **2020**, *10*, 3462. (d) Galván, A.; Fañanás, F. J.; Rodríguez, F. Multicomponent and Multicatalytic Reactions – A Synthetic Strategy Inspired by Nature. *Eur. J. Inorg. Chem.* **2017**, *2016*, 1306. (e) Marks, T. L. L.; Tobin, J. Orthogonal tandem catalysis. *Nat. Chem.* **2015**, *7*, 477. (f) Wasilke, J. C.; Obrey, S. J.; Baker, R. T.; Bazan, G. C. Concurrent tandem catalysis. *Chem. Rev.* **2005**, *105*, 1001.

28. (a) Bair, J. S.; Schramm, Y.; Sergeev, A. G.; Clot, E.; Eisenstein, O.; Hartwig, J. F. Linear-Selective Hydroarylation of Unactivated Terminal and Internal Olefins with Trifluoromethyl-Substituted Arenes. *J. Am. Chem. Soc.* **2014**, *136*, 13098. (b) Saper, N. I.; Ohgi, A.; Small, D. W.; Semba, K.; Nakao, Y.; Hartwig, J. F. Nickel-catalysed anti-Markovnikov hydroarylation of unactivated alkenes with unactivated arenes facilitated by non-covalent interactions. *Nat. Chem.* **2020**, *12*, 276.

29. (a) Gaide, T.; Bianga, J.; Schlipköter, K.; Behr, A.; Vorholt, A. J. Linear Selective Isomerization/Hydroformylation of Unsaturated Fatty Acid Methyl Esters: A Bimetallic Approach. *ACS Catal.* **2017**, *7*, 4163. (b) Alagona, G.; Ghio, C. Rhodium-Catalyzed Hydroformylation of Ketal-Masked β-Isophorone: Computational Explanation for the Unexpected Reaction Evolution of the Tertiary Rh-Alkyl via an Exocyclic β-Elimination Derivative. *The Journal of Physical Chemistry A* **2015**, *119*, 5117. (c) Börner, M. V.-H.; Lutz, D.; Armin Isomerization–Hydroformylation Tandem Reactions. *ACS Catal.* **2014**, *4*, 1706. (d) Yu, S.; Chie, Y.-m.; Guan, Z.-h.; Zhang, X. Highly regioselective isomerization-hydroformylation of internal olefins to linear aldehyde using Rh complexes with tetraphosphorus ligands. *Org. Lett.* **2008**, *10*, 3469. (e) Yan, Y.; Zhang, X.; Zhang, X. A tetraphosphorus ligand for highly regioselective isomerization-hydroformylation of internal olefins. *J. Am. Chem. Soc.* **2006**, *128*, 16058. (f) Paganelli, S.; Battois, F.; Marchetti, M.; Lazzaroni, R.; Settambolo, R.; Rocchiccioli, S. Rhodium catalyzed hydroformylation of β-isophorone: An unexpected result. *J. Mol. Catal. A: Chem.* **2006**, *246*, 195. (g) Bronger, R. P. J.; Kamer, P. C. J.; van Leeuwen, P. W. N. M. Influence of the Bite Angle on the Hydroformylation of Internal Olefins to Linear Aldehydes. *Organometallics* **2003**, *22*, 5358. (h) Klein, H.; Jackstell, R.; Wiese, K.-D.; Borgmann, C.; Beller, M. Highly Selective Catalyst Systems for the Hydroformylation of Internal Olefins to Linear Aldehydes. *Angew. Chem. Int. Ed.* **2001**, *40*, 3408. (i) van der Veen, L. A.; Kamer, P. C. J.; van Leeuwen, P. W. N. M. Hydroformylation of Internal Olefins to Linear Aldehydes with Novel Rhodium Catalysts. *Angew. Chem. Int. Ed.* **1999**, *38*, 336. (j) Azzaroni, F.; Biscarini, P.; Bordoni, S.; Longoni, G.; Venturini, E. Catalytic hydroformylation of (1*S*,5*S*)-(−)- and (1*R*,5*R*)-(+)-*β*-pinene: stereoselective synthesis and spectroscopic characterization of (1*S*,2*R*,5*S*)-, (1*S*,2*S*,5*S*)-, (1*R*,2*R*,5*R*)- and (1*R*,2*S*,5*R*)-10-formylpinane. *J. Organomet. Chem.* **1996**, *508*, 59. (k) dos Santos, E. N.; Pittman, C. U.; Toghiani, H. Hydroformylation of α- and β-pinene catalysed by rhodium and cobalt carbonyls. *J. Mol. Catal.* **1993**, *83*, 51. (l) Tsutomu, M.; Mamoru, K.; Masayasu, S.; Shiro, S.; Atsushi, O.; Ken-ichi, M. Behavior of Amine in Rhodium Complex–Tertiary Amine Catalyst System Active for Hydrogenation of Aldehyde under Oxo Reaction Conditions. *Bull. Chem. Soc. Jpn.* **1984**, *57*, 577.

30. Seayad, A.; Ahmed, M.; Klein, H.; Jackstell, R.; Gross, T.; Beller, M. Internal olefins to linear amines. *Science* **2002**, *297*, 1676.

31. (a) Yarosh, O. G.; Zhilitskaya, L. V.; Yarosh, N. K.; Albanov, A. I.; Voronkov, M. G. Hydrosilylation of Cyclohexene, 1-Methylcyclohexene, and Isopropylidenecyclohexane. *Russ. J. Gen. Chem.* **2004**, *74*, 1895. (b) Benkeser, R. A.; Muench, W. C. The Addition Rates of Dichloro- and Trichlorosilane to 2-Pentene and 1-Octene. *J.*

Organomet. Chem. **1980**, *184*, C3. (c) Bank, H. M.; Saam, J. C.; Speier, J. L. The Addition of Silicon Hydrides to Olefinic Double Bonds. IX. Addition of sym-Tetramethyldisiloxane to Hexene-1, -2, and -3. *J. Org. Chem.* **1964**, *29*, 792. (d) Saam, J.; Speier, J. The Addition of Silicon Hydrides to Olefinic Double Bonds. Part VI. Addition to Branched Olefins. *J. Am. Chem. Soc.* **1961**, *83*, 1351.

32. Zieliński, G. K.; Grela, K. Tandem Catalysis Utilizing Olefin Metathesis Reactions. *Chem. Eur. J.* **2016**, *22*, 9440.

33. Cossy, J.; Bargiggia, F.; BouzBouz, S. Tandem Cross-Metathesis/Hydrogenation/Cyclization Reactions by Using Compatible Catalysts. *Org. Lett.* **2003**, *5*, 459.

34. Chen, J.-R.; Li, C.-F.; An, X.-L.; Zhang, J.-J.; Zhu, X.-Y.; Xiao, W.-J. Ru-Catalyzed Tandem Cross-Metathesis/Intramolecular-Hydroarylation Sequence. *Angew. Chem. Int. Ed.* **2008**, *47*, 2489.

35. Dornan, P. K.; Wickens, Z. K.; Grubbs, R. H. Tandem Z-Selective Cross-Metathesis/Dihydroxylation: Synthesis of anti-1,2-Diols. *Angew. Chem. Int. Ed.* **2015**, *54*, 7134.

36. Börner, A. F., R., Tandem and Other Sequential Reactions Using a Hydroformylation Step. In *Hydroformylation: Fundamentals, Processes, and Applications in Organic Synthesis*, Wiley-VCH Verlag GmbH & Co. KGaA: 2016; pp 379.

37. (a) Yuki, Y.; Takahashi, K.; Tanaka, Y.; Nozaki, K. Tandem Isomerization/Hydroformylation/Hydrogenation of Internal Alkenes to *n*-Alcohols Using Rh/Ru Dual- or Ternary-Catalyst Systems. *J. Am. Chem. Soc.* **2013**, *135*, 17393. (b) Takahashi, K.; Yamashita, M.; Nozaki, K. Tandem Hydroformylation/Hydrogenation of Alkenes to Normal Alcohols Using Rh/Ru Dual Catalyst or Ru Single Component Catalyst. *J. Am. Chem. Soc.* **2012**, *134*, 18746. (c) Kohei, T.; Makoto, Y.; Takeo, I.; Koji, N.; Kyoko, N. High-Yielding Tandem Hydroformylation/Hydrogenation of a Terminal Olefin to Produce a Linear Alcohol Using a Rh/Ru Dual Catalyst System. *Angew. Chem. Int. Ed.* **2010**, *49*, 4488.

38. (a) Crudden, C. M.; Ziebenhaus, C.; Rygus, J. P. G.; Ghozati, K.; Unsworth, P. J.; Nambo, M.; Voth, S.; Hutchinson, M.; Laberge, V. S.; Maekawa, Y.; Imao, D. Iterative protecting group-free cross-coupling leading to chiral multiply arylated structures. *Nat. Commun.* **2016**, *7*, 11065. (b) Rygus, J. P. G.; Crudden, C. M. Enantiospecific and Iterative Suzuki–Miyaura Cross-Couplings. *J. Am. Chem. Soc.* **2017**, *139*, 18124. (c) Mlynarski, S. N.; Schuster, C. H.; Morken, J. P. Asymmetric synthesis from terminal alkenes by cascades of diboration and cross-coupling. *Nature* **2014**, *505*, 386.

39. Brown, H. C.; Heydkamp, W. R.; Breuer, E.; Murphy, W. S. The Reaction of Organoboranes with Chloramine and with Hydroxylamine-*O*-sulfonic Acid. A Convenient Synthesis of Amines from Olefins via Hydroboration. *J. Am. Chem. Soc.* **1964**, *86*, 3565.

40. Alam, M. G.; Tshabalala, T. A.; Ojwach, S. O. Metal-Catalyzed Alkene Functionalization Reactions Towards Production of Detergent and Surfactant Feedstocks. *J. Surfactants Deterg.* **2017**, *20*, 75.

41. (a) Gartside, R. J. Process for the production of linear alpha olefins and ethylene. US6727396B2, 2004. (b) Bala Ramachandran, S. C., Robert J. Gartside, Shane Kleindienst, Wolfgang Ruettinger, Saeed Alerasool Olefin isomerization and metathesis catalyst. US 2010/0056839 A1, 2009. (c) Consorti, C. S.; Aydos, G. L. P.; Dupont, J. Tandem isomerisation–metathesis catalytic processes of linear olefins in ionic liquid biphasic system. *Chem. Commun.* **2010**, *46*, 9058. (d) Ohlmann, D. M.; Tschauder, N.; Stockis, J.-P.; Gooßen, K.; Dierker, M.; Gooßen, L. J. Isomerizing Olefin Metathesis as a Strategy To Access Defined Distributions of Unsaturated Compounds from Fatty Acids. *J. Am. Chem. Soc.* **2012**, *134*, 13716. (e) Baader, S.; Ohlmann, D. M.; Gooßen, L. J. Isomerizing Ethenolysis as an Efficient Strategy for Styrene Synthesis. *Chem. Eur. J.* **2013**, *19*, 9807. (f) Dobereiner, G. E.; Erdogan, G.; Larsen, C. R.; Grotjahn, D. B.; Schrock, R. R. A One-Pot Tandem Olefin Isomerization/Metathesis-Coupling (ISOMET) Reaction. *ACS Catal.* **2014**, *4*, 3069. (g) Hulea, V. Direct transformation of butenes or ethylene into propylene by cascade catalytic reactions. *Catal. Sci. Technol.* **2019**, *9*, 4466. (h) Pollini, J.; Pankau, W. M.; Gooßen, L. J. Isomerizing Olefin Metathesis. *Chem. Eur. J.* **2019**, *25*, 7416. (i) De, S.; Sivendran, N.; Maity, B.; Pirkl, N.; Koley, D.; Gooßen, L. J. Dinuclear PdI Catalysts in Equilibrium Isomerizations: Mechanistic Understanding, in Silico Casting, and Catalyst Development. *ACS Catal.* **2020**, *10*, 4517. (j) Flook, M. M.; Jiang, A. J.; Schrock, R. R.; Müller, P.; Hoveyda, A. H. Z-Selective Olefin Metathesis Processes Catalyzed by a Molybdenum Hexaisopropylterphenoxide Monopyrrolide Complex. *J. Am. Chem. Soc.* **2009**, *131*, 7962.

42. Lutz, E. F. Shell higher olefins process. *J. Chem. Educ.* **1986**, *63*, 202.

43. (a) Haibach, M. C.; Kundu, S.; Brookhart, M.; Goldman, A. S. Alkane Metathesis by Tandem Alkane-Dehydrogenation–Olefin-Metathesis Catalysis and Related Chemistry. *Acc. Chem. Res.* **2012**, *45*, 947. (b) Goldman, A. S.; Roy, A. H.; Huang, Z.; Ahuja, R.; Schinski, W.; Brookhart, M. Catalytic Alkane Metathesis by Tandem Alkane Dehydrogenation-Olefin Metathesis. *Science* **2006**, *312*, 257.

44. Jia, X.; Qin, C.; Friedberger, T.; Guan, Z.; Huang, Z. Efficient and selective degradation of polyethylenes into liquid fuels and waxes under mild conditions. *Sci. Adv.* **2016**, *2*, e1501591.

Chapter 2

Multicatalytic Approach to the Hydroaminomethylation of α-Olefins

2.1 Introduction

Amines are ubiquitous in industrial, biological, and synthetic chemistry. Many industrial products either contain linear amines or are synthesized from amines,[1] and some of the most commonly prescribed pharmaceuticals contain 1-aminoalkyl groups (Scheme 1). Such amines are most commonly synthesized by the amination of alcohols, the reductive amination of aldehydes, or the reduction of amides, nitriles, or nitro compounds.[1] However, the starting materials for these processes are often synthesized from olefins; therefore, a method for the synthesis of amines from olefins would be more direct, less expensive, and more environmentally benign than the multi-step alternatives.

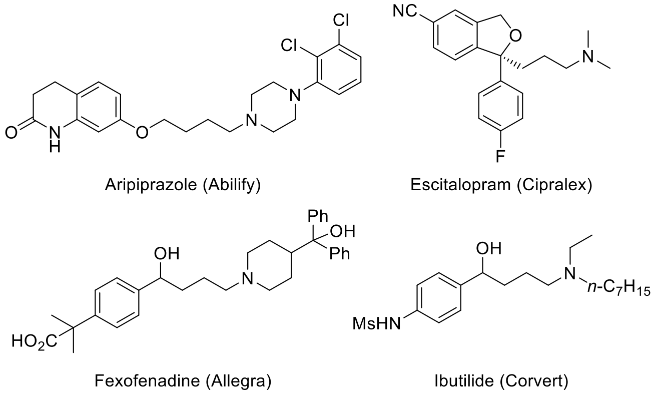

Aripiprazole (Abilify)

Escitalopram (Cipralex)

Fexofenadine (Allegra)

Ibutilide (Corvert)

Scheme 1. APIs containing aminoalkyl groups

The hydroaminomethylation of olefins is an atom-economical and operationally simple reaction involving hydroformylation of an olefin to form an aldehyde and reductive amination of this aldehyde to form an amine.[2] The reaction is commonly conducted with a rhodium-based catalyst ligated by a diphosphine (Scheme 2A). Several limitations, such as the high pressure of synthesis gas (usually around 60 bar) required to achieve acceptable yields,[2a,2b] have diminished the utility of this reaction. In addition, self-condensation of the aldehyde, hydrogenation of the aldehyde, and hydrogenation of the olefin have been reported to compete with hydroaminomethylation.[2a]

Hydroaminomethylation is difficult to achieve, in part, because the properties of the most active catalysts for hydroformylation are quite different from those of the most active catalysts for reductive amination.[3] Moreover the reductive amination process must not be strongly inhibited by carbon monoxide. A single catalyst that meets these criteria and catalyzes hydroaminomethylations at low pressures and temperatures has not been identified. In 2003, Beller reported one of the most active and regioselective systems comprising the combination of $[Rh(COD)_2]BF_4$ with Xantphos, but these reactions were conducted with 40 bar of syngas at 125 °C (Scheme 2A).[4] Hydroaminomethylations reported by Eilbracht, Alper, Whiteker, Zhang, and others occur under similar conditions.[5] A set of hydroaminomethylations reported by Beller occurred at the lower temperature of 60 °C. However, these reactions were limited to those of vinylarenes, and high pressures (30 bar, 1:5 $CO:H_2$) were still required. [6]

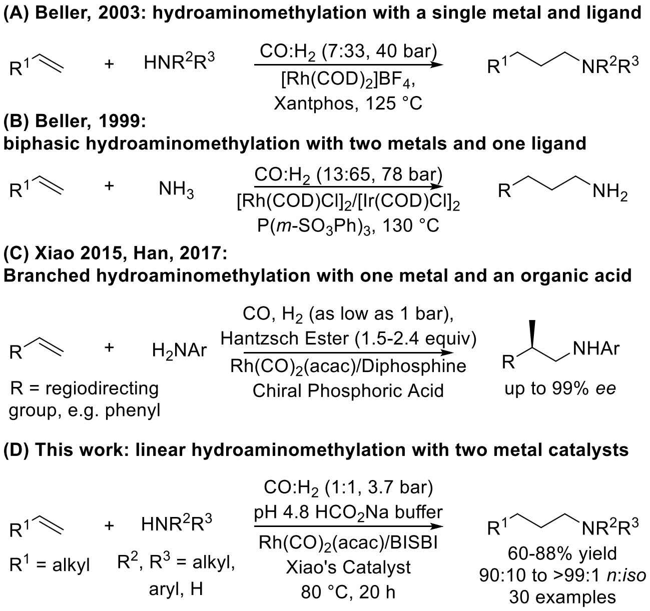
(A) Beller, 2003: hydroaminomethylation with a single metal and ligand
R1
+
HNR2R3
CO:H2 (7:33, 40 bar)
[Rh(COD)2]BF4,
Xantphos, 125 °C
R1
NR2R3
(B) Beller, 1999:
biphasic hydroaminomethylation with two metals and one ligand
R1
+
NH3
CO:H2 (13:65, 78 bar)
[Rh(COD)Cl]2/[Ir(COD)Cl]2
P(m-SO3Ph)3, 130 °C
R
NH2
(C) Xiao 2015, Han, 2017:
Branched hydroaminomethylation with one metal and an organic acid
R
+
H2NAr
CO, H2 (as low as 1 bar),
Hantzsch Ester (1.5-2.4 equiv)
Rh(CO)2(acac)/Diphosphine
Chiral Phosphoric Acid
R
NHAr
R = regiodirecting group, e.g. phenyl
up to 99% ee
(D) This work: linear hydroaminomethylation with two metal catalysts
R1
+
HNR2R3
CO:H2 (1:1, 3.7 bar)
pH 4.8 HCO2Na buffer
Rh(CO)2(acac)/BISBI
Xiao's Catalyst
80 °C, 20 h
R1
NR2R3
R1 = alkyl
R2, R3 = alkyl, aryl, H
60-88% yield
90:10 to >99:1 n:iso
30 examples

Scheme 2. Approaches to hydroaminomethylation

We envisioned a new approach in which two catalysts, one for each step, would react by mechanisms that are distinct and independent from each other, enabling hydroaminomethylation to occur under conditions that are milder than those with a single catalyst.[7] Beller and Luo published hydroaminomethylations conducted with a single phosphine and two metals, but these reactions still required high pressures of synthesis gas and high temperatures (Scheme 2B).[8] Following a different design, Xiao and Han published hydroaminomethylations catalyzed by the combination of a rhodium-based catalyst for the hydroformylation step and a chiral phosphoric acid for the reductive amination step that form enantioenriched, branched amines from α- and β-functionalized olefins (Scheme 2C). However, these systems have not been shown to catalyze linear-selective hydroaminomethylations of unfunctionalized alkenes, and the organic catalyst requires an expensive Hantzsch ester to reduce the imine intermediate.[7a,7b,9]

Herein, we report a linear-selective hydroaminomethylation of α-olefins catalyzed by two distinct metal complexes and an approach to the reductive amination step not applied previously to hydroaminomethylation (Scheme 2D). A rhodium-diphosphine complex catalyzes the hydroformylation step, and a phosphine-free, cyclometallated iridium complex catalyzes the reductive amination step by transfer hydrogenation. Key features of this work include the identification of a catalyst for reductive amination that is not poisoned by CO and the use of buffered formic acid for the reduction step. With this system, aromatic, heteroaromatic, and aliphatic amines are formed in high yields and in high regioselectivities with pressures of synthesis gas and temperatures that are significantly lower than those used previously for hydroaminomethylation.

Our strategy for a low-pressure, multicatalytic hydroaminomethylation was based on the hypotheses that the high pressures of hydrogen in existing systems for hydroaminomethylation are required to ensure that reductive amination is faster than self-condensation of the aldehyde and that the reductive amination step of hydroaminomethylation is slow because catalysts for this step tend to be inhibited by carbon monoxide. In this case, a reductive amination catalyst that is unaffected by carbon monoxide could be combined with a suitable hydroformylation catalyst to conduct hydroaminomethylations at low pressures of synthesis gas. A complex that catalyzes reductive amination by transfer hydrogenation might meet this criterion.

2.2 Results and discussion

To test this reaction design, we studied the hydroaminomethylation of 1-decene (**1a**) with aniline (**2a**) in the presence of formic acid, the highly active and selective hydroformylation catalyst generated from $Rh(CO)_2(acac)$ and BISBI, and various complexes known to catalyze the transfer hydrogenation of imines and iminium ions (Table 1). The most well-known catalysts for reductive amination by transfer hydrogenation consist of a metal capable of transferring a hydride and a ligand capable of transferring a proton to a polarized multiple bond.[10] However, amine **3aa** formed in poor yield from olefin **1a** in the presence of ruthenium diamine complexes **C1** and **C2** (entries 1–4), even though these complexes are known to be active for transfer hydrogenation of imines. The group 9 congeners (catalysts **C3**-**C5**) of catalysts **C1** and **C2** are active for the reductive amination of aldehydes by transfer hydrogenation.[11] However, amine **3aa** formed with low regioselectivity and in poor yield in the presence of catalysts **C3**, **C4**, and **C5** and in the presence of $Rh(CO)_2(acac)$ and BISBI (entries 5–7). Control experiments indicated that complexes **C3**-**C5** either degrade into unselective catalysts for hydroformylation or are themselves unselective catalysts for hydroformylation under the conditions in Table 1. This reactivity of the reductive amination catalyst toward hydroformylation leads to low *n*:*iso* ratios of the amine product. Amine **3aa** also formed in low yields in the presence of catalyst **C6** (entry 8). All of the hydroaminomethylations conducted with catalysts **C1**-**C6** (entries 1-8) proceeded to high conversions; the major side products of the reactions formed from self-condensation of undecanal.

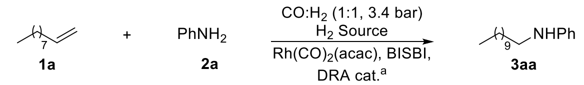

Entry	DRA Cat.[a]	H_2 Source	Hydroformylation Ligand	Yield[b]	*n:iso*
1	**C1**	5:2 HCO_2H:TEA	BISBI	33	97:3
2	**C1**	HCO_2Na buffer[c]	BISBI	10	72:28
3	**C2**	5:2 HCO_2H:TEA	BISBI	29	98:2
4	**C2**	HCO_2Na buffer[c]	BISBI	10	70:30
5	**C3**	5:2 HCO_2H:TEA	BISBI	29	59:41
6	**C4**	5:2 HCO_2H:TEA	BISBI	34	88:12
7	**C5**	5:2 HCO_2H:TEA	BISBI	34	72:28
8	**C6**	5:2 HCO_2H:TEA	BISBI	48	85:15
9	**C7**	5:2 HCO_2H:TEA	BISBI	30	96:4
10	**C7**	HCO_2Na buffer[c]	BISBI	91	98:2
11	**C7**	HCO_2Na buffer[c]	Xantphos	82	98:2
12	**C7**	HCO_2Na buffer[c]	DPEPhos	75	90:10
13	**C7**	none	BISBI	0	N/A
14[d]	**C7**	HCO_2Na buffer[c]	BISBI	83	99:1
15[e]	**C7**	HCO_2Na buffer[c]	BISBI	76	99:1
16[f]	**C7**	HCO_2Na buffer[c]	BISBI	8	68:32
17	none	HCO_2Na buffer[c]	BISBI	0	N/A

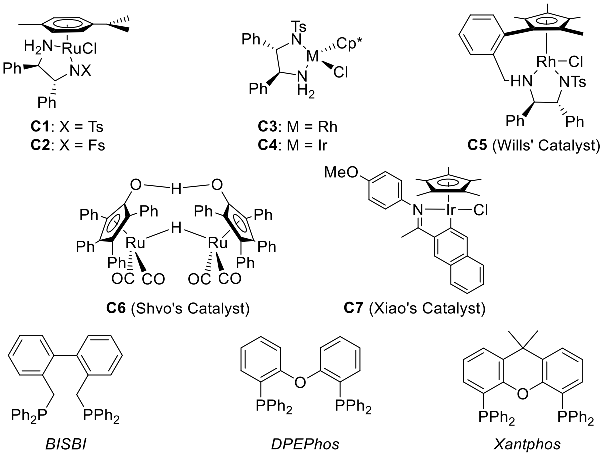

Conditions: 1-decene (0.5 mmol), aniline (0.75 mmol), H_2 source (500 µL), 9:1 PhMe:MeOH (2.5 mL), $Rh(CO)_2(acac)$ (0.5 mol%), hydroformylation ligand (2.5 mol%), reduction catalyst (1 mol%), 80 °C, 20 h. [a]Direct Reductive Amination catalyst. [b]Yield of all constitutional isomers of amine **3aa**, determined by GC against dodecane as an internal standard. [c]Aqueous sodium formate buffer at pH 4.8. [d]0.25 mol% $Rh(CO)_2(acac)$, 1.25 mol% BISBI, 0.5 mol% **C7**. [e]0.125 mol% $Rh(CO)_2(acac)$, 0.625 mol% BISBI, 0.25 mol% **C7**. [f]With no $Rh(CO)_2(acac)$

Table 1. Evaluation of conditions for the hydroaminomethylation of 1-decene with aniline

To increase the rate of reductive amination of undecanal relative to that of its self-condensation, we sought catalysts for transfer hydrogenation that might be more stable to carbon monoxide than catalysts **C1**-**C6**. Reports that catalyst **C7** is more active for the reduction of *N*-*p*-anisylketimines than catalyst **C4** and the robustness of catalyst **C7** endowed by cyclometallation prompted us to attempt hydroaminomethylations with catalyst **C7** as a catalyst for reductive amination.[12]

Initial studies with catalyst **C7** showed that amine **3aa** formed in only 30% yield from olefin **1a**, CO, H_2, and amine **2a** in the presence of catalyst **C7** and the combination of $Rh(CO)_2(acac)$, and BISBI with a 5:2 HCO_2H:Et_3N azeotrope as the reducing agent (entry 11). On the basis of prior literature showing that the reductive amination of acetophenone with *p*-anisidine catalyzed by complex **C7** occurs significantly more rapidly with an aqueous sodium formate buffer at pH 4.8 as the reducing agent than with a 5:2 HCO_2H:Et_3N azeotrope as the reducing agent,[13,14] we conducted the hydroaminomethylation of olefin **1a** with amine **2a** with this reducing agent in the presence of **C7**. Amine **3aa** formed in 91% yield under these conditions (entry 10). Amine **3aa** formed in lower yields in the presence of XantPhos and DPEPhos than in the presence of BISBI (entries 11–12), and the product did not form in the absence of formate (entry 13). The hydroaminomethylation occurred at lower loadings of the two catalysts with only a small sacrifice in yield (entries 14-15). Amine **3aa** formed in 8% yield and 68:32 *n*:*iso* in the presence of catalyst **C7** with no $Rh(CO)_2(acac)$ present (entry 16), indicating that catalyst **C7** is only slightly active towards hydroformylation under the developed conditions. Amine **3aa** did not form in the absence of a reductive amination catalyst (entry 17).

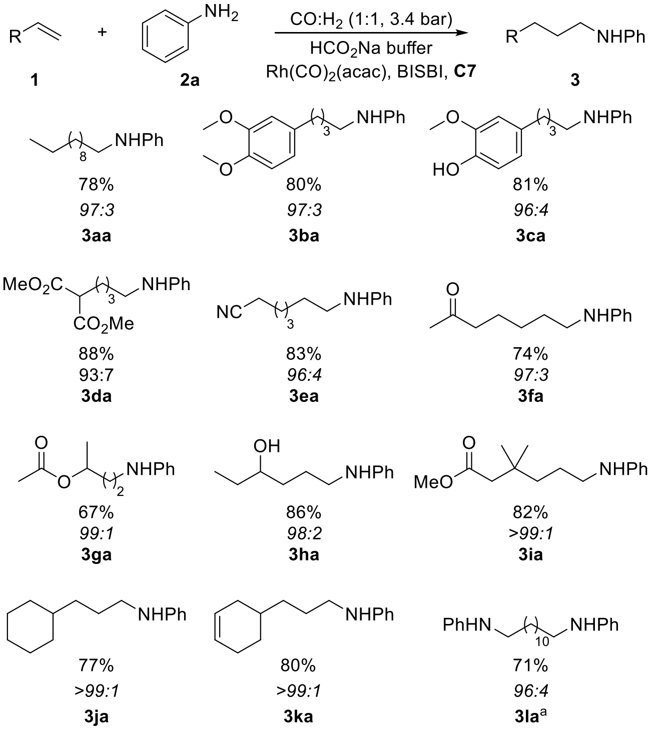
R
NH2
1
2a
CO:H2 (1:1, 3.4 bar)
HCO2Na buffer
Rh(CO)2(acac), BISBI, C7
R
NHPh
3
NHPh
78%
97:3
3aa
NHPh
80%
97:3
3ba
NHPh
HO
81%
96:4
3ca
MeO2C
NHPh
CO2Me
88%
93:7
3da
NC
NHPh
83%
96:4
3ea
O
NHPh
74%
97:3
3fa
O
NHPh
67%
99:1
3ga
OH
NHPh
86%
98:2
3ha
O
MeO
NHPh
82%
>99:1
3ia
NHPh
77%
>99:1
3ja
NHPh
80%
>99:1
3ka
PhHN
NHPh
71%
96:4
3la^a

Conditions: olefin (0.5 mmol), aniline (0.75 mmol), pH 4.8 aqueous sodium formate buffer (500 μL), CO:H_2 (1:1, 3.4 bar), $Rh(CO)_2(acac)$ (0.5 mol%), BISBI (2.5 mol%), Xiao's catalyst (1 mol%), 9:1 PhMe:MeOH (2.5 mL), 80 °C, 20 h. All yields reported are isolated yields. Regioselectivities were determined by GC analysis of the crude reaction mixture. [a]0.25 mmol olefin.

Table 2. Hydroaminomethylations of various olefins with aniline

We attribute the high yields and regioselectivities of the reaction in entry 10 to several factors. First, Xiao's cyclometallated catalyst is not significantly inhibited by low pressures of CO; control experiments indicated that the yield of the reductive amination of undecanal catalyzed by complex **C7** was the same in the absence of CO as in the presence of 1.7 bar of CO. In contrast, complexes **C1**, **C2** and **C6** were poisoned by CO, even at this low pressure (see the supporting information for details). Second, Xiao's catalyst is compatible with the aqueous HCO_2Na buffer, a mild, inexpensive hydrogen surrogate. Finally, Xiao's catalyst does not hydrogenate imines by a metal-ligand bifunctional mechanism.[12] Instead, Xiao's catalyst transfers a hydride to an iminium ion that is formed by protonation of an imine or enamine in an acidic medium.[12]

The scope of olefins that undergo this hydroaminomethylation is illustrated by the examples in Table 2. Phenols (**3ca**), malonates (**3da**), nitriles (**3ea**), enolizable ketones (**3fa**), allylic acetates (**3ga**), allylic alcohols (**3ha**), and disubstituted olefins (**3ka**) were all tolerated. Olefins bearing electron-withdrawing groups in the allylic position reacted with excellent regioselectivities (**1b**, **1c**, **1d**, **1g**, **1h**); such β-functionalized olefins often undergo hydroformylations with low *n*:*iso* ratios, due to their tendencies to isomerize to internal olefins. Sterically hindered α-olefins (**1g**, **1i**, **1j**, **1k**) also underwent hydroaminomethylation. As expected, the regioselectivities of the reactions of these alkenes were higher than those of reactions of less hindered alkenes. In addition, the double hydroaminomethylation of olefin **1l** proceeded in high yield and with high regioselectivity.

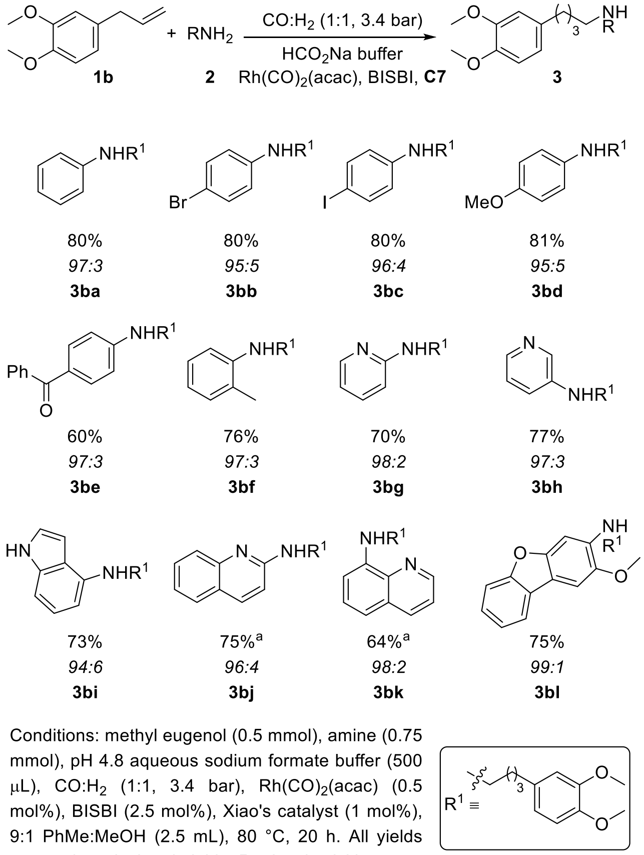

Conditions: methyl eugenol (0.5 mmol), amine (0.75 mmol), pH 4.8 aqueous sodium formate buffer (500 μL), $CO:H_2$ (1:1, 3.4 bar), $Rh(CO)_2(acac)$ (0.5 mol%), BISBI (2.5 mol%), Xiao's catalyst (1 mol%), 9:1 PhMe:MeOH (2.5 mL), 80 °C, 20 h. All yields reported are isolated yields. Regioselectivities were determined by GC analysis of the crude reaction mixture. [a]1.25 mmol amine

Table 3. Hydroaminomethylations of methyl eugenol with various arylamines

The scope of arylamines that undergo hydroaminomethylation was studied with the olefin methyl eugenol (**1b**) as the coupling partner. The results are given in Table 3. Both electron-poor (**2b**, **2c**, **2e**) and electron-rich (**2d**) anilines underwent hydroaminomethylation. Anilines bearing *ortho* substituents (**2f**) and those bearing ketones (**2e**) also underwent hydroaminomethylation.

The scope of heteroarylamines that undergo hydroaminomethylation with olefin **1b** is also shown in Table 3. Heteroarylamines are widespread in pharmaceuticals and agrochemicals, but hydroaminomethylations with such regents are limited.[15] For reference, we conducted the reaction of olefin **1b** with 2-aminopyridine (**2g**) under standard conditions for hydroaminomethylation (125 °C, 40 bar 1:5 CO:H_2) with the single catalyst formed from the combination of $[RhCOD_2]BF_4$ and Xantphos. Only trace amounts of amine **3bg** formed; the major species present in the crude reaction mixture was the starting olefin **1b**.[16] In contrast, the reactions of methyl eugenol with heteroarylamines, including aminopyridines (**2g**, **2h**), aminoindoles (**2i**), aminoquinolines (**2j**, **2k**), and aminodibenzofurans (**2l**) occurred in good yield under the conditions we developed with two catalysts. Even heteroarylamines capable of chelating metal catalysts (**2k**) reacted. This contrast in reactivity demonstrates the unusual compatibility of the new system for hydroaminomethylation with biologically important heteroarenes.

Alkylamines might be expected to be quenched by the acidic buffer containing formic acid, but both primary and secondary alkylamines underwent hydroaminomethylation under the conditions we developed with two catalysts and a pH 4.8 formate buffer (Table 4). Both cyclic (**2m**, **2n**, **2o**, **2p**) and acyclic (**2q**, **2r**, **2s**) secondary amines underwent the hydroaminomethylation. Sterically hindered aliphatic amines were less reactive towards hydroaminomethylation than unhindered aliphatic amines, presumably due to slow reduction of sterically hindered iminium ions. Primary aliphatic amines (**2t**) also underwent hydroaminomethylation to form secondary amines without the formation of tertiary amines.

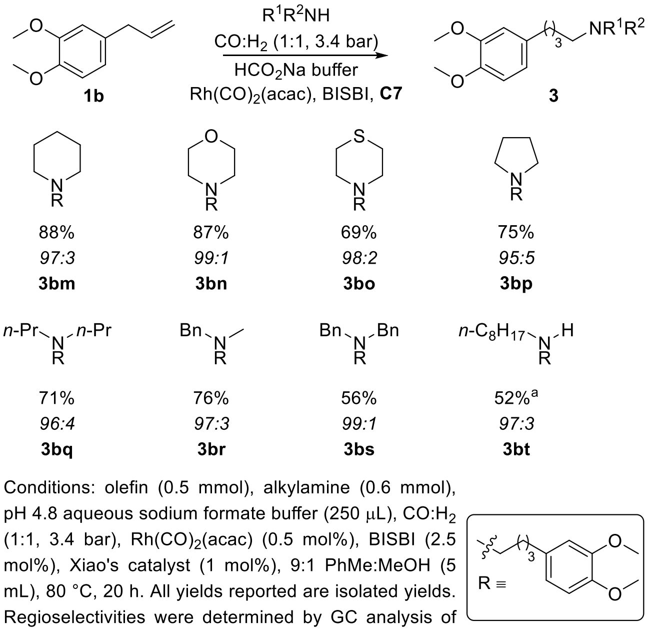

Conditions: olefin (0.5 mmol), alkylamine (0.6 mmol), pH 4.8 aqueous sodium formate buffer (250 μL), CO:H_2 (1:1, 3.4 bar), $Rh(CO)_2(acac)$ (0.5 mol%), BISBI (2.5 mol%), Xiao's catalyst (1 mol%), 9:1 PhMe:MeOH (5 mL), 80 °C, 20 h. All yields reported are isolated yields. Regioselectivities were determined by GC analysis of the crude reaction mixture. [a]2.5 equiv octylamine.

Table 4. Hydroaminomethylations of methyl eugenol with various aliphatic amines

To demonstrate further the applicability of this work to the preparation of medicinally relevant amines, we synthesized amine **3mt**, the active ingredient in a drug sold under the generic name ibutilide (Scheme 3). Under the conditions in Scheme 3, olefin **1m** underwent hydroaminomethylation in 76% yield. Previous examples of this hydroaminomethylation occurred in significantly lower yields and required pressures of syngas that are much higher than those in the current work.[5e]

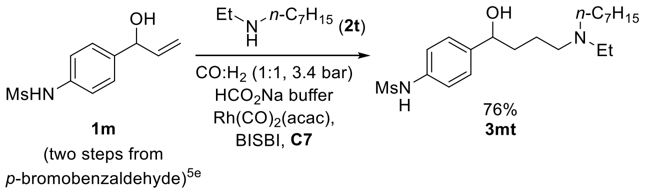
Et-NH-n-C$_7$H$_{15}$ (**2t**)
CO:H$_2$ (1:1, 3.4 bar)
HCO$_2$Na buffer
Rh(CO)$_2$(acac),
BISBI, **C7**
OH
MsHN
1m
(two steps from
p-bromobenzaldehyde)[5e]
n-C$_7$H$_{15}$
N
Et
MsN
H
76%
3mt

Conditions for Hydroaminomethylation: olefin (0.5 mmol), alkylamine (0.6 mmol), pH 4.8 aqueous sodium formate buffer (250 μL), CO:H$_2$ (1:1, 3.4 bar), Rh(CO)$_2$(acac) (1 mol%), BISBI (5 mol%), Xiao's catalyst (2 mol%), 9:1 PhMe:MeOH (5 mL), 80 °C, 20 h.

Scheme 3. Synthesis of Ibutilide

Finally, the hydroaminomethylations reported in this work can be conducted easily on large scales and at atmospheric pressure of syngas. The hydroaminomethylation of 6 mmol of methyl eugenol with aniline gave 1.24 g of amine **3ba** (71% yield, Scheme 4. By adjusting the ratio of CO to H$_2$ to 1:2 CO:H$_2$, the reaction of 1-decene (**1a**) with aniline (**2a**) formed *N*-undecyl aniline (**3aa**) in 65% yield at a total pressure of only 1 atm at 70 °C (Scheme 5).

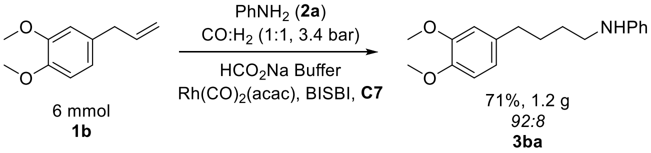
PhNH$_2$ (**2a**)
CO:H$_2$ (1:1, 3.4 bar)
HCO$_2$Na Buffer
Rh(CO)$_2$(acac), BISBI, **C7**
O
O
6 mmol
1b
NHPh
71%, 1.2 g
92:8
3ba

Conditions: methyl eugenol (6 mmol), aniline (9 mmol), pH 4.8 aqueous sodium formate buffer (6 mL), CO:H$_2$ (1:1, 3.4 bar), Rh(CO)$_2$(acac) (0.5 mol%), BISBI (2.5 mol%), Xiao's catalyst (1 mol%), 9:1 PhMe:MeOH (30 mL), 80 °C, 20 h.

Scheme 4. Hydroaminomethylation on a 6-mmol scale

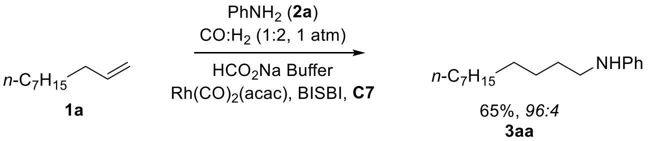
PhNH$_2$ (**2a**)
CO:H$_2$ (1:2, 1 atm)
HCO$_2$Na Buffer
Rh(CO)$_2$(acac), BISBI, **C7**
n-C$_7$H$_{15}$
1a
n-C$_7$H$_{15}$
NHPh
65%, *96:4*
3aa

Conditions: 1-decene (0.15 mmol), aniline (0.23 mmol), pH 4.8 aqueous sodium formate buffer (250 μL), CO:H$_2$ (1:2, 15 psi), Rh(CO)$_2$(acac) (2 mol%), BISBI (8 mol%), Xiao's catalyst (2 mol%), 9:1 PhMe:MeOH (750 μL), 70 °C, 64 h.

Scheme 5. Hydroaminomethylation at atmospheric pressure

2.3 Conclusion

In summary, we have developed a scalable, linear-selective, dual-catalytic hydroaminomethylation of α-olefins occurring at low temperature and pressure by exploiting the combination of a catalyst for hydroformylation and a catalyst for reductive amination that is active under carbon monoxide and that reduces imines by transfer hydrogenation. The pressures and temperatures of the reaction are the lowest reported for linear-selective hydroaminomethylations, and the reactions can even be conducted at atmospheric pressure of synthesis gas. The reaction occurs with a broad range of olefins and amines and is uniquely suitable for the preparation of a wide range of medicinally relevant heteroarylamines. Efforts to further increase the activity of dual catalysts and the scope of reactants are ongoing.

2.4 Experimental

2.4.1 General methods and materials

All reagents were purchased from commercial suppliers and used as received unless otherwise noted. Toluene and methanol were purchased from EMD and used as received. The aqueous pH 4.8 HCO_2H/HCO_2Na buffer was prepared according to the method of Xiao and co-workers.[13] Hydroaminomethylations were conducted in a Biotage Endeavor Catalyst Screening System. Crude reaction mixtures were analyzed by gas chromatography (GC) on an Agilent 7890 GC equipped with an HP-5 column (25 m x 0.20 mm x 0.33 μm film) and an FID detector. Quantitative analysis by GC was conducted with dodecane as an internal standard. The products of catalytic reactions were purified by flash column chromatography with a Teledyne Isco CombiFlash® R_f system and RediSep R_f Gold™ columns. All NMR spectra were recorded at the University of California, Berkeley NMR facility. Proton-NMR spectra were recorded on Bruker AVB-400, AVQ-400, AV-500 and AV-600 instruments with operating frequencies of 400, 400, 500, and 600 MHz, respectively, and Carbon-13 NMR spectra were recorded on a Bruker AV-600 instrument with a ^{13}C operating frequency of 150 MHz. Chemical shifts (δ) are reported in ppm relative to those of residual solvent signals ($CDCl_3$ $\delta = 7.26$ for ^{1}H NMR and $\delta = 77.0$ for ^{13}C NMR, Acetone-d_6 $\delta = 2.05$ for ^{1}H NMR and $\delta = 206.3, 29.8$ for ^{13}C NMR). High-resolution mass spectra were recorded in electrospray ionization mode on an Agilent Q-TOF spectrometer in the Lawrence Berkeley National Laboratory Catalysis Center at the University of California, Berkeley. FTIR spectra were recorded on a Bruker Vertex80 Time-Resolved FTIR spectrometer in the Lawrence Berkeley National Laboratory Catalysis Center at the University of California, Berkeley.

2.4.2 Synthesis of Xiao's catalyst

The following procedure was adapted from the procedure reported by Xiao and co-workers.[13]

(*E*)-*N*-(4-Methoxyphenyl)-1-(naphthalen-2-yl)ethan-1-imine (**S1**)

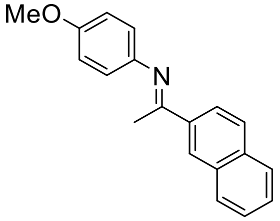

A 100 mL round-bottom flask was charged with a stir bar, 2-acetylnapthalene (2.81 g, 16.5 mmol, 1.00 equiv), *p*-anisidine (1.99 g, 16.2 mmol, 0.982 equiv), activated 4 Å molecular sieves (4.0 g), and toluene (58 mL). The mixture was heated at 120 °C for 18 h, cooled to room temperature, filtered over magnesium sulfate, and concentrated *in vacuo* to afford imine **S1** as a dark-yellow solid. The solid was recrystallized from ether/hexanes to afford imine **S1** (1.06 g, 3.83 mmol, 24% yield). The ^{1}H-NMR spectrum of the product matched the spectrum reported by Xiao.[13]

Xiao's Catalyst (C7)

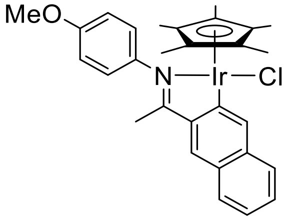

A 100 mL round-bottom flask was charged with a stir bar and CH_2Cl_2 (25 mL). The flask was sealed with a septum and sparged with N_2 for 1 h. The septum was briefly removed, and the flask was quickly charged with $[Cp^*IrCl_2]_2$ (1.39 g, 1.74 mmol, 1.00 equiv), imine **S1** (1.06 g, 3.83 mmol, 2.20 equiv), and NaOAc (2.85 g, 34.8 mmol, 9.09 equiv). The flask was sealed with a septum and stirred at room temperature for 24 h, after which time a deep red color was observed. The crude reaction mixture was filtered through a plug of Celite and concentrated *in vacuo* to afford a red solid. The crude product was recrystallized from hexanes/CH_2Cl_2 (10:1) to afford Xiao's catalyst as a red-orange crystalline solid (1.56 g, 2.39 mmol, 70% yield). The ^{1}H-NMR spectrum of the product matched the spectrum reported by Xiao.[13]

2.4.3 General procedures for hydroaminomethylations

Preparation of catalyst stock solutions

Catalyst stock solutions were made to conduct seven reactions simultaneously. Under air, a vial was charged with $Rh(CO)_2(acac)$ (5.2 mg, 0.020 mmol, 0.5 mol%), 2,2'-bis(diphenylphosphinomethyl)-1,1'-biphenyl (BISBI, 55.4 mg, 0.101 mmol, 2.5 mol%), and Xiao's catalyst (26.1 mg, 0.0401 mmol, 1.0 mol%). The solids were dissolved in dichloromethane (4.00 mL), and the resulting deep-red solution was drawn into a Hamilton gastight syringe. Aliquots of this stock solution (500 μL) were added to seven different glass liner tubes compatible with the Biotage Endeavor Catalyst Screening System, and the solvent was evaporated under a flow of nitrogen.

Hydroaminomethylations with arylamines

An aliquot of the catalyst stock solution (0.500 mL, 0.50 mol% $Rh(CO)_2(acac)$, 2.5 mol% BISBI, 1.0 mol% Xiao's catalyst) was plated (*see above*) onto a glass liner tube. Under air, the tube was sequentially charged with toluene: methanol (9:1, vol:vol, 2.5 mL), olefin (0.5 mmol, 1.0 equiv), pH 4.8 aqueous sodium formate buffer (500 μL), and amine (0.75 mmol, 1.5 equiv) and loaded into a Biotage Endeavor Catalyst Screening System. At room temperature, the reaction vessels were purged with N_2 (1x), pressurized to 25 psi with CO, and brought to a total pressure of 50 psi with H_2. The reaction mixture was heated at 80 °C for 20 h with mechanical stirring (400 rpm), after which time the vessel was cooled to 40 °C, purged with N_2 (1x), and removed from the Endeavor reactor. The crude reaction mixture was diluted with aqueous, saturated sodium bicarbonate (10 mL) and extracted into diethyl ether or ethyl acetate (20 mL, 3x). The combined extracts were dried over Na_2SO_4, analyzed by gas chromatography, concentrated *in vacuo*, and purified by flash chromatography.

Hydroaminomethylations with alkylamines

An aliquot of the catalyst stock solution (0.500 mL, 0.50 mol% $Rh(CO)_2(acac)$, 2.5 mol% BISBI, 1.0 mol% Xiao's catalyst) was plated onto a glass liner tube (*see above*). Under air, the tube was sequentially charged with toluene: methanol (9:1, vol:vol, 5.00 mL), olefin (0.5 mmol, 1.0

equiv), pH 4.8 aqueous sodium formate buffer (250 μL), and amine (0.60 mmol, 1.2 equiv) and loaded into a Biotage Endeavor Catalyst Screening System. At room temperature, the reaction vessels were purged with N_2 (1x), pressurized to 25 psi with CO, and brought to a total pressure of 50 psi with H_2 at room temperature. The reaction mixture was heated at 80 °C for 20 h with mechanical stirring (400 rpm), after which time the vessel was cooled to 40 °C, purged with N_2 (1x), and removed from the Endeavor reactor. The crude reaction mixture was diluted with 10% aqueous K_2CO_3 (10 mL) and extracted into diethyl ether or ethyl acetate (20 mL, 3x). The combined extracts were dried over Na_2SO_4, analyzed by gas chromatography, concentrated *in vacuo*, and purified by flash chromatography.

2.4.4 Impact of CO on the DRA of undecanal

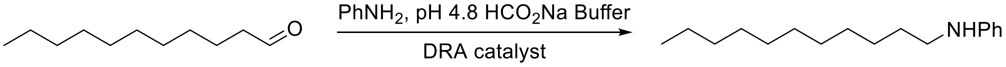
O
$PhNH_2$, pH 4.8 HCO_2Na Buffer
DRA catalyst
NHPh

DRA cat.	1 h, 0 psi CO	1 h, 25 psi CO	20 h, 0 psi CO	20 h, 25 psi CO
C7	93%	94%	93%	90%
C1	32%	8%	40%	11%
C2	46%	9%	43%	11%
C6	12%	12%	23%	17%

Conditions: Undecanal (0.5 mmol), aniline (0.75 mmol), pH 4.8 HCO_2Na buffer (500 μL), 9:1 PhMe:MeOH (vol:vol, 2.5 mL), 80 °C, yields determined by GC with dodecane as an internal standard.

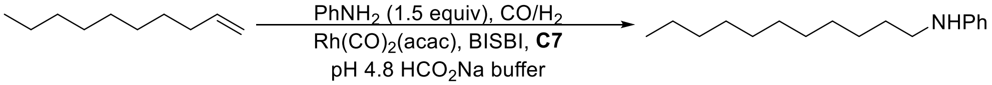
$PhNH_2$ (1.5 equiv), CO/H_2
$Rh(CO)_2(acac)$, BISBI, **C7**
pH 4.8 HCO_2Na buffer
NHPh

P_{CO} (psi)	P_{tot} (psi)	yield (GC)
25	50	94
50	75	99
75	100	98
100	125	94
125	150	75
150	175	59
200	225	48

Conditions: 1-decene (0.5 mmol), aniline (0.75 mmol), pH 4.8 HCO_2Na buffer (500 μL), H_2 (25 psi), CO, $Rh(CO)_2(acac)$ (0.5 mol%), BISBI (2.5 mol%), **C7**, (1 mol%), 9:1 PhMe:MeOH (vol:vol, 2.5 mL), 80 °C, 20 h, yields determined by GC with dodecane as an internal standard.

2.4.5 Control experiments

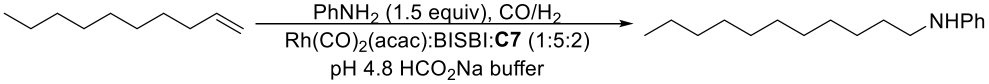
PhNH$_2$ (1.5 equiv), CO/H$_2$
Rh(CO)$_2$(acac):BISBI:**C7** (1:5:2)
pH 4.8 HCO$_2$Na buffer
NHPh

Entry	Rh(CO)$_2$(acac)	DRA Cat	Yield (GC)	*n*:*iso*
1	0.5 mol%	**C7**	91	98:2
2	0 mol%	**C7**	8	68:32
3	0 mol%	**C6**	0	N/A
4[a]	0.5 mol%	**C7**	0	N/A

Conditions: 1-decene (0.5 mmol), aniline (0.75 mmol), pH 4.8 HCO$_2$Na buffer (500 μL), H$_2$ (25 psi), CO (25 psi), Rh(CO)$_2$(acac) (0.5 mol%), BISBI (2.5 mol%), DRA Cat (1 mol%), 9:1 PhMe:MeOH (vol:vol, 2.5 mL), 80 °C, 20 h, yields determined by GC with dodecane as an internal standard.

[a] Without synthesis gas.

2.4.6 Catalytic hydroaminomethylations

2.4.6.1 Reactions of olefins with aniline (Table 1)

***N*-Undecylaniline (3aa)**

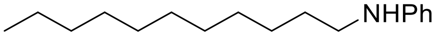

The hydroaminomethylation of 1-decene (95.0 μL, 0.502 mmol) with aniline (68.4 μL, 0.751 mmol, 1.50 equiv) was conducted according to the general procedure for hydroaminomethylations with arylamines. The product was isolated by silica chromatography (12 g silica, 0% → 5% EtOAc/hexanes gradient). Amine **3aa** was obtained (96.2 mg, 78% yield) as a pale-yellow oil. ^{1}H NMR (600 MHz, $CDCl_3$) δ 7.23 (t, J = 7.9 Hz, 2H), 6.75 (t, J = 7.3 Hz, 1H), 6.65 (d, J = 7.8 Hz, 2H), 3.96 – 3.32 (br s, 1H), 3.15 (t, J = 7.2, 2H), 1.67 (quin, J = 7.3 Hz, 2H), 1.49 – 1.27 (m, 16H), 0.96 (t, J = 7.0 Hz, 3H); ^{13}C NMR (151 MHz, $CDCl_3$) δ 148.6, 129.2, 117.1, 112.7, 44.0, 32.0, 29.7, 29.7, 29.6, 29.5, 29.4, 29.4, 27.2, 22.7, 14.2; ATR-IR: 3393, 3050, 2999, 2932, 2855, 2833, 1601, 1509, 1462, 1417, 1372, 1321, 1258, 1234, 1179, 1153, 1139, 1072, 1026, 992, 953, 937, 911, 864, 853, 805, 747, 692, 633, 596, 558, 508, 461, 403 cm^{-1}; HRMS (ESI/QTOF) m/z: $[M + H]^+$ Calcd for $C_{17}H_{30}N^+$ 248.2373; Found 248.2368. NMR spectra matched the literature.[17]

N-(4-(3,4-Dimethoxyphenyl)butyl)aniline (3ba)

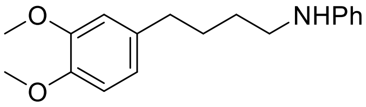

The hydroaminomethylation of methyl eugenol (91.0 μL, 0.500 mmol) with aniline (68.4 μL, 0.751 mmol, 1.50 equiv) was conducted according to the general procedure for hydroaminomethylations with arylamines. The product was isolated by silica chromatography (12 g silica, 0% → 10% EtOAc/hexanes gradient). Amine **3ba** was obtained (120.2 mg, 80% yield) as a dark-yellow oil. ^{1}H NMR (600 MHz, $CDCl_3$) δ 7.21 (t, *J* = 7.9 Hz, 2H), 6.83 (d, J = 8.0 Hz, 1H), 6.79 – 6.71 (m, 3 H), 6.63 (d, J = 8.0 Hz, 2H), 3.90 (s, 3H), 3.89 (s, 3H), 3.80 – 3.30 (br s, 1H), 3.16 (t, J = 6.9 Hz, 2H), 2.65 (t, J = 7.5 Hz, 2H), 1.81–1.64 (m, 4H); ^{13}C NMR (151 MHz, $CDCl_3$) δ 148.9, 148.5, 147.2, 134.9, 129.2, 120.2, 117.1, 112.7, 111.8, 111.3, 55.9, 55.8, 43.8, 35.3, 29.2, 29.1; ATR-IR: 3393, 3050, 2999, 2932, 2855, 2833, 1601, 1509, 1462, 1417, 1372, 1321, 1258, 1234, 1179, 1153, 1139, 1072, 1026, 992, 953, 937, 911, 864, 853, 805, 747, 692, 633, 596, 558, 508, 461, 403 cm^{-1}; HRMS (ESI/QTOF) m/z: $[M + H]^+$ Calcd for $C_{18}H_{24}NO_2^+$ 286.1802; Found 286.1813.

2-Methoxy-4-(4-(phenylamino)butyl)phenol (3ca)

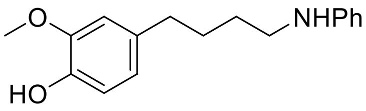

The hydroaminomethylation of eugenol (77.0 μL, 0.500 mmol) with aniline (68.4 μL, 0.751 mmol, 1.50 equiv) was conducted according to the general procedure for hydroaminomethylations with arylamines. The product was isolated by silica chromatography (40 g silica, 0% → 15% EtOAc/hexanes gradient). Amine **3ca** was obtained (108.9 mg, 81% yield) as a white solid. ^{1}H NMR (600 MHz, $CDCl_3$) δ 7.22 (t, J = 7.9 Hz, 2H), 6.91 – 6.86 (m, 1H), 6.76 – 6.70 (m, 3H), 6.67 – 6.61 (d, J = 8.0 Hz, 2H), 5.18 – 3.67 (m, 2H), 3.90 (s, 3H), 3.17 (t, J = 6.9 Hz, 2H), 2.64 (t, J = 7.5 Hz, 2H), 1.79 – 1.65 (m, 4H); ^{13}C NMR (151 MHz, $CDCl_3$) δ 148.4, 146.4, 143.7, 134.2, 129.2, 120.9, 117.2, 114.2, 112.8, 110.0, 55.9, 43.9, 35.4, 29.2, 29.1; ATR-IR: 3280, 2997, 2924, 2832, 1600, 1521, 1506, 1474, 1447, 1383, 1308, 1280, 1247, 1214, 1155, 1124, 1102, 1088, 1035, 998, 923, 884, 870, 849, 801, 747, 712, 691, 636, 592, 551, 517, 503, 478, 457, 414 cm^{-1}; HRMS (ESI/QTOF) m/z: $[M + H]^+$ Calcd for $C_{17}H_{22}NO_2^+$ 272.1645; Found 272.1633.

Dimethyl 2-(4-(phenylamino)butyl)malonate (3da)

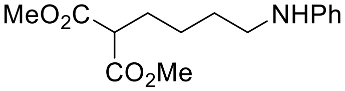

The hydroaminomethylation of dimethyl allylmalonate (80.0 μL, 0.498 mmol) with aniline (68.4 μL, 0.751 mmol, 1.51 equiv) was conducted according to the general procedure for hydroaminomethylations with arylamines. The product was isolated by silica chromatography (12 g silica, 0% → 30% EtOAc/hexanes gradient). Amine **3da** was obtained (122.6 mg, 88% yield) as a dark-yellow oil. ^{1}H NMR (600 MHz, $CDCl_3$) δ 7.17 (t, *J* = 7.9 Hz, 2H), 6.69 (t, *J* = 7.3 Hz, 1H), 6.59 (d, *J* = 7.9 Hz, 2H), 3.93 – 3.45 (br s, 1H), 3.74 (s, 6H), 3.39 (t, *J* = 7.5 Hz, 1H), 3.12 (t, *J* = 7.1 Hz, 2H), 1.96 (q, *J* = 7.6 Hz, 2H), 1.65 (quin, *J* = 7.3 Hz, 2H), 1.56 – 1.34 (m, 2H);^{13}C NMR (151 MHz, $CDCl_3$) δ 169.8, 148.3, 129.2, 117.1, 112.7, 52.5, 51.5, 43.5, 29.0, 28.5, 24.9; ATR-IR: 3405, 2952, 2862, 1729, 1602, 1507, 1434, 1256, 1198, 1152, 1120, 1012, 911, 869, 749, 732, 693, 509 cm^{-1}; HRMS (ESI/QTOF) m/z: $[M + H]^+$ Calcd for $C_{15}H_{22}NO_4^+$ 280.1543; Found 280.1540.

7-(Phenylamino)heptanenitrile (3ea)

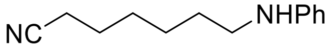

The hydroaminomethylation of 5-hexene nitrile (57.0 μL, 0.501 mmol) with aniline (68.4 μL, 0.751 mmol, 1.50 equiv) was conducted according to the general procedure for hydroaminomethylations with arylamines. The product was isolated by silica chromatography (12 g silica, slow 0% → 15% EtOAc/hexanes gradient). Amine **3ea** was obtained (83.7 mg, 82% yield) as a pale-yellow oil. ^{1}H NMR (600 MHz, $CDCl_3$) δ 7.22–7.16 (t, J = 7.9 Hz, 2H), 6.71 (t, J = 7.3 Hz, 1H), 6.64 – 6.59 (d, J = 8.0 Hz, 2H), 3.93 – 3.28 (br s, 1H), 3.13 (t, J = 7.1 Hz, 2H), 2.34 (t, J = 7.1 Hz, 2H), 1.71 – 1.60 (m, 4H), 1.55 – 1.41 (m, 4H); ^{13}C NMR (151 MHz, $CDCl_3$) δ 148.4, 129.2, 119.7, 117.2, 112.7, 43.7, 29.2, 28.5, 26.4, 25.3, 17.1; ATR-IR: 3396, 2930, 2857, 2245, 1601, 1506, 1476, 1428, 1319, 1261, 1179, 1120, 991, 869, 748, 693, 509 cm^{-1}; HRMS (ESI/QTOF) m/z: $[M + H]^+$ Calcd for $C_{13}H_{19}N_2^+$ 203.1543; Found 203.1542.

7-(Phenylamino)heptan-2-one (3fa)

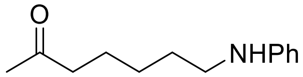

The hydroaminomethylation of 5-hexen-2-one (58.0 μL, 0.501 mmol) with aniline (68.4 μL, 0.751 mmol, 1.50 equiv) was conducted according to the general procedure for hydroaminomethylations with arylamines. The product was isolated by silica chromatography (12 g silica, slow 0% → 20% EtOAc/hexanes gradient). Amine **3fa** was obtained (75.8 mg, 74% yield) as a pale-yellow oil. ^{1}H NMR (600 MHz, $CDCl_3$) δ 7.17 (t, *J* = 7.7 Hz, 2H), 6.69 (t, *J* = 7.3 Hz, 1H), 6.60 (d, *J* = 8.0 Hz, 2H), 3.92 – 3.18 (br s, 1H), 3.11 (t, *J* = 7.1 Hz, 2H), 2.45 (t, *J* = 7.3 Hz, 2H), 2.14 (s, 3H), 1.63 (quin, *J* = 7.4 Hz, 4H), 1.44 – 1.36 (m, 2H); ^{13}C NMR (151 MHz, $CDCl_3$) δ 208.9, 148.4, 129.2, 117.1, 112.7, 43.7, 43.5, 29.9, 29.3, 26.6, 23.5; ATR-IR: 3395, 3051, 3021, 2931, 2858, 1709, 1602, 1506, 1477, 1431, 1358, 1319, 1258, 1224, 1178, 1161, 1119, 1076, 1028, 991, 910, 868, 747, 732, 692, 647, 595, 510 cm^{-1}; HRMS (ESI/QTOF) m/z: $[M + H]^+$ Calcd for $C_{13}H_{20}NO^+$ 206.1539; Found 206.154.

5-(Phenylamino)pentan-2-yl acetate (3ga)

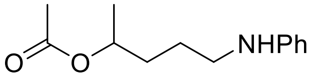

The hydroaminomethylation of but-3-en-2-yl acetate (63.0 μL, 0.498 mmol) with aniline (68.4 μL, 0.751 mmol, 1.51 equiv) was conducted according to the general procedure for hydroaminomethylations with arylamines. The product was isolated by silica chromatography (12 g silica, 0% → 15% EtOAc/hexanes gradient). Amine **3ga** was obtained (73.9 mg, 67% yield) as a pale-yellow oil. ^{1}H NMR (600 MHz, $CDCl_3$) δ 7.19 (t, *J* = 7.9 Hz, 2H), 6.74 – 6.68 (t, J = 7.2 Hz, 1H), 6.61 (d, *J* = 8.0 Hz, 2H), 4.96 (td, *J* = 6.6, 5.2 Hz, 1H), 3.93 – 3.25 (br s, 1H), 3.13 (t, *J* = 6.6 Hz, 2H), 2.05 (s, 3H), 1.76 – 1.58 (m, 4H), 1.25 (d, *J* = 6.3 Hz, 3H); ^{13}C NMR (151 MHz, $CDCl_3$) δ ^{13}C NMR (151 MHz, CDCl3) δ 170.8, 148.3, 129.2, 117.2, 112.7, 70.6, 43.7, 33.4, 25.4, 21.3, 20.0.; ATR-IR: 3397, 2936, 1724, 1602, 1506, 1372, 1320, 1240, 1179, 1152, 1124, 1080, 1019, 952, 911, 868, 747, 692, 610, 508 cm^{-1}; HRMS (ESI/QTOF) m/z: [M + H]$^+$ Calcd for $C_{13}H_{20}NO_2^+$ 222.1489; Found 222.1493.

6-(Phenylamino)hexan-3-ol (3ha)

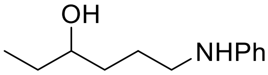

The hydroaminomethylation of 1-penten-3-ol (51.0 μL, 0.496 mmol) with aniline (68.4 μL, 0.751 mmol, 1.51 equiv) was conducted according to the general procedure for hydroaminomethylations with arylamines. The product was isolated by silica chromatography (12 g silica, 15% → 40% EtOAc/hexanes gradient). Amine **3ha** was obtained (82.5 mg, 86% yield) as a pale-yellow oil. ^{1}H NMR (600 MHz, $CDCl_3$) δ 7.18 (t, J = 7.9 Hz, 2H), 6.70 (t, J = 7.2 Hz, 1H), 6.62 (d, J = 7.9 Hz, 2H), 3.57 (tt, J = 8.2, 4.4 Hz, 1H), 3.15 (t, J = 6.7 Hz, 2H), 2.24 (d, J = 486.8 Hz, 2H), 1.83 – 1.31 (m, 6H), 0.96 (t, J = 7.4 Hz, 3H); ^{13}C NMR (151 MHz, $CDCl_3$) δ 148.4, 129.2, 117.3, 112.9, 73.0, 44.1, 34.4, 30.3, 25.8, 9.9; ATR-IR: 3359, 3052, 3021, 2960, 2932, 2873, 1602, 1504, 1477, 1462, 1430, 1375, 1320, 1256, 1179, 1154, 1085, 1028, 991, 966, 909, 867, 840, 747, 731, 691, 646, 569, 507 cm^{-1}; HRMS (ESI/QTOF) m/z: $[M + H]^+$ Calcd for $C_{12}H_{20}NO^+$ 194.1539; Found 194.1532.

Methyl 3,3-dimethyl-6-(phenylamino)hexanoate (3ia)

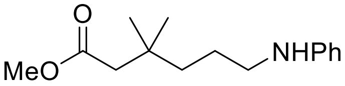

The hydroaminomethylation of methyl 3,3-dimethyl-4-pentenoate (79.0 μL, 0.494 mmol) with aniline (68.4 μL, 0.751 mmol, 1.52 equiv) was conducted according to the general procedure for hydroaminomethylations with arylamines. The product was isolated by silica chromatography (12 g silica, 0% → 10% EtOAc/hexanes gradient). Amine **3ia** was obtained (101.9 mg, 82% yield) as a pale-yellow oil. ^{1}H NMR (600 MHz, $CDCl_3$) δ 7.19 (t, *J* = 7.9 Hz, 2H), 6.70 (t, J = 7.3 Hz, 1H), 6.62 (d, J = 8.0 Hz, 2H), 3.94 – 3.42 (br s, 1H), 3.66 (s, 3H), 3.10 (t, J = 7.0 Hz, 2H), 2.25 (s, 2H), 1.67 – 1.58 (m, 2H), 1.46 – 1.39 (m, 2H), 1.03 (s, 6H); ^{13}C NMR (151 MHz, $CDCl_3$) δ 172.7, 148.4, 129.2, 117.0, 112.6, 51.2, 45.6, 44.5, 39.2, 33.1, 27.4, 24.3; ATR-IR: 3401, 2952, 1729, 1602, 1506, 1471, 1433, 1368, 1321, 1232, 1179, 1128, 1066, 1015, 992, 911, 867, 747, 692, 619, 508 cm^{-1}; HRMS (ESI/QTOF) m/z: $[M + H]^+$ Calcd for $C_{15}H_{24}NO_2^+$ 250.1802; Found 250.1806.

N-(3-Cyclohexylpropyl)aniline (3ja)

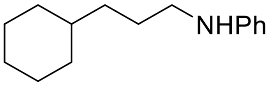

The hydroaminomethylation of 4-vinylcyclohexene (68.0 μL, 0.497 mmol) with aniline (68.4 μL, 0.751 mmol, 1.51 equiv) was conducted according to the general procedure for hydroaminomethylations with arylamines. The product was isolated by silica chromatography (12 g silica, 0% → 10% EtOAc/hexanes slow gradient). Amine **3ja** was obtained (82.7 mg, 77% yield) as a pale-yellow oil; ^{1}H NMR (600 MHz, $CDCl_3$) δ 7.22 (t, *J* = 7.9 Hz, 2H), 6.74 (t, *J* = 7.3 Hz, 1H), 6.65 (d, *J* = 8.0 Hz, 2H), 3.83 – 3.45 (br s, 1H), 3.13 (t, *J* = 7.2 Hz, 2H), 1.85 – 1.58 (m, 7H), 1.37 – 1.15 (m, 6H), 1.02 – 0.90 (m, 2H); ^{13}C NMR (151 MHz, $CDCl_3$) δ 148.6, 129.2, 117.1, 112.7, 44.4, 37.5, 34.9, 33.4, 26.9, 26.7, 26.4; ATR-IR: 3412, 3051, 2919, 2848, 1601, 1504, 1476, 1447, 1319, 1259, 1178, 1152, 1115, 991, 865, 745, 690, 507 cm^{-1}; HRMS (ESI/QTOF) m/z: $[M + H]^+$ Calcd for $C_{15}H_{24}N^+$ 218.1903; Found 218.1900.

N-(3-(Cyclohex-3-en-1-yl)propyl)aniline (3ka)

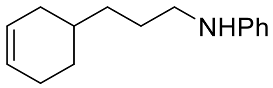

The hydroaminomethylation of 4-vinylcyclohexene (65.0 μL, 0.499 mmol) with aniline (68.4 μL, 0.751 mmol, 1.51 equiv) was conducted according to the general procedure for hydroaminomethylations with arylamines. The product was isolated by silica chromatography (12 g silica, 0% → 10% EtOAc/hexanes slow gradient). Amine **3ka** was obtained (86.0 mg, 80% yield) as a pale-yellow oil; ^{1}H NMR (600 MHz, $CDCl_3$) δ 7.24 (t, *J* = 7.9 Hz, 2H), 6.75 (t, *J* = 7.3 Hz, 1H), 6.66 (d, *J* = 8.0 Hz, 2H), 5.78 – 5.69 (m, 2H), 3.91 – 3.27 (br s, 1H), 3.16 (t, *J* = 7.2 Hz, 2H), 2.25 – 2.05 (m, 3H), 1.89 – 1.57 (m, 5H), 1.51 – 1.25 (m, 3H); ^{13}C NMR (151 MHz, $CDCl_3$) δ 148.5, 129.2, 127.1, 126.5, 117.1, 112.7, 44.3, 34.1, 33.4, 31.9, 29.0, 27.0, 25.3; ATR-IR: 3410, 3019, 2910, 1601, 1504, 1476, 1453, 1431, 1318, 1260, 1178, 1153, 1120, 1029, 992, 912, 867, 745, 690, 652, 506 cm^{-1}; HRMS (ESI/QTOF) m/z: $[M + H]^+$ Calcd for $C_{15}H_{22}N^+$ 216.1747; Found 216.1750.

*N*¹, *N*¹²-Diphenyldodecane-1,12-diamine (3la)

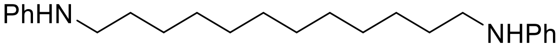

The hydroaminomethylation of 1,9-decadiene (46.0 μL, 0.249 mmol) with aniline (68.4 μL, 0.751 mmol, 1.51 equiv) was conducted according to the general procedure for hydroaminomethylations with arylamines. The product was isolated by silica chromatography (12 g silica, 0% → 10% EtOAc/hexanes slow gradient). Amine **3la** was obtained (62.4 mg, 71% yield) as a white solid. ^{1}H NMR (600 MHz, $CDCl_3$) δ 7.20 (t, *J* = 7.7 Hz, 4H), 6.72 (t, *J* = 7.3 Hz, 2H), 6.63 (d, *J* = 8.0 Hz, 4H), 3.61 (s, 2H), 3.12 (t, *J* = 7.1 Hz, 4H), 1.64 (quin, *J* = 7.3 Hz, 4H), 1.52 – 1.21 (m, 16H); ^{13}C NMR (151 MHz, $CDCl_3$) δ 148.5, 129.2, 117.0, 112.7, 44.0, 29.6, 29.5, 27.2 (Note: only four ^{13}C resonances in the aliphatic region were observed, likely due to overlap between peaks with similar chemical shifts); ATR-IR: 3412, 3399, 3050, 2918, 2847, 1912, 1675, 1599, 1504, 1479, 1464, 1428, 1378, 1337, 1317, 1266, 1241, 1195, 1178, 1151, 1119, 1072, 1049, 1027, 991, 909, 867, 839, 746, 725, 690, 618, 549, 508 cm^{-1}; HRMS (ESI/QTOF) m/z: $[M + H]^+$ Calcd for $C_{24}H_{37}N_2^+$ 353.2951; Found 353.2943.

2.4.6.2 Reactions of methyl eugenol with arylamines (Table 2)

4-Bromo-*N*-(4-(3,4-dimethoxyphenyl)butyl)aniline (3bb)

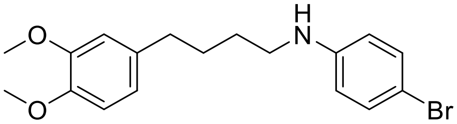

The hydroaminomethylation of methyl eugenol (86.0 μL, 0.500 mmol) with *p*-bromoaniline (130.6 mg, 0.759 mmol, 1.52 equiv) was conducted according to the general procedure for hydroaminomethylations with arylamines. The product was isolated by silica chromatography (12 g silica, 0% → 20% EtOAc/hexanes slow gradient). Amine **3bb** was obtained (126.9 mg, 81% yield) as a yellow solid. ^{1}H NMR (600 MHz, $CDCl_3$) δ 7.23 (d, *J* = 8.4 Hz, 2H), 6.80 (d, *J* = 7.9 Hz, 1H), 6.73 (m, 2H), 6.45 (d, *J* = 8.4 Hz, 2H), 3.87 (s, 3H), 3.86 (s, 3H), 3.81 – 3.51 (br s, 1H), 3.08 (t, *J* = 7.0 Hz, 2H), 2.61 (t, *J* = 7.6 Hz, 2H), 1.71 (quin, *J* = 7.3 Hz, 2H), 1.64 (quin, *J* = 7.0 Hz, 2H); ^{13}C NMR (151 MHz, $CDCl_3$) δ 148.8, 147.3, 147.2, 134.7, 131.8, 120.2, 114.2, 111.7, 111.3, 108.5, 55.9, 55.8, 43.8, 35.2, 29.0, 28.9; ATR-IR: 3390, 2999, 2932, 2855, 2834, 1593, 1512, 1498, 1463, 1417, 1399, 1372, 1319, 1293, 1258, 1234, 1177, 1154, 1139, 1072, 1027, 909, 852, 811, 763, 729, 696, 645, 633, 595, 560, 501, 460 cm^{-1}; HRMS (ESI/QTOF) m/z: $[M + H]^+$ Calcd for $C_{18}H_{23}BrNO_2^+$ 364.0914; Found 364.0912.

4-Iodo-*N*-(4-(3,4-dimethoxyphenyl)butyl)aniline (3bc)

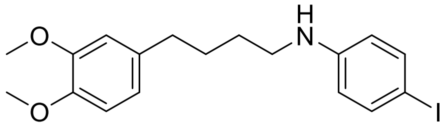

The hydroaminomethylation of methyl eugenol (86.0 µL, 0.500 mmol) with *p*-iodoaniline 164.3 mg, 0.750 mmol, 1.50 equiv) was conducted according to the general procedure for hydroaminomethylations with arylamines. The product was isolated by silica chromatography (12 g silica, 5% → 20% EtOAc/hexanes slow gradient). Amine **3bc** was obtained (164.9 mg, 80% yield) as a white solid. ^{1}H NMR (600 MHz, $CDCl_3$) δ 7.40 (d, *J* = 8.4 Hz, 2H), 6.80 (d, *J* = 7.9 Hz, 1H), 6.76 – 6.63 (m, 2H), 6.36 (d, *J* = 8.7 Hz, 2H), 3.87 (s, 3H), 3.86 (s, 3H), 3.73 – 3.38 (br s, 1H), 3.09 (t, *J* = 6.9 Hz, 2H), 2.61 (t, *J* = 7.5 Hz, 2H), 1.71 (p, *J* = 7.3 Hz, 2H), 1.63 (p, *J* = 13.6, 6.9 Hz, 2H); ^{13}C NMR (151 MHz, $CDCl_3$) δ 148.8, 147.9, 147.2, 137.7, 134.7, 120.2, 114.9, 111.7, 111.3, 77.4, 55.9, 55.8, 43.6, 35.2, 29.0, 28.9; ATR-IR: 3368, 2996, 2915, 2854, 2825, 1591, 1511, 1464, 1448, 1416, 1398, 1368, 1341, 1324, 1296, 1260, 1238, 1178, 1155, 1140, 1121, 1029, 975, 898, 855, 845, 810, 763, 694, 634, 600, 543, 505, 467, 441, 409 cm^{-1}; HRMS (ESI/QTOF) m/z: $[M + H]^+$ Calcd for $C_{18}H_{23}INO_2^+$ 412.0768; Found 412.0761.

N-(4-(3,4-Dimethoxyphenyl)butyl)-4-methoxyaniline (3bd)

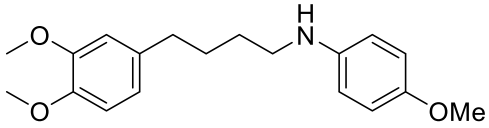

The hydroaminomethylation of methyl eugenol (86.0 μL, 0.500 mmol) with *p*-methoxyaniline (95.8 mg, 0.778 mmol, 1.56 equiv) was conducted according to the general procedure for hydroaminomethylations with arylamines. The product was isolated by silica chromatography (12 g silica, 0% → 20% EtOAc/hexanes slow gradient). Amine **3bd** was obtained (145.2 mg, 80% yield) as a yellow solid. ^{1}H NMR (600 MHz, $CDCl_3$) δ 6.83 – 6.77 (m, 3H), 6.76 – 6.71 (m, 2H), 6.58 (d, *J* = 8.9 Hz, 2H), 3.88 (s, 3H), 3.86 (s, 3H), 3.75 (s, 3H), 3.48 – 3.22 (m, 1H), 3.10 (t, *J* = 7.0 Hz, 2H), 2.62 (t, *J* = 7.6 Hz, 2H), 1.73 (quin, *J* = 7.0 Hz, 2H), 1.65 (quin, *J* = 7.0 Hz, 2H); ^{13}C NMR (151 MHz, $CDCl_3$) δ 152.0, 148.8, 147.1, 142.7, 134.9, 120.2, 114.9, 114.1, 111.7, 111.2, 77.4, 77.2, 77.0, 55.9, 55.8, 55.8, 44.9, 35.3, 29.2, 29.1; ATR-IR: 3387, 2997, 2932, 2855, 2832, 1607, 1590, 1510, 1463, 1441, 1417, 1326, 1232, 1179, 1154, 1139, 1094, 1027, 910, 852, 818, 763, 730, 645, 632, 595, 519, 461 cm^{-1}; HRMS (ESI/QTOF) m/z: $[M + H]^+$ Calcd for $C_{19}H_{26}NO_3^+$ 316.1907; Found 316.1901.

(4-((4-(3,4-Dimethoxyphenyl)butyl)amino)phenyl)(phenyl)methanone (3be)

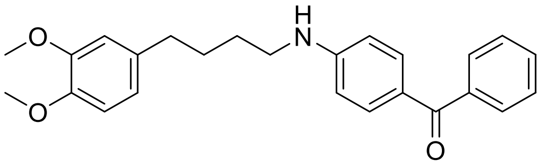

The hydroaminomethylation of methyl eugenol (86.0 μL, 0.500 mmol) with 4-aminobenzophenone (148.3 mg, 0.752 mmol) conducted according to the general procedure for hydroaminomethylations with arylamines. The product was isolated by silica chromatography (12 g silica, 10% → 30% EtOAc/hexanes slow gradient). Amine **3be** was obtained (116.2 mg, 60% yield) as a yellow solid. ^{1}H NMR (600 MHz, $CDCl_3$) δ 7.89 – 7.58 (m, 4H), 7.51 (t, *J* = 7.4 Hz, 1H), 7.43 (t, *J* = 7.5 Hz, 2H), 6.79 (d, *J* = 7.8 Hz, 1H), 6.75 – 6.65 (m, 2H), 6.55 (d, *J* = 8.4 Hz, 2H), 4.75 – 4.13 (br s, 1H), 3.85 (s, 3H), 3.84 (s, 3H), 3.36 – 3.02 (m, 2H), 2.60 (t, *J* = 7.3 Hz, 2H), 2.13 – 1.46 (m, 4H); ^{13}C NMR (151 MHz, $CDCl_3$) δ 195.1, 152.2, 148.8, 147.2, 139.2, 134.6, 133.0, 131.1, 129.4, 128.0, 125.7, 120.2, 111.7, 111.2, 111.2, 55.9, 55.8, 43.1, 35.1, 28.9, 28.8; ATR-IR: 3353, 2927, 1627, 1583, 1562, 1514, 1479, 1461, 1448, 1438, 1418, 1348, 1315, 1284, 1260, 1240, 1227, 1186, 1176, 1142, 1100, 1073, 1044, 1031, 1000, 940, 921, 861, 854, 836, 808, 788, 764, 747, 710, 702, 690, 628, 618, 597, 578, 565, 505, 423, 406 cm^{-1}; HRMS (ESI/QTOF) m/z: $[M + H]^+$ Calcd for $C_{25}H_{28}NO_3^+$ 390.2064; Found 390.2056.

N-(4-(3,4-Dimethoxyphenyl)butyl)-2-methylaniline (3bf)

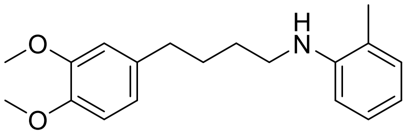

The hydroaminomethylation of methyl eugenol (86.0 μL, 0.500 mmol) with *o*-toluidine (79.7 μL, 0.750 mmol, 1.50 equiv) was conducted according to the general procedure for hydroaminomethylations with arylamines. The product was isolated by silica chromatography (12 g silica, 0% → 10% EtOAc/hexanes slow gradient). Amine **3bf** was obtained (113.3 mg, 76% yield) as a white solid. ^{1}H NMR (600 MHz, $CDCl_3$) δ 7.18 (t, *J* = 7.7 Hz, 1H), 7.09 (d, *J* = 7.3 Hz, 1H), 6.84 (d, *J* = 8.0 Hz, 1H), 6.81 – 6.75 (m, 2H), 6.70 (t, *J* = 7.4 Hz, 1H), 6.66 (d, *J* = 8.0 Hz, 1H), 3.92 (s, 3H), 3.90 (s, 3H), 3.60 – 3.39 (br s, 1H), 3.23 (t, *J* = 6.8 Hz, 2H), 2.68 (t, *J* = 7.3 Hz, 2H), 2.17 (s, 3H), 1.84 – 1.71 (m, 4H); ^{13}C NMR (151 MHz, $CDCl_3$) δ 148.9, 147.2, 146.3, 134.9, 130.0, 127.1, 121.7, 120.2, 116.7, 111.7, 111.3, 111.2, 109.6, 55.9, 55.8, 43.8, 35.3, 29.2, 17.5; IR (KBr, thin film): 3409, 3055, 3017, 3004, 2957, 2930, 2887, 2849, 2597, 1605, 1585, 1511, 1482, 1468, 1440, 1416, 1377, 1352, 1338, 1317, 1298, 1284, 1256, 1235, 1225, 1191, 1180, 1153, 1135, 1082, 1068, 1052, 1035, 1021, 987, 963, 944, 922, 909, 850, 810, 763, 749, 741, 718, 637, 615, 559, 536, 492, 441 cm^{-1}; HRMS (ESI/QTOF) m/z: $[M + H]^+$ Calcd for $C_{19}H_{26}NO_2^+$ 300.1958; Found 300.1950.

N-(4-(3,4-Dimethoxyphenyl)butyl)pyridin-2-amine (3bg)

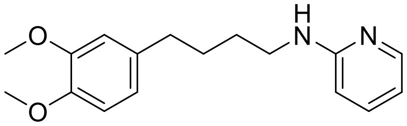

The hydroaminomethylation of methyl eugenol (86.0 µL, 0.500 mmol) with 2-aminopyridine (71.0 mg, 0.754 mmol, 1.51 equiv) was conducted according to the general procedure for hydroaminomethylations with arylamines. The product was isolated by silica chromatography (12 g silica, 20% → 50% EtOAc/hexanes slow gradient). Amine **3bg** was obtained (102.5 mg, 70% yield) as a white solid. ^{1}H NMR (600 MHz, $CDCl_3$) δ 8.05 (dd, *J* = 5.1, 1.8 Hz, 1H), 7.37 (ddd, *J* = 8.8, 7.0, 2.0 Hz, 1H), 6.76 (d, *J* = 7.9 Hz, 1H), 6.72 – 6.64 (m, 2H), 6.51 (dd, *J* = 7.1, 5.0 Hz, 1H), 6.32 (d, *J* = 8.4 Hz, 1H), 4.78 – 4.47 (br s, 1H), 3.84 (s, 3H), 3.82 (s, 3H), 3.26 (q, *J* = 6.5 Hz, 2H), 2.58 (t, *J* = 7.5 Hz, 2H), 1.75 – 1.57 (m, 4H); ^{13}C NMR (151 MHz, $CDCl_3$) δ 158.8, 148.8, 148.1, 147.1, 137.3, 134.8, 120.1, 112.5, 111.7, 111.2, 106.4, 55.9, 55.8, 42.0, 35.2, 29.1, 29.0; ATR-IR: 3257, 2999, 2932, 2859, 2834, 1601, 1572, 1514, 1465, 1449, 1438, 1416, 1387, 1333, 1304, 1292, 1262, 1233, 1190, 1154, 1137, 1080, 1026, 981, 943, 914, 848, 811, 765, 733, 632, 596, 560, 517, 464, 412 cm^{-1}; HRMS (ESI/QTOF) m/z: [M + H]+ Calcd for C17H23N2O2+ 287.1754; Found 287.1752.

N-(4-(3,4-Dimethoxyphenyl)butyl)pyridin-3-amine (3bh)

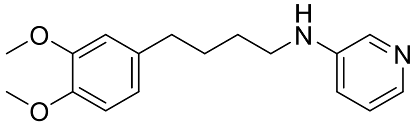

The hydroaminomethylation of methyl eugenol (86.0 μL, 0.500 mmol) with 3-aminopyridine (70.1 mg, 0.745 mmol, 1.49 equiv) was conducted according to the general procedure for hydroaminomethylations with arylamines. The product was isolated by silica chromatography (12 g silica, 25% → 70% EtOAc/hexanes slow gradient). Amine **3bh** was obtained (110.6 mg, 77% yield) as a yellow solid. ^{1}H NMR (600 MHz, $CDCl_3$) δ 7.96 (d, *J* = 2.9 Hz, 1H), 7.88 (d, *J* = 4.6 Hz, 1H), 7.01 (dd, *J* = 8.4, 4.7 Hz, 1H), 6.78 (d, *J* = 8.3 Hz, 1H), 6.75 (d, *J* = 7.9 Hz, 1H), 6.72 – 6.64 (m, 2H), 4.03 – 3.84 (br s, 1H), 3.81 (s, 3H), 3.80 (s, 3H), 3.07 (t, *J* = 6.9 Hz, 2H), 2.56 (t, *J* = 7.5 Hz, 2H), 1.67 (quin, *J* = 7.4 Hz, 2H), 1.61 (quin, *J* = 7.1 Hz, 2H); ^{13}C NMR (151 MHz, $CDCl_3$) δ 148.7, 147.1, 144.4, 138.2, 135.8, 134.7, 123.7, 120.1, 118.2, 111.6, 111.2, 55.9, 55.8, 43.3, 35.1, 29.0, 28.8; ATR-IR: 3259, 3002, 2934, 2857, 2253, 1588, 1513, 1464, 1417, 1259, 1234, 1190, 1154, 1139, 1027, 909, 853, 794, 764, 726, 708, 644, 595, 559, 460, 414 cm^{-1}; HRMS (ESI/QTOF) m/z: $[M + H]^+$ Calcd for $C_{17}H_{23}N_2O_2^+$ 287.1754; Found 287.1755.

N-(4-(3,4-Dimethoxyphenyl)butyl)-1H-indol-4-amine (3bi)

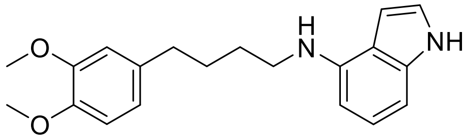

The hydroaminomethylation of methyl eugenol (86.0 µL, 0.500 mmol) with 4-aminoindole (99.4 mg, 0.752 mmol, 1.50 equiv) was conducted according to the general procedure for hydroaminomethylations with arylamines. The product was isolated by silica chromatography (12 g silica, 15% → 30% EtOAc/hexanes slow gradient). Amine **3bi** was obtained (117.6 mg, 73% yield) as a blue-gray solid. ^{1}H NMR (600 MHz, $CDCl_3$) δ 8.20 (s, 1H), 7.11 (t, *J* = 7.9 Hz, 1H), 7.07 – 7.01 (m, 1H), 6.89 – 6.72 (m, 4H), 6.50 – 6.41 (m, 1H), 6.33 (d, *J* = 7.6 Hz, 1H), 4.11 – 3.69 (m, 7H), 3.34 (t, *J* = 6.4 Hz, 2H), 2.67 (t, *J* = 7.1 Hz, 2H), 1.97 – 1.63 (m, 4H); ^{13}C NMR (151 MHz, $CDCl_3$) δ 148.8, 147.1, 141.6, 136.4, 135.0, 123.4, 121.9, 120.2, 116.7, 111.8, 111.3, 101.2, 99.2, 98.4, 55.9, 55.8, 43.9, 35.3, 29.3, 29.2; ATR-IR: 3411, 3350, 3007, 2929, 2855, 1589, 1513, 1474, 1461, 1445, 1412, 1370, 1332, 1301, 1256, 1233, 1189, 1155, 1140, 1105, 1027, 954, 897, 848, 810, 764, 735, 671, 632, 613, 585, 565, 534, 456 cm^{-1}; HRMS (ESI/QTOF) m/z: $[M + H]^+$ Calcd for $C_{20}H_{25}N_2O_2^+$ 325.1911; Found 325.1907.

N-(4-(3,4-Dimethoxyphenyl)butyl)quinolin-2-amine (3bj)

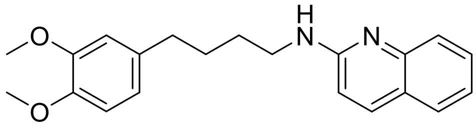

The hydroaminomethylation of methyl eugenol (86.0 µL, 0.500 mmol) with 2-aminoquinoline (180.5 mg, 1.25 mmol, 2.50 equiv) was conducted according to the general procedure for hydroaminomethylations with arylamines. The product was isolated by silica chromatography (12 g silica, 15% → 40% EtOAc/hexanes slow gradient). Amine **3bj** was obtained (125.4 mg, 75% yield) as a yellow oil. ^{1}H NMR (600 MHz, $CDCl_3$) δ 7.78 (d, *J* = 8.9 Hz, 1H), 7.68 (d, *J* = 8.4 Hz, 1H), 7.56 (d, *J* = 8.0 Hz, 1H), 7.52 (t, *J* = 7.7 Hz, 1H), 7.19 (t, *J* = 7.4 Hz, 1H), 6.78 (d, *J* = 8.0 Hz, 1H), 6.75 – 6.66 (m, 2H), 6.60 (d, *J* = 8.9 Hz, 1H), 5.32 – 4.58 (m, 1H), 3.84 (s, 3H), 3.83 (s, 3H), 3.51 (q, *J* = 6.4 Hz, 2H), 2.62 (t, *J* = 7.3 Hz, 2H), 1.84 – 1.57 (m, 4H); ^{13}C NMR (151 MHz, $CDCl_3$) δ 157.0, 148.8, 147.9, 147.1, 137.3, 134.9, 129.5, 127.4, 125.9, 123.3, 121.9, 120.2, 111.7, 111.2, 111.2, 55.9, 55.8, 41.5, 35.2, 29.3, 29.0; ATR-IR: 3389, 3051, 3001, 2933, 2856, 2252, 1679, 1618, 1570, 1513, 1463, 1418, 1400, 1371, 1348, 1312, 1258, 1233, 1191, 1154, 1140, 1027, 908, 854, 817, 780, 756, 727, 646, 621, 596, 561, 524, 475 cm^{-1}; HRMS (ESI/QTOF) m/z: $[M + H]^+$ Calcd for $C_{21}H_{25}N_2O_2^+$ 337.1911; Found 337.1909.

N-(4-(3,4-Dimethoxyphenyl)butyl)quinolin-8-amine (3bk)

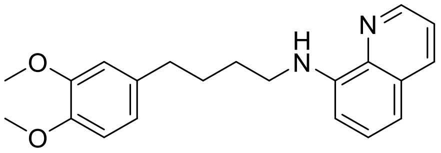

The hydroaminomethylation of methyl eugenol (86.0 µL, 0.500 mmol) with 8-aminoquinoline (180.2 mg, 1.25 mmol, 2.50 equiv) was conducted according to the general procedure for hydroaminomethylations with arylamines. The product was isolated by silica chromatography (12 g silica, 5% → 10% EtOAc/hexanes slow gradient). Amine **3bk** was obtained (107.3 mg, 64% yield) as a yellow solid. ^{1}H NMR (600 MHz, $CDCl_3$) δ 8.71 (d, *J* = 4.2 Hz, 1H), 8.05 (d, *J* = 8.3 Hz, 1H), 7.49 – 7.29 (m, 2H), 7.04 (d, *J* = 8.2 Hz, 1H), 6.94 – 6.70 (m, 3H), 6.6 6 (d, *J* = 7.6 Hz, 1H), 6.57 – 5.77 (br s, 1H), 3.87 (s, 3H), 3.87 (s, 3H), 3.35 (t, *J* = 6.6 Hz, 2H), 2.66 (t, *J* = 7.3 Hz, 2H), 2.14 – 1.48 (m, 4H); ^{13}C NMR (151 MHz, $CDCl_3$) δ 148.8, 147.1, 146.7, 144.9, 138.1, 135.9, 134.9, 128.7, 127.8, 121.3, 120.2, 113.5, 111.7, 111.2, 104.4, 55.9, 55.8, 43.3, 35.3, 29.2, 28.9; ATR-IR: 3399, 3040, 3001, 2933, 2855, 2252, 1609, 1575, 1514, 1463, 1418, 1380, 1337, 1259, 1233, 1191, 1154, 1139, 1124, 1088, 1028, 908, 852, 817, 803, 790, 764, 726, 645, 544, 457, 421 cm^{-1}; HRMS (ESI/QTOF) m/z: $[M + H]^+$ Calcd for $C_{21}H_{25}N_2O_2^+$ 337.1911; Found 337.1908.

N-(4-(3,4-Dimethoxyphenyl)butyl)-2-methoxydibenzo[b,d]furan-3-amine (3bl)

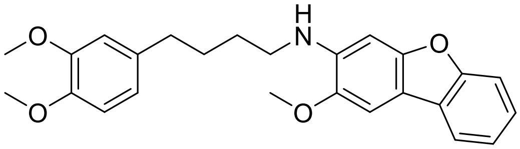

The hydroaminomethylation of methyl eugenol (86.0 μL, 0.500 mmol) with 2-methoxy-3-aminodibenzofuran (162.8 mg, 0.763 mmol, 1.53 equiv) was conducted according to the general procedure for hydroaminomethylations with arylamines. The product was isolated by silica chromatography (24 g silica, 5% → 10% EtOAc/hexanes slow gradient). Amine **3bl** was obtained (153.6, 76% yield) as a yellow-orange solid. ^{1}H NMR (600 MHz, $CDCl_3$) δ 7.86 – 7.67 (m, 1H), 7.56 – 7.40 (m, 1H), 7.33 – 7.24 (m, 3H), 6.81 (d, *J* = 7.8 Hz, 1H), 6.79 – 6.66 (m, 3H), 4.89 – 4.27 (br s, 1H), 3.96 (s, 3H), 3.89 (s, 3H), 3.87 (s, 3H), 3.23 (t, *J* = 6.5 Hz, 2H), 2.65 (t, *J* = 7.0 Hz, 2H), 1.96 – 1.54 (m, 4H); ^{13}C NMR (151 MHz, $CDCl_3$) δ 155.7, 152.6, 148.8, 147.2, 144.0, 139.4, 134.8, 125.7, 124.0, 122.2, 120.2, 118.6, 111.7, 111.3, 111.2, 111.0, 100.4, 92.5, 56.0, 55.9, 55.8, 43.6, 35.2, 29.1, 28.8; ATR-IR: 3429, 3002, 2935, 2835, 2252, 1632, 1607, 1591, 1513, 1485, 1463, 1430, 1360, 1299, 1281, 1259, 1234, 1220, 1198, 1152, 1103, 1028, 906, 865, 840, 811, 725, 647, 629, 561, 440 cm^{-1}; HRMS (ESI/QTOF) m/z: $[M + H]^+$ Calcd for $C_{25}H_{28}NO_4^+$ 406.2013; Found 406.2013.

2.4.6.3 Reactions of methyl eugenol with aliphatic amines (Table 3)

1-(4-(3,4-Dimethoxyphenyl)butyl)piperidine (3bm)

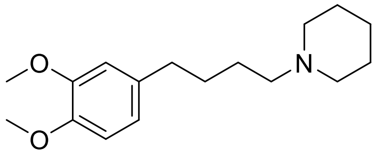

The hydroaminomethylation of methyl eugenol (86.0 μL, 0.500 mmol) with piperidine (59.3 μL, 0.600 mmol, 1.20 equiv) was conducted according to the general procedure for hydroaminomethylations with aliphatic amines. The product was isolated by silica chromatography (12 g silica, isocratic 10% EtOAc/hexanes followed by 0.5% Et_3N, 2% MeOH, 97.5% EtOAc). Amine **3bm** was obtained (121.5 mg, 88% yield) as a brown oil. ^1H NMR (600 MHz, $CDCl_3$) δ 6.78 (d, *J* = 7.9 Hz, 1H), 6.74–6.65 (m, 2H), 3.87 (s, 3H), 3.85 (s, 3H), 2.57 (t, *J* = 7.5 Hz, 2H), 2.47–2.17 (m, 6H), 1.64–1.47 (m, 8H), 1.47–1.33 (m, 2H); ^{13}C NMR (151 MHz, $CDCl_3$) δ 148.7, 147.0, 135.2, 120.1, 111.7, 111.2, 59.4, 55.9, 55.8, 54.7, 35.5, 29.8, 26.6, 26.0, 24.5; ATR-IR: 2931, 2853, 2799, 2761, 1590, 1513, 1463, 1416, 1349, 1259, 1234, 1191, 1153, 1139, 1029, 858, 803, 763, 732, 634, 596, 560, 462 cm^{-1}; HRMS (ESI/QTOF) m/z: $[M + H]^+$ Calcd for $C_{17}H_{28}NO_2^+$ 278.2115; Found 278.2111.

4-(4-(3,4-Dimethoxyphenyl)butyl)morpholine (3bn)

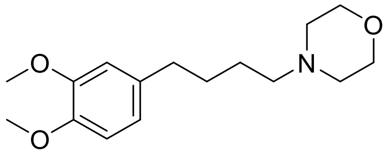

The hydroaminomethylation of methyl eugenol (86.0 µL, 0.500 mmol) with morpholine (60.2 µL, 0.688 mmol, 1.38 equiv) was conducted according to the general procedure for hydroaminomethylations with aliphatic amines. The product was isolated by silica chromatography (12 g silica, isocratic 10% EtOAc/hexanes followed by 0.5% Et_3N, 2% MeOH, 97.5% EtOAc). Amine **3bn** was obtained (122.0 mg, 87% yield) as a brown oil. ^1H NMR (600 MHz, $CDCl_3$) δ 6.75 (d, *J* = 7.9 Hz, 1H), 6.72–6.65 (m, 2H), 3.84 (s, 3H), 3.82 (s, 3H), 3.68 (t, *J* = 4.7 Hz, 4H), 2.55 (t, *J* = 7.6 Hz, 2H), 2.52 – 2.34 (br s, 4H), 2.32 (d, *J* = 7.6 Hz, 2H), 1.63 – 1.55 (m, 2H), 1.54 – 1.46 (m, 2H); ^{13}C NMR (151 MHz, $CDCl_3$) δ 148.7, 147.0, 135.0, 120.1, 111.7, 111.1, 66.9, 58.9, 55.9, 55.7, 53.7, 35.4, 29.4, 26.1; ATR-IR: 2997, 2934, 2854, 2807, 2766, 2686, 1680, 1607, 1590, 1514, 1463, 1417, 1358, 1332, 1305, 1260, 1235, 1191, 1154, 1140, 1116, 1070, 1028, 967, 913, 864, 803, 764, 729, 697, 644, 626, 612, 595, 562, 520, 502, 460 cm^{-1}; HRMS (ESI/QTOF) m/z: $[M + H]^+$ Calcd for $C_{16}H_{26}NO_3^+$ 280.1907; Found 280.1899.

4-(4-(3,4-Dimethoxyphenyl)butyl)thiomorpholine (3bo)

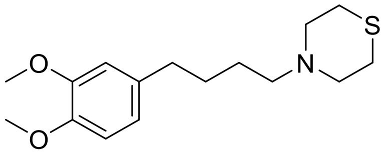

The hydroaminomethylation of methyl eugenol (86.0 μL, 0.500 mmol) with thiomorpholine (60.3 μL, 0.600 mmol, 1.20 equiv) was conducted according to the general procedure for hydroaminomethylations with aliphatic amines. The product was isolated by silica chromatography (12 g silica, isocratic 10% EtOAc/hexanes followed by 0.5% Et_3N, 2% MeOH, 97.5% EtOAc). Amine **3bo** was obtained (101.8 mg, 69% yield) as a pale-yellow oil. ^{1}H NMR (600 MHz, $CDCl_3$) δ 6.78 (d, *J* = 8.0 Hz, 1H), 6.75 – 6.63 (m, 2H), 3.86 (s, 3H), 3.85 (s, 3H), 2.80 – 2.61 (m, 8H), 2.56 (t, *J* = 7.6 Hz, 2H), 2.41 – 2.29 (m, 2H), 1.66 – 1.54 (m, 2H), 1.53 – 1.40 (m, 2H); ^{13}C NMR (151 MHz, $CDCl_3$) δ 148.7, 147.0, 135.0, 120.1, 111.7, 111.1, 59.2, 55.9, 55.8, 55.0, 35.3, 29.5, 28.0, 26.1; ATR-IR: 2997, 2933, 2857, 2806, 2769, 2253, 1676, 1607, 1590, 1514, 1463, 1416, 1374, 1340, 1322, 1258, 1234, 1191, 1154, 1139, 1079, 1028, 951, 912, 852, 803, 763, 729, 669, 644, 596, 560, 425 cm^{-1}; HRMS (ESI/QTOF) m/z: $[M + H]^+$ Calcd for $C_{16}H_{26}NO_2S^+$ 296.1679; Found 296.1687.

1-(4-(3,4-Dimethoxyphenyl)butyl)pyrrolidine (3bp)

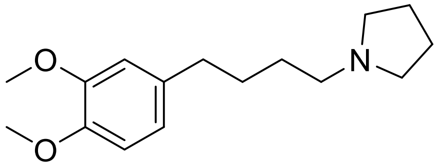

The hydroaminomethylation of methyl eugenol (86.0 µL, 0.500 mmol) with pyrrolidine (49.3 µL, 0.600 mmol, 1.20 equiv) was conducted according to the general procedure for hydroaminomethylations with aliphatic amines. The product was isolated by silica chromatography (12 g silica, isocratic 10% EtOAc/hexanes followed by 0.5% Et_3N, 2% MeOH, 97.5% EtOAc). Amine **3bp** was obtained (99.2 mg, 75% yield) as a yellow oil. ^{1}H NMR (600 MHz, $CDCl_3$) δ 6.77 (d, *J* = 7.9 Hz, 1H), 6.70 (d, *J* = 8.0 Hz, 2H), 3.86 (s, 3H), 3.84 (s, 3H), 2.57 (t, *J* = 7.6 Hz, 2H), 2.53 – 2.39 (m, 6H), 1.76 (quin, *J* = 3.1 Hz, 4H), 1.72 – 1.49 (m, 4H); ^{13}C NMR (151 MHz, $CDCl_3$) δ 148.9, 147.2, 135.4, 120.3, 111.9, 111.3, 56.6, 56.0, 55.9, 54.3, 35.6, 29.9, 28.8, 23.5; ATR-IR: IR (KBr, thin film): 3952, 3931, 3866, 3845, 3826, 3812, 3792, 3775, 3765, 3750, 3734, 3640, 3579, 3554, 3518, 3492, 3443, 3398, 3348, 3334, 3270, 3219, 3194, 3174, 3153, 3132, 3055, 2995, 2932, 2875, 2858, 2833, 2785, 2744, 2690, 2578, 2559, 2540, 2492, 2478, 2433, 2415, 2376, 2334, 2314, 2280, 2253, 2228, 2215, 2198, 2189, 2173, 2153, 2143, 2118, 2093, 2077, 2062, 2040, 2016, 2006, 1992, 1972, 1964, 1952, 1930, 1905, 1856, 1839, 1737, 1642, 1607, 1590, 1463, 1417, 1387, 1350, 1328, 1259, 1235, 1192, 1154, 1140, 1079, 1065, 912, 876, 851, 803, 764, 697, 641, 595, 561, 520, 504, 466, 416, 402 cm^{-1}; HRMS (ESI/QTOF) m/z: $[M + H]^+$ Calcd for $C_{16}H_{26}NO_2^+$ 264.1958; Found 264.1944.

4-(3,4-Dimethoxyphenyl)-*N*,*N*-dipropylbutan-1-amine (3bq)

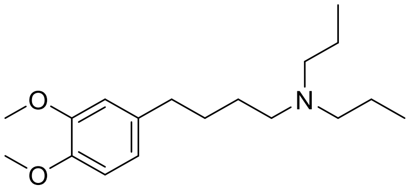

The hydroaminomethylation of methyl eugenol (86.0 µL, 0.500 mmol) with dipropylamine (82.3 µL, 0.600 mmol, 1.20 equiv) was conducted according to the general procedure for hydroaminomethylations with aliphatic amines. The product was isolated by silica chromatography (12 g silica, isocratic 10% EtOAc/hexanes followed by 0.5% Et_3N, 2% MeOH, 97.5% EtOAc). Amine **3bq** was obtained (103.5 mg, 71 % yield) as a pale-yellow oil. ^{1}H NMR (600 MHz, $CDCl_3$) δ 6.78 (d, *J* = 8.1 Hz, 1H), 6.74 – 6.53 (m, 2H), 3.86 (s, 3H), 3.85 (s, 3H), 2.56 (t, *J* = 7.7 Hz, 2H), 2.41 (t, *J* = 7.6 Hz, 2H), 2.34 (t, *J* = 7.6 Hz, 4H), 1.70 – 1.52 (m, 2H), 1.52 – 1.29 (m, 6H), 0.86 (t, *J* = 7.3 Hz, 6H); ^{13}C NMR (151 MHz, $CDCl_3$) δ 148.7, 147.0, 135.4, 120.1, 111.7, 111.2, 56.3, 55.9, 55.7, 54.0, 35.5, 29.6, 26.8, 20.2, 12.0; ATR-IR: 2955, 2933, 2870, 2833, 2797, 2254, 1591, 1514, 1464, 1417, 1378, 1337, 1259, 1235, 1191, 1155, 1140, 1078, 1030, 911, 849, 803, 764, 730, 645, 595, 560, 519, 503, 461 cm^{-1}; HRMS (ESI/QTOF) m/z: $[M + H]^+$ Calcd for $C_{18}H_{32}NO_2^+$ 294.2428; Found 294.2414.

_N_-Benzyl-4-(3,4-dimethoxyphenyl)-_N_-methylbutan-1-amine (3br)

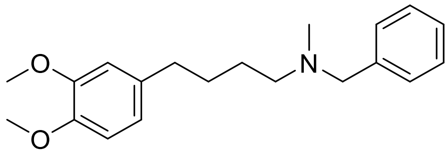

The hydroaminomethylation of methyl eugenol (86.0 μL, 0.500 mmol) with *N*-benzylmethylamine (77.4 μL, 0.600 mmol, 1.20 equiv) was conducted according to the general procedure for hydroaminomethylations with aliphatic amines. The product was isolated by silica chromatography (12 g silica, isocratic 10% EtOAc/hexanes followed by 0.5% Et_3N, 2% MeOH, 97.5% EtOAc). Amine **3br** was obtained (119.2 mg, 76% yield) as a yellow oil. ^1H NMR (600 MHz, $CDCl_3$) δ 7.36 – 7.21 (m, 5H), 6.79 (d, *J* = 7.9 Hz, 1H), 6.74 – 6.66 (m, 2H), 3.87 (s, 3H), 3.86 (s, 3H), 3.48 (s, 2H), 2.56 (t, *J* = 7.6 Hz, 2H), 2.39 (t, *J* = 7.3 Hz, 2H), 2.18 (s, 3H), 1.64 (quin, *J* = 7.4 Hz, 2H), 1.56 (quin, *J* = 7.3 Hz, 2H); ^{13}C NMR (151 MHz, $CDCl_3$) δ 148.8, 147.1, 139.3, 135.3, 129.0, 128.2, 126.9, 120.2, 111.8, 111.2, 62.4, 57.3, 55.9, 55.8, 42.3, 35.4, 29.4, 27.0; ATR-IR: 2937, 2837, 2789, 2253, 1671, 1591, 1515, 1464, 1453, 1418, 1259, 1234, 1192, 1155, 1141, 1028, 906, 852, 806, 764, 725, 699, 647, 468 cm^{-1}; HRMS (ESI/QTOF) m/z: $[M + H]^+$ Calcd for $C_{20}H_{28}NO_2^+$ 314.2115; Found 314.2113.

***N*,*N*-Dibenzyl-4-(3,4-dimethoxyphenyl)butan-1-amine (3bs)**

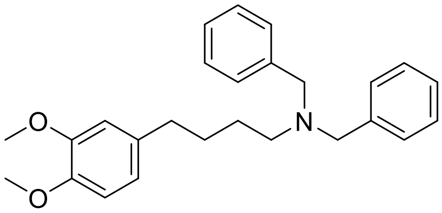

The hydroaminomethylation of methyl eugenol (86.0 μL, 0.500 mmol) with *N*,*N*-dibenzylamine (115.3 mg, 0.600 mmol, 1.20 equiv) was conducted according to the general procedure for hydroaminomethylations with aliphatic amines. The product was isolated by silica chromatography (12 g silica, isocratic 15% EtOAc/hexanes followed by 0.5% Et_3N, 2% MeOH, 97.5% EtOAc). Amine **3bs** was obtained (109.3 mg, 56% yield) as a pale-yellow oil; ^{1}H NMR (600 MHz, $CDCl_3$) δ 7.39 (d, *J* = 7.5 Hz, 4H), 7.33 (t, *J* = 7.5 Hz, 4H), 7.25 (t, *J* = 7.4 Hz, 2H), 6.79 (d, *J* = 8.6 Hz, 1H), 6.72 – 6.63 (m, 2H), 3.88 (s, 3H), 3.87 (s, 3H), 3.57 (s, 4H), 2.57 – 2.40 (m, 4H), 1.71 – 1.49 (m, 4H); ^{13}C NMR (151 MHz, $CDCl_3$) δ 148.7, 147.0, 140.0, 135.3, 128.8, 128.1, 126.7, 120.1, 111.7, 111.1, 58.3, 55.9, 55.8, 53.1, 35.2, 29.0, 26.5; ATR-IR: 3061, 3027, 2934, 2833, 2794, 2253, 1590, 1514, 1494, 1464, 1452, 1417, 1365, 1259, 1235, 1191, 1154, 1140, 1074, 1028, 968, 908, 849, 805, 764, 728, 697, 646, 563, 466 cm^{-1}; HRMS (ESI/QTOF) m/z: $[M + H]^+$ Calcd for $C_{26}H_{32}NO_2^+$ 390.2428; Found 390.2422.

N-(4-(3,4-Dimethoxyphenyl)butyl)octan-1-amine (3bt)

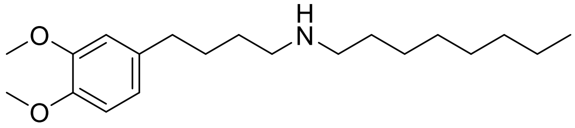

The hydroaminomethylation of methyl eugenol (86.0 µL, 0.500 mmol) with octylamine (206.5 µL, 1.25 mmol, 2.50 equiv) was conducted according to the general procedure for hydroaminomethylations with aliphatic amines. The product was isolated by silica chromatography (12 g silica, isocratic 15% EtOAc/hexanes followed by 0.5% Et_3N, 2% MeOH, 97.5% EtOAc). Amine **3bt** was obtained (82.8 mg, 52% yield) as a pale-yellow oil. ^1H NMR (600 MHz, $CDCl_3$) δ 6.73 (d, J = 8.1 Hz, 1H), 6.67 (d, J = 7.5 Hz, 2H), 3.82 (s, 3H), 3.80 (s, 3H), 2.80 – 2.25 (m, 6H), 1.66 – 1.11 (m, 17H), 0.84 (t, J = 6.9 Hz, 3H); ^{13}C NMR (151 MHz, $CDCl_3$) δ 148.7, 147.0, 135.1, 120.1, 111.7, 111.2, 55.8, 55.7, 50.1, 49.9, 35.4, 31.8, 30.1, 29.8, 29.5, 29.4, 29.2, 27.4, 22.6, 14.0; ATR-IR: 2925, 2852, 2784, 1676, 1590, 1516, 1463, 1418, 1378, 1334, 1260, 1235, 1192, 1155, 1142, 1028, 916, 858, 809, 763, 732, 633, 596, 565, 462 cm^{-1}; HRMS (ESI/QTOF) m/z: $[M + H]^+$ Calcd for $C_{20}H_{36}NO_2^+$ 322.2741; Found 322.2741.

2.4.7 Application to the synthesis of Ibutilide

N-(4-Formylphenyl)methanesulfonamide (5)

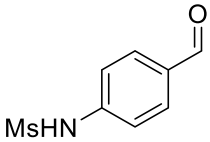

Aldehyde **5** was prepared from *p*-bromobenzaldehyde and methanesulfonamide by the method of Navarro and cowarkers.[18] Aldehyde **5** was obtained (2.22 g, 70%) as a light orange solid. Spectral data matched those published previously.[5e,18] ^{1}H NMR (500 MHz, Acetone-d_6) δ 9.98 (s, 1H), 8.00 – 7.88 (m, 2H), 7.64 – 7.45 (m, 2H), 3.17 (s, 3H).

N-(4-(1-Hydroxyallyl)phenyl)methanesulfonamide (1m)

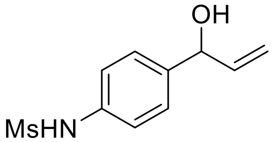

A new bottle of vinylmagnesium bromide (1 M in THF) was opened in a nitrogen-filled glovebox. An oven-dried round-bottom flask equipped with a magnetic stirring bar was cooled to room temperature in the glovebox, and vinylmagnesium bromide (3.00 mL, 3.00 mmol) was added to the flask. A solution of aldehyde **5** (272 mg, 1.37 mmol) in dry, degassed THF (4.5 mL) was drawn into a gastight syringe in the glovebox, and the needle was capped with a septum. The round-bottom flask was capped with a septum, removed from the glovebox, and cooled in an ice bath. The solution of aldehyde **5** in THF was added dropwise with stirring to the round-bottom flask at 0 °C under a flow of nitrogen. The reaction mixture was warmed to room temperature, stirred for 24 h, quenched with saturated NH_4Cl, extracted into ether (3x), washed with water, washed with brine, and dried over Na_2SO_4. The product was isolated by silica chromatography (ca. 60 g silica, slow gradient 0% → 10% MeOH/DCM). Olefin **1m** was obtained as a thick, pale-yellow oil (221.6 mg, 71%). Spectral data matched those published previously.[5e] ^{1}H NMR (400 MHz, Acetone-d_6) δ 8.49 (s, 1H), 7.40 – 7.31 (m, 2H), 7.31 – 7.24 (m, 2H), 5.98 (ddd, J = 17.2, 10.3, 5.9 Hz, 1H), 5.29 (dt, J = 17.1, 1.7 Hz, 1H), 5.14 (t, J = 5.3 Hz, 1H), 5.05 (dt, J = 10.3, 1.5 Hz, 1H), 4.46 (d, J = 4.3 Hz, 1H), 2.94 (s, 3H).

***N*-(4-(4-(Ethyl(heptyl)amino)-1-hydroxybutyl)phenyl)methanesulfonamide** (ibutilide, **3mt**)

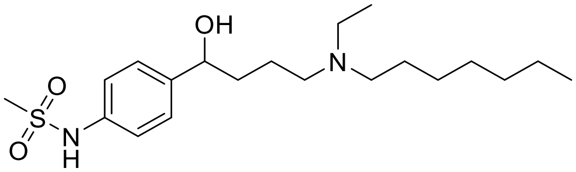

An aliquot of the catalyst stock solution (0.500 mL, 1.0 mol% $Rh(CO)_2(acac)$, 5.0 mol% BISBI, 2.0 mol% Xiao's catalyst) was plated onto a glass liner tube (*see above*). Under air, olefin **1m** (112.6 mg, 0.495 mmol) was added as a solution in toluene methanol (9:1, vol: vol, 5.00 mL). The tube was charged with pH 4.8 aqueous sodium formate buffer (250 µL) and *N*-ethylheptan-1-amine (109.8 µL, 0.600 mmol, 1.29 equiv) and loaded into a Biotage Endeavor Catalyst Screening System. At room temperature, the reaction vessels were purged with N_2 (1x), pressurized to 25 psi with CO, and brought to a total pressure of 50 psi with H_2 at room temperature. The reaction mixture was heated at 80 °C for 20 h with mechanical stirring (400 rpm), after which time the vessel was cooled to 40 °C, purged with N_2 (1x), and removed from the Endeavor reactor. The crude reaction mixture was diluted with 10% aqueous K_2CO_3 (10 mL) and extracted into ethyl acetate (20 mL, 3x). The combined extracts were dried over Na_2SO_4, and the product isolated by silica chromatography (4 g silica, slow 0% → 10% MeOH/DCM gradient followed by 0.5% Et_3N, 2% MeOH, 97.5% EtOAc). Amine **3mt** was obtained (144.9 mg, 76% yield) as a yellow oil. Spectral data matched the literature.[5e] ^{1}H NMR (300 MHz, Acetone-d_6) δ 7.52 – 7.35 (m, 2H), 7.35 – 7.18 (m, 2H), 7.25 – 5.95 (br s, 2H), 4.66 (dd, J = 7.7, 4.0 Hz, 1H), 2.96 (s, 3H), 2.73 – 2.32 (m, 6H), 1.95 – 1.22 (m, 14H), 1.06 (t, J = 7.1 Hz, 3H), 0.92 (t, J = 4.6, 2.4 Hz, 3H).

2.4.8 Procedure for hydroaminomethylation on a 6 mmol scale

N-(4-(3,4-Dimethoxyphenyl)butyl)aniline (3ba)

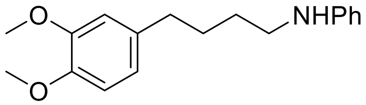

A 100 mL round-bottom flask was charged with Xiao's catalyst (38.0 mg, 0.0583 mmol), $Rh(CO)_2(acac)$ (8.2 mg, 0.0318 mmol), and BISBI (87.5 mg, 0.159 mmol). The catalysts were diluted with a 9:1 vol:vol mixture of toluene: methanol (31 mL). The flask was then charged with methyl eugenol (1.055 mL, 6.31 mmol), pH 4.8 aqueous sodium formate buffer (6 mL), and *N*-ethylheptylamine (838.1 μL). The flask was capped with a septum that was punctured with a needle, and the flask was placed in a 300 mL Parr stainless-steel autoclave. The autoclave was purged once with 1:1 $CO:H_2$, pressurized with 1:1 $CO:H_2$ to 50 psi with a low-pressure regulator, heated at 80 °C for 20 h, and cooled to room temperature. The crude reaction mixture was diluted with 10% aqueous K_2CO_3 and extracted into diethyl ether (20 mL, 3x). The combined extracts were dried over Na_2SO_4, analyzed by gas chromatography, concentrated *in vacuo*, and purified by silica chromatography (~60 g silica, 0 → 10% ethyl acetate hexanes gradient). Amine **3ba** was obtained (1.24 g, 71%) as a pale-yellow oil.

2.4.9 Procedure for hydroaminomethylation at 1 atm syngas

N-Undecylaniline (3aa)

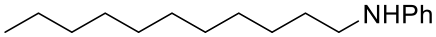

An aliquot of the catalyst stock solution (0.500 mL, 2.0 mol% $Rh(CO)_2(acac)$, 8.0 mol% BISBI, 2.0 mol% Xiao's catalyst) was plated onto a glass liner tube (*see above*). Under air, the tube was sequentially charged with toluene: methanol (9:1, vol:vol, 750 μL), olefin **1a** (28.0 μL, 0.148 mmol), pH 4.8 aqueous sodium formate buffer (250 μL), and amine **2a** (20.3 μL, 0.224 mmol, 1.52 equiv) and loaded into a Biotage Endeavor Catalyst Screening System. At room temperature, the reaction vessels were purged with N_2 (1x), pressurized to 5 psi with CO, and brought to a total pressure of 15 psi with H_2. The reaction mixture was heated at 70 °C for 64 h with mechanical stirring (400 rpm), after which time the vessel was cooled to 40 °C, purged with N_2 (1x), and removed from the Endeavor reactor. The crude reaction mixture was diluted with aqueous, saturated sodium bicarbonate (10 mL) and extracted into diethyl ether or ethyl acetate (20 mL, 3x). The combined extracts were dried over Na_2SO_4, analyzed by gas chromatography, concentrated *in vacuo*, and purified by flash chromatography (24 g silica, slow 0% → 5% EtOAc/hexanes gradient). Amine **3aa** was obtained (23.7 mg, 65% yield) as a pale-yellow oil.

2.4.10 Spectra of novel compounds

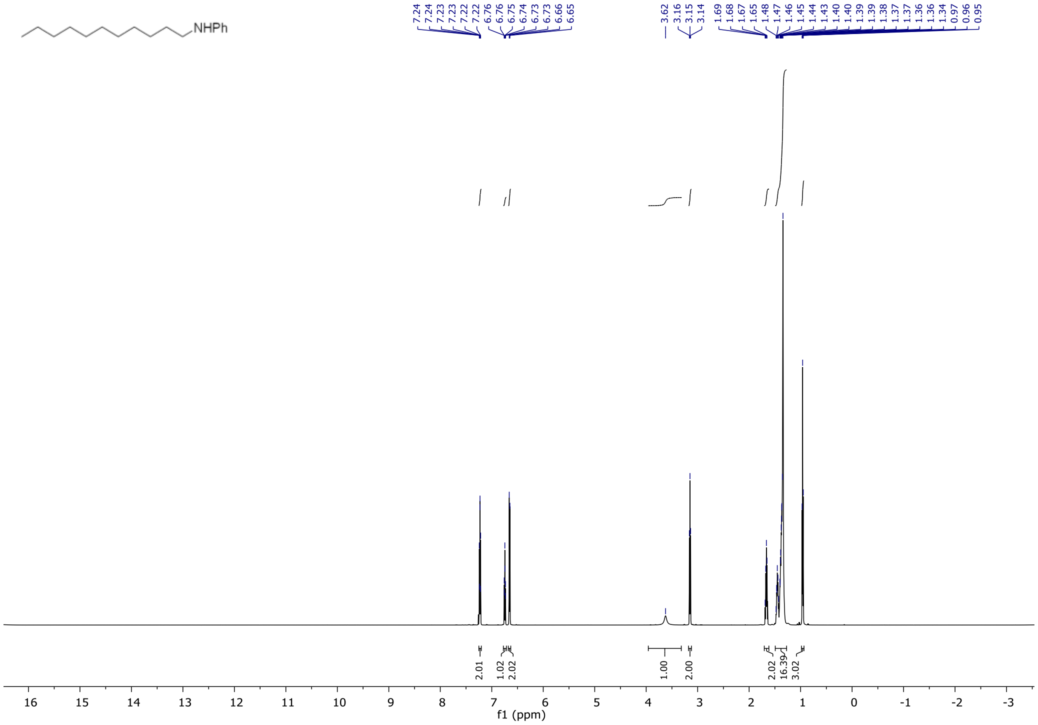

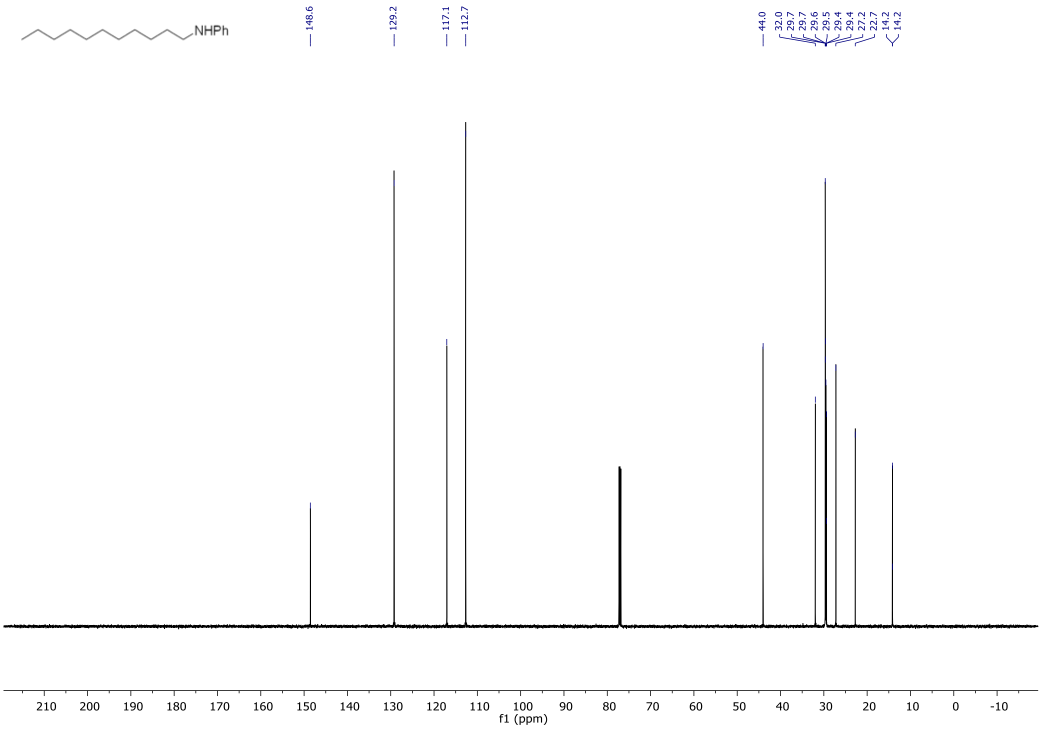
NHPh
148.6
129.2
117.1
112.7
44.0
32.0
29.7
29.7
29.6
29.5
29.4
29.4
27.2
22.7
14.2
14.2
210
200
190
180
170
160
150
140
130
120
110
100
90
80
70
60
50
40
30
20
10
0
-10
f1 (ppm)

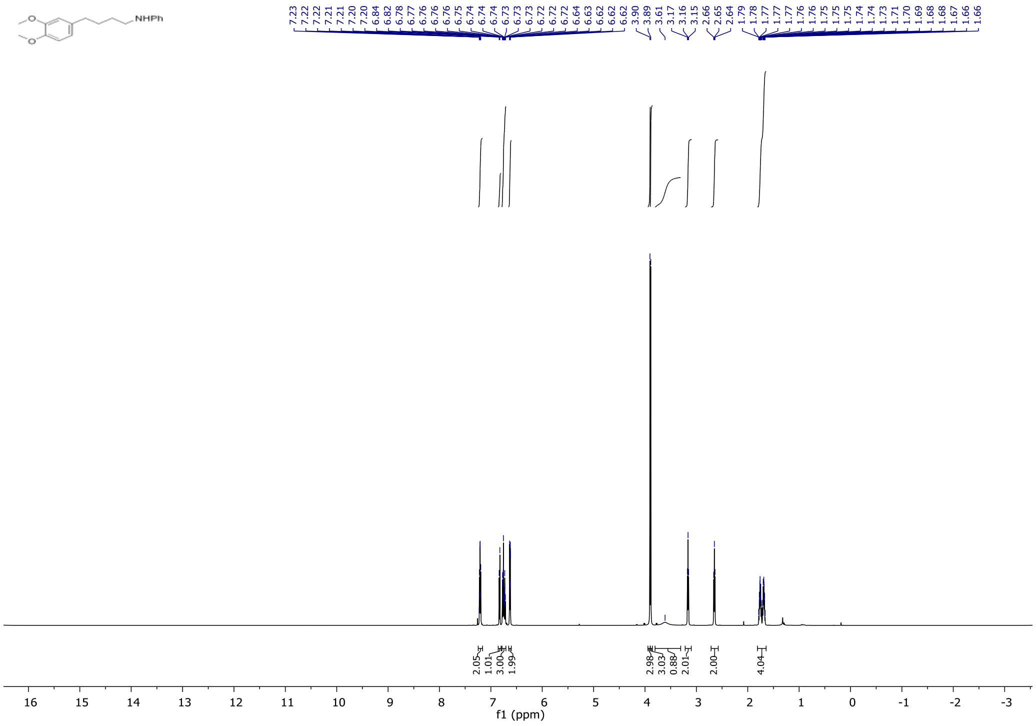
NHPh
O
O
7.23
7.22
7.22
7.21
7.21
7.20
7.20
6.84
6.82
6.78
6.77
6.76
6.76
6.75
6.74
6.74
6.74
6.73
6.73
6.73
6.72
6.72
6.64
6.63
6.62
6.62
3.90
3.89
3.61
3.17
3.16
3.15
2.66
2.65
2.64
1.79
1.78
1.77
1.77
1.77
1.76
1.76
1.75
1.75
1.74
1.74
1.73
1.71
1.70
1.69
1.68
1.68
1.67
1.66
1.66
2.05
1.01
3.00
1.99
2.98
3.03
0.88
2.01
2.00
4.04
16
15
14
13
12
11
10
9
8
7
6
5
4
3
2
1
0
-1
-2
-3
f1 (ppm)

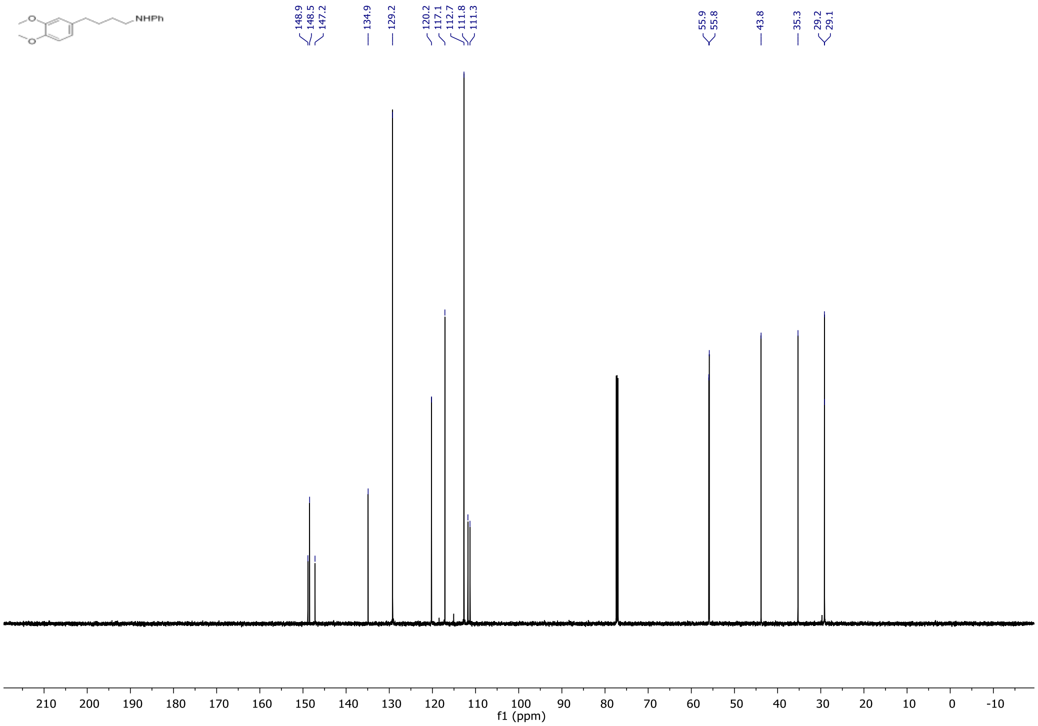
O
O
NHPh
148.9
148.5
147.2
134.9
129.2
120.2
117.1
112.7
111.8
111.3
55.9
55.8
43.8
35.3
29.2
29.1
210
200
190
180
170
160
150
140
130
120
110
100
90
80
70
60
50
40
30
20
10
0
-10
f1 (ppm)

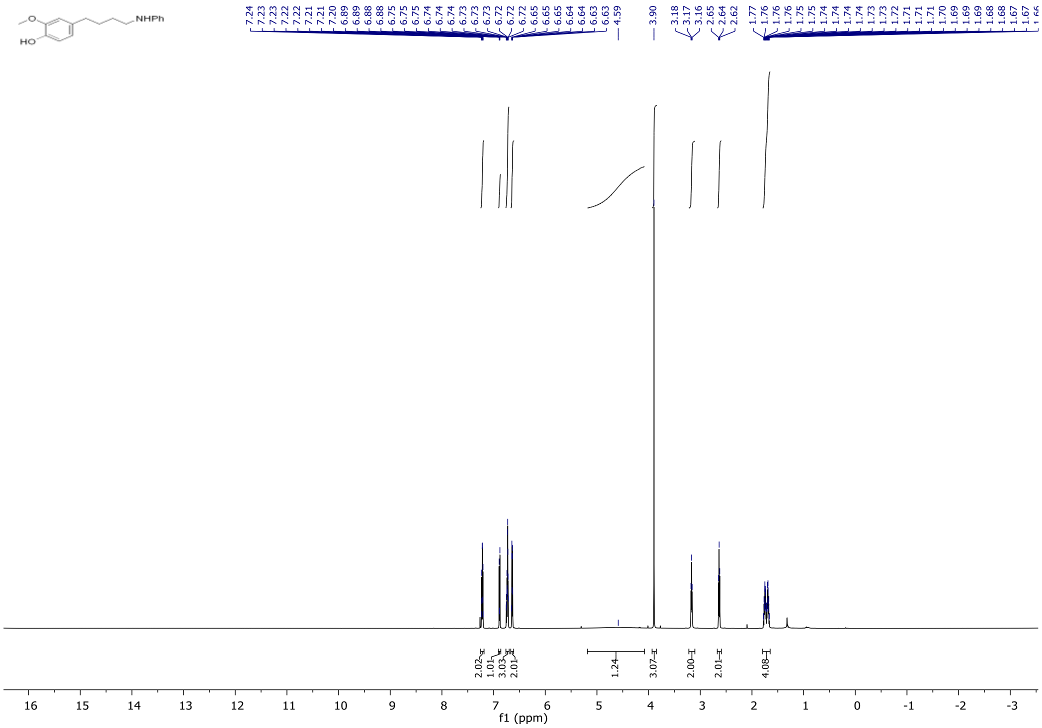

NHPh
O
HO
7.24
7.23
7.23
7.22
7.22
7.21
7.21
7.20
6.89
6.89
6.88
6.88
6.75
6.75
6.75
6.74
6.74
6.74
6.73
6.73
6.73
6.72
6.72
6.72
6.65
6.65
6.65
6.64
6.64
6.63
6.63
4.59
3.90
3.18
3.17
3.16
2.65
2.64
2.62
1.77
1.76
1.76
1.76
1.75
1.75
1.74
1.74
1.74
1.74
1.73
1.73
1.72
1.71
1.71
1.71
1.70
1.69
1.69
1.69
1.68
1.68
1.67
1.67
2.02
1.01
3.03
2.01
1.24
3.07
2.00
2.01
4.08
16
15
14
13
12
11
10
9
8
7
6
5
4
3
2
1
0
-1
-2
-3
f1 (ppm)

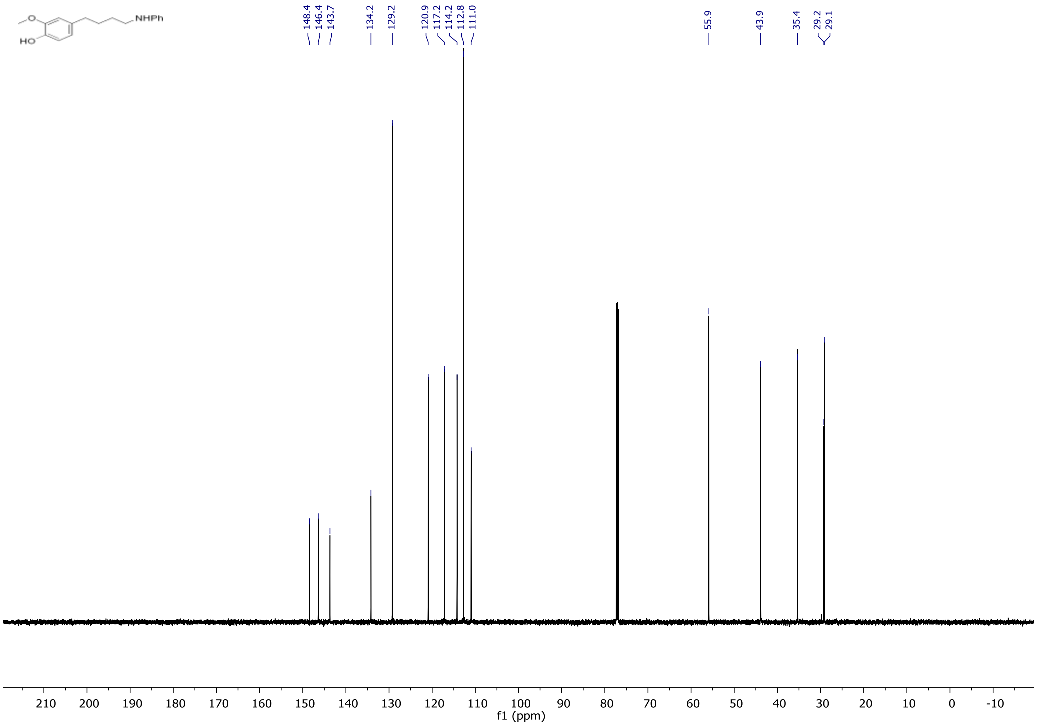
O
HO
NHPh
148.4
146.4
143.7
134.2
129.2
120.9
117.2
114.2
112.8
111.0
55.9
43.9
35.4
29.2
29.1
210
200
190
180
170
160
150
140
130
120
110
100
90
80
70
60
50
40
30
20
10
0
-10
f1 (ppm)

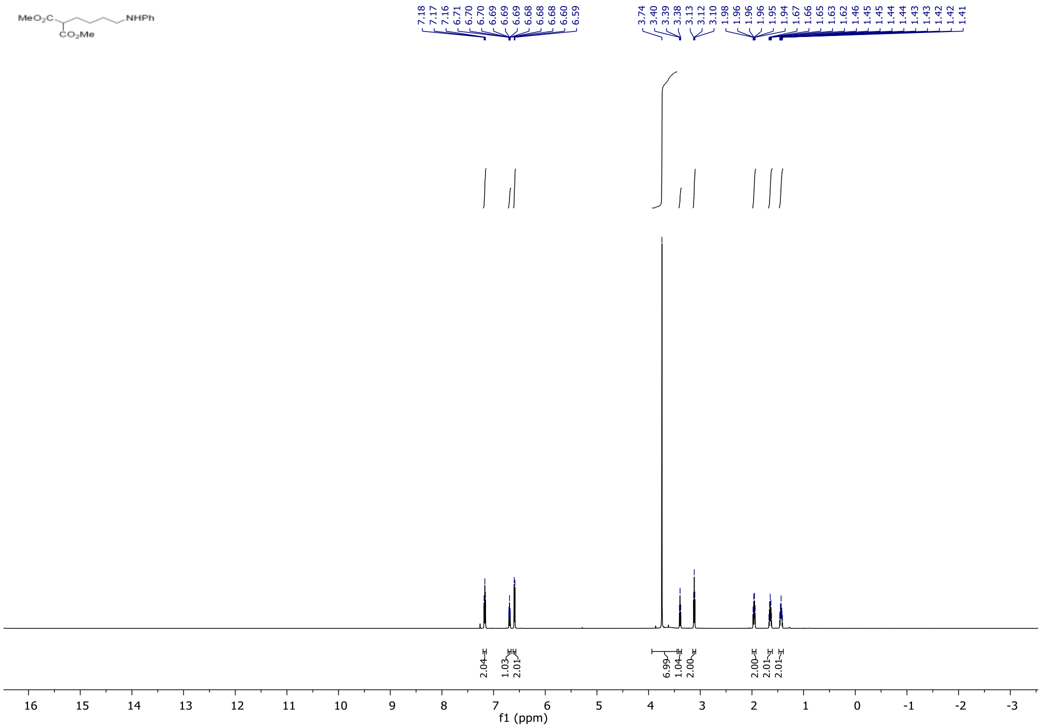
MeO2C
CO2Me
NHPh
7.18
7.17
7.16
6.71
6.70
6.69
6.69
6.69
6.68
6.68
6.60
6.59
3.74
3.40
3.39
3.38
3.13
3.12
3.10
1.98
1.96
1.96
1.96
1.95
1.94
1.67
1.66
1.65
1.63
1.62
1.46
1.45
1.45
1.44
1.43
1.43
1.42
1.41
2.04
1.03
2.01
6.99
1.04
2.00
2.00
2.01
2.01
16
15
14
13
12
11
10
9
8
7
6
5
4
3
2
1
0
-1
-2
-3
f1 (ppm)

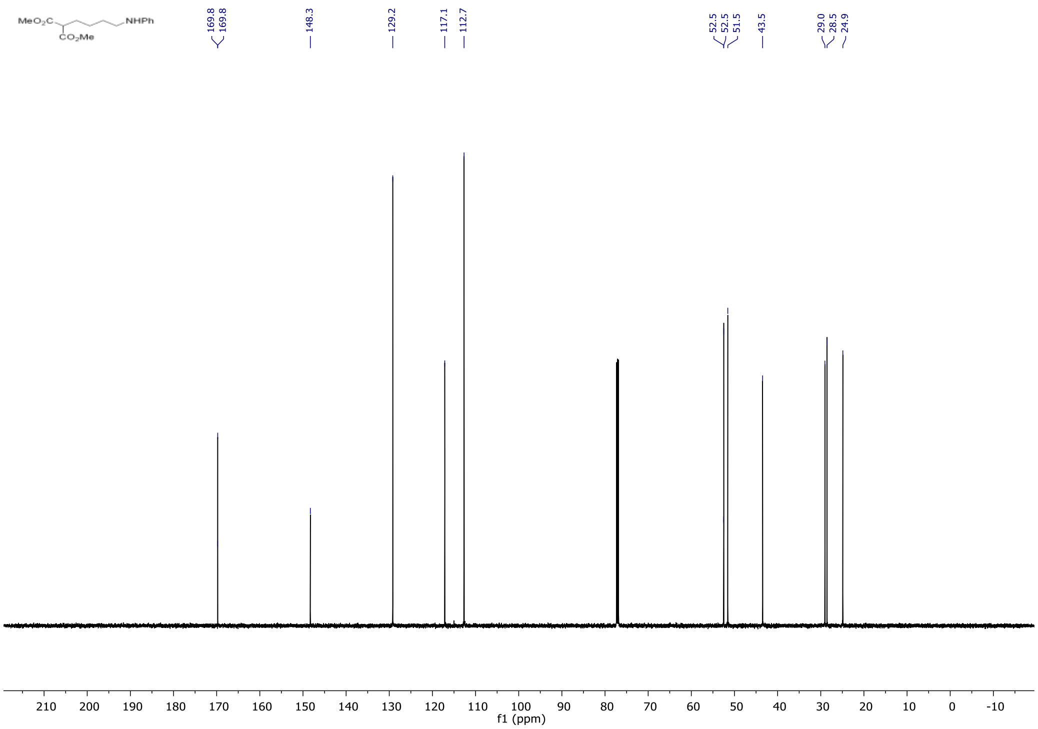
MeO2C
CO2Me
NHPh
169.8
169.8
148.3
129.2
117.1
112.7
52.5
52.5
51.5
43.5
29.0
28.5
24.9
210
200
190
180
170
160
150
140
130
120
110
100
90
80
70
60
50
40
30
20
10
0
-10
f1 (ppm)

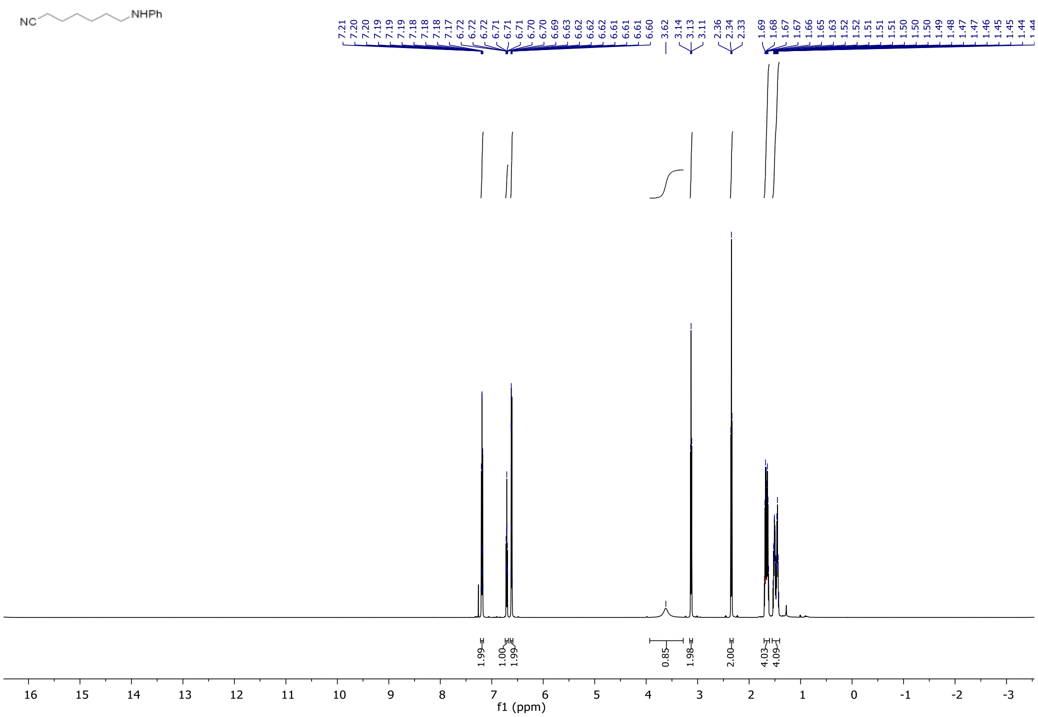
NC
NHPh
7.21
7.20
7.20
7.19
7.19
7.19
7.18
7.18
7.18
7.17
6.72
6.72
6.71
6.71
6.71
6.70
6.69
6.63
6.62
6.62
6.61
6.61
6.61
6.60
3.62
3.14
3.13
3.11
2.36
2.34
2.33
1.69
1.68
1.67
1.66
1.65
1.63
1.52
1.52
1.51
1.51
1.50
1.50
1.50
1.49
1.48
1.47
1.46
1.45
1.44
1.99
1.00
1.99
0.85
1.98
2.00
4.03
4.09
16
15
14
13
12
11
10
9
8
7
6
5
4
3
2
1
0
-1
-2
-3
f1 (ppm)

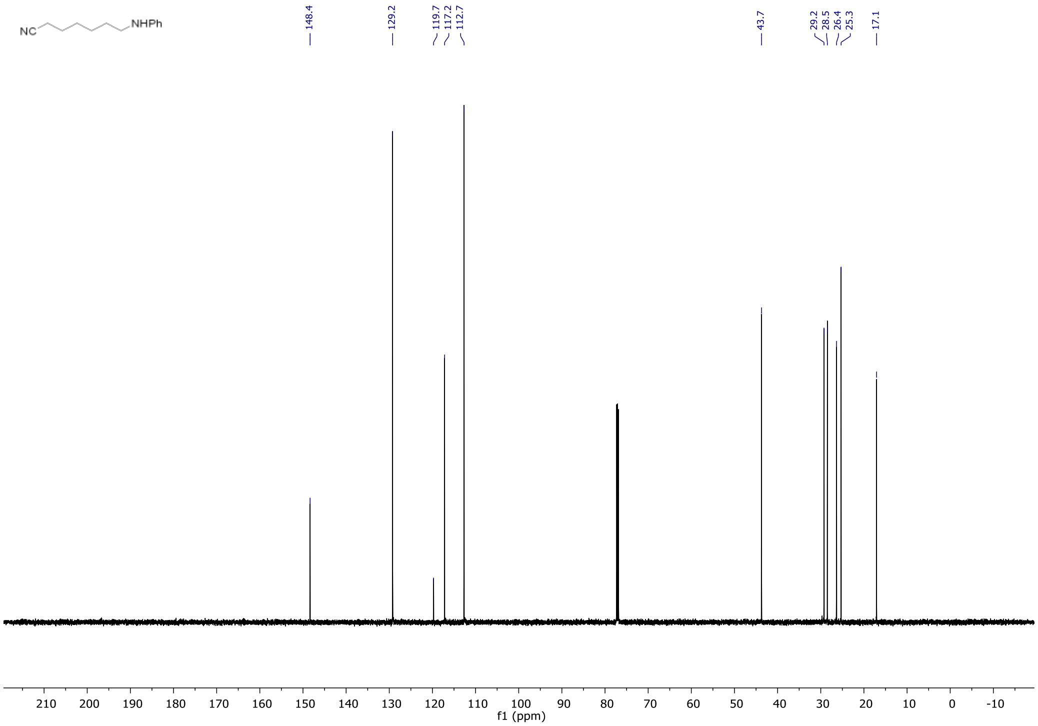
NC
NHPh
148.4
129.2
119.7
117.2
112.7
43.7
29.2
28.5
26.4
25.3
17.1
210 200 190 180 170 160 150 140 130 120 110 100 90 80 70 60 50 40 30 20 10 0 -10
f1 (ppm)

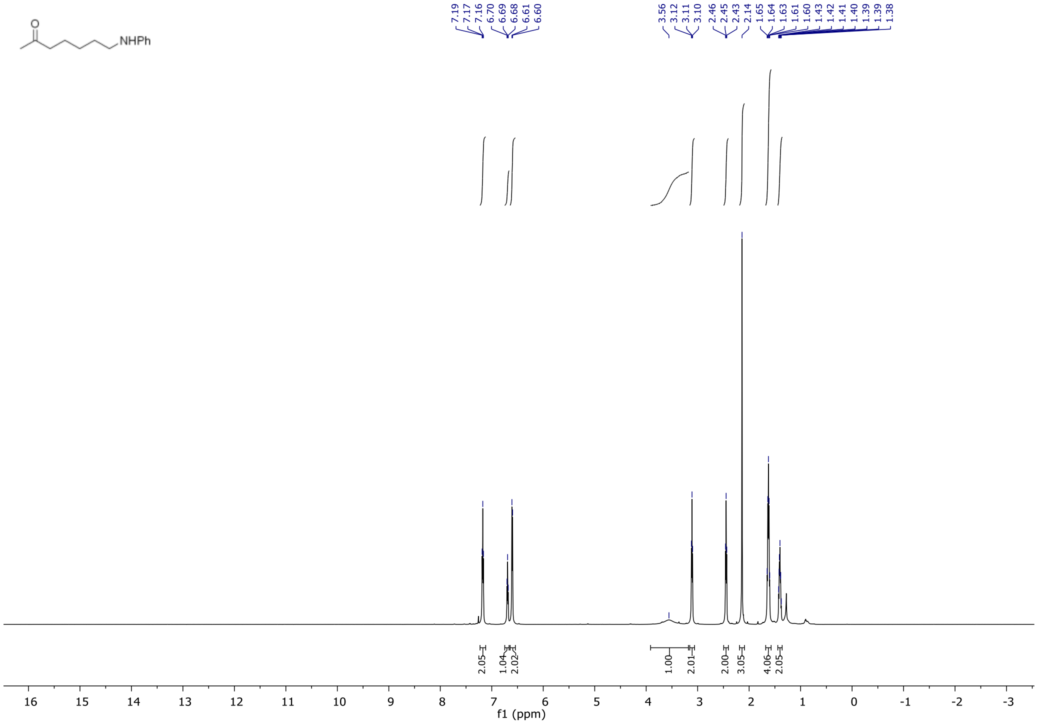
O
NHPh
7.19
7.17
7.16
6.70
6.69
6.68
6.61
6.60
3.56
3.12
3.11
3.10
2.46
2.45
2.43
2.14
1.65
1.64
1.63
1.61
1.60
1.43
1.42
1.41
1.40
1.39
1.39
1.38
2.05
1.04
2.02
1.00
2.01
2.00
3.05
4.06
2.05
16
15
14
13
12
11
10
9
8
7
6
5
4
3
2
1
0
-1
-2
-3
f1 (ppm)

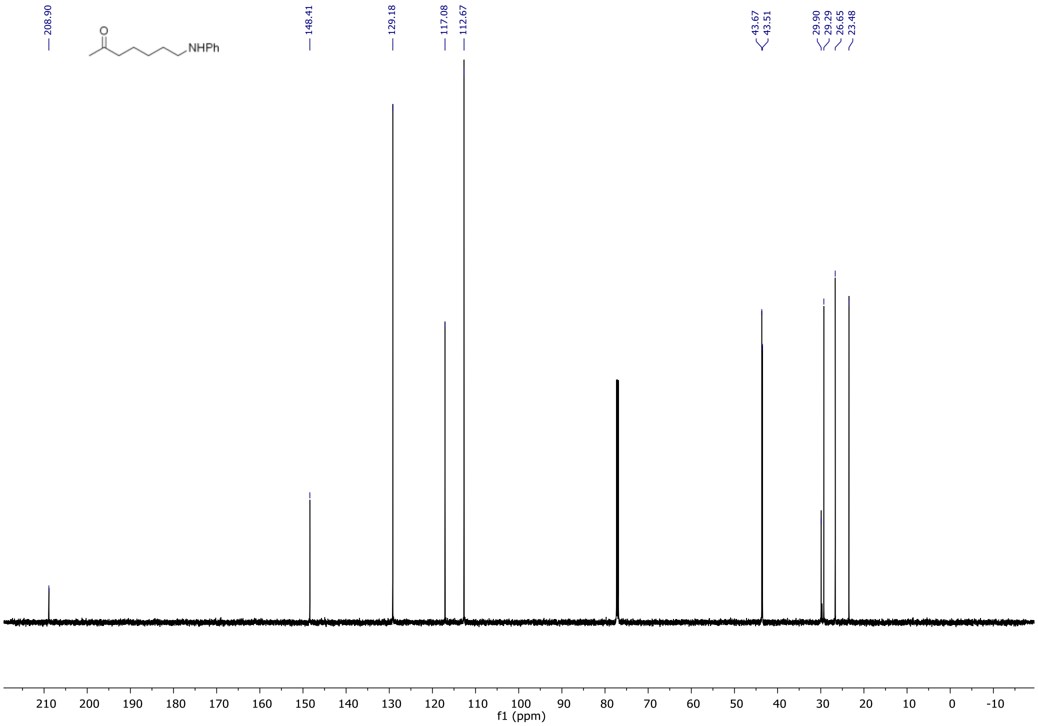
208.90
148.41
129.18
117.08
112.67
43.67
43.51
29.90
29.29
26.65
23.48
O
NHPh
210
200
190
180
170
160
150
140
130
120
110
100
90
80
70
60
50
40
30
20
10
0
-10
f1 (ppm)

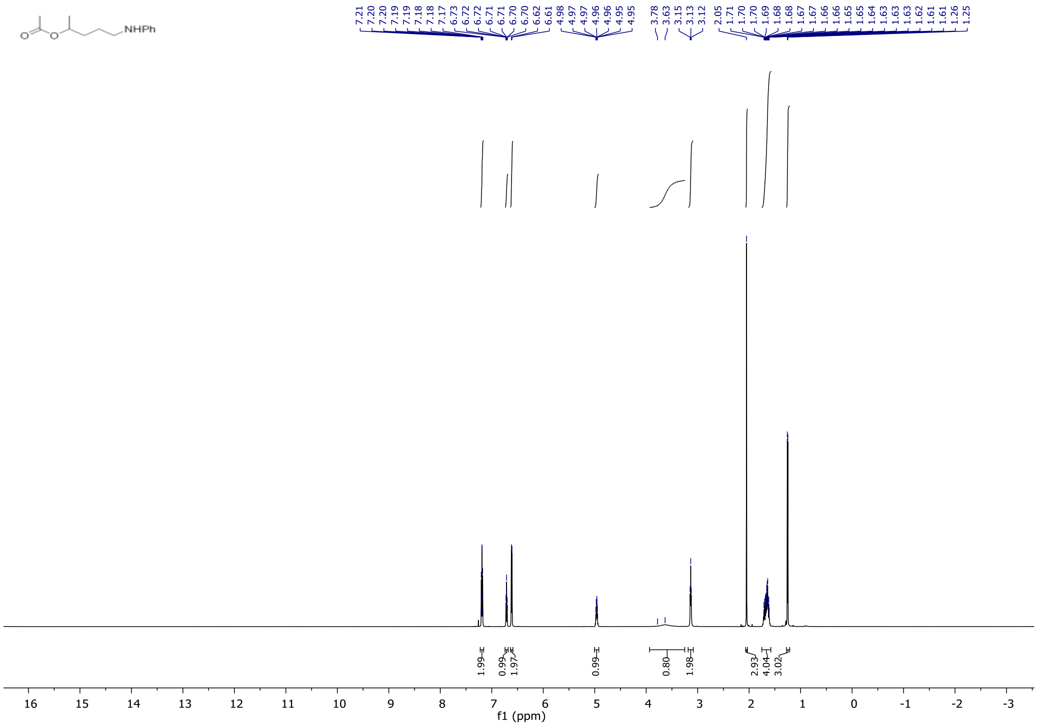
NHPh
O
O
7.21
7.20
7.20
7.19
7.19
7.18
7.18
7.17
6.73
6.72
6.72
6.71
6.71
6.70
6.70
6.62
6.61
4.98
4.97
4.97
4.96
4.96
4.95
4.95
3.78
3.63
3.15
3.13
3.12
2.05
1.71
1.70
1.70
1.69
1.68
1.68
1.67
1.67
1.66
1.66
1.65
1.65
1.64
1.63
1.63
1.62
1.61
1.61
1.26
1.25
1.99
0.99
1.97
0.99
0.80
1.98
2.93
4.04
3.02
16
15
14
13
12
11
10
9
8
7
6
5
4
3
2
1
0
-1
-2
-3
f1 (ppm)

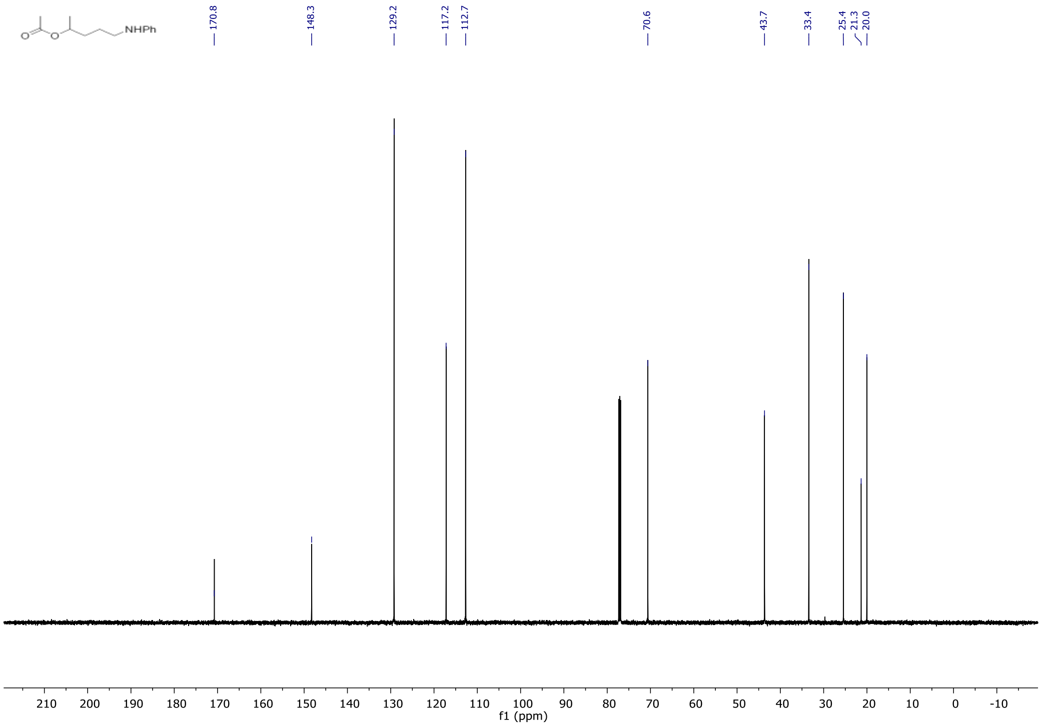
NHPh
O
O
170.8
148.3
129.2
117.2
112.7
70.6
43.7
33.4
25.4
21.3
20.0
210
200
190
180
170
160
150
140
130
120
110
100
90
80
70
60
50
40
30
20
10
0
-10
f1 (ppm)

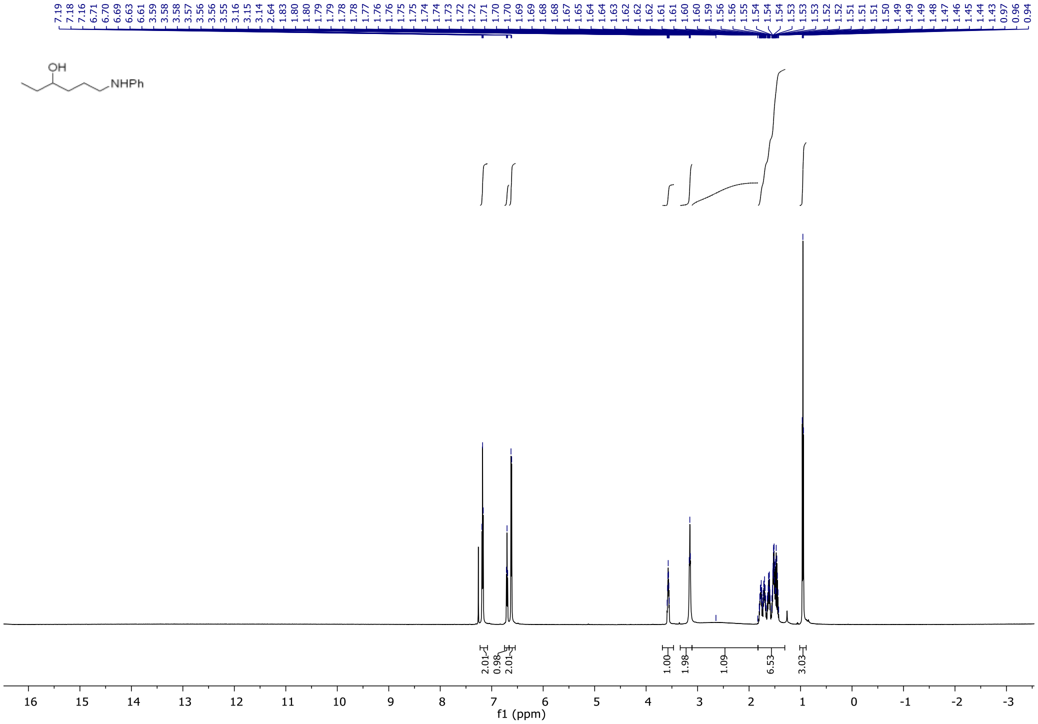

OH
NHPh
2.01
0.98
2.01
1.00
1.98
1.09
6.53
3.03
16
15
14
13
12
11
10
9
8
7
6
5
4
3
2
1
0
-1
-2
-3
f1 (ppm)

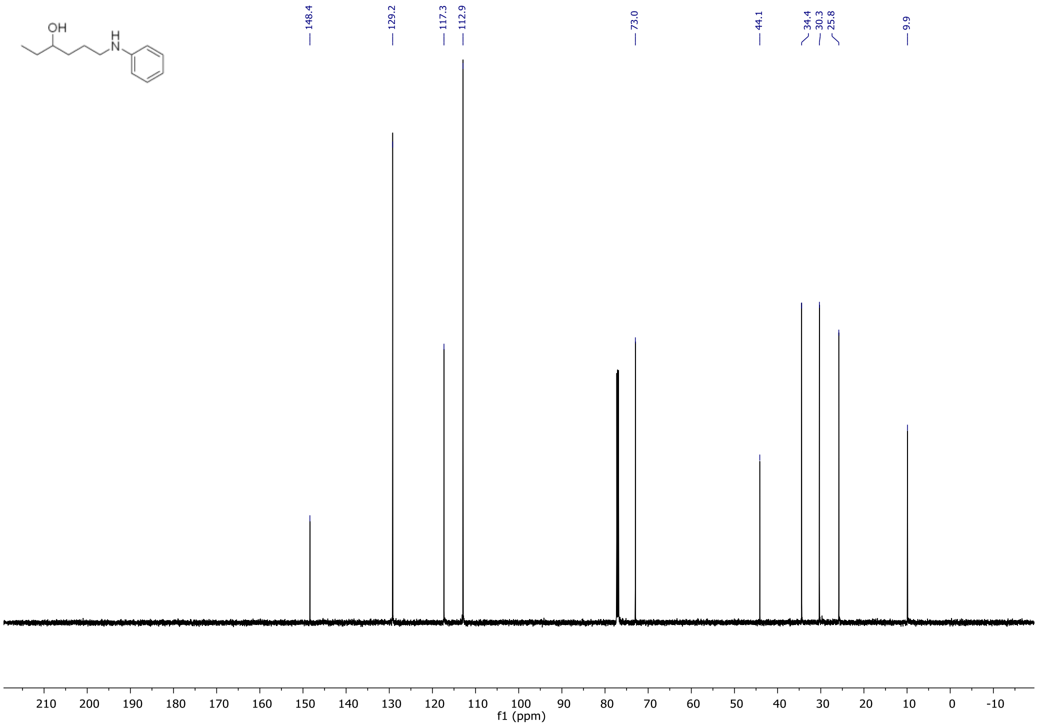
OH
H
N
148.4
129.2
117.3
112.9
73.0
44.1
34.4
30.3
25.8
9.9
210
200
190
180
170
160
150
140
130
120
110
100
90
80
70
60
50
40
30
20
10
0
-10
f1 (ppm)

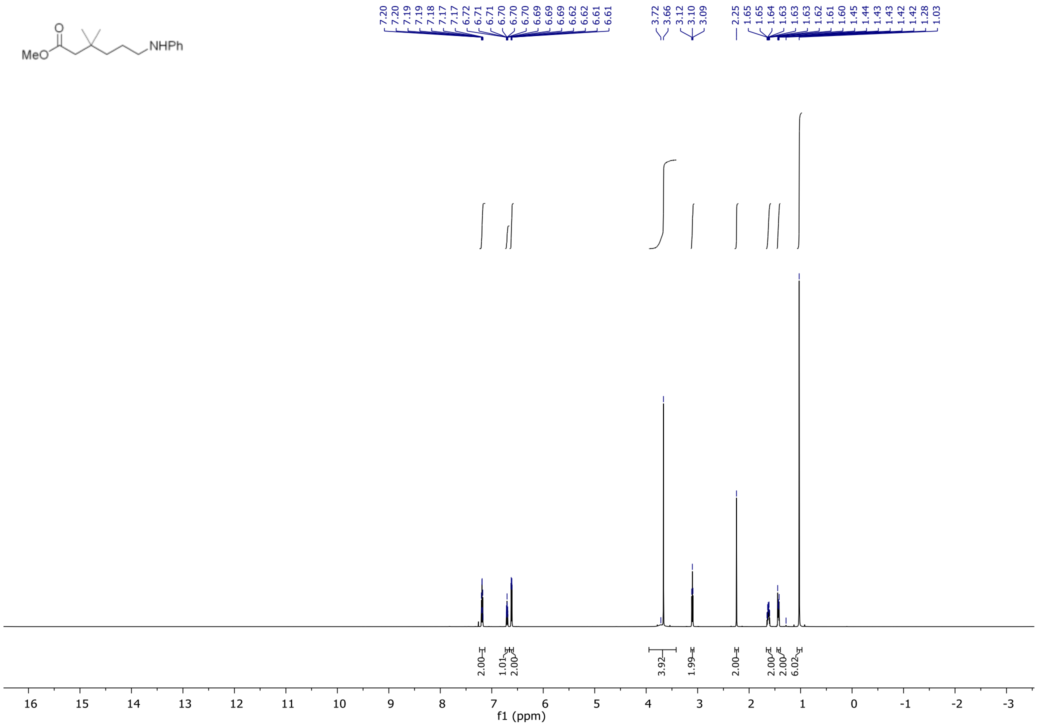
MeO
O
NHPh
7.20
7.20
7.19
7.19
7.18
7.17
7.17
6.72
6.71
6.71
6.70
6.70
6.70
6.69
6.69
6.62
6.62
6.61
6.61
3.72
3.66
3.12
3.10
3.09
2.25
1.65
1.65
1.64
1.63
1.63
1.63
1.62
1.61
1.60
1.45
1.44
1.43
1.43
1.42
1.42
1.28
1.03
2.00
1.01
2.00
3.92
1.99
2.00
2.00
2.00
6.02
16
15
14
13
12
11
10
9
8
7
6
5
4
3
2
1
0
-1
-2
-3
f1 (ppm)

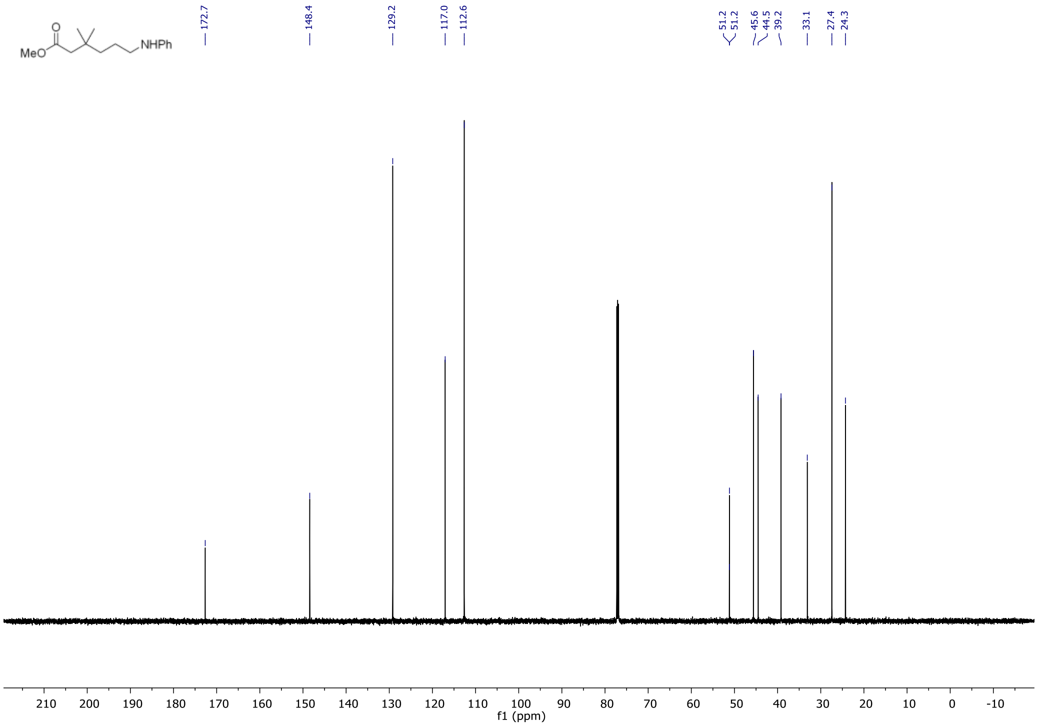
MeO
O
NHPh
172.7
148.4
129.2
117.0
112.6
51.2
51.2
45.6
44.5
39.2
33.1
27.4
24.3
210
200
190
180
170
160
150
140
130
120
110
100
90
80
70
60
50
40
30
20
10
0
-10
f1 (ppm)

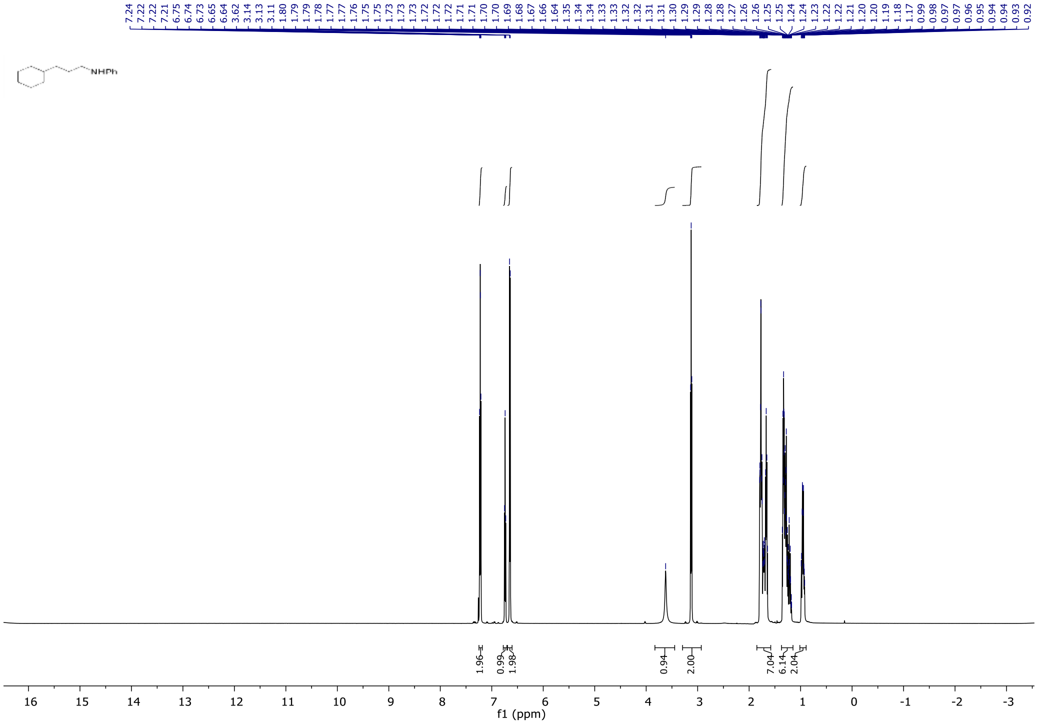
7.24
7.22
7.22
7.21
6.75
6.74
6.73
6.65
6.64
3.62
3.14
3.13
3.11
1.80
1.79
1.79
1.78
1.77
1.77
1.76
1.75
1.75
1.73
1.73
1.73
1.72
1.72
1.72
1.71
1.71
1.70
1.70
1.69
1.68
1.67
1.66
1.64
1.35
1.34
1.34
1.33
1.33
1.32
1.32
1.31
1.30
1.29
1.29
1.28
1.28
1.27
1.26
1.25
1.25
1.24
1.24
1.24
1.23
1.22
1.22
1.21
1.20
1.20
1.19
1.18
1.17
0.99
0.98
0.97
0.97
0.96
0.95
0.94
0.94
0.93
0.92
NHPh
1.96
0.99
1.98
0.94
2.00
7.04
6.14
2.04
16
15
14
13
12
11
10
9
8
7
6
5
4
3
2
1
0
-1
-2
-3
f1 (ppm)

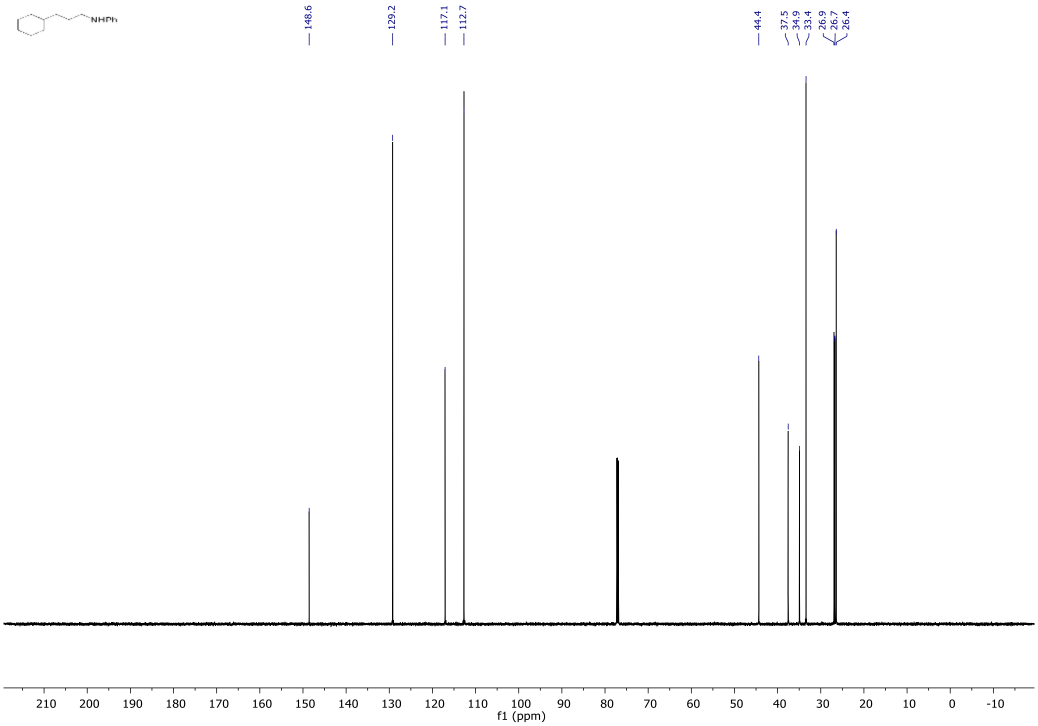
NHPh
148.6
129.2
117.1
112.7
44.4
37.5
34.9
33.4
26.9
26.7
26.4
210
200
190
180
170
160
150
140
130
120
110
100
90
80
70
60
50
40
30
20
10
0
-10
f1 (ppm)

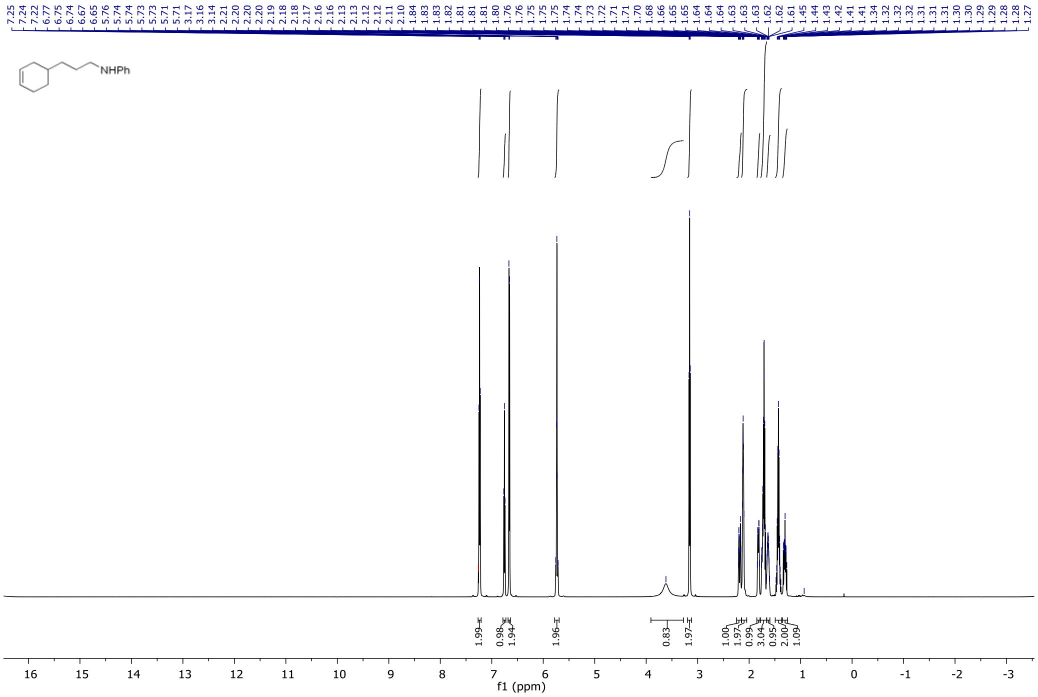
7.25 7.24 7.22 6.77 6.75 6.74 6.67 6.65 5.76 5.74 5.74 5.73 5.73 5.71 3.17 3.16 3.14 2.21 2.20 2.20 2.19 2.18 2.18 2.17 2.16 2.16 2.13 2.13 2.12 2.12 2.11 2.10 1.84 1.83 1.83 1.82 1.81 1.81 1.81 1.80 1.76 1.76 1.75 1.75 1.75 1.74 1.74 1.73 1.72 1.71 1.71 1.70 1.68 1.66 1.65 1.65 1.64 1.64 1.63 1.63 1.63 1.62 1.62 1.61 1.45 1.44 1.43 1.42 1.41 1.41 1.34 1.32 1.32 1.32 1.31 1.31 1.30 1.29 1.29 1.28 1.28 1.27
NHPh
1.99
0.98
1.94
1.96
0.83
1.97
1.00
1.97
0.99
3.04
0.95
2.00
1.09
16 15 14 13 12 11 10 9 8 7 6 5 4 3 2 1 0 -1 -2 -3
f1 (ppm)

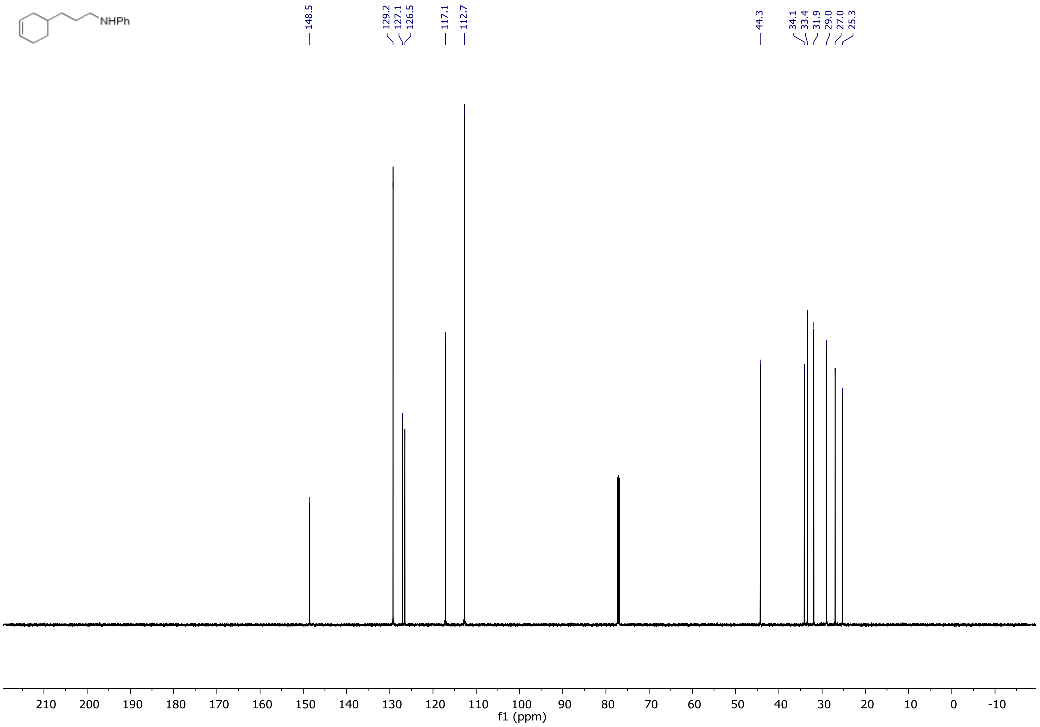
NHPh
148.5
129.2
127.1
126.5
117.1
112.7
44.3
34.1
33.4
31.9
29.0
27.0
25.3
210
200
190
180
170
160
150
140
130
120
110
100
90
80
70
60
50
40
30
20
10
0
-10
f1 (ppm)

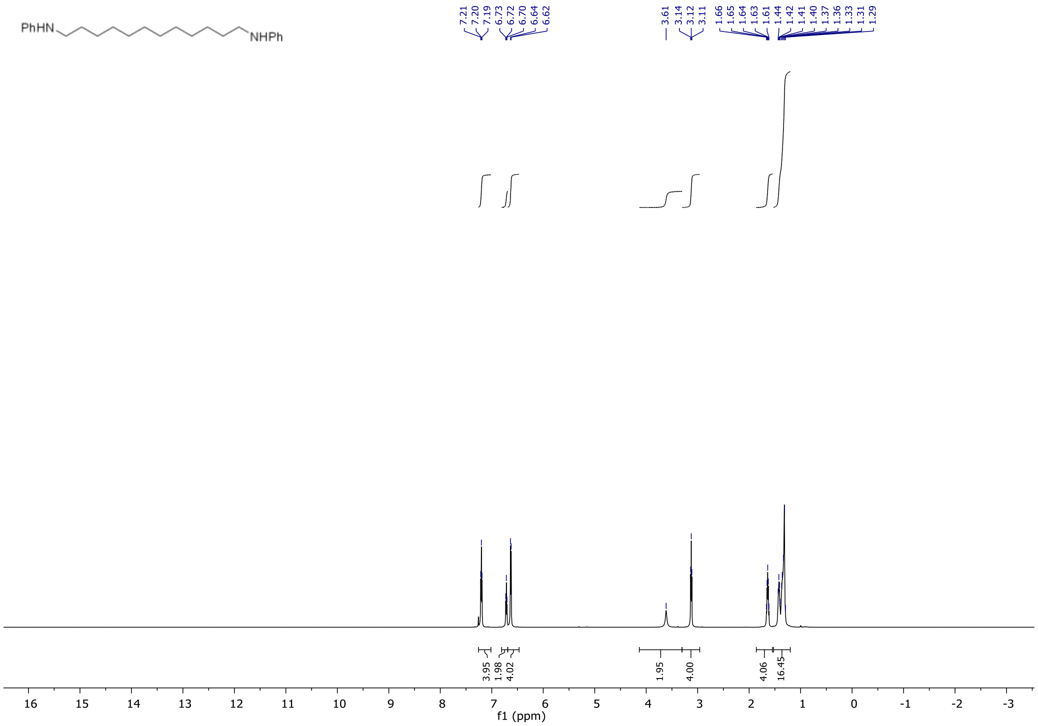
PhHN
NHPh
7.21
7.20
7.19
6.73
6.72
6.70
6.64
6.62
3.61
3.14
3.12
3.11
1.66
1.65
1.64
1.63
1.61
1.44
1.42
1.41
1.40
1.37
1.36
1.33
1.31
1.29
3.95
1.98
4.02
1.95
4.00
4.06
16.45
16
15
14
13
12
11
10
9
8
7
6
5
4
3
2
1
0
-1
-2
-3
f1 (ppm)

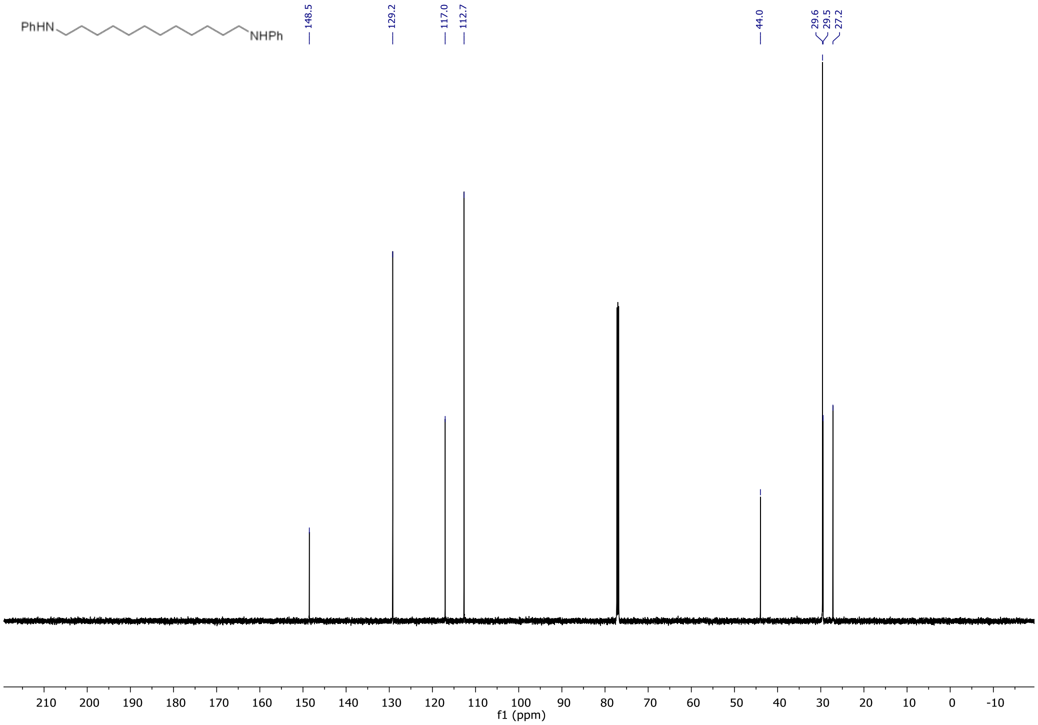
PhHN
NHPh
148.5
129.2
117.0
112.7
44.0
29.6
29.5
27.2
210
200
190
180
170
160
150
140
130
120
110
100
90
80
70
60
50
40
30
20
10
0
-10
f1 (ppm)

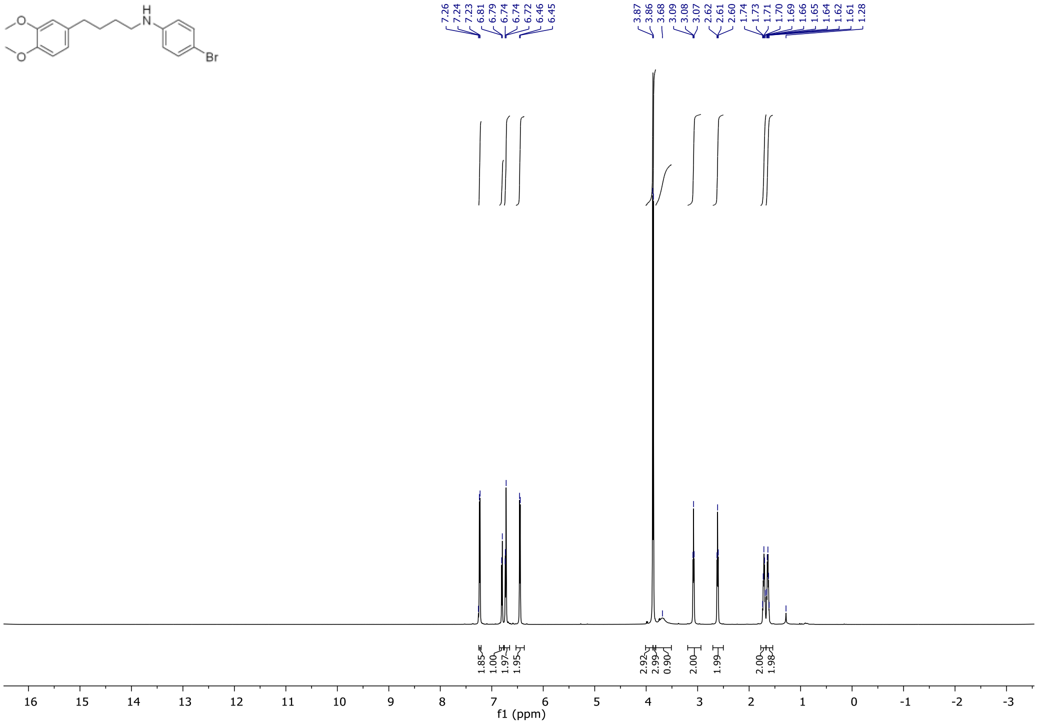
H
N
O
O
Br
7.26
7.24
7.23
6.81
6.79
6.74
6.74
6.72
6.46
6.45
3.87
3.86
3.68
3.09
3.08
3.07
2.62
2.61
2.60
1.74
1.73
1.71
1.70
1.69
1.66
1.65
1.64
1.62
1.61
1.28
1.85
1.00
1.97
1.95
2.92
2.99
0.90
2.00
1.99
2.00
1.98
16
15
14
13
12
11
10
9
8
7
6
5
4
3
2
1
0
-1
-2
-3
f1 (ppm)

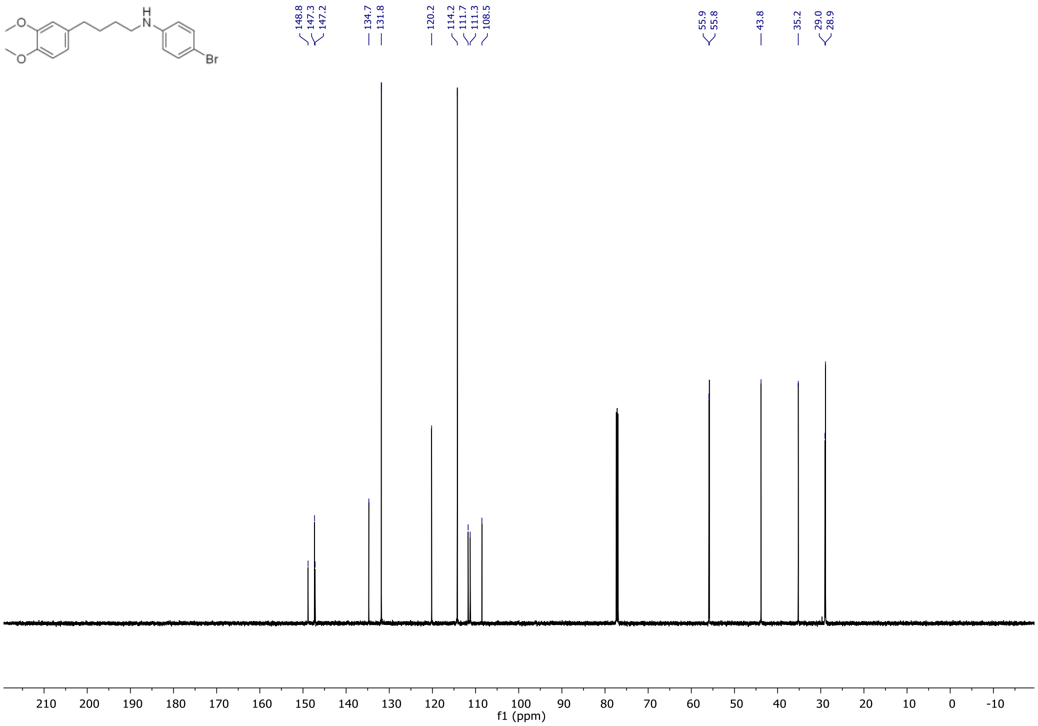
O
O
H
N
Br
148.8
147.3
147.2
134.7
131.8
120.2
114.2
111.7
111.3
108.5
55.9
55.8
43.8
35.2
29.0
28.9
210
200
190
180
170
160
150
140
130
120
110
100
90
80
70
60
50
40
30
20
10
0
-10
f1 (ppm)

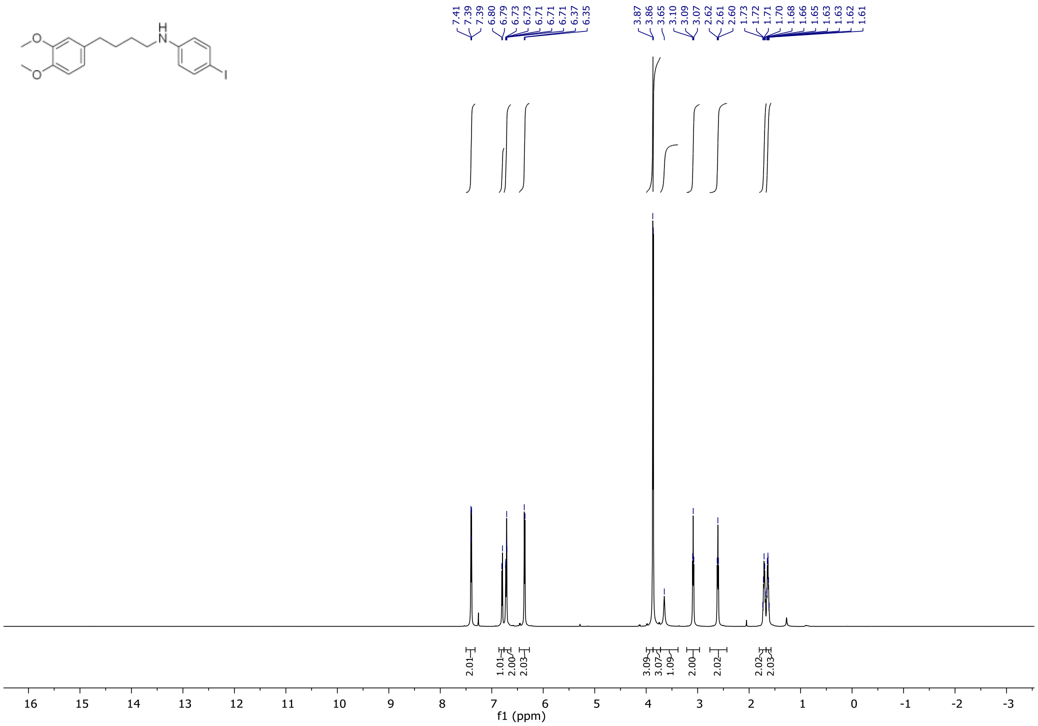
H
N
O
O
I
7.41
7.39
7.39
6.80
6.79
6.73
6.73
6.71
6.71
6.71
6.37
6.35
3.87
3.86
3.65
3.10
3.09
3.07
2.62
2.61
2.60
1.73
1.72
1.71
1.70
1.68
1.66
1.65
1.63
1.63
1.62
1.61
2.01
1.01
2.00
2.03
3.09
3.07
1.09
2.00
2.02
2.02
2.03
16
15
14
13
12
11
10
9
8
7
6
5
4
3
2
1
0
-1
-2
-3
f1 (ppm)

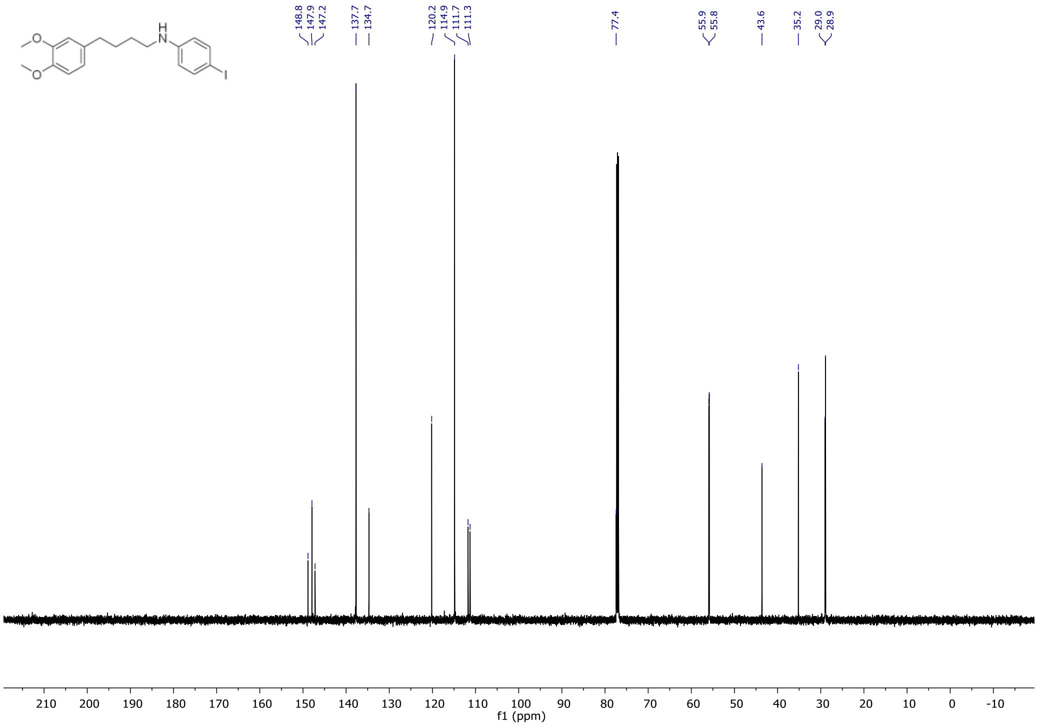
148.8
147.9
147.2
137.7
134.7
120.2
114.9
111.7
111.3
77.4
55.9
55.8
43.6
35.2
29.0
28.9
210 200 190 180 170 160 150 140 130 120 110 100 90 80 70 60 50 40 30 20 10 0 -10
f1 (ppm)
O
O
H
N
I

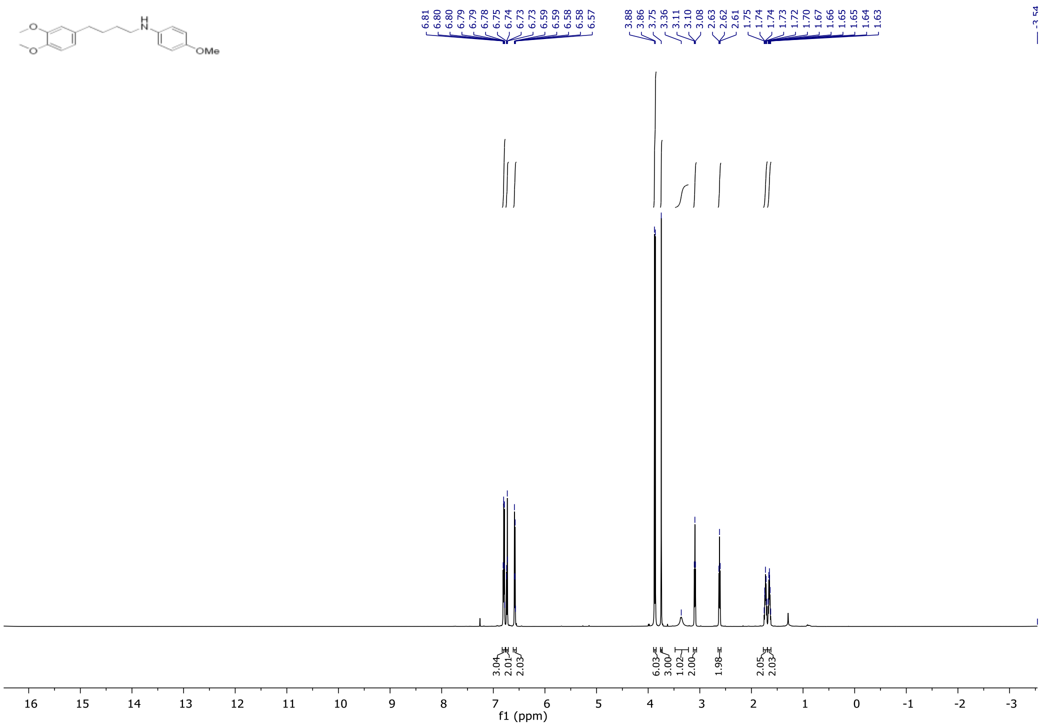
OMe
H
N
6.81
6.80
6.80
6.79
6.79
6.78
6.75
6.74
6.73
6.73
6.59
6.59
6.58
6.58
6.57
3.88
3.86
3.75
3.36
3.11
3.10
3.08
2.63
2.62
2.61
1.75
1.74
1.74
1.73
1.72
1.70
1.67
1.66
1.65
1.65
1.64
1.63
-3.54
3.04
2.01
2.03
6.03
3.00
1.02
2.00
1.98
2.05
2.03
16
15
14
13
12
11
10
9
8
7
6
5
4
3
2
1
0
-1
-2
-3
f1 (ppm)

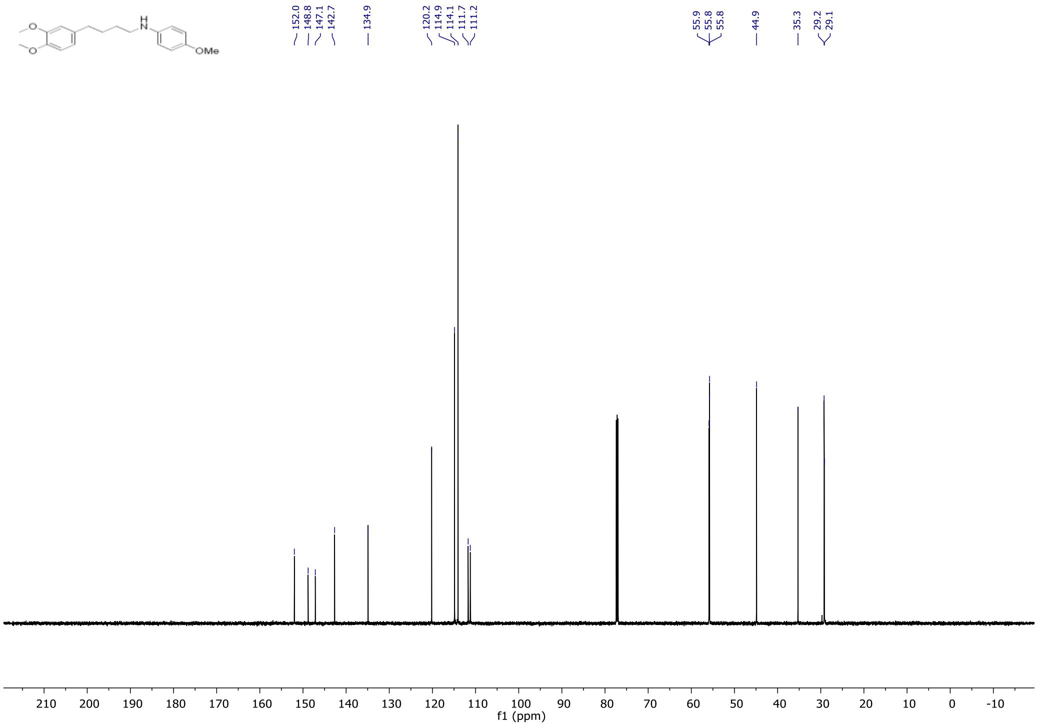

OMe
N
H
152.0
148.8
147.1
142.7
134.9
120.2
114.9
114.1
111.7
111.2
55.9
55.8
55.8
44.9
35.3
29.2
29.1
210
200
190
180
170
160
150
140
130
120
110
100
90
80
70
60
50
40
30
20
10
0
-10
f1 (ppm)

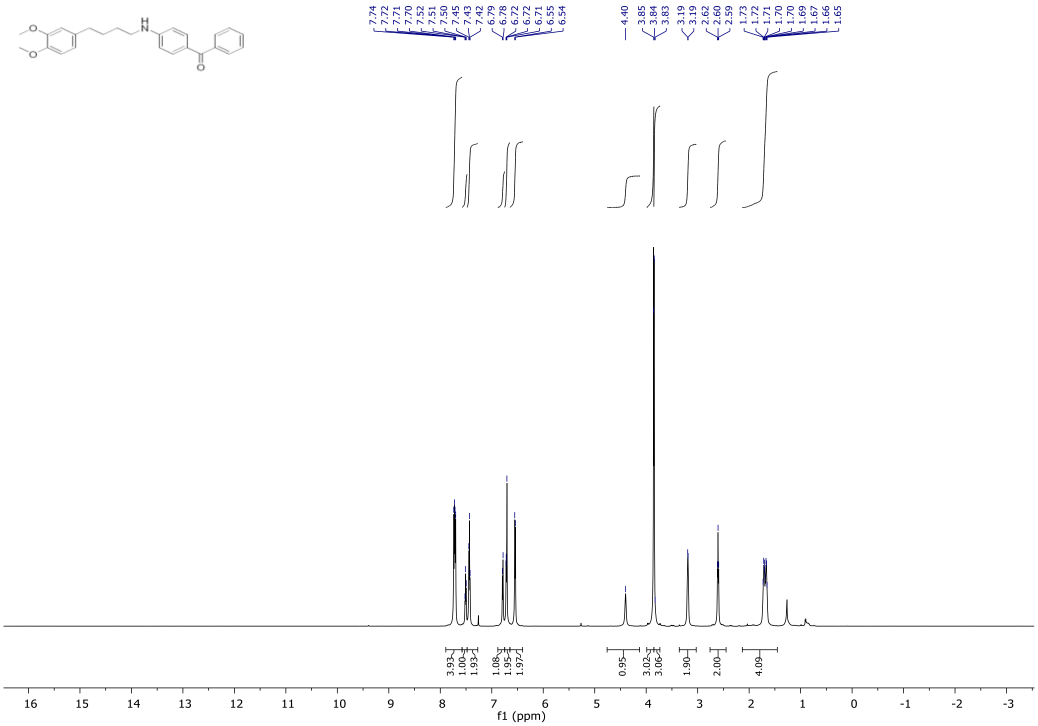
7.74
7.72
7.71
7.70
7.52
7.51
7.50
7.45
7.43
7.42
6.79
6.78
6.72
6.72
6.71
6.55
6.54
4.40
3.85
3.84
3.83
3.19
3.19
2.62
2.60
2.59
1.73
1.72
1.71
1.70
1.70
1.69
1.67
1.66
1.65
3.93
1.00
1.93
1.08
1.95
1.97
0.95
3.02
3.06
1.90
2.00
4.09
16
15
14
13
12
11
10
9
8
7
6
5
4
3
2
1
0
-1
-2
-3
f1 (ppm)

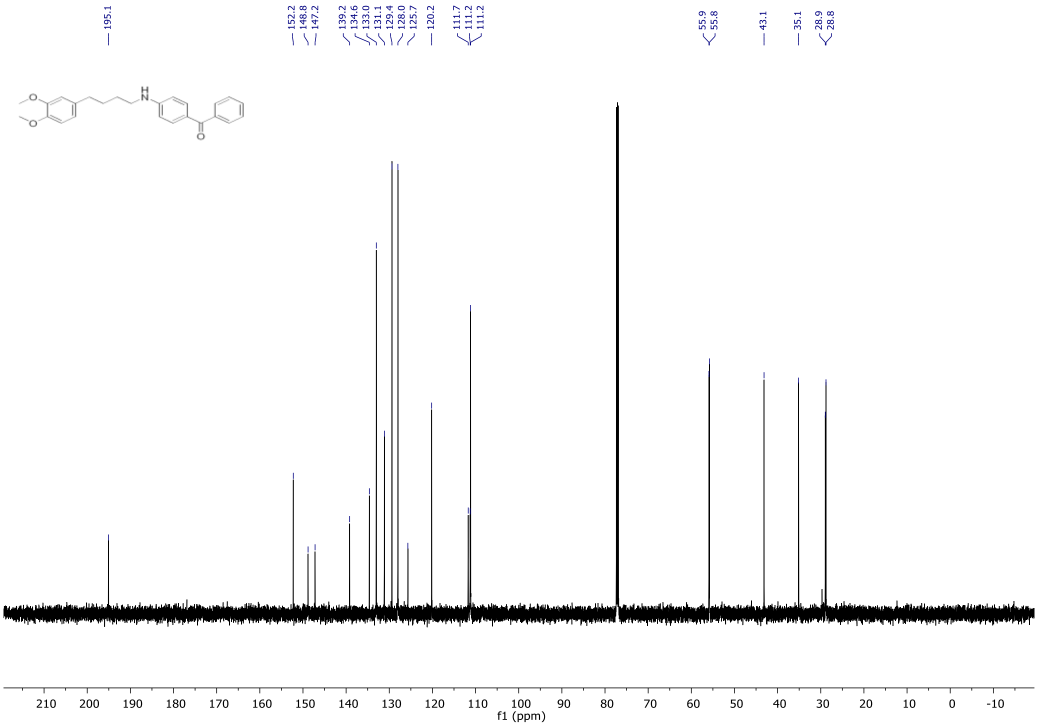
195.1
152.2
148.8
147.2
139.2
134.6
133.0
131.1
129.4
128.0
125.7
120.2
111.7
111.2
111.2
55.9
55.8
43.1
35.1
28.9
28.8
O
O
H
N
O
210
200
190
180
170
160
150
140
130
120
110
100
90
80
70
60
50
40
30
20
10
0
-10
f1 (ppm)

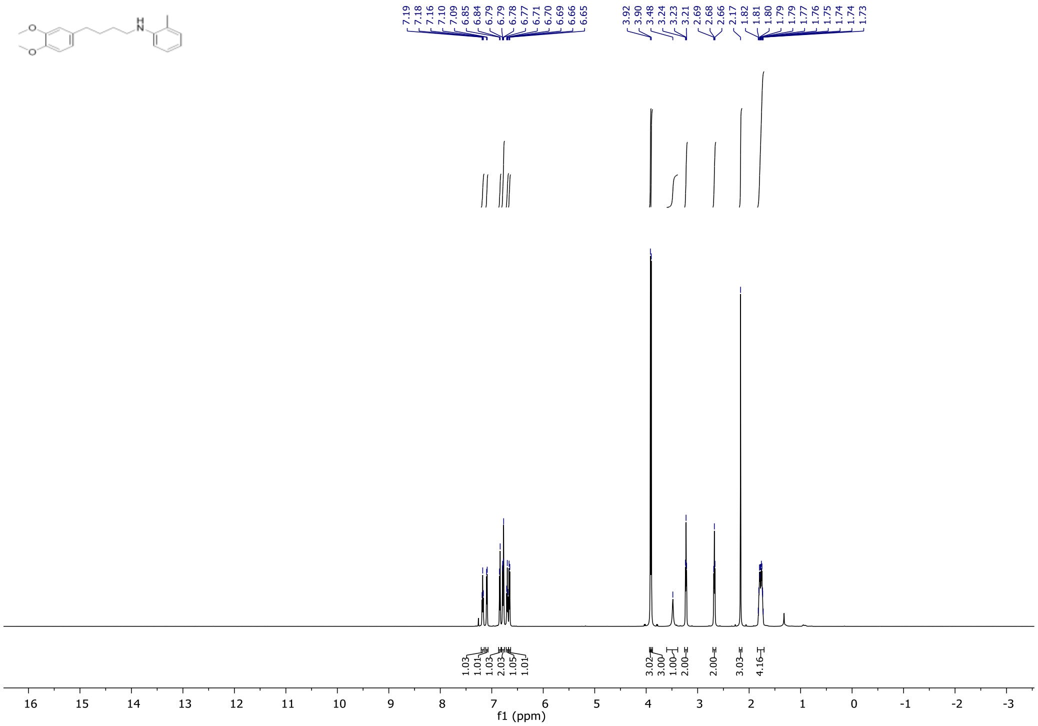
N
H
O
O
7.19
7.18
7.16
7.10
7.09
6.85
6.84
6.79
6.79
6.78
6.77
6.71
6.70
6.69
6.66
6.65
3.92
3.90
3.48
3.24
3.23
3.21
2.69
2.68
2.66
2.17
1.82
1.81
1.80
1.79
1.79
1.77
1.76
1.75
1.74
1.74
1.73
1.03
1.01
1.03
2.03
1.05
1.01
3.02
3.00
1.00
2.00
2.00
3.03
4.16
16
15
14
13
12
11
10
9
8
7
6
5
4
3
2
1
0
-1
-2
-3
f1 (ppm)

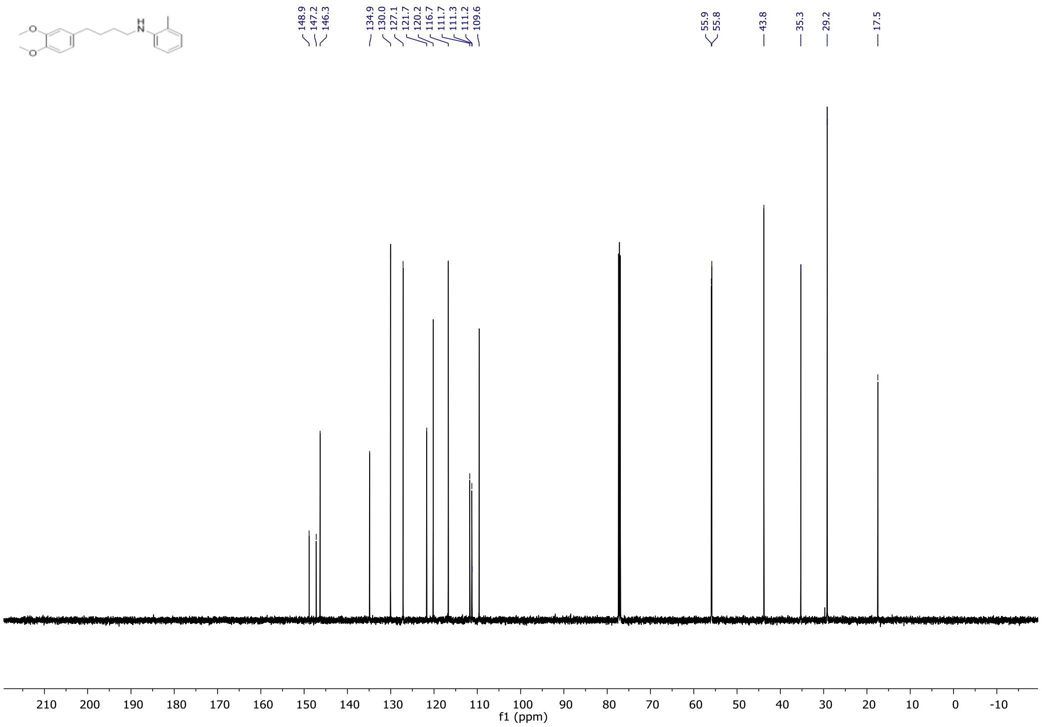
O
O
H
N
148.9
147.2
146.3
134.9
130.0
127.1
121.7
120.2
116.7
111.7
111.3
111.2
109.6
55.9
55.8
43.8
35.3
29.2
17.5
210
200
190
180
170
160
150
140
130
120
110
100
90
80
70
60
50
40
30
20
10
0
-10
f1 (ppm)

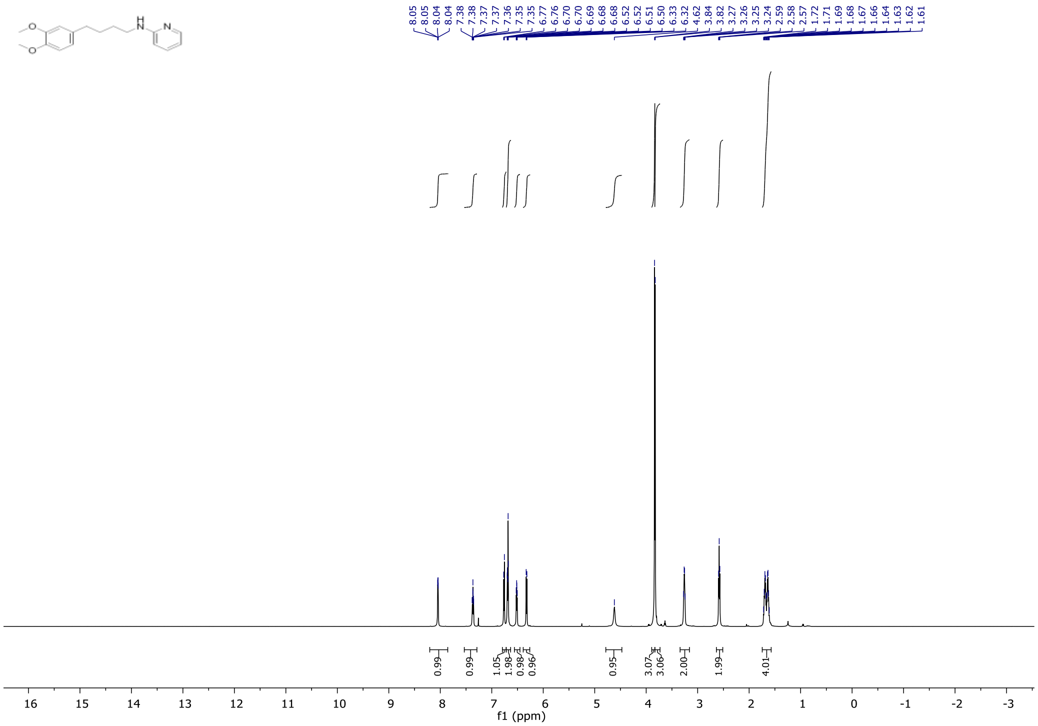
O
O
H
N
N
8.05
8.05
8.04
8.04
7.38
7.37
7.37
7.36
7.35
7.35
6.77
6.76
6.70
6.69
6.68
6.68
6.52
6.52
6.51
6.50
6.33
6.32
4.62
3.84
3.82
3.27
3.26
3.25
3.24
2.59
2.58
2.57
1.72
1.71
1.69
1.68
1.67
1.66
1.64
1.63
1.62
1.61
0.99
0.99
1.05
1.98
0.98
0.96
0.95
3.07
3.06
2.00
1.99
4.01
16
15
14
13
12
11
10
9
8
7
6
5
4
3
2
1
0
-1
-2
-3
f1 (ppm)

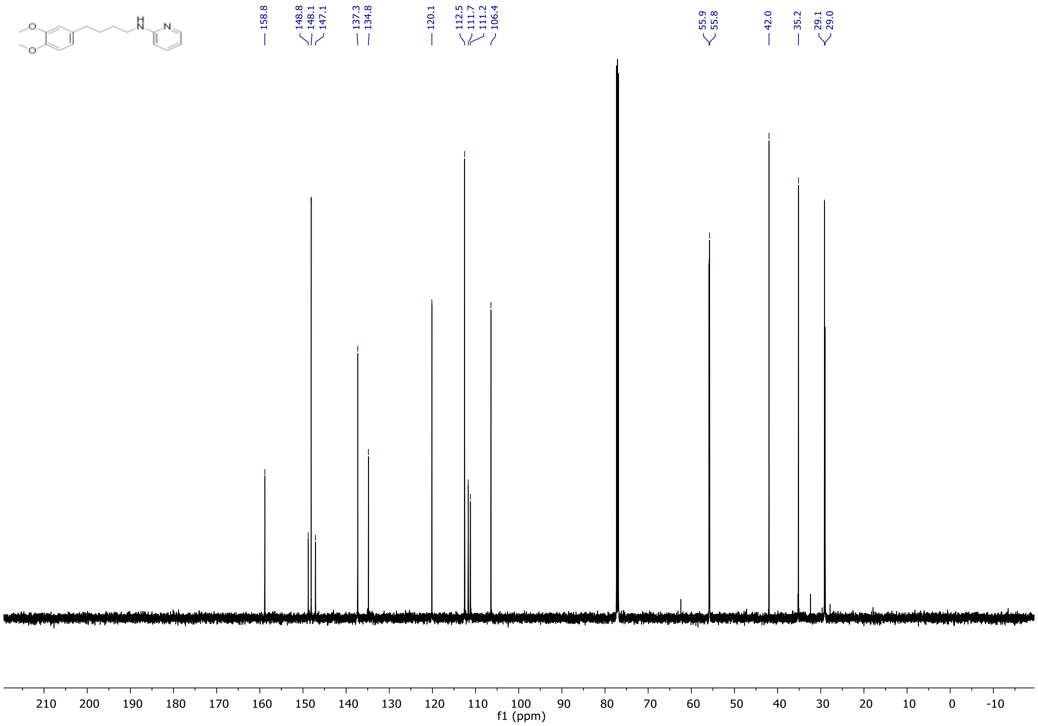
158.8
148.8
148.1
147.1
137.3
134.8
120.1
112.5
111.7
111.2
106.4
55.9
55.8
42.0
35.2
29.1
29.0
210
200
190
180
170
160
150
140
130
120
110
100
90
80
70
60
50
40
30
20
10
0
-10
f1 (ppm)

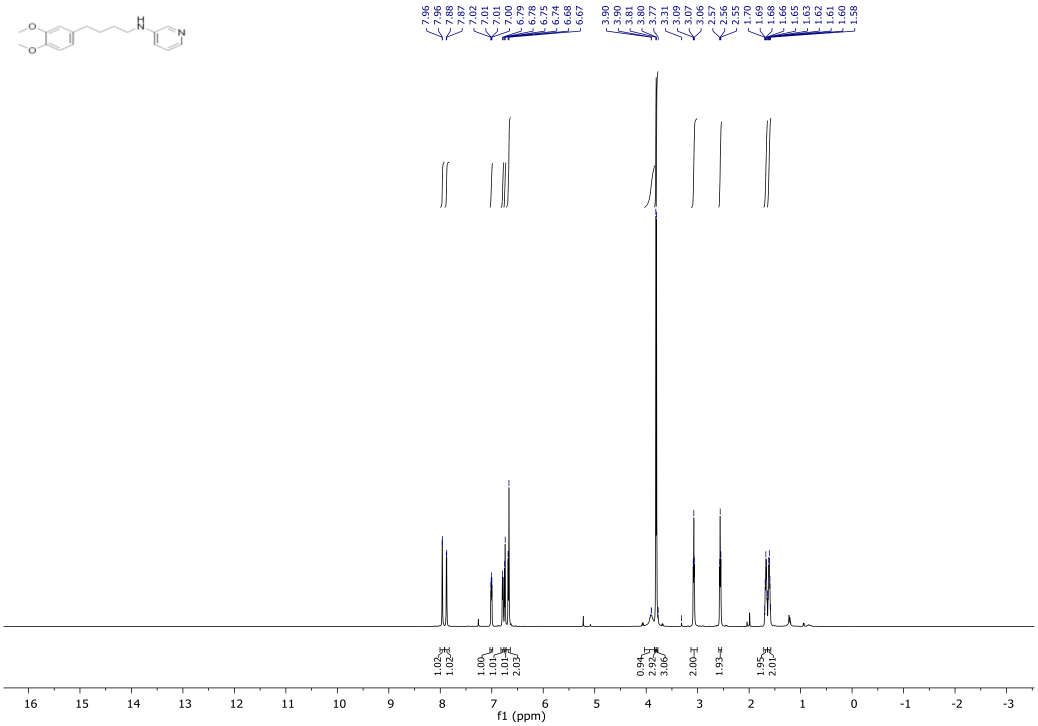
O
O
H
N
N
7.96
7.96
7.88
7.87
7.02
7.01
7.01
7.00
6.79
6.78
6.75
6.74
6.68
6.67
3.90
3.90
3.81
3.80
3.77
3.31
3.09
3.07
3.06
2.57
2.56
2.55
1.70
1.69
1.68
1.66
1.65
1.63
1.62
1.61
1.60
1.58
1.02
1.02
1.00
1.01
1.01
2.03
0.94
2.92
3.06
2.00
1.93
1.95
2.01
16
15
14
13
12
11
10
9
8
7
6
5
4
3
2
1
0
-1
-2
-3
f1 (ppm)

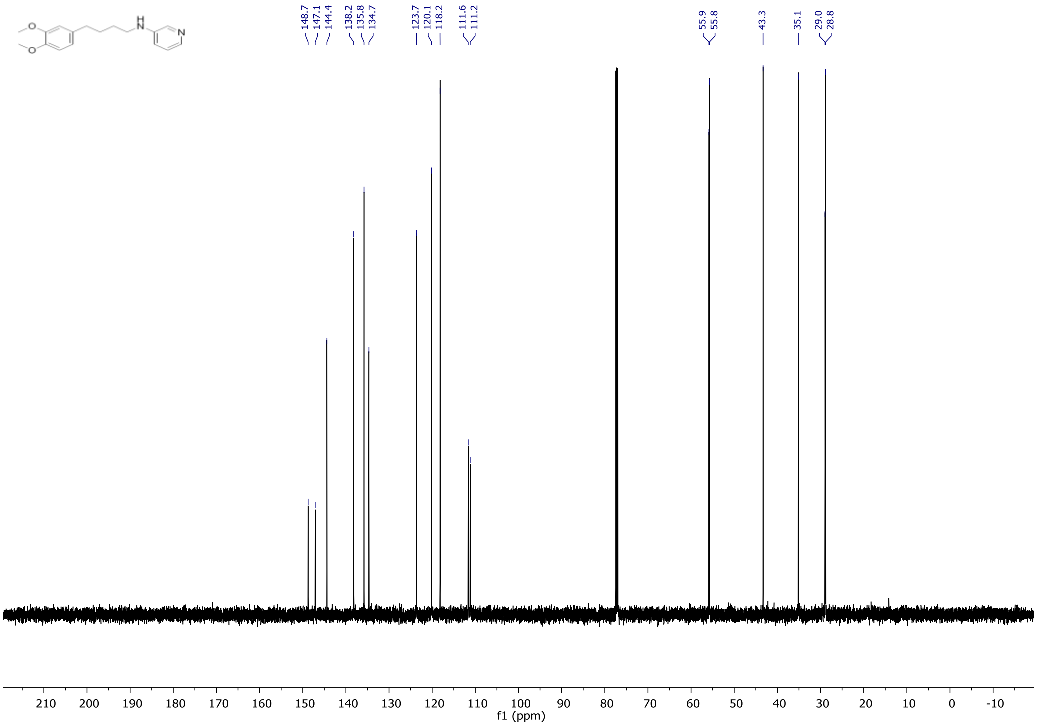
148.7
147.1
144.4
138.2
135.8
134.7
123.7
120.1
118.2
111.6
111.2
55.9
55.8
43.3
35.1
29.0
28.8
O
O
N
H
N
210
200
190
180
170
160
150
140
130
120
110
100
90
80
70
60
50
40
30
20
10
0
-10
f1 (ppm)

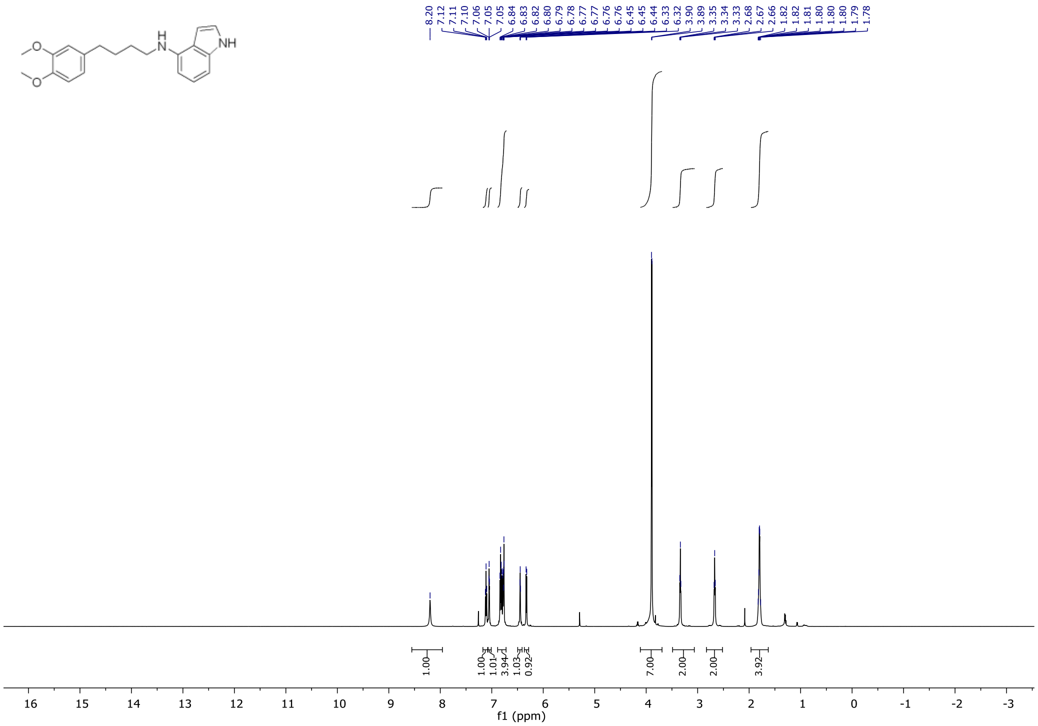
O
O
H
N
NH
8.20
7.12
7.11
7.10
7.06
7.05
7.05
6.84
6.83
6.82
6.80
6.79
6.78
6.77
6.76
6.76
6.45
6.45
6.44
6.33
6.32
3.90
3.89
3.35
3.34
3.33
2.68
2.67
2.66
1.82
1.82
1.81
1.80
1.80
1.80
1.79
1.78
1.00
1.00
1.01
3.94
1.03
0.92
7.00
2.00
2.00
3.92
16
15
14
13
12
11
10
9
8
7
6
5
4
3
2
1
0
-1
-2
-3
f1 (ppm)

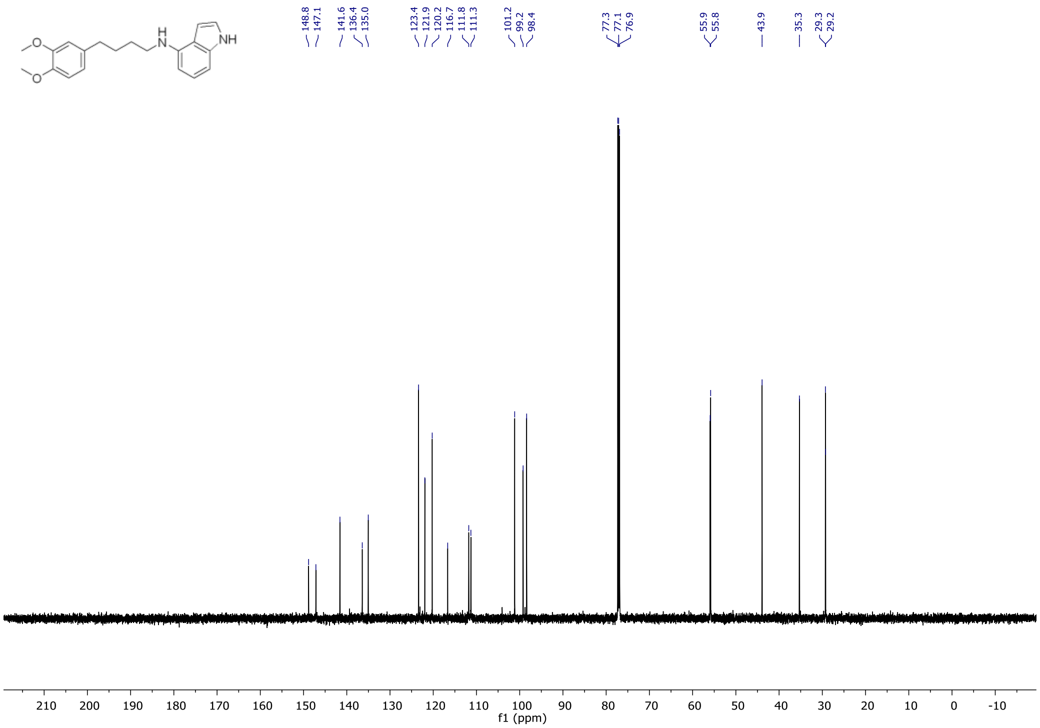

O
O
H
N
NH
148.8
147.1
141.6
136.4
135.0
123.4
121.9
120.2
116.7
111.8
111.3
101.2
99.2
98.4
77.3
77.1
76.9
55.9
55.8
43.9
35.3
29.3
29.2
210
200
190
180
170
160
150
140
130
120
110
100
90
80
70
60
50
40
30
20
10
0
-10
f1 (ppm)

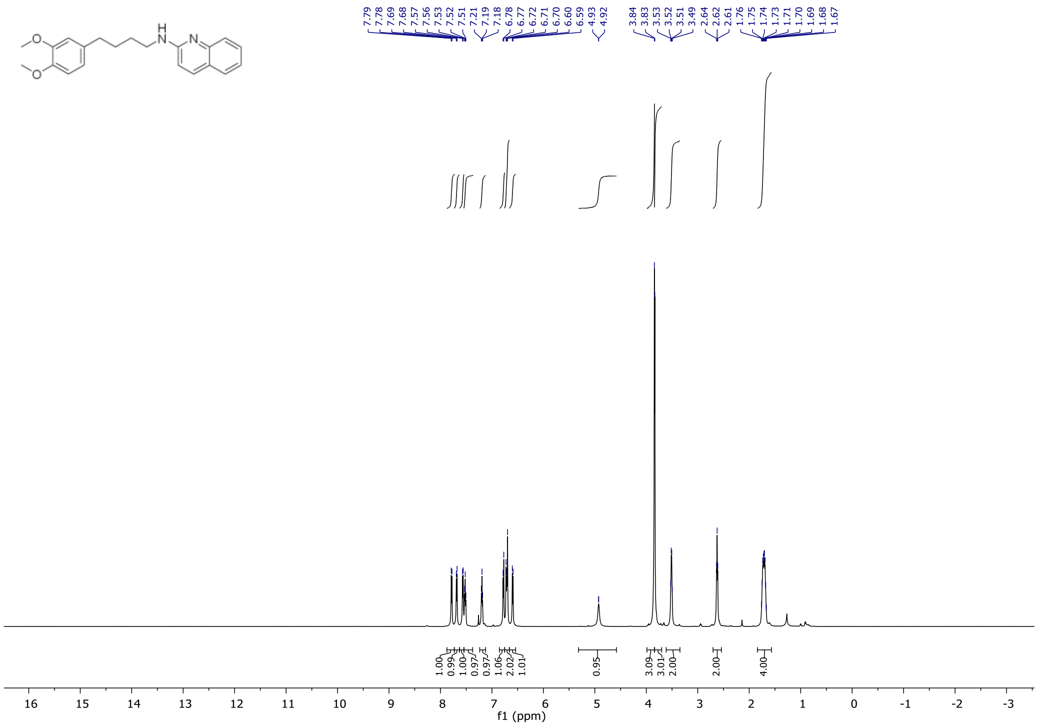

O
O
H
N
N
7.79
7.78
7.69
7.68
7.57
7.56
7.53
7.52
7.51
7.21
7.19
7.18
6.78
6.77
6.72
6.71
6.70
6.60
6.59
4.93
4.92
3.84
3.83
3.53
3.52
3.51
3.49
2.64
2.62
2.61
1.76
1.75
1.74
1.73
1.71
1.70
1.69
1.68
1.67
1.00
0.99
1.00
0.97
0.97
1.06
2.02
1.01
0.95
3.09
3.01
2.00
2.00
4.00
16
15
14
13
12
11
10
9
8
7
6
5
4
3
2
1
0
-1
-2
-3
f1 (ppm)

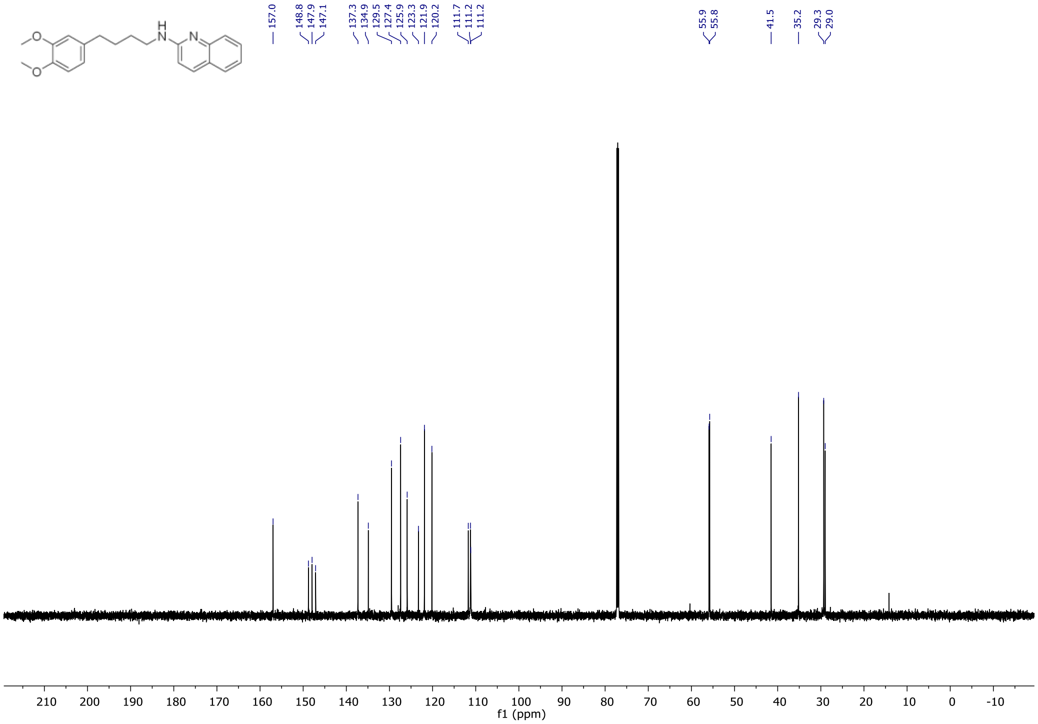
O
O
H
N
N
157.0
148.8
147.9
147.1
137.3
134.9
129.5
127.4
125.9
123.3
121.9
120.2
111.7
111.2
111.2
55.9
55.8
41.5
35.2
29.3
29.0
210
200
190
180
170
160
150
140
130
120
110
100
90
80
70
60
50
40
30
20
10
0
-10
f1 (ppm)

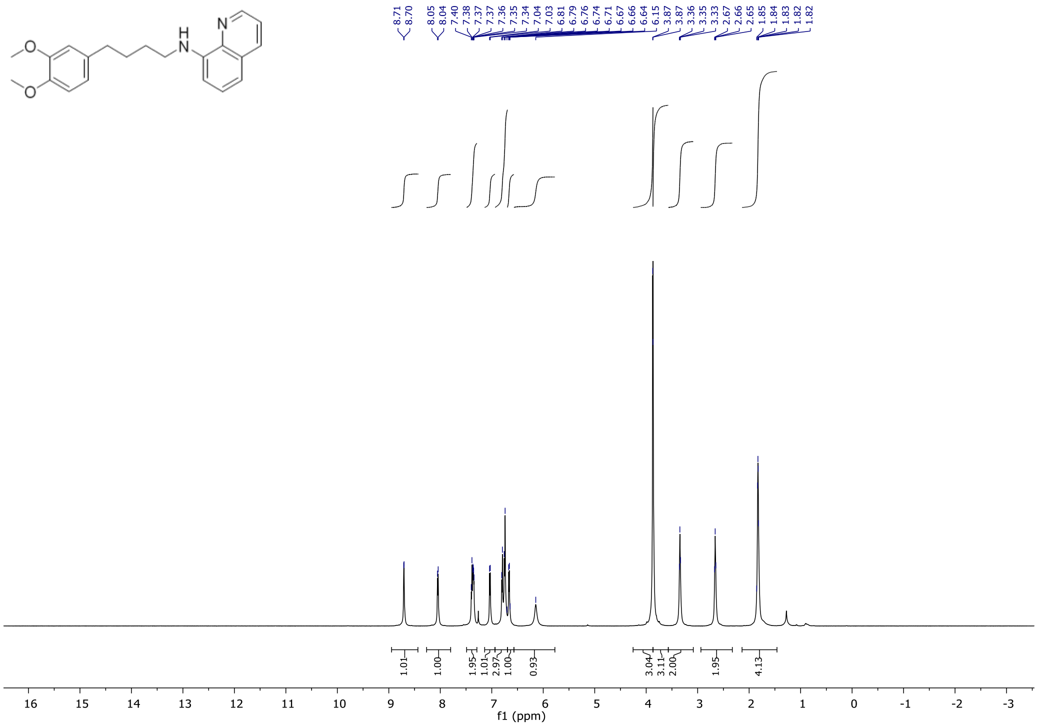
O
O
H
N
N
8.71
8.70
8.05
8.04
7.40
7.38
7.37
7.37
7.36
7.35
7.34
7.04
7.03
6.81
6.79
6.76
6.74
6.71
6.67
6.66
6.64
6.15
3.87
3.87
3.36
3.35
3.33
2.67
2.66
2.65
1.85
1.84
1.83
1.82
1.82
1.01
1.00
1.95
1.01
2.97
1.00
0.93
3.04
3.11
2.00
1.95
4.13
16
15
14
13
12
11
10
9
8
7
6
5
4
3
2
1
0
-1
-2
-3
f1 (ppm)

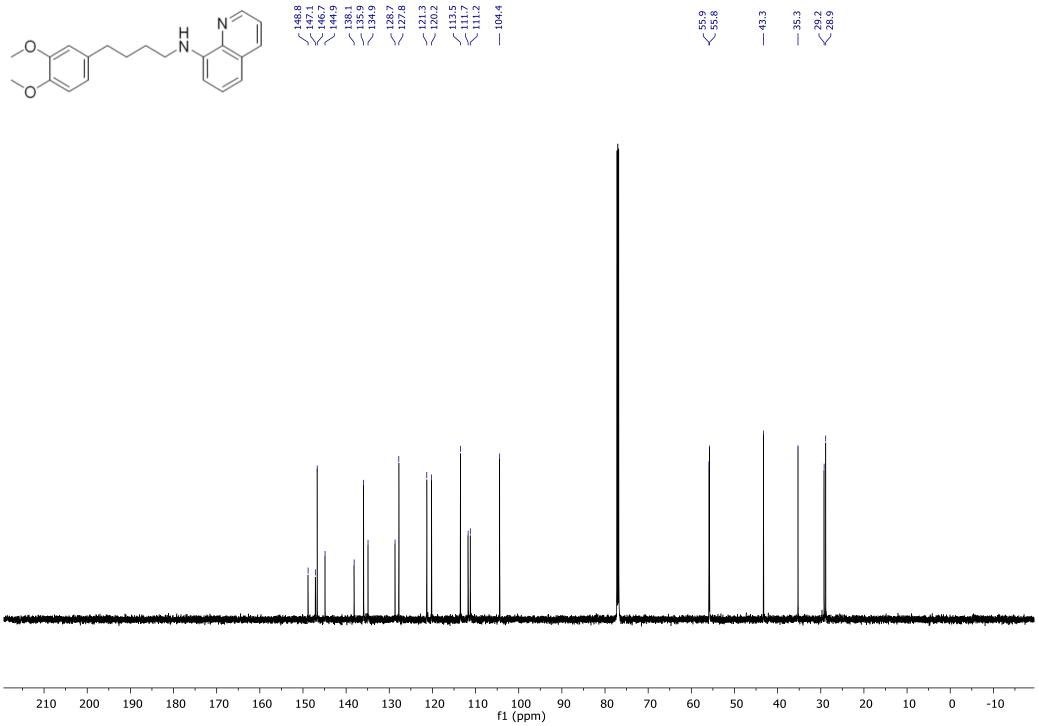
148.8
147.1
146.7
144.9
138.1
135.9
134.9
128.7
127.8
121.3
120.2
113.5
111.7
111.2
104.4
55.9
55.8
43.3
35.3
29.2
28.9
210 200 190 180 170 160 150 140 130 120 110 100 90 80 70 60 50 40 30 20 10 0 -10
f1 (ppm)
O
O
H
N
N

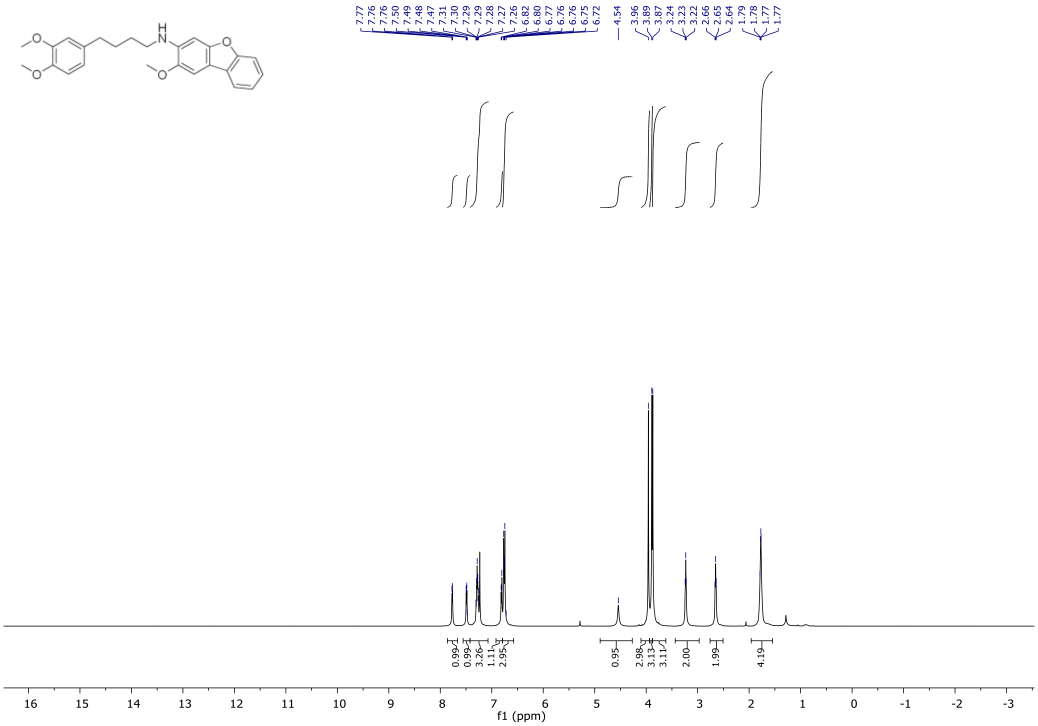
H
N
O
O
O
O

7.77
7.76
7.76
7.50
7.49
7.48
7.47
7.31
7.30
7.29
7.29
7.28
7.27
7.26
6.82
6.80
6.77
6.76
6.76
6.75
6.72
4.54
3.96
3.89
3.87
3.24
3.23
3.22
2.66
2.65
2.64
1.79
1.78
1.77
1.77
0.99
0.99
3.26
1.11
2.95
0.95
2.98
3.13
3.11
2.00
1.99
4.19
16
15
14
13
12
11
10
9
8
7
6
5
4
3
2
1
0
-1
-2
-3
f1 (ppm)

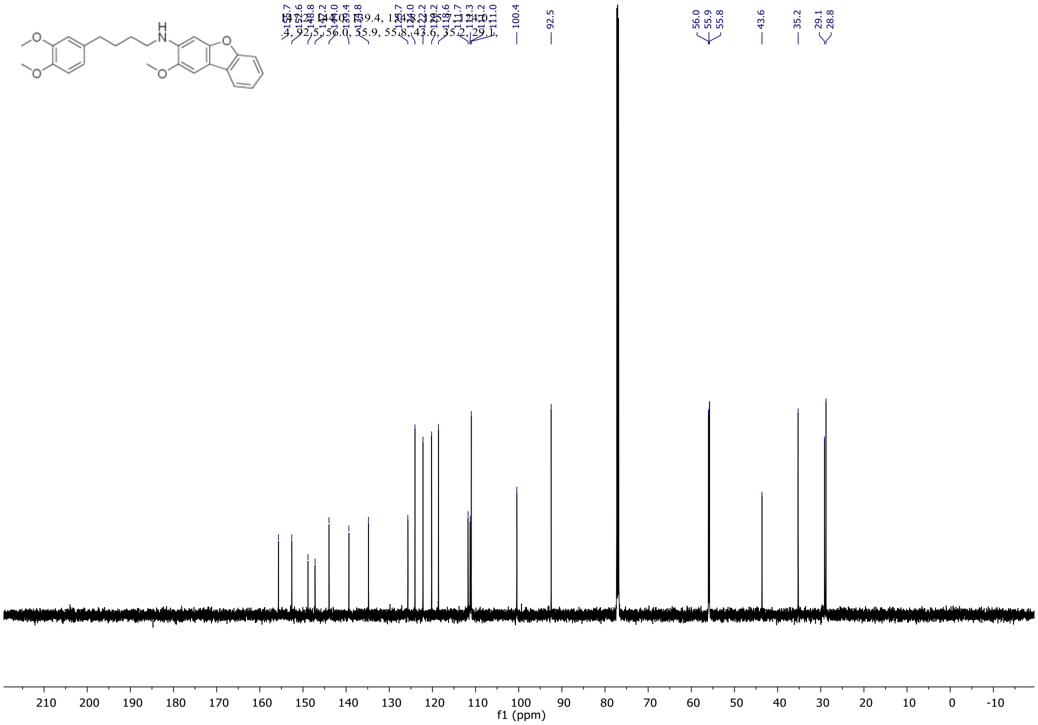
155.7
152.6
148.8
147.2
144.0
139.4
134.8
125.7
124.0
122.2
120.2
118.6
111.7
111.3
111.2
111.0
100.4
92.5
56.0
55.9
55.8
43.6
35.2
29.1
28.8
147.2, 144.0, 139.4, 134.8, 125.7, 124.0,
.4, 92.5, 56.0, 55.9, 55.8, 43.6, 35.2, 29.1,
H
N
O
O
O
O
210
200
190
180
170
160
150
140
130
120
110
100
90
80
70
60
50
40
30
20
10
0
-10
f1 (ppm)

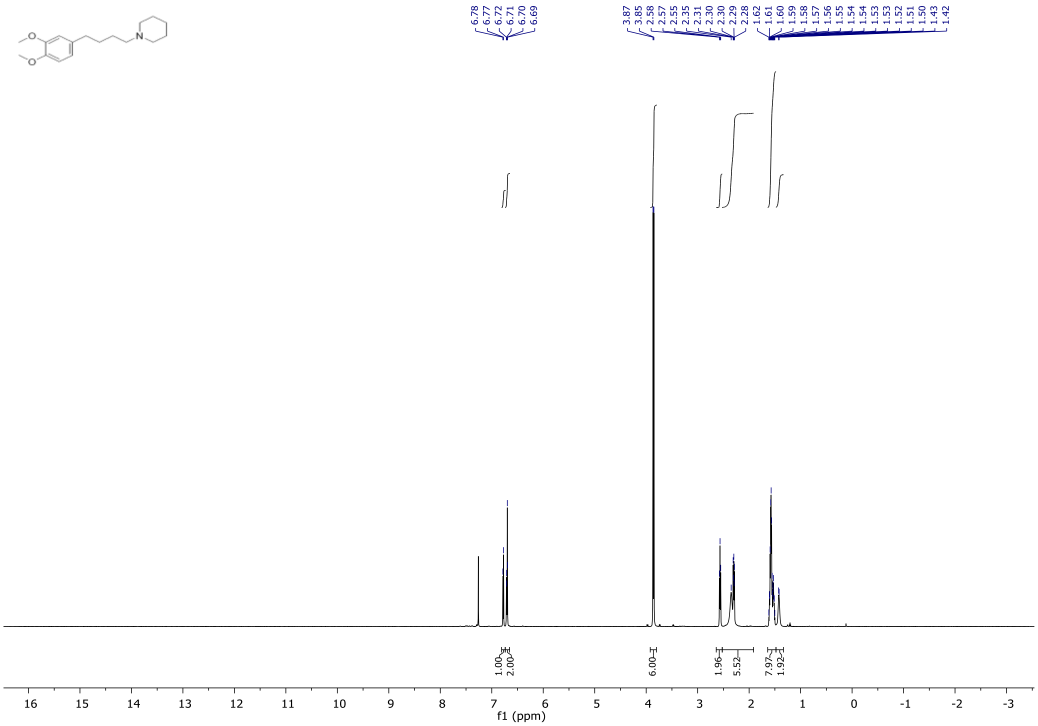
N
O
O
6.78
6.77
6.72
6.71
6.70
6.69
3.87
3.85
2.58
2.57
2.55
2.35
2.31
2.30
2.30
2.29
2.28
1.62
1.61
1.60
1.59
1.58
1.57
1.56
1.55
1.54
1.54
1.53
1.53
1.52
1.51
1.50
1.43
1.42
1.00
2.00
6.00
1.96
5.52
7.97
1.92
16
15
14
13
12
11
10
9
8
7
6
5
4
3
2
1
0
-1
-2
-3
f1 (ppm)

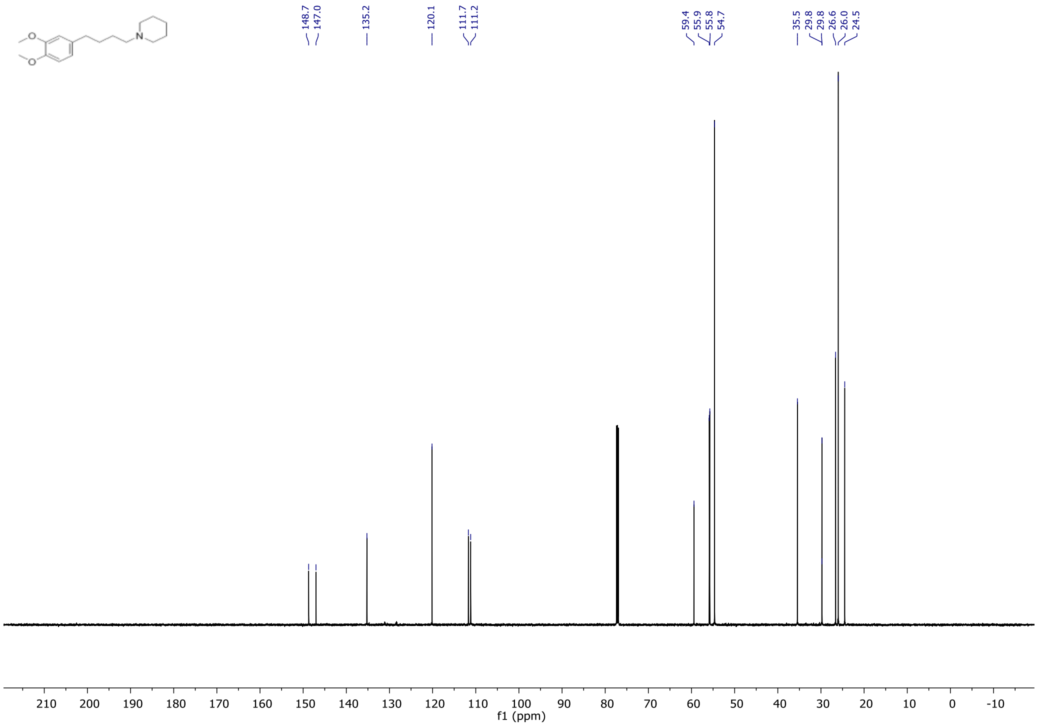
O
O
N
148.7
147.0
135.2
120.1
111.7
111.2
59.4
55.9
55.8
54.7
35.5
29.8
29.8
26.6
26.0
24.5
210
200
190
180
170
160
150
140
130
120
110
100
90
80
70
60
50
40
30
20
10
0
-10
f1 (ppm)

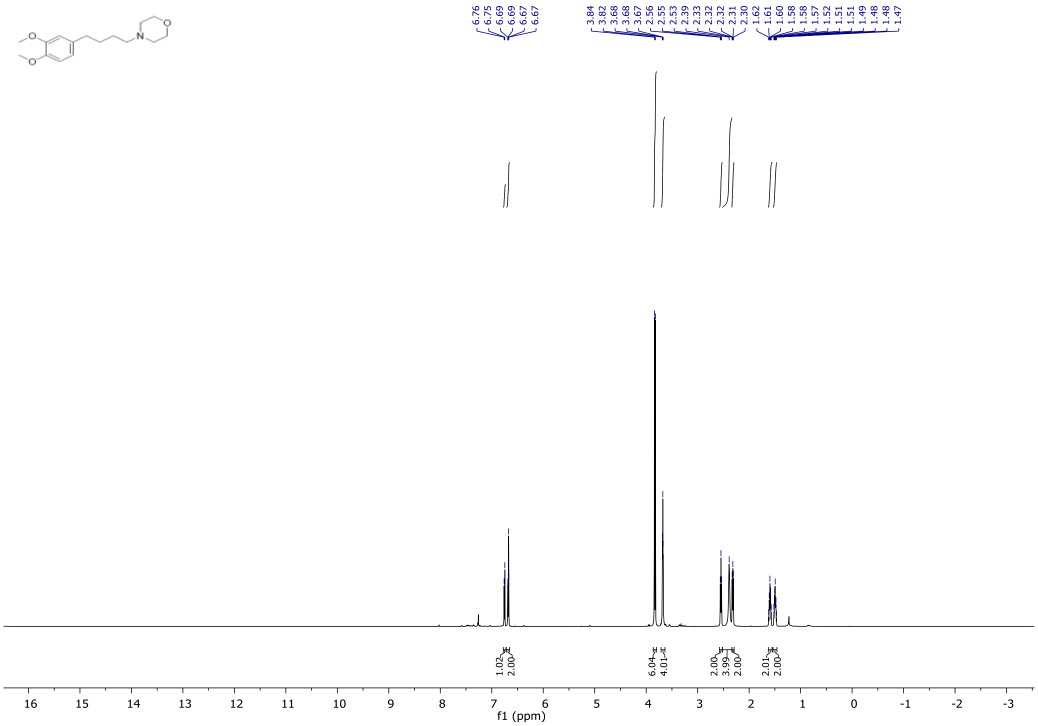
O
O
N
O
6.76
6.75
6.69
6.69
6.67
6.67
3.84
3.82
3.68
3.68
3.67
2.56
2.55
2.53
2.39
2.33
2.32
2.32
2.31
2.30
1.62
1.61
1.60
1.58
1.58
1.57
1.52
1.51
1.49
1.48
1.47
1.02
2.00
6.04
4.01
2.00
3.99
2.00
2.01
2.00
16
15
14
13
12
11
10
9
8
7
6
5
4
3
2
1
0
-1
-2
-3
f1 (ppm)

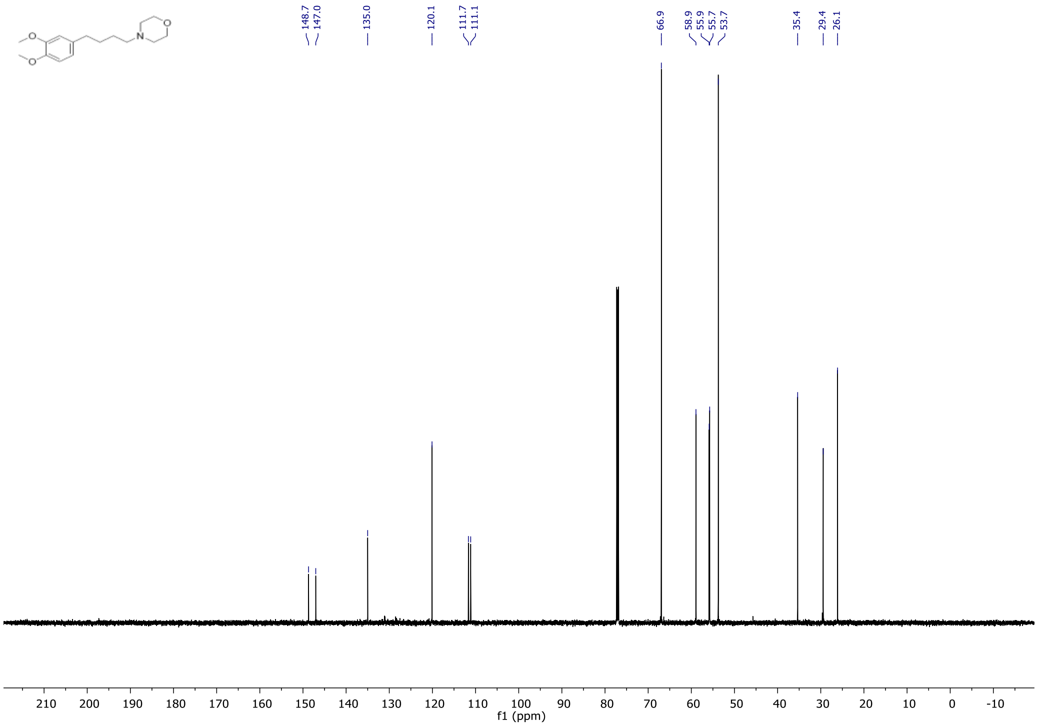
148.7
147.0
135.0
120.1
111.7
111.1
66.9
58.9
55.9
55.7
53.7
35.4
29.4
26.1
O
O
N
O
210
200
190
180
170
160
150
140
130
120
110
100
90
80
70
60
50
40
30
20
10
0
-10
f1 (ppm)

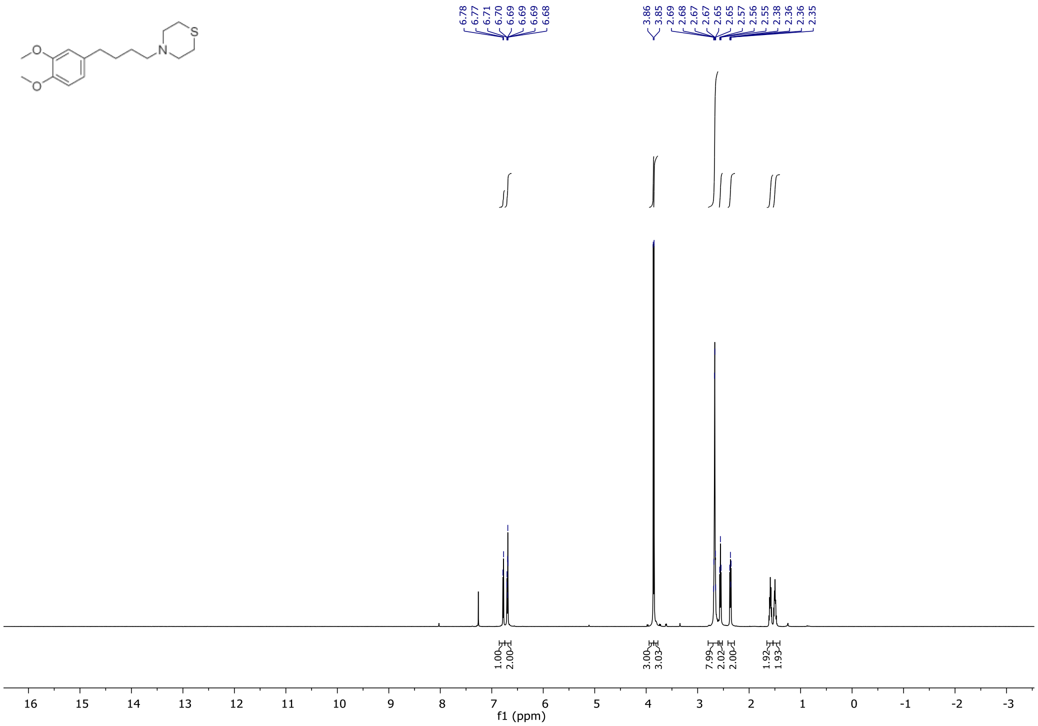
O
O
N
S
6.78
6.77
6.71
6.70
6.69
6.69
6.69
6.68
3.86
3.85
2.69
2.68
2.67
2.67
2.65
2.65
2.57
2.56
2.55
2.38
2.36
2.36
2.35
1.00
2.00
3.00
3.03
7.99
2.02
2.00
1.92
1.93
16
15
14
13
12
11
10
9
8
7
6
5
4
3
2
1
0
-1
-2
-3
f1 (ppm)

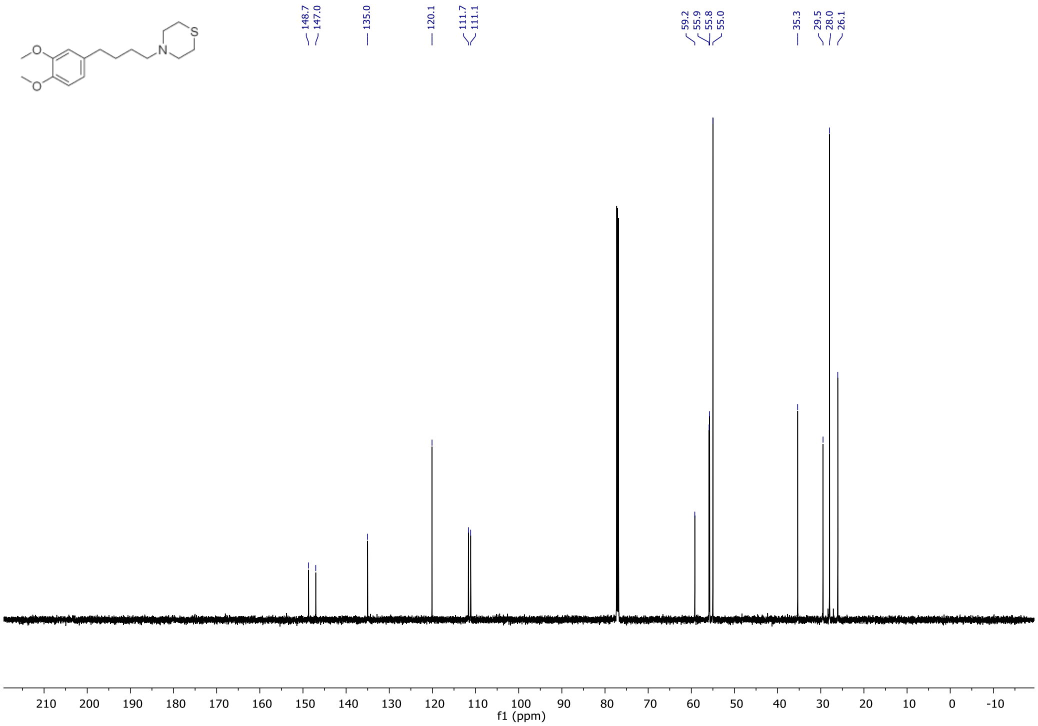
O
O
N
S
148.7
147.0
135.0
120.1
111.7
111.1
59.2
55.9
55.8
55.0
35.3
29.5
28.0
26.1
210
200
190
180
170
160
150
140
130
120
110
100
90
80
70
60
50
40
30
20
10
0
-10
f1 (ppm)

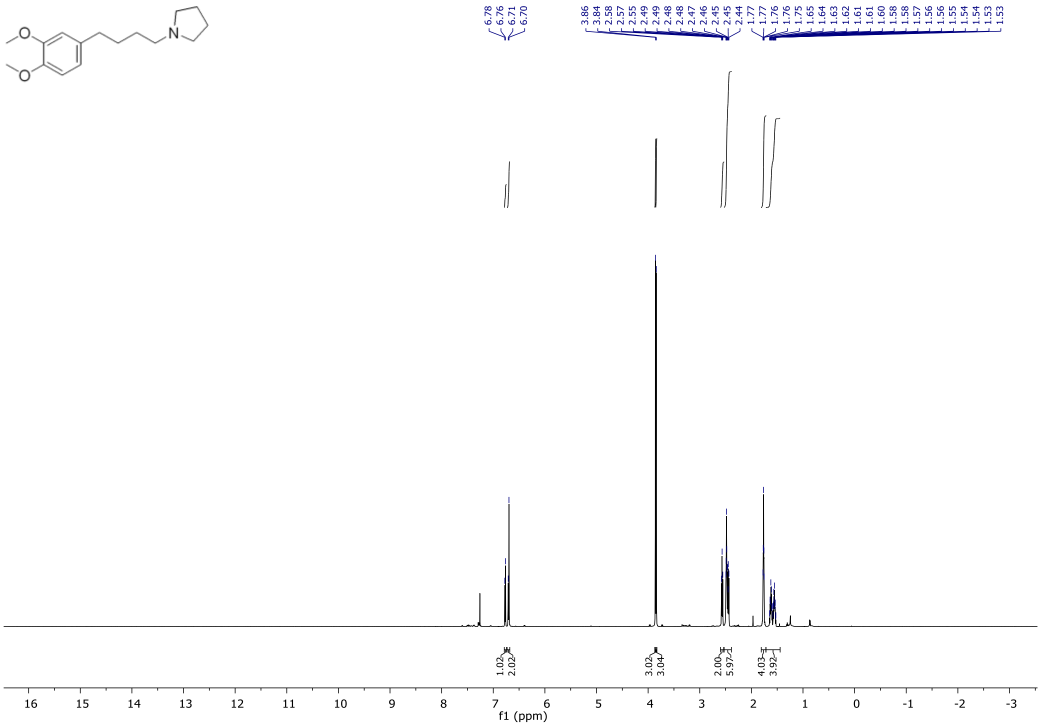
6.78
6.76
6.71
6.70
3.86
3.84
2.58
2.57
2.55
2.49
2.49
2.48
2.48
2.47
2.46
2.45
2.45
2.44
1.77
1.77
1.76
1.75
1.65
1.64
1.63
1.62
1.61
1.61
1.60
1.58
1.57
1.56
1.56
1.55
1.54
1.53
1.53
O
O
N
1.02
2.02
3.02
3.04
2.00
5.97
4.03
3.92
16
15
14
13
12
11
10
9
8
7
6
5
4
3
2
1
0
-1
-2
-3
f1 (ppm)

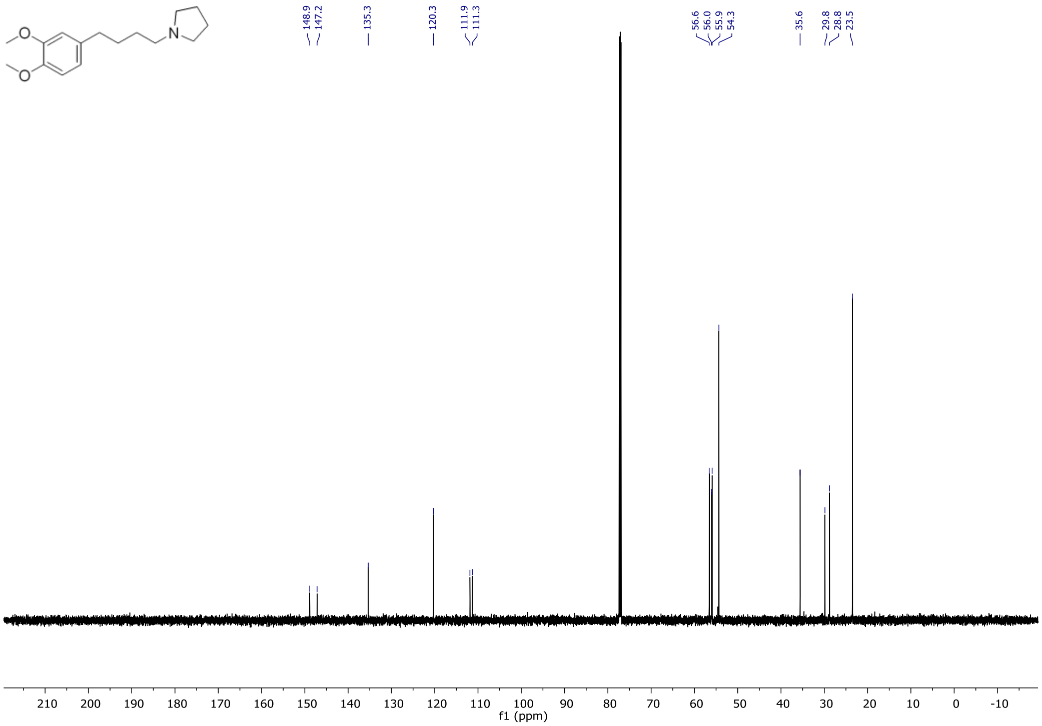
O
O
N
148.9
147.2
135.3
120.3
111.9
111.3
56.6
56.0
55.9
54.3
35.6
29.8
28.8
23.5
210
200
190
180
170
160
150
140
130
120
110
100
90
80
70
60
50
40
30
20
10
0
-10
f1 (ppm)

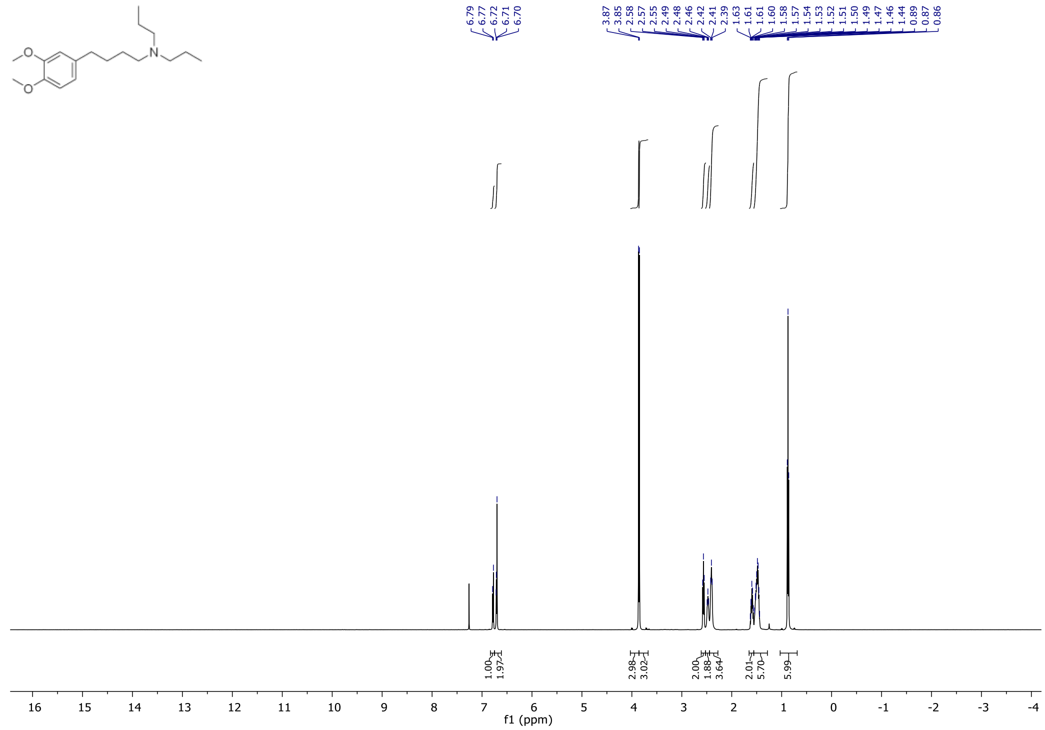
O
O
N
6.79
6.77
6.72
6.71
6.70
3.87
3.85
2.58
2.57
2.55
2.49
2.48
2.46
2.42
2.41
2.39
1.63
1.61
1.61
1.60
1.58
1.57
1.54
1.53
1.52
1.51
1.50
1.49
1.47
1.46
1.44
0.89
0.87
0.86
1.00
1.97
2.98
3.02
2.00
1.88
3.64
2.01
5.70
5.99
16
15
14
13
12
11
10
9
8
7
6
5
4
3
2
1
0
-1
-2
-3
-4
f1 (ppm)

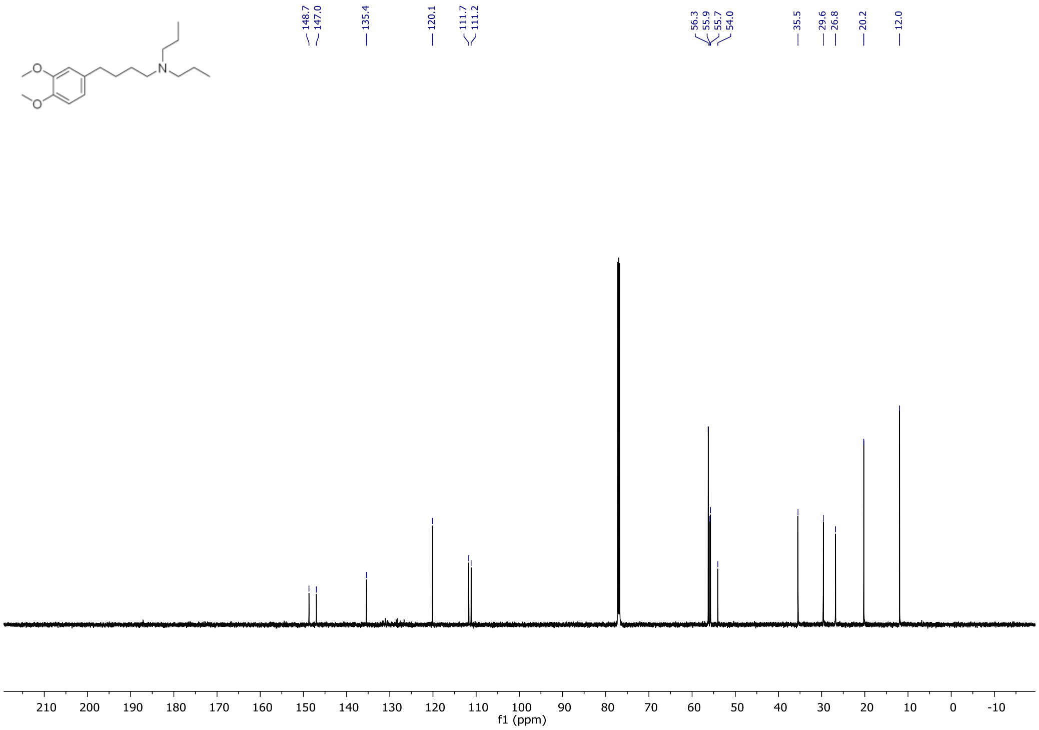
O
O
N
148.7
147.0
135.4
120.1
111.7
111.2
56.3
55.9
55.7
54.0
35.5
29.6
26.8
20.2
12.0
210
200
190
180
170
160
150
140
130
120
110
100
90
80
70
60
50
40
30
20
10
0
-10
f1 (ppm)

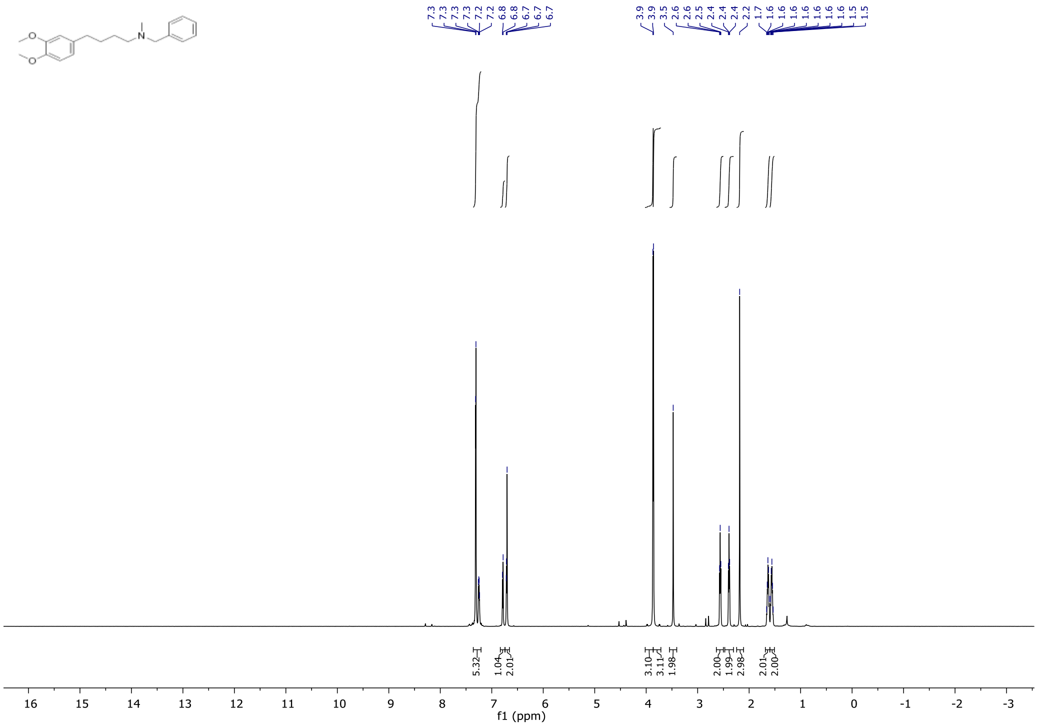
7.3
7.3
7.3
7.3
7.2
7.2
6.8
6.8
6.7
6.7
6.7
3.9
3.9
3.5
2.6
2.6
2.5
2.4
2.4
2.4
2.2
1.7
1.6
1.6
1.6
1.6
1.6
1.6
1.5
1.5
N
O
O
5.32
1.04
2.01
3.10
3.11
1.98
2.00
1.99
2.98
2.01
2.00
16
15
14
13
12
11
10
9
8
7
6
5
4
3
2
1
0
-1
-2
-3
f1 (ppm)

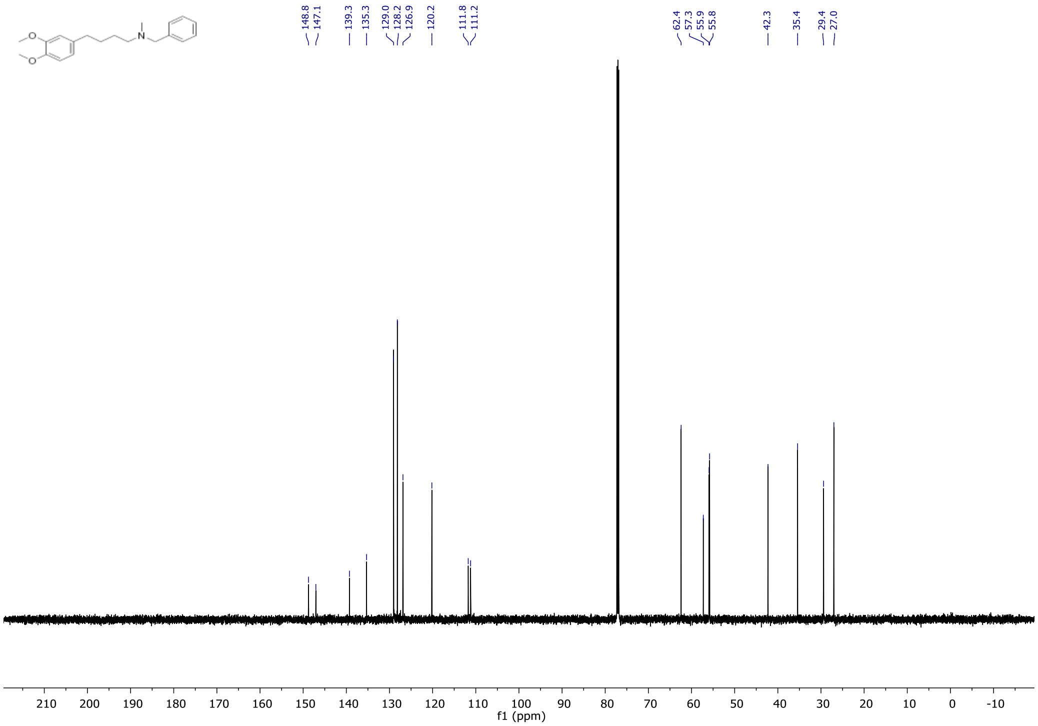
148.8
147.1
139.3
135.3
129.0
128.2
126.9
120.2
111.8
111.2
62.4
57.3
55.9
55.8
42.3
35.4
29.4
27.0
210
200
190
180
170
160
150
140
130
120
110
100
90
80
70
60
50
40
30
20
10
0
-10
f1 (ppm)
O
O
N

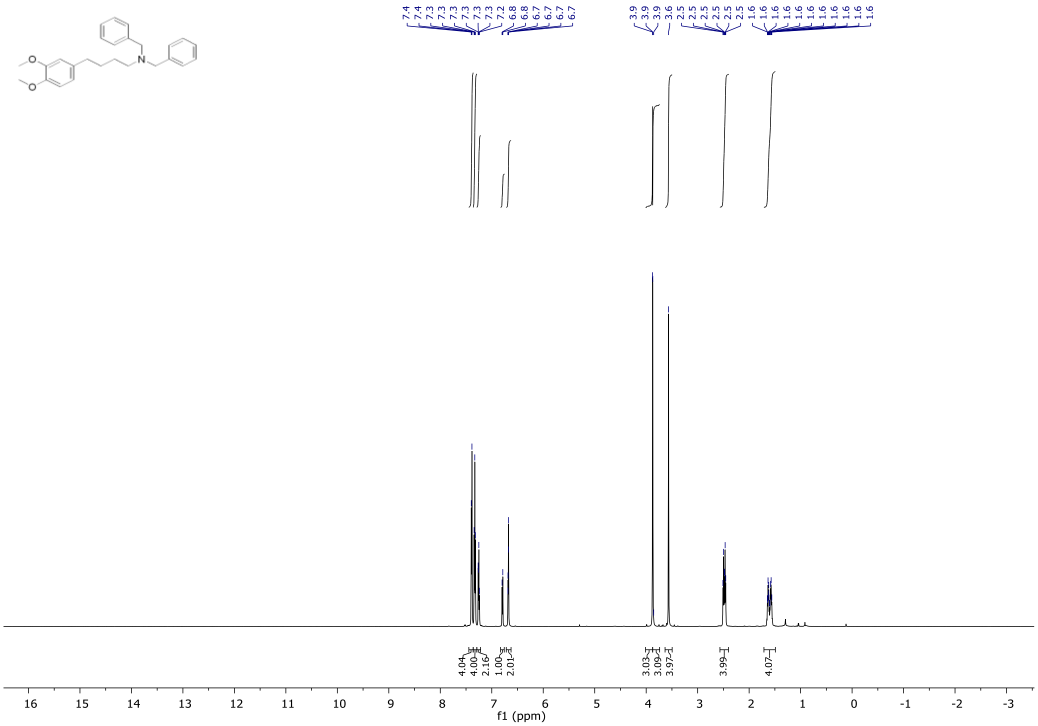
O
O
N
7.4
7.4
7.3
7.3
7.3
7.3
7.3
7.3
7.2
6.8
6.8
6.7
6.7
6.7
6.7
3.9
3.9
3.9
3.6
2.5
2.5
2.5
2.5
2.5
2.5
1.6
1.6
1.6
1.6
1.6
1.6
1.6
1.6
1.6
1.6
1.6
4.04
4.00
2.16
1.00
2.01
3.03
3.09
3.97
3.99
4.07
16
15
14
13
12
11
10
9
8
7
6
5
4
3
2
1
0
-1
-2
-3
f1 (ppm)

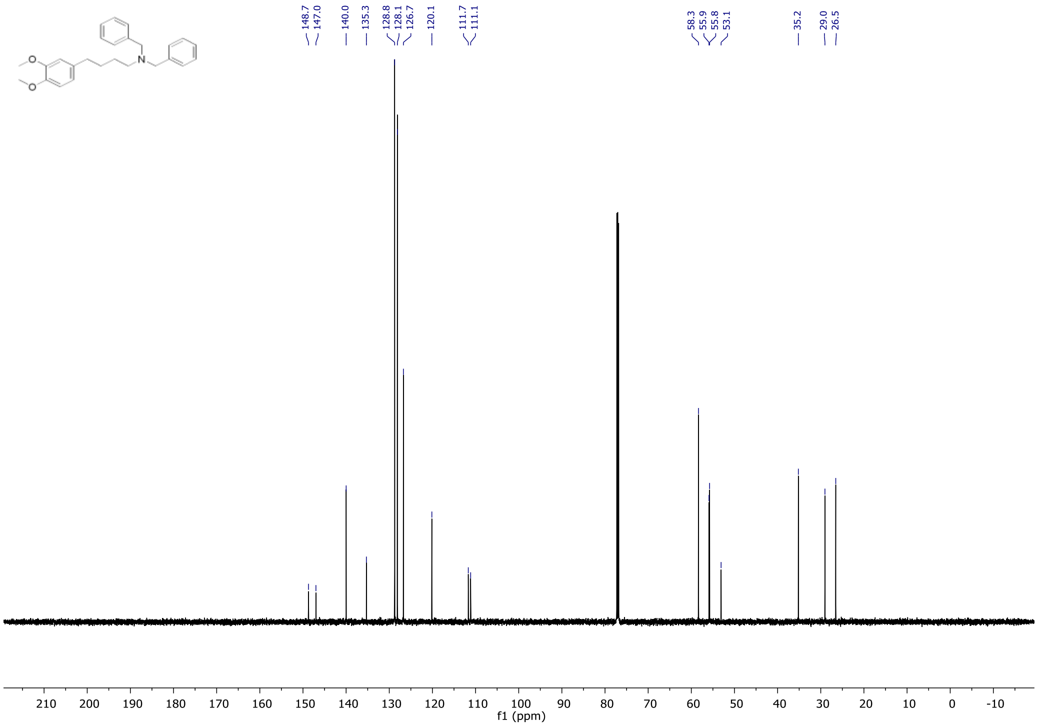
O
O
N
148.7
147.0
140.0
135.3
128.8
128.1
126.7
120.1
111.7
111.1
58.3
55.9
55.8
53.1
35.2
29.0
26.5
210 200 190 180 170 160 150 140 130 120 110 100 90 80 70 60 50 40 30 20 10 0 -10
f1 (ppm)

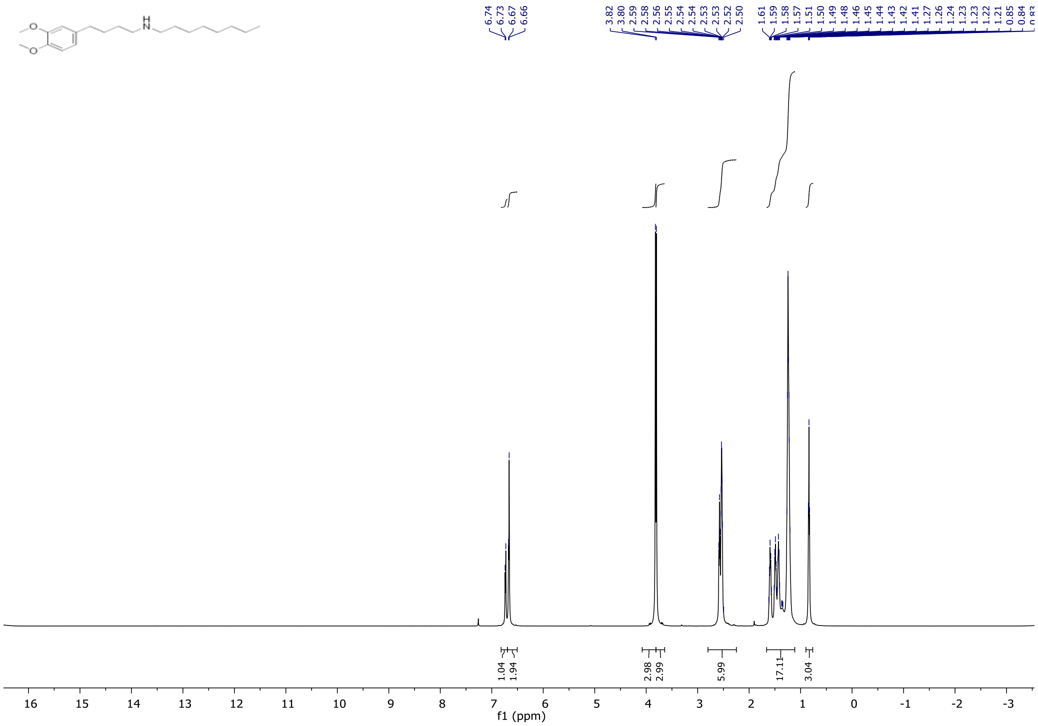
6.74
6.73
6.67
6.66
3.82
3.80
2.59
2.58
2.56
2.55
2.54
2.54
2.53
2.53
2.52
2.50
1.61
1.59
1.58
1.57
1.51
1.50
1.49
1.48
1.46
1.45
1.44
1.43
1.42
1.41
1.27
1.26
1.24
1.23
1.23
1.22
1.21
0.85
0.84
O
O
H
N
1.04
1.94
2.98
2.99
5.99
17.11
3.04
16
15
14
13
12
11
10
9
8
7
6
5
4
3
2
1
0
-1
-2
-3
f1 (ppm)

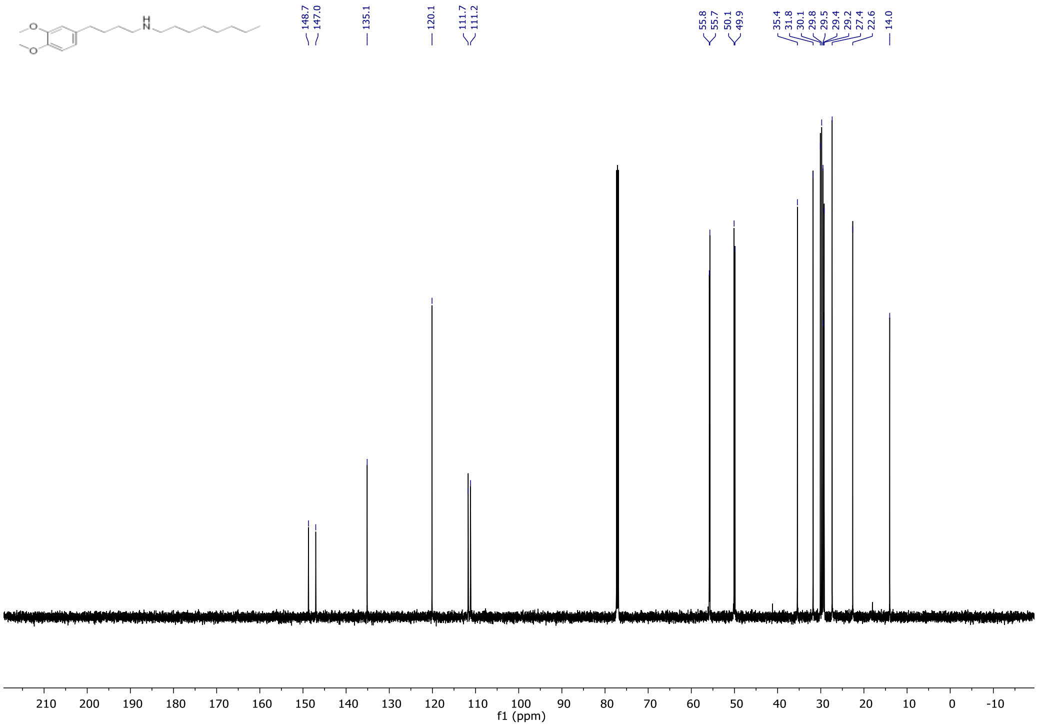
O
O
H
N
148.7
147.0
135.1
120.1
111.7
111.2
55.8
55.7
50.1
49.9
35.4
31.8
30.1
29.8
29.5
29.4
29.2
27.4
22.6
14.0
210
200
190
180
170
160
150
140
130
120
110
100
90
80
70
60
50
40
30
20
10
0
-10
f1 (ppm)

2.5 References

Parts of this chapter were reprinted with permission from:
"Multicatalytic Approach to the Hydroaminomethylation of α-Olefins"
Hanna, S.; Holder, J.; Hartwig, J. F. *Angew. Chem. Int. Ed.* **2019**, *58*, 3368-3372.

1. (a) Hayes, K. S. Industrial processes for manufacturing amines. *Appl. Catal., A* **2001**, *221*, 187. (b) Roose, P.; Eller, K.; Henkes, E.; Rossbacher, R.; Höke, H., *Amines, Aliphatic*. 2015.

2. (a) Crozet, D.; Urrutigoity, M.; Kalck, P. Recent Advances in Amine Synthesis by Catalytic Hydroaminomethylation of Alkenes. *ChemCatChem* **2011**, *3*, 1102. (b) Chen, C. D., X.-Q.; Zhang, X. Recent progress in rhodium-catalyzed hydroaminomethylation. *Org. Chem. Front.* **2016**, *3*, 1359. (c) Kalck, P.; Urrutigoïty, M. Tandem Hydroaminomethylation Reaction to Synthesize Amines from Alkenes. *Chem. Rev.* **2018**, *118*, 3833.

3. Hartwig, J. F., *Organotransition Metal Chemistry: From Bonding to Catalysis*. 1 ed.; University Science Books: Mill Valley, California, 2009.

4. Ahmed, M.; Seayad, A. M.; Jackstell, R.; Beller, M. Amines made easily: A highly selective hydroaminomethylation of olefins. *J. Am. Chem. Soc.* **2003**, *125*, 10311.

5. (a) Seayad, A.; Ahmed, M.; Klein, H.; Jackstell, R.; Gross, T.; Beller, M. Internal olefins to linear amines. *Science* **2002**, *297*, 1676. (b) Ahmed, M.; Bronger, R. P. J.; Jackstell, R.; Kamer, P. C. L.; van Leeuwen, P. W. N. M.; Beller, M. Highly selective hydroaminomethylation of internal alkenes to give linear amines. *Chem. Eur. J.* **2006**, *12*, 8979. (c) Vieira, T. O.; Alper, H. Rhodium(I)-catalyzed hydroaminomethylation of 2-isopropenylanilines as a novel route to 1,2,3,4-tetrahydroquinolines. *Chem. Commun.* **2007**, 2710. (d) Liu, G.; Huang, K.; Cai, C.; Cao, B.; Chang, M.; Wu, W.; Zhang, X. Highly Regioselective Hydroaminomethylation of Terminal Olefins to Linear Amines Using Rh Complexes with a Tetrabi Phosphorus Ligand. *Chem. Eur. J.* **2011**, *17*, 14559. (e) Briggs, J. R.; Klosin, J.; Whiteker, G. T. Synthesis of Biologically Active Amines via Rhodium−Bisphosphite-Catalyzed Hydroaminomethylation. *Org. Lett.* **2005**, *7*, 4795. (f) Whiteker, G. T. Synthesis of Fexofenadine via Rhodium-Catalyzed Hydroaminomethylation. *Top. Catal.* **2010**, *53*, 1025. (g) Liu, G.; Huang, K.; Cao, B.; Chang, M.; Li, S.; Yu, S.; Zhou, L.; Wu, W.; Zhang, X. Highly Regioselective Isomerization-Hydroaminomethylation of Internal Olefins Catalyzed by Rh Complex with Tetrabi-Type Phosphorus Ligands. *Org. Lett.* **2012**, *14*, 102. (h) Wu, L.; Fleischer, I.; Jackstell, R.; Beller, M. Efficient and Regioselective Ruthenium-catalyzed Hydro-aminomethylation of Olefins. *J. Am. Chem. Soc.* **2013**, *135*, 3989. (i) Liu, G.; Li, Z.; Geng, H.; Zhang, X. Rhodium-catalyzed regioselective hydroaminomethylation of terminal olefins with pyrrole-based tetraphosphorus ligands. *Catal. Sci. Technol.* **2014**, *4*, 917. (j) Liu, J.; Kubis, C.; Franke, R.; Jackstell, R.; Beller, M. From Internal Olefins to Linear Amines: Ruthenium-Catalyzed Domino Water–Gas Shift/Hydroaminomethylation Sequence. *ACS Catal.* **2016**, *6*, 907. (k) Subhani, M. A.; Mueller, K.-S.; Eilbracht, P. Chiral Polyamino Alcohols via Hydroaminomethylation: A New Class of Polyamines for Dendritic Cores and Ligand Precursors. *Adv. Synth. Catal.* **2009**, *351*, 2113. (l) Schmidt, A.; Marchetti, M.; Eilbracht, P. Regioselective hydroaminomethylation of 1,1-diaryl-allyl-alcohols: a new access to 4,4-diarylbutylamines. *Tetrahedron* **2004**, *60*, 11487.

6. Routaboul, L.; Buch, C.; Klein, H.; Jackstell, R.; Beller, M. An improved protocol for the selective hydroaminomethylation of arylethylenes. *Tetrahedron Lett.* **2005**, *46*, 7401.

7. (a) Takahashi, K.; Yamashita, M.; Nozaki, K. Tandem Hydroformylation/Hydrogenation of Alkenes to Normal Alcohols Using Rh/Ru Dual Catalyst or Ru Single Component Catalyst. *J. Am. Chem. Soc.* **2012**, *134*, 18746. (b) Kohei, T.; Makoto, Y.; Takeo, I.; Koji, N.; Kyoko, N. High-Yielding Tandem Hydroformylation/Hydrogenation of a Terminal Olefin to Produce a Linear Alcohol Using a Rh/Ru Dual Catalyst System. *Angew. Chem. Int. Ed.* **2010**, *49*, 4488. (c) Yuki, Y.; Takahashi, K.; Tanaka, Y.; Nozaki, K. Tandem Isomerization/Hydroformylation/Hydrogenation of Internal Alkenes to *n*-Alcohols Using Rh/Ru Dual- or Ternary-Catalyst Systems. *J. Am. Chem. Soc.* **2013**, *135*, 17393.

8. (a) Zimmermann, B.; Herwig, J.; Beller, M. The First Efficient Hydroaminomethylation with Ammonia: With Dual Metal Catalysts and Two-Phase Catalysis to Primary Amines. *Angew. Chem. Int. Ed.* **1999**, *38*, 2372. (b) Wang, Y.; Zhang, C.; Luo, M.; Chen, H.; Li, X. J. Hydroaminomethylation of high alkenes with dual-metal catalysts in a biphasic aqueous/organic system. *Arkivoc* **2008**, *xi*, 165.

9. (a) Villa-Marcos, B.; Xiao, J. Metal and organo-catalysed asymmetric hydroaminomethylation of styrenes. *Chinese J. Catal.* **2015**, *36*, 106. (b) Han, J. M.; Xing-Han, L.; Zhi, Y. Enantioselective Hydroaminomethylation of Olefins Enabled by Rh/Brønsted Acid Relay Catalysis. *Org. Lett.* **2017**, *19*, 1076.

10. (a) Wang, D.; Astruc, D. The Golden Age of Transfer Hydrogenation. *Chem. Rev.* **2015**, *115*, 6621. (b) Takao Ikariya, M. S., *Bifunctional Molecular Catalysis*. Springer-Verlag Berlin Heidelberg: 2011; Vol. 37, p 212. (c) Gordon, P. A. D.; John, C. The mechanism of enantioselective ketone reduction with Noyori and Noyori–Ikariya bifunctional catalysts. *Dalton Trans.* **2016**, *45*, 6741.

11. Blacker, J.; Martin, J., Scale-Up Studies in Asymmetric Transfer Hydrogenation. In *Asymmetric Catalysis on Industrial Scale*, Wiley-VCH Verlag GmbH & Co. KGaA: 2004; pp 201.

12. (a) Wang, C.; Pettman, A.; Bacsa, J.; Xiao, J. A Versatile Catalyst for Reductive Amination by Transfer Hydrogenation. *Angew. Chem.* **2010**, *122*, 7710. (b) Talwar, D.; Salguero, N. P.; Robertson, C. M.; Xiao, J. Primary Amines by Transfer Hydrogenative Reductive Amination of Ketones by Using Cyclometalated IrIII Catalysts. *Chem. Eur. J.* **2014**, *20*, 245. (c) Xiao, W. T.; Chunho, L.; Xiaofeng, W.; Jianliang Cyclometalated Iridium Complexes as Highly Active Catalysts for the Hydrogenation of Imines. *Synlett* **2013**, *25*, 81.

13. Lei, Q.; Wei, Y.; Talwar, D.; Wang, C.; Xue, D.; Xiao, J. Fast Reductive Amination by Transfer Hydrogenation “on Water”. *Chem. Eur. J.* **2013**, *19*, 4021.

14. The precise pH of the buffer strongly influences the outcomes of reductive aminations with Xiao's catalyst. Under basic conditions, neither imines nor ketones are protonated, and the reduction does not occur. In contrast, under highly acidic conditions, amines, ketones, and imines are protonated and both the chemoselectivity for the reduction of C=N bonds and the rate of the reductive amination are low. See reference 14.

15. Ahmed, M.; Buch, C.; Routaboul, L.; Jackstell, R.; Klein, H.; Spannenberg, A.; Beller, M. Hydroaminomethylation with novel rhodium-carbene complexes: An efficient catalytic approach to pharmaceuticals. *Chem. Eur. J.* **2007**, *13*, 1594.

16. Reaction Conditions: 0.5 mmol methyl eugenol, 0.5 mmol 2-aminopyridine, 40 bar CO:H2 (1:5), [Rh(COD)2]BF4 (0.1 mol%), Xantphos (0.4 mol%), 1.5 mL PhMe:MeOH (1:1), 125 °C, 20 h

17. Pan, Y.; Luo, Z.; Han, J.; Xu, X.; Chen, C.; Zhao, H.; Xu, L.; Fan, Q.; Xiao, J. B(C6F5)3-Catalyzed Deoxygenative Reduction of Amides to Amines with Ammonia Borane. *Adv. Synth. Catal.* **2019**, *361*, 2301.

18. Rosen, B. R.; Ruble, J. C.; Beauchamp, T. J.; Navarro, A. Mild Pd-Catalyzed N-Arylation of Methanesulfonamide and Related Nucleophiles: Avoiding Potentially Genotoxic Reagents and Byproducts. *Org. Lett.* **2011**, *13*, 2564.

Chapter 3

Contra-thermodynamic Olefin Isomerization by Chain-Walking Hydrofunctionalization and Formal Retro-hydrofunctionalization

3.1 Introduction

Generally, internal alkenes are more stable than their terminal counterparts. This greater stability originates from a hyperconjugative interaction between the alkyl substituents and the π* orbital of an olefin. Because the isomerization of terminal olefins to internal olefins is exergonic, many such isomerizations have been reported (Scheme 1). Classical methods for the isomerization of olefins involve proton transfers catalyzed by acid or base. Transition-metal-catalyzed isomerizations of alkenes occur by one of several pathways shown in Scheme 1,[1] but all such catalytic isomerizations involve the conversion of terminal olefins to internal olefins or the conversion of one internal olefin to another internal olefin because terminal olefins are less stable than internal olefins.

Inspired by biological processes in which downhill hydrolyses and redox processes are coupled to thermodynamically uphill steps, we sought to develop one or more exergonic chemical processes that could be coupled to an endergonic isomerization of internal olefins to terminal olefins. The term contra-thermodynamic describes reactions that couple an increase in free energy of one synthetically valuable process to additional exergonic processes. Several multi-step approaches to contra-thermodynamic olefin isomerization have been reported;[2] however, strategies to form the terminal alkene with high selectivity have been limited to translocation of a double bond by only one carbon unit.[3] No examples of reactions that lead to the selective migration of a double bond beyond a single carbon unit have been reported previously.

Such a method for the selective, contra-thermodynamic translocation of a double bond over multiple carbon units would enable chemists to conduct subsequent reactions at sites that are remote from the starting alkene. For example, the terminal olefins formed by such an isomerization could undergo a variety of difunctionalizations or hydrofunctionalizations that cannot occur in concert with chain walking of metal-alkyl intermediates. Long-range isomerizations also could be used to modify the structures of natural products, such as terpenes, containing alkenes. Finally, on a different scale, long-range, contra-thermodynamic isomerizations could enable the valorization of mixtures of internal olefins to isomerically pure linear α-olefins.

To develop a long-range, contra-thermodynamic olefin isomerization, we envisioned that chain-walking hydrofunctionalization of an internal alkene could be conducted in concert with retro-hydrofunctionalization (Scheme 1: *This Work*). We report the formation of terminal alkenes from internal alkenes by combining platinum-catalyzed hydrosilylation with a new method for the conversion of alkylsilanes to terminal alkenes. This process enables the translocation of the carbon-carbon double bond through multiple secondary sites, as well as through a combination of secondary and tertiary sites to form the terminal alkene.

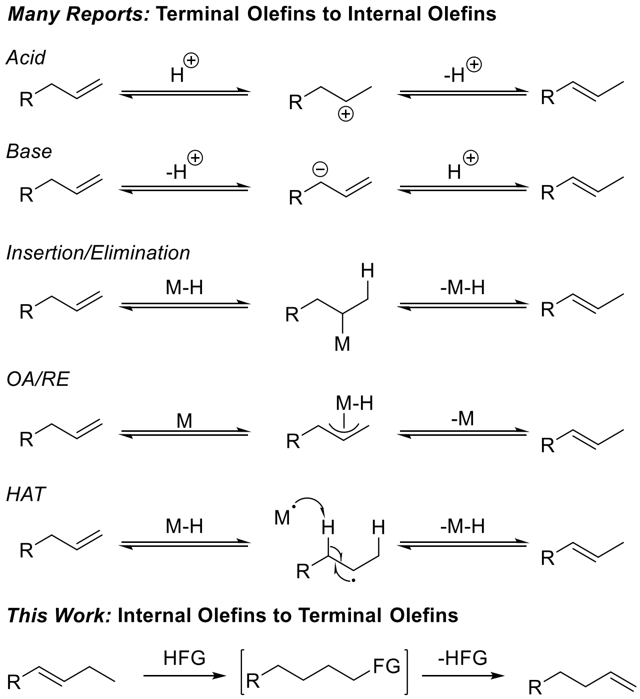
Many Reports: Terminal Olefins to Internal Olefins
Acid
Base
Insertion/Elimination
OA/RE
HAT
This Work: Internal Olefins to Terminal Olefins
HFG
-HFG

Scheme 1. Thermodynamic vs. contra-thermodynamic positional olefin isomerizations

A variety of chain-walking hydrofunctionalizations,[4] including hydrosilylations,[5] hydroborations,[6] hydrocyanations,[7] hydroformylations,[8] and alkoxycarbonylations,[9] are known, and several retro-hydrofunctionalizations have been developed. However, none of these retro-hydrofunctionalizations have been combined with hydrofunctionalizations to enable the contra-thermodynamic isomerization of alkenes. Retro-hydrocyanation, which was developed by Morandi, proceeds by the net transfer of hydrogen cyanide to a strained olefin (Scheme 2).[10] A similar retro-hydroformylation developed by Dong involves the net transfer of formaldehyde to a strained olefin, and a retro-hydroformylation reported by Nozaki involves the extrusion of synthesis gas from the system.[11] While retro-hydrocyanation and retro-hydroformylation have been developed, the *n*:*iso* ratios of chain-walking hydrocyanations and chain-walking hydroformylations are lower than those of other chain-walking hydrofunctionalizations, and the current catalysts for these transformations rarely undergo isomerization through tertiary centers (Keuleman's rule).

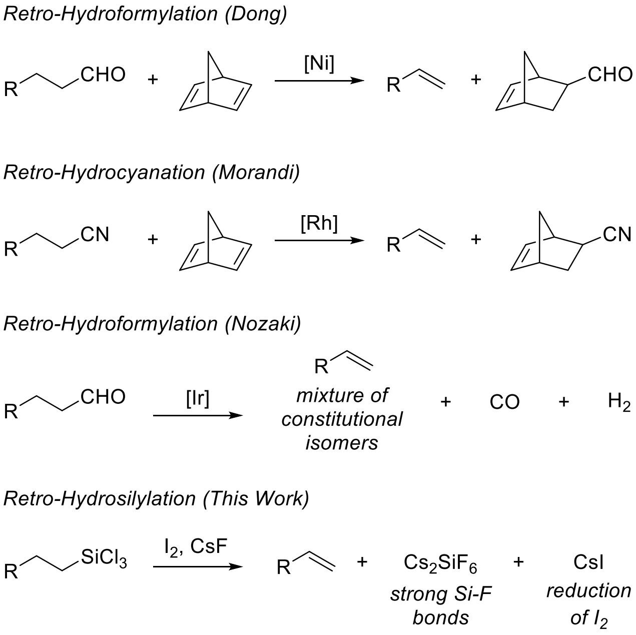
Retro-Hydroformylation (Dong)
R
CHO
+
[Ni]
R
+
CHO
Retro-Hydrocyanation (Morandi)
R
CN
+
[Rh]
R
+
CN
Retro-Hydroformylation (Nozaki)
R
CHO
[Ir]
R
mixture of constitutional isomers
+
CO
+
H2
Retro-Hydrosilylation (This Work)
R
SiCl3
I2, CsF
R
+
Cs2SiF6
strong Si-F bonds
+
CsI
reduction of I2

Scheme 2. Retro-hydrofunctionalizations

In contrast to chain-walking hydroformylations and hydrocyanations, platinum-catalyzed hydrosilylations proceed with exceptionally high *n:iso* ratios because the catalyst undergoes fast isomerization of internal metal alkyls to terminal metal alkyls and selective reductive elimination of the terminal metal alkyl intermediate with the silyl group. In addition, chain-walking hydrosilylations of internal olefins with trichlorosilane proceed without solvent and with low loadings of Speier's catalyst (H_2PtCl_6), making this class of hydrofunctionalization conducive to the development of a one-pot isomerization. Finally, platinum catalysts for hydrosilylation "walk" through tertiary centers, a prerequisite for movement of a double bond through branched portions of a molecule. However, retro-hydrosilylation is not a known reaction.[12]

Retro-hydrosilylation is challenging to develop because the microscopic reverse of hydrosilylation involves the oxidative addition of a C–Si bond, which is a rare reaction. Therefore, we designed a new approach to the conversion of alkylsilanes to olefins. By this process, the typically nucleophilic silyl group would be oxidized to a nucleofuge, which would undergo base-promoted conversion to a terminal olefin. Specifically, alkylsilanes would be oxidized to alkyl halides through pentafluorosilicate intermediates,[13] and the resulting alkyl halides would undergo classical eliminations *in situ*. In contrast to the retro-hydrofunctionalizations driven by the release of ring strain or by the extrusion of gases, this approach would couple the endergonic retro-hydrosilylation to the exergonic reduction of iodine and formation of strong Si–F bonds. The approach would constitute a formal retro-hydrosilylation because it does not proceed by the microscopic reverse of hydrosilylation.

3.2 Results and discussion

To test this design, we conducted the reaction of branched alkylsilane **2a** with an oxidant and a fluoride source (Table 1). We imagined that treating this silane with cesium fluoride and iodine would trigger a domino sequence involving the formation of a pentafluorosilicate, iodination, and elimination. Indeed, silane **2a** reacted with cesium fluoride and iodine in DMF for 20 h at 100 °C to form 4-*tert*-butylmethylenecyclohexane (olefin **3a**) in 82% yield (entry 1); in this process, the cesium fluoride functions as both a reagent for activation of the silane and a base for elimination of the halide. In the presence of 6 equivalents of CsF, olefin **3a** formed in only trace amounts (entry 2). In this case, the corresponding alkyl iodide was the major product formed, indicating that the formal retro-hydrosilylation process can be stopped prior to elimination. Reactions with KF in place of CsF (entry 3), larger numbers of equivalents of I_2 than 1.1 (entry 4), or solvents other than DMF (entries 5-7) gave olefin **3a** in lower yields than reactions conducted with the standard conditions in entry 1. Although NIS and NBS are known to halogenate alkyl pentafluorosilicates, these compounds were not suitable oxidants for this transformation (entries 8-9). A lower yield was observed when the formal retro-hydrosilylation was conducted at 50 °C instead of 100 °C (entry 10).

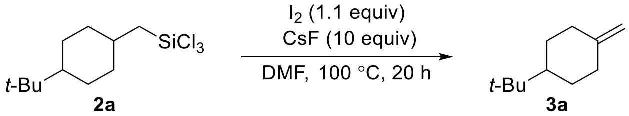

entry	change from above conditions	yield **3a**[a]
1	none	82%
2	6 equiv CsF	0%[b]
3	KF instead of CsF	31%
4	2 equiv I2	73%
5	ACN instead of DMF	68%
6	*i*PrOH instead of DMF	60%
7	toluene instead of DMF	0%[b]
8	NIS instead of I2	9%
9	NBS instead of I2	0%
10	50 °C	48%

[a] Yields were determined by ^{1}H NMR spectroscopy with trichloroethylene as an internal standard
[b] Major product observed was alkyl iodide intermediate

Table 1. Formal retro-hydrosilylation of β-branched alkylsilanes

Upon subjecting the linear alkylsilane **2b** to the conditions developed for the formal retro-hydrosilylation of branched silane **2a**, a significant quantity of octadecyl fluoride (**4b**) formed, along with terminal olefin **3b** (Table 2, entry 1). This result indicates that that alkyl iodide intermediates lacking *β*-branching undergo competitive S_N2 and E2 processes with cesium fluoride. We hypothesized that arresting the formal retro-hydrosilylation of silane **2b** at alkyl iodide **5b** by conducting the iodination process with exactly 6 equivalents of CsF would enable the elimination to be conducted with a base known to favor E2 elimination over S_N2 substitution. Indeed, the reaction of silane **2b** with 6 equivalents of CsF formed octadecyl iodide in 62% yield, along with trace olefin and no alkyl fluoride (entry 2). Treatment of this crude reaction mixture with a hindered alkoxide base (NaO*t*Bu) at room temperature leads to a classical elimination reaction and provided olefin **3b** in 65% overall yield (entry 3).

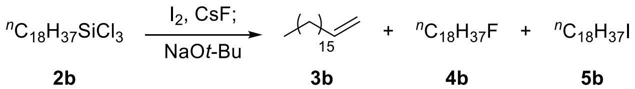

entry	CsF (equiv)	yield **3b**[a]	yield **4b**[a]	yield **5b**[a]
1[b]	10	54%	23%	0%
2[b]	6	0%	0%	62%
3	6	65%	0%	0%
4[c]	6	0%	0%	0%
5[d]	6	33%	0%	10%

Conditions: Silane (0.1 mmol), Iodine (1.1 equiv), CsF, DMF, 100 °C, 20 h; NaO*t*-Bu (5 equiv), rt, 20 h. [a]Yields were determined by ^1H NMR spectroscopy with trichloroethylene as an internal standard. [b]No second step conducted. [c]Both steps conducted simultaneously. [d]Under air, no protection from light.

Table 2. Formal retro-hydrosilylation of linear alkylsilanes

Having developed conditions for the formal retro-hydrosilylation of both linear and *β*-branched alkylsilanes, we hypothesized that this reaction could be conducted on crude silanes prepared by chain-walking hydrosilylation. In this case, a one-pot, contra-thermodynamic olefin isomerization would result. Indeed, treatment of a variety of internal olefins with $HSiCl_3$ in the presence of Speier's catalyst and subsequent subjection of the crude alkylsilane to the conditions that induce formal retro-hydrosilylation gave terminal olefins in good yields with excellent *n*:*iso* selectivities (Scheme 3). No internal olefins were observed by ^1H NMR spectroscopy in any of the crude samples; that is, the *n*:*iso* ratios of the products were all greater than 99:1. Internal olefins **1c**, **1d**, and **1e**, underwent isomerization to 1-octene (olefin **3c**) in moderate to good yields, indicating that both short-range and long-range isomerizations occur. In fact, 7-tetradecene (olefin **1f**) underwent isomerization over six positions to form 1-tetradecene (olefin **3f**) in good yield. Diene **1g**, which contains a terminal olefin and an internal olefin, underwent isomerization to α,ω-diene **3g**, the sole diene formed in the reaction. In this case, the quantity of each reagent was twice that of reactions of substrates lacking alkenes because both olefins underwent hydrosilylation and retro-hydrosilylation. This example demonstrates that terminal olefins are tolerated passively because hydrosilylation-retro-hydrosilylation sequences on terminal and internal alkene are degenerate.

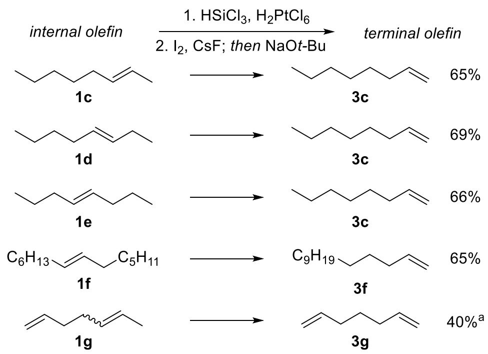

internal olefin
1. HSiCl3, H2PtCl6
2. I2, CsF; then NaOt-Bu
terminal olefin
1c
3c
65%
1d
3c
69%
1e
3c
66%
C6H13
C5H11
1f
C9H19
3f
65%
1g
3g
40%a

Step 1: Internal olefin (1 mmol), $HSiCl_3$ (2 equiv), H_2PtCl_6 (0.2 mol% in 2 mL isopropanol), 100 °C, 20 h, neat reaction, sealed vessel. Step 2: I_2 (1.1 equiv), CsF (6 equiv), DMF (0.25 M), 100 °C, 20 h; then NaO*t*-Bu, rt, 20 h. Yields were determined by ^1H NMR spectroscopy with trichloroethylene as internal standard. [a]10 equiv CsF, 2.2 equiv I_2, and 10 equiv NaO*t*-Bu.

Scheme 3. Contra-thermodynamic isomerizations of internal olefins to α-olefins

In addition to isomerizations through linear alkyl chains, isomerizations through branched chains that entail the formation of tertiary metal alkyl intermediates occurred (Scheme 4). For example, cyclic, trisubstituted olefin **1h** underwent isomerization to the 1,1-disubstituted olefin **3h** in good yield. Long-range isomerizations of endocyclic olefins **1i** and **1j** to terminal olefin **3i** through tertiary centers also occurred in good yields. Acyclic olefins also underwent isomerization through branched alkyl chains. For example, the long-range isomerization of acyclic 1,2-disubstituted olefin **1k** to 1,1-disubstituted olefin **3k** proceeded in good yield. Additionally, the isomerization tolerates steric hindrance at the starting alkene. Conversion of the hindered, trisubstituted olefin **1l**, which bears a *tert*-butyl substituent α to the double bond, to olefin **3l** occurred in good yield.

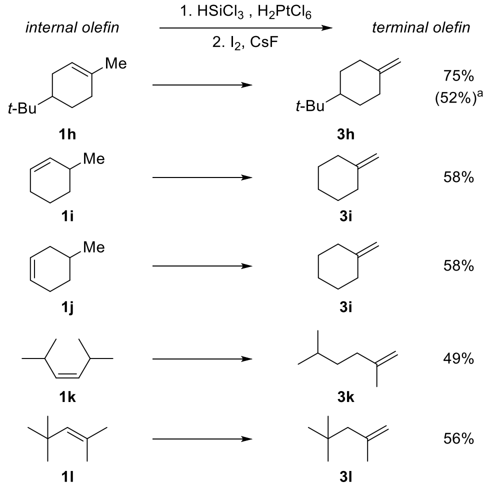

internal olefin
1. HSiCl3 , H2PtCl6
2. I2, CsF
terminal olefin
Me
t-Bu
1h
t-Bu
3h
75%
(52%)a
Me
1i
3i
58%
Me
1j
3i
58%
1k
3k
49%
1l
3l
56%

Step 1: Internal olefin (1 mmol), $HSiCl_3$ (2 equiv), H_2PtCl_6 (0.2 mol% in 2 mL isopropanol), 100 °C, 20 h, neat reaction, sealed vessel. Step 2: I_2 (1.1 equiv), CsF (10 equiv), DMF (0.40 M), 100 °C, 20 h. Yields were determined by ^1H NMR spectroscopy with trichloroethylene as internal standard. [a]Isolated yield indicated in parentheses.

Scheme 4. Contra-thermodynamic isomerization of internal olefins through branched alkyl chains to 1,1-disubstituted olefins

Finally, this type of contra-thermodynamic isomerization can be conducted on large scales. The isomerization of olefin **1h** to olefin **3h** occurred in 71% isolated yield on a gram scale (Scheme 5).

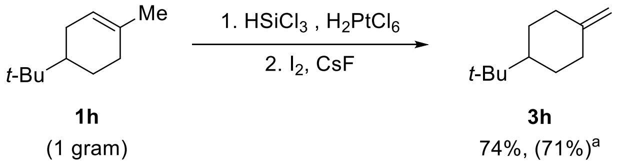

Step 1: Internal olefin (6.2 mmol), $HSiCl_3$ (2 equiv), H_2PtCl_6 (0.2 mol% in 2 mL isopropanol), 100 °C, 20 h, neat reaction, sealed vessel. Step 2: I_2 (1.1 equiv), CsF (10 equiv), DMF (0.40 M), 100 °C, 20 h. Yields were determined by ^{1}H NMR spectroscopy with trichloroethylene as internal standard. [a]Isolated yield indicated in parentheses.

Scheme 5. Contra-thermodynamic isomerization on a gram scale

3.3 Conclusion

In conclusion, we have developed a strategy for contra-thermodynamic olefin isomerization that combines chain-walking hydrosilylation with a formal retro-hydrosilylation. While other hydrofunctionalizations could be envisioned to be applicable to this process for the isomerization of alkenes, platinum-catalyzed hydrosilylation was chosen because of its high *n*:*iso* ratios, compatibility with trisubstituted olefins, low catalyst loadings, and solvent-free conditions. In contrast to previous retro-hydrofunctionalizations, the present retro-hydrosilylation is driven by redox processes and by the formation of strong Si–F bonds. Development of additional isomerizations that proceed through chain-walking hydrofunctionalization and retro-hydrofunctionalization is ongoing. Particular attention is being given to hydrofunctionalizations that are suitable for industrial processes and to those with expanded functional group tolerance.

3.4 Experimental

3.4.1 General information

All air-sensitive manipulations were conducted under an inert atmosphere in a nitrogen-filled glovebox or by standard Schlenk techniques. Unless stated otherwise, reagents and solvents were purchased from commercial suppliers and used without further purification. TLC plates were visualized by staining with $KMnO_4$. All NMR spectra were recorded at the University of California, Berkeley NMR facility. Proton-NMR spectra were recorded on Bruker AVB-400, AVQ-400, AV-500, and AV-600 instruments with operating frequencies of 400, 400, 500, and 600 MHz, respectively, and Carbon-13 NMR spectra were recorded on a Bruker AV-600 instrument with a ^{13}C operating frequency of 151 MHz. Chemical shifts (δ) are reported in ppm relative to those of residual solvent signals ($CDCl_3$ $\delta = 7.26$ for ^{1}H NMR spectra and $\delta = 77.16$ for ^{13}C NMR spectra). The following abbreviations were used in reporting NMR data: s, singlet; d, doublet; t, triplet; q, quartet; p, pentet; hept, heptet; m, multiplet.

3.4.2 Synthesis of substrates

4-(^{t}Butyl)-1-methylcyclohex-1-ene

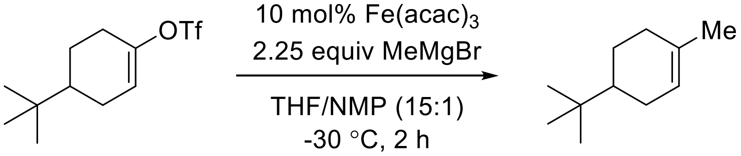

The following procedure was adapted from the literature.[14] In a nitrogen-filled glove box, an oven-dried 500 mL round bottomed flask equipped with a magnetic stir bar was charged with 4-(tert-butyl)cyclohex-1-en-1-yl trifluoromethanesulfonate[15] (3.436 g, 12.00 mmol, 1 equiv) and THF (60 mL). Anhydrous $Fe(acac)_3$ (423.6 mg, 1.199 mmol, 10 mol%) was transferred to the flask with NMP (12 mL) and THF (120 mL). The reaction mixture was sealed with a septum, removed from the glove box, maintained under N_2, and cooled to –30 °C in an *o*-xylene/dry ice bath. Methyl magnesium bromide (3.0 M in Et_2O, 9.00 mL, 27.0 mmol, 2.25 equiv) was added dropwise. After complete addition of Grignard reagent, the reaction was stirred at –30 °C for 2 hours. After this time, saturated aqueous NH_4Cl was added (50 mL), the reaction mixture was warmed to room temperature, and the biphasic mixture was concentrated under reduced pressure. The resulting residue was dissolved in pentane (100 mL), washed with water (8 x 40 mL), dried over sodium sulfate, and concentrated under reduced pressure. Column chromatography on silica gel (isocratic, pentane) afforded 4-(tert-butyl)-1-methylcyclohex-1-ene as a colorless liquid (1.379 g, 9.056 mmol, 75% yield).

3.4.3 General procedure for contra-thermodynamic olefin isomerizations

Step 1: Chain-walking hydrosilylation

In a nitrogen-filled glove box, a heavy-walled Schlenk flask with a single opening (5–10 mL) equipped with a magnetic stir bar was charged with internal olefin (1 mmol, 1 equiv) and 2.0 µL of a stock solution prepared by dissolving 100 mg H_2PtCl_6•$6H_2O$ in 200 µL of isopropanol (~1.0 mg H_2PtCl_6•$6H_2O$, 0.0020 mmol, 0.20 mol%). The Schlenk flask was sealed with a Teflon plug, removed from the glove box, and cooled to 0 °C. Trichlorosilane (202 µL, 2.00 mmol, 2.00 equiv) was added to the reaction mixture under N_2, and the Schlenk flask was sealed and heated at 100 °C for 20 h. After this time, the reaction mixture was cooled to room temperature and subjected to high vacuum (<1000 mtorr) for 15 minutes to remove excess $HSiCl_3$. The Schlenk flask was then backfilled with N_2 and transferred to a nitrogen-filled glove box.

Step 2: Formal retro-hydrosilylation

Procedure A (for preparing 1,1-disubstituted olefins):

In a nitrogen-filled glovebox and in the dark, a solution of iodine (279.2 mg, 1.100 mmol, 1.100 equiv) in dry DMF (2.50 mL) and anhydrous cesium fluoride powder (1.519 g, 10.00 mmol, 10.00 equiv) were added to the Schlenk flask containing crude alkyl trichlorosilane from step 1. The Schlenk flask was sealed, stirred at room temperature for 15 minutes, and heated with vigorous stirring at 100 °C for 20 h in the dark. After this time, the reaction mixture was carefully diluted with $CDCl_3$ (5 mL) in a fume hood, and trichloroethylene (90.0 µL, 1.00 equiv) was added. An aliquot of this mixture was filtered through a 0.2 µm PTFE syringe filter and analyzed by ^1H NMR spectroscopy.

Procedure B (for preparing monosubstituted olefins):

In a nitrogen-filled glovebox and in the dark, a solution of iodine (279.2 mg, 1.100 mmol, 1.100 equiv) in dry DMF (4.00 mL) and anhydrous cesium fluoride powder (911.0 mg, 6.000 mmol, 6.000 equiv) were added to the Schlenk flask containing crude alkyl trichlorosilane from step 1. The Schlenk flask was sealed, stirred at room temperature for 15 minutes, and heated with vigorous stirring at 100 °C for 20 h in the dark. After this time, the reaction mixture was cooled to room temperature, and dry sodium *tert*-butoxide (480.5 mg, 5.000 mmol, 5.000 equiv) was added. The reaction mixture was stirred at room temperature for 20 h with protection from light. After this time, the reaction mixture was carefully diluted with $CDCl_3$ (5 mL) in a fume hood, and trichloroethylene (90.0 µL, 1.00 equiv) was added. An aliquot of this mixture was filtered through a 0.2 µm PTFE syringe filter and analyzed by ^1H NMR spectroscopy.

3.4.4 Products of olefin isomerization

1-Octene (3c)

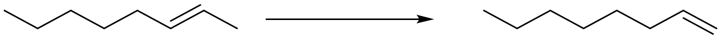

Prepared from (*E*)-2-octene (112.2 mg, 1.000 mmol) according to general procedure B.
^{1}H NMR Yield: 65%

1-Octene (3c)

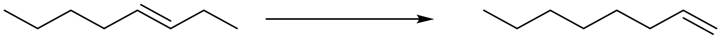

Prepared from (*E*)-3-octene (110.9 mg, 0.9946 mmol) according to general procedure B.
^{1}H NMR Yield: 69%

1-Octene (3c)

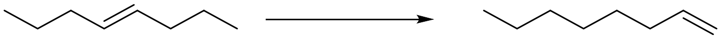

Prepared from (*E*)-4-octene (111.6 mg, 1.000 mmol) according to general procedure B.
^{1}H NMR Yield: 66%

1-Tetradecene (3f)

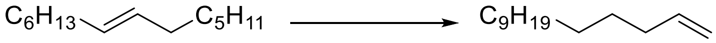

Prepared from (*E*)-7-tetradecene (192.0 mg, 0.978 mmol) according to general procedure B.
^{1}H NMR Yield 65%

1,6-Heptadiene (3g)

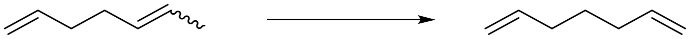

Prepared from 1,5-heptadiene (95.3 mg, 0.991 mmol) according to general procedure B, with 4 equivalents $HSiCl_3$, 0.4 mol% $H_2PtCl_6•6H_2O$, 10 equivalents of CsF, 2.2 equivalents of I_2, 8 mL of DMF, and 10 equivalents of NaO*t*-Bu.
^{1}H NMR Yield: 40%

1-(*tert*-Butyl)-4-methylenecyclohexane (3h)

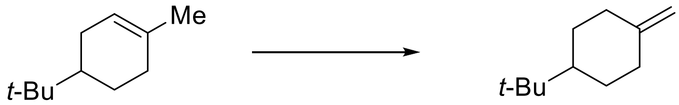

Prepared from 4-(*tert*-butyl)-1-methylcyclohex-1-ene (148.1 mg, 0.9726 mmol) according to general procedure A.

This procedure was also repeated on a 1-gram scale (952.0 mg, 6.252 mmol)

^{1}H NMR Yield: 75% (150 mg scale)

^{1}H NMR Yield: 74% (1 g scale)

Isolation of olefin 3h: The NMR sample and crude reaction mixture were combined and carefully diluted with water (100 mL), and the resulting mixture was extracted with pentane (3 x 50 mL). The combined organic layers were pink in color (residual iodine) and were decolorized by washing with 2 M sodium thiosulfate (3 x 20 mL). The combined layers were washed with water (5 x 20 mL) and brine (1 x 20 mL), dried over sodium sulfate, and carefully concentrated *in vacuo* to afford a pale-yellow liquid. Column chromatography on silica gel (isocratic, pentane, R_f ~ 0.9) followed by careful concentration *in vacuo* afforded pure 1-(*tert*-butyl)-4-methylenecyclohexane (**3h**) as a clear, colorless liquid (79.0 mg, 0.519 mmol, 53% yield, small scale; 671.4 mg, 4.409 mmol, 71%, large scale). The lower isolated yield relative to ^{1}H NMR yield on small scale is largely attributed to the volatility of the product (b.p. = 53 °C at 8 torr).[16]

^{1}H and ^{13}C NMR spectra of the product matched the literature.[16]

^{1}H NMR (400 MHz, $CDCl_3$) δ 4.58 (t, J = 1.7 Hz, 2H), 2.33 (d, J = 13.6 Hz, 2H), 1.98 (t, J = 13.3 Hz, 2H), 1.86 (d, J = 11.6 Hz, 2H), 1.20 – 0.96 (m, 3H), 0.85 (s, 9H).

^{13}C NMR (151 MHz, $CDCl_3$) δ 150.4, 106.3, 48.1, 35.5, 32.6, 29.1, 27.8.

Methylenecyclohexane (3i)

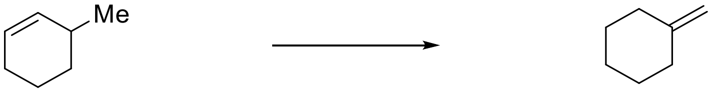

Prepared from 3-methylcyclohex-1-ene (98.4 mg, 1.02 mmol) according to general procedure A.
^{1}H NMR Yield: 58%

Methylenecyclohexane (3i)

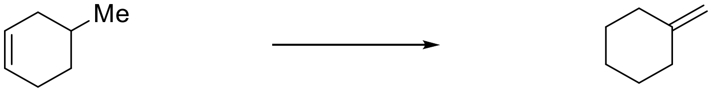

Prepared from 4-methylcyclohex-1-ene (95.4 mg, 0.992 mmol) according to general procedure A.
^{1}H NMR Yield: 58%

2,5-Dimethylhex-1-ene (3k)

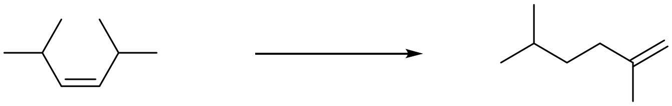

Prepared from (*Z*)-2,5-dimethylhex-3-ene (110.1 mg, 0.9811 mmol) according to general procedure A.
^{1}H NMR Yield: 49%

2,4,4-Trimethylpent-1-ene (3l)

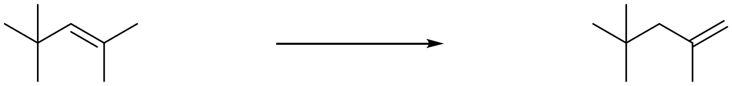

Prepared from 2,4,4-trimethylpent-2-ene (110.6 mg, 0.9856 mmol) according to general procedure A.
^{1}H NMR Yield: 56%

3.4.6 ^{1}H NMR and ^{13}C NMR Spectra

Crude ^{1}HNMR spectra were recorded in CDCl$_3$/DMF mixtures, causing some variability in chemical shifts.

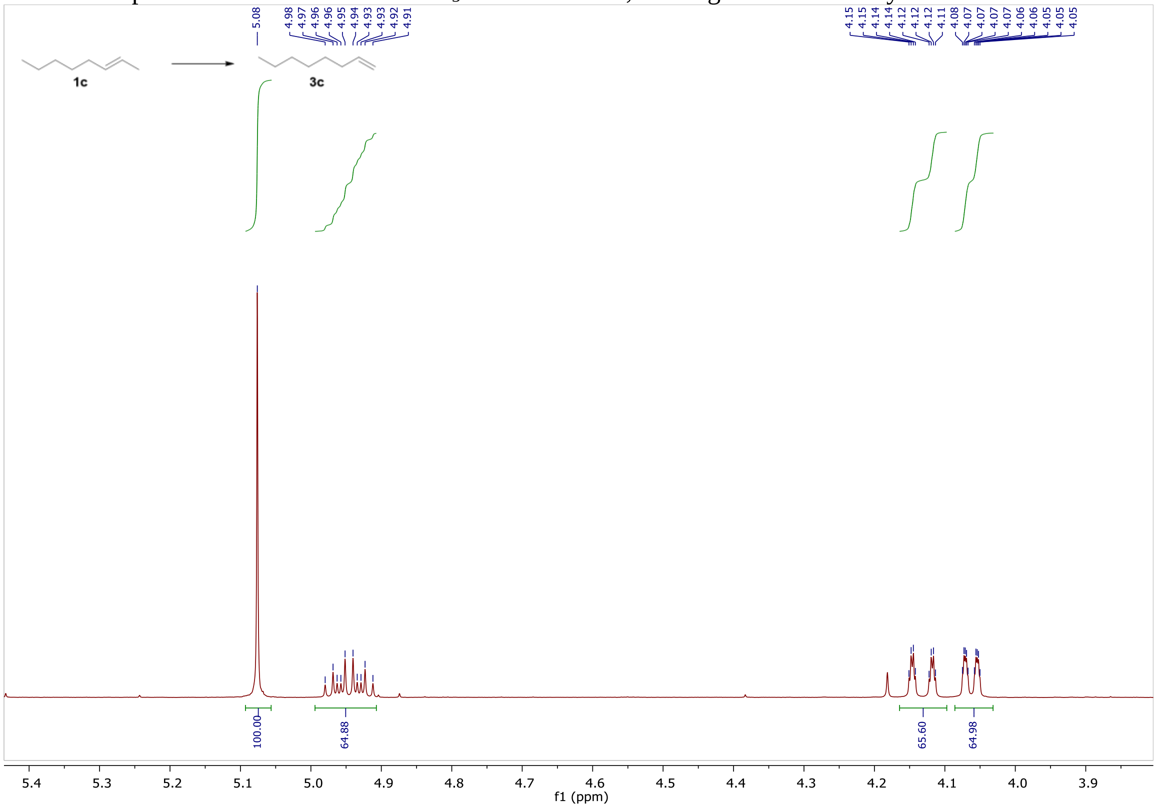

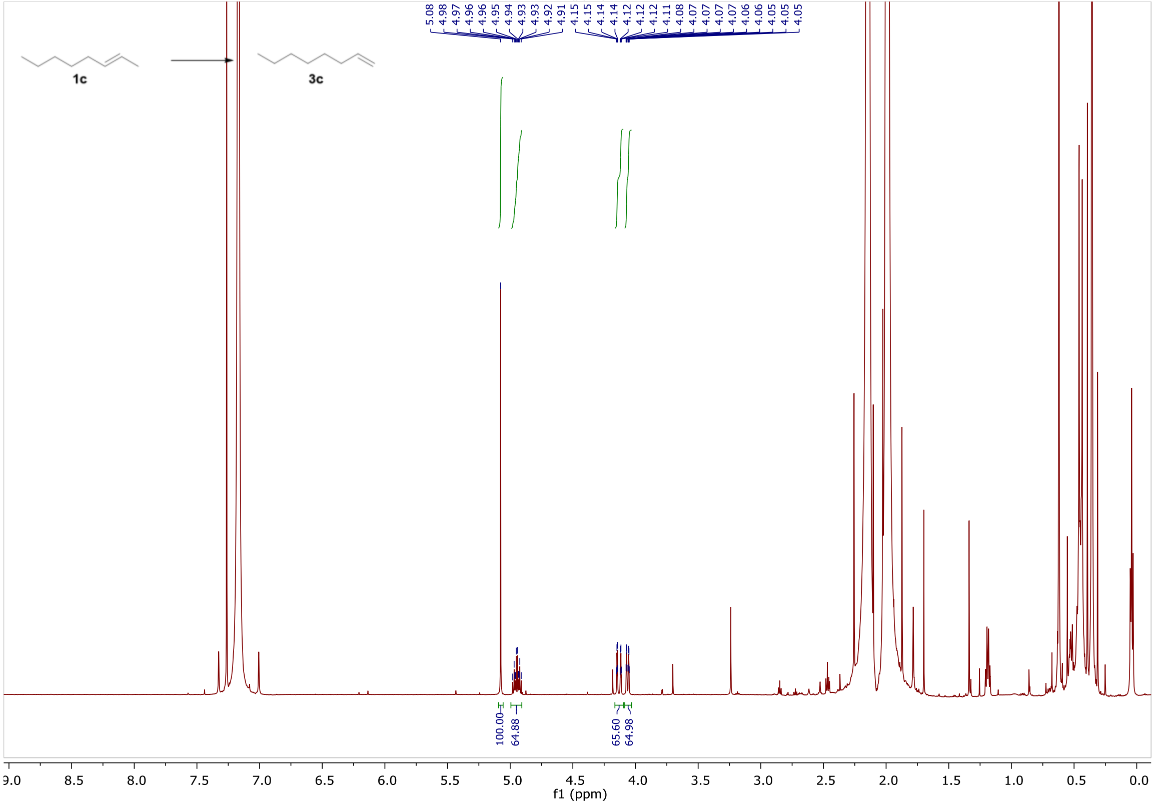

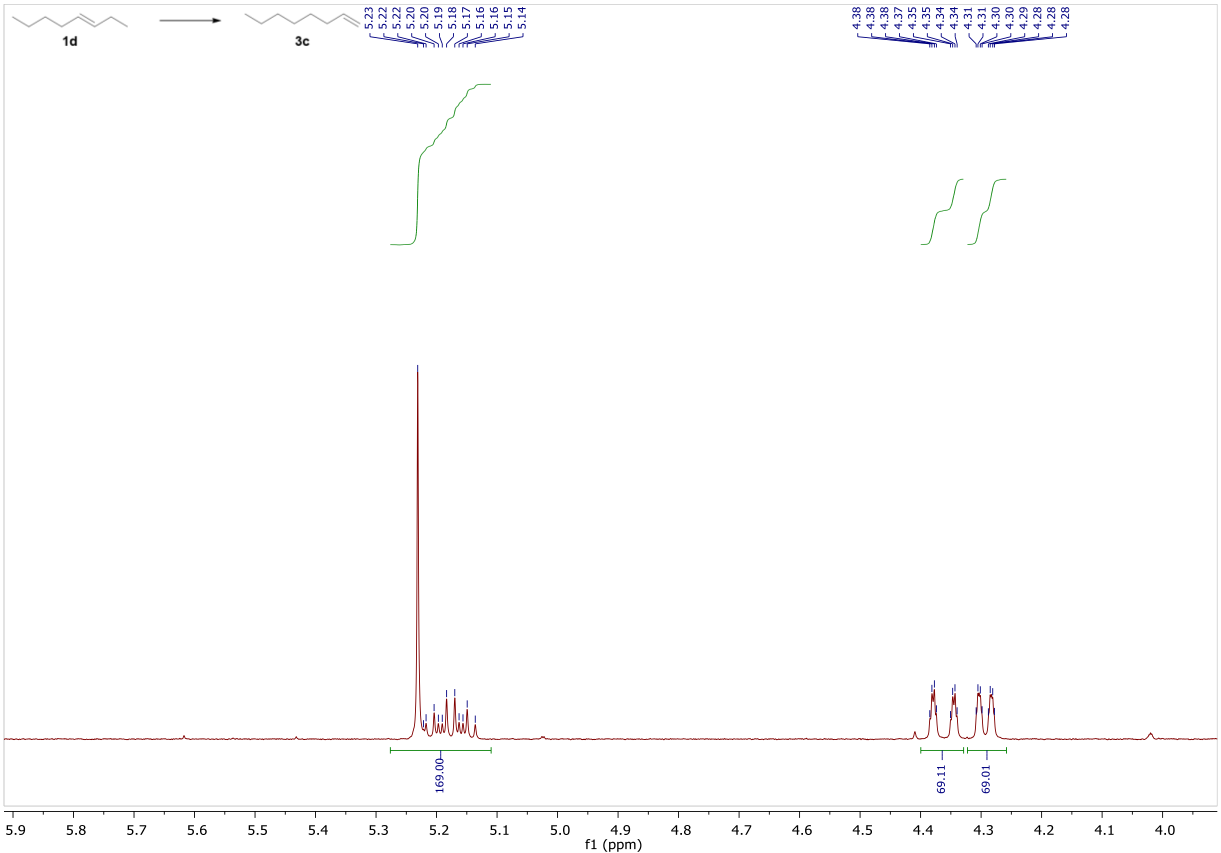
1d
3c
5.23
5.22
5.22
5.20
5.20
5.19
5.18
5.17
5.16
5.15
5.14
4.38
4.38
4.38
4.37
4.35
4.35
4.34
4.34
4.31
4.31
4.30
4.29
4.28
4.28
4.28
169.00
69.11
69.01
5.9
5.8
5.7
5.6
5.5
5.4
5.3
5.2
5.1
5.0
4.9
4.8
4.7
4.6
4.5
4.4
4.3
4.2
4.1
4.0
f1 (ppm)

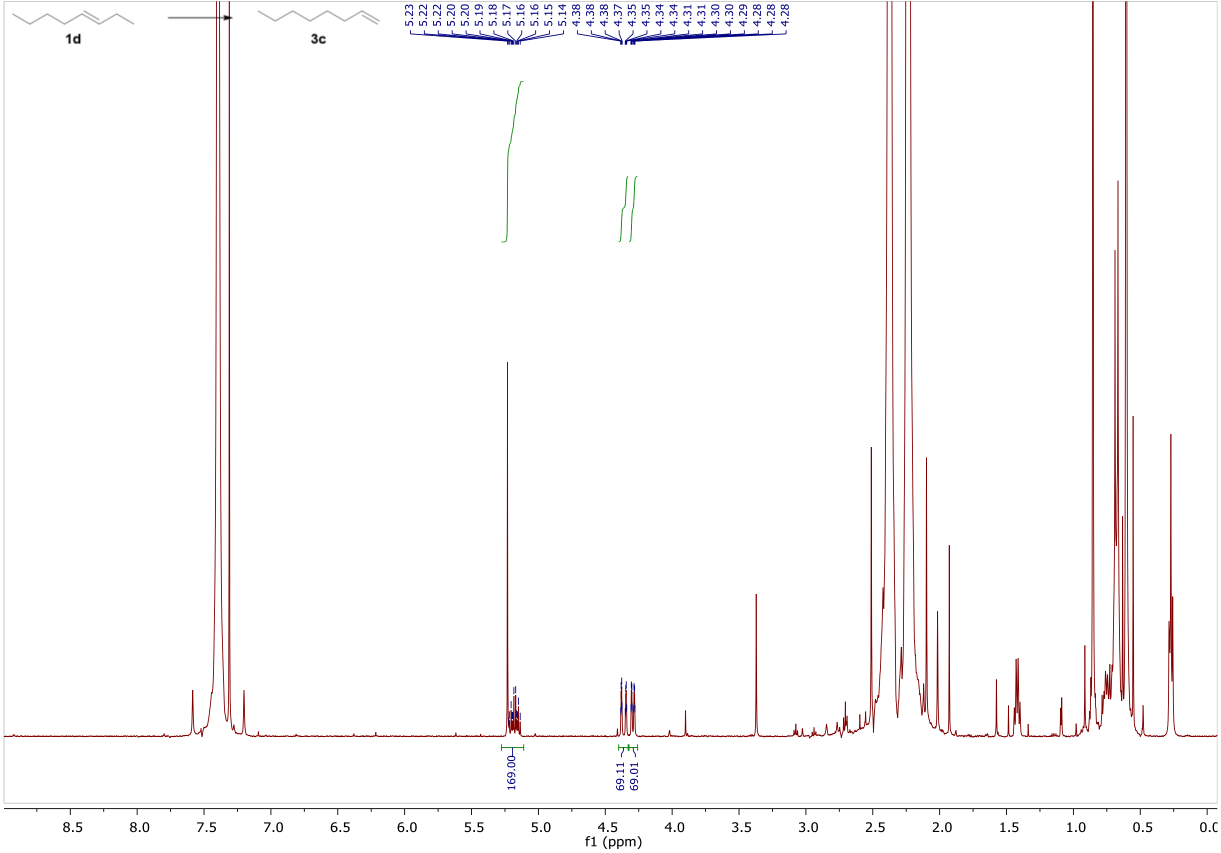
1d
3c
5.23
5.22
5.22
5.20
5.19
5.18
5.17
5.16
5.16
5.15
5.14
4.38
4.38
4.37
4.35
4.35
4.34
4.34
4.31
4.31
4.30
4.29
4.28
4.28
4.28
169.00
69.11
69.01
8.5
8.0
7.5
7.0
6.5
6.0
5.5
5.0
4.5
4.0
3.5
3.0
2.5
2.0
1.5
1.0
0.5
0.0
f1 (ppm)

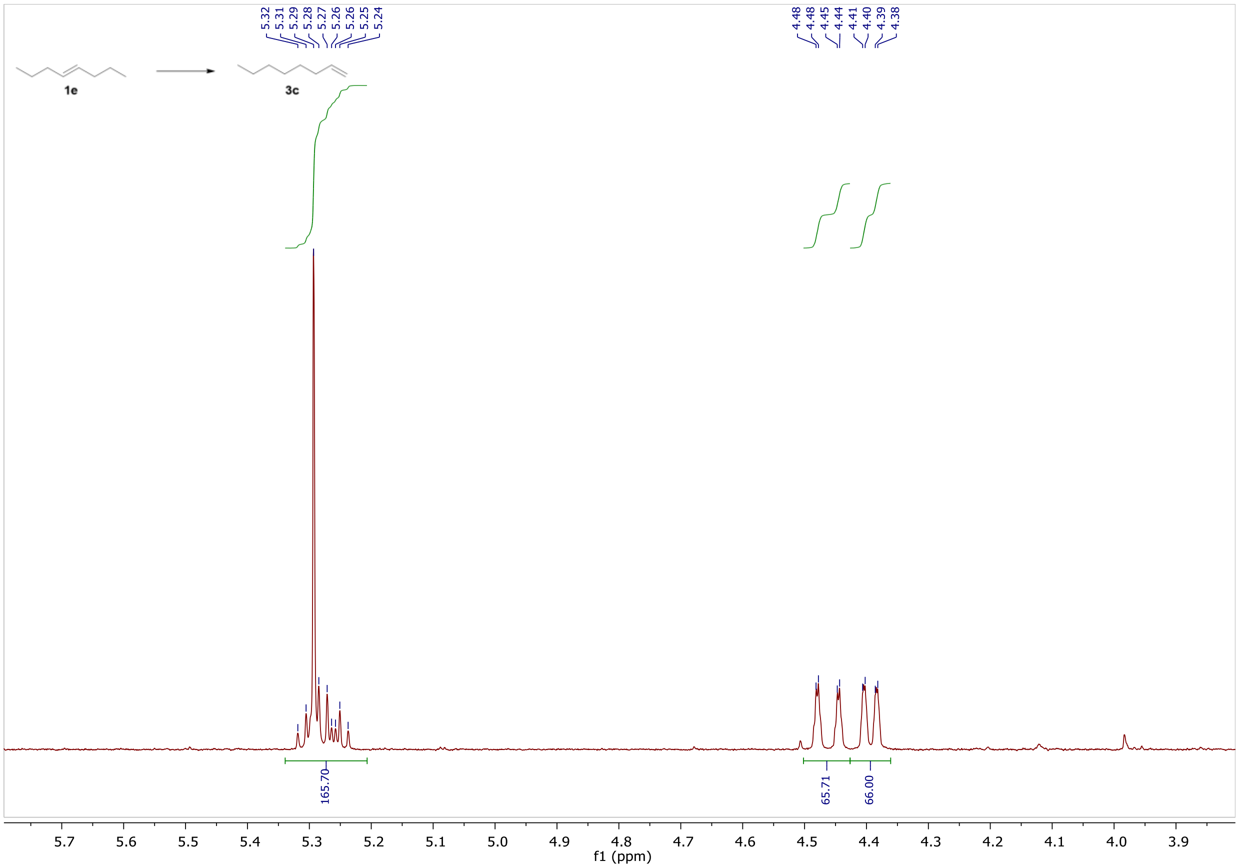
5.32
5.31
5.29
5.28
5.27
5.26
5.26
5.25
5.24
4.48
4.48
4.45
4.44
4.41
4.40
4.39
4.38
1e
3c
165.70
65.71
66.00
5.7
5.6
5.5
5.4
5.3
5.2
5.1
5.0
4.9
4.8
4.7
4.6
4.5
4.4
4.3
4.2
4.1
4.0
3.9
f1 (ppm)

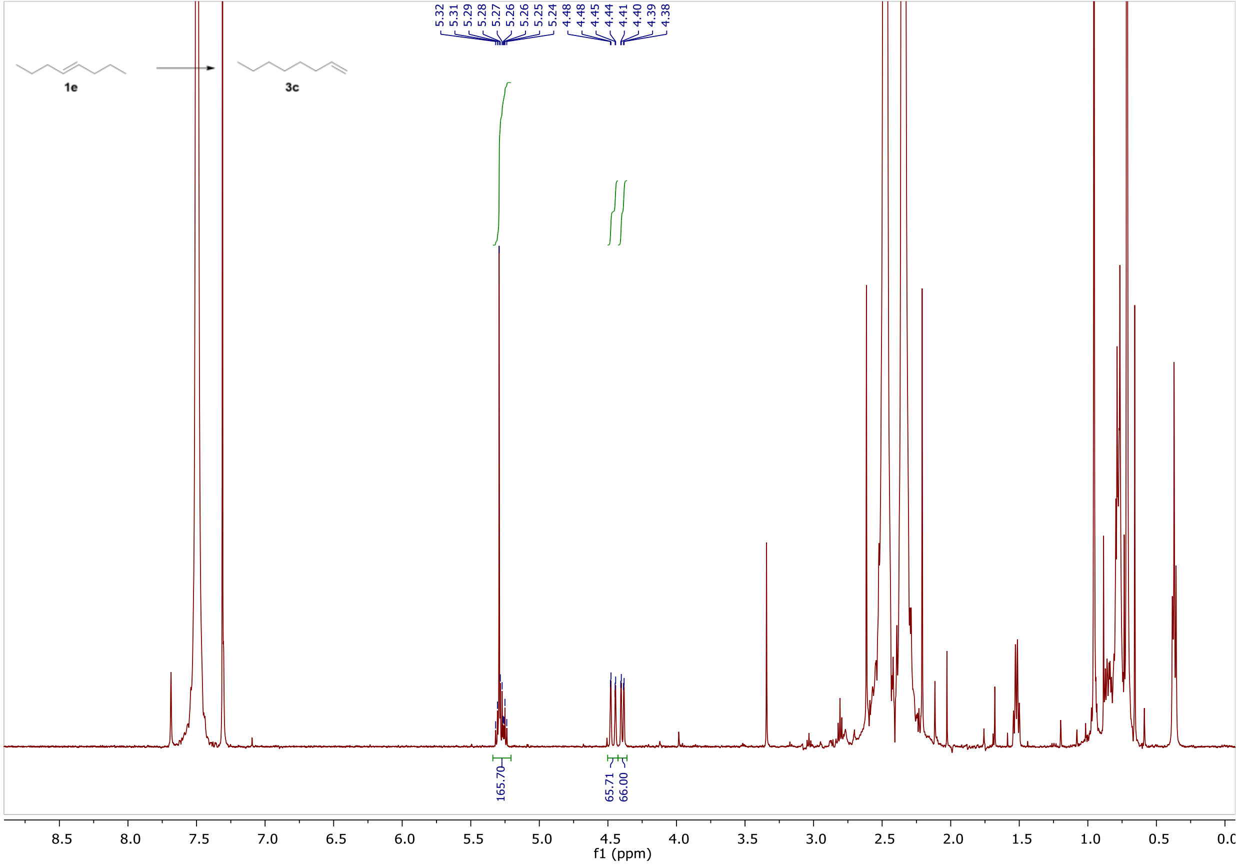
5.32
5.31
5.29
5.28
5.27
5.26
5.26
5.25
5.24
4.48
4.48
4.45
4.44
4.41
4.40
4.39
4.38
1e
3c
165.70
65.71
66.00
8.5
8.0
7.5
7.0
6.5
6.0
5.5
5.0
4.5
4.0
3.5
3.0
2.5
2.0
1.5
1.0
0.5
0.0
f1 (ppm)

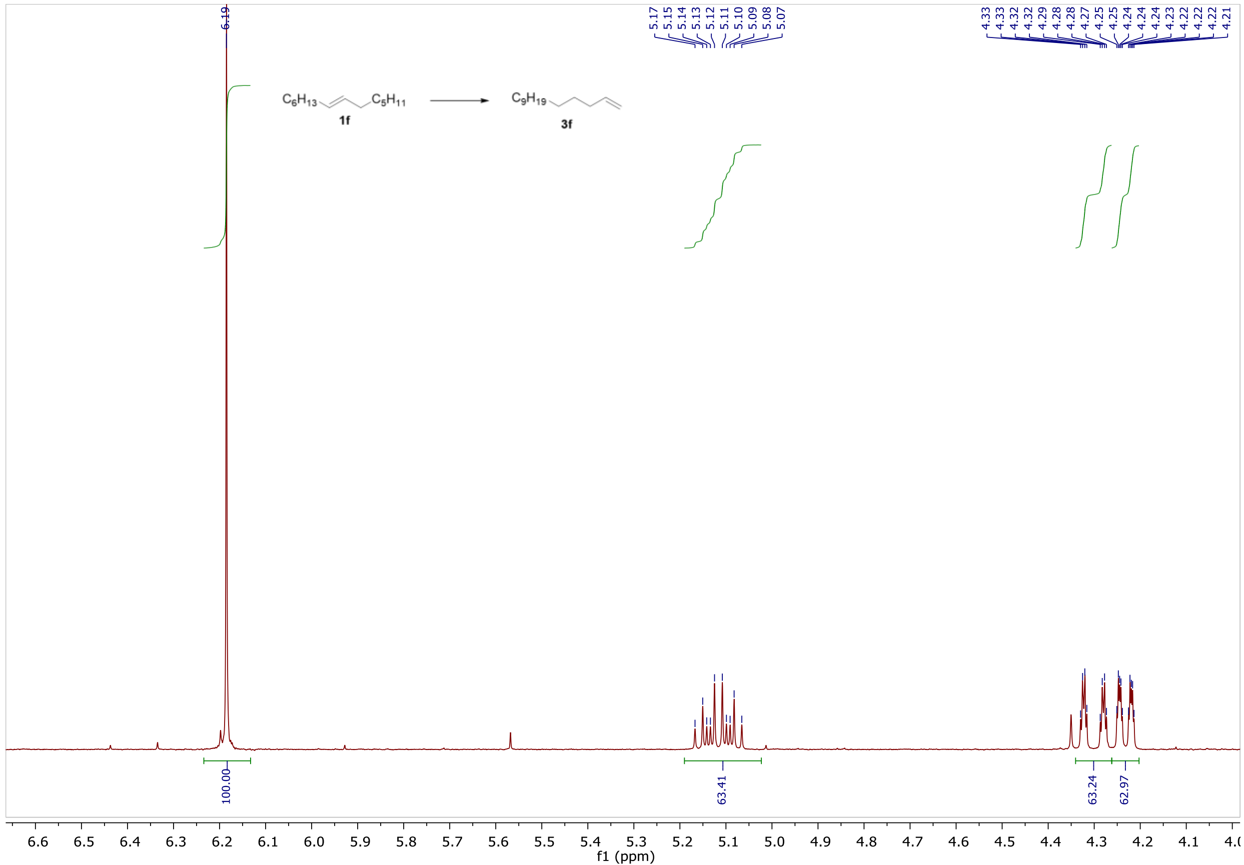

C6H13 C5H11
1f
C9H19
3f
6.19
5.17 5.15 5.14 5.13 5.12 5.11 5.10 5.09 5.08 5.07
4.33 4.33 4.32 4.32 4.29 4.28 4.28 4.27 4.25 4.25 4.24 4.24 4.24 4.24 4.23 4.22 4.22 4.22 4.21
100.00
63.41
63.24
62.97
6.6 6.5 6.4 6.3 6.2 6.1 6.0 5.9 5.8 5.7 5.6 5.5 5.4 5.3 5.2 5.1 5.0 4.9 4.8 4.7 4.6 4.5 4.4 4.3 4.2 4.1 4.0
f1 (ppm)

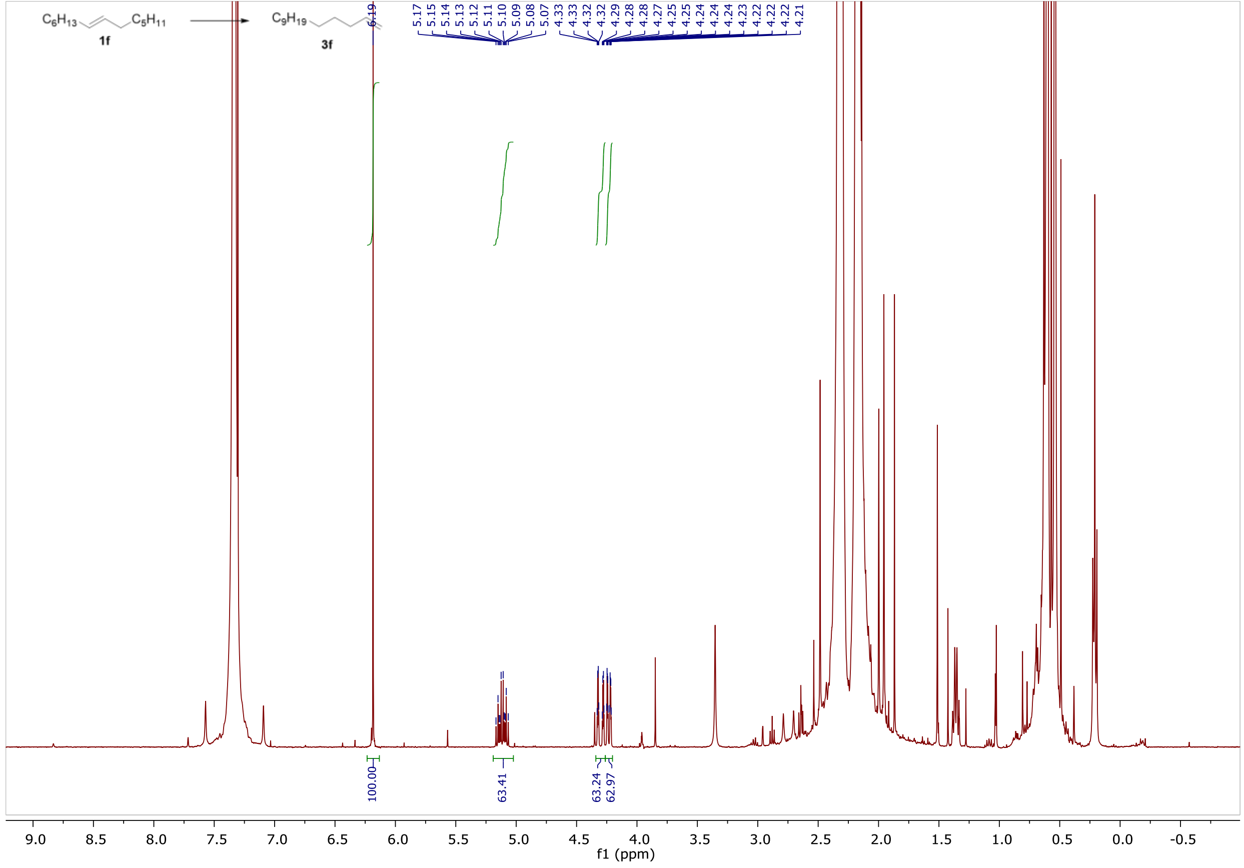

C6H13 C5H11
1f
C9H19
3f
6.19
5.17 5.15 5.14 5.13 5.12 5.11 5.10 5.09 5.08 5.07
4.33 4.33 4.32 4.32 4.29 4.28 4.28 4.27 4.25 4.25 4.24 4.24 4.24 4.24 4.23 4.22 4.22 4.22 4.21
100.00
63.41
63.24
62.97
9.0 8.5 8.0 7.5 7.0 6.5 6.0 5.5 5.0 4.5 4.0 3.5 3.0 2.5 2.0 1.5 1.0 0.5 0.0 -0.5
f1 (ppm)

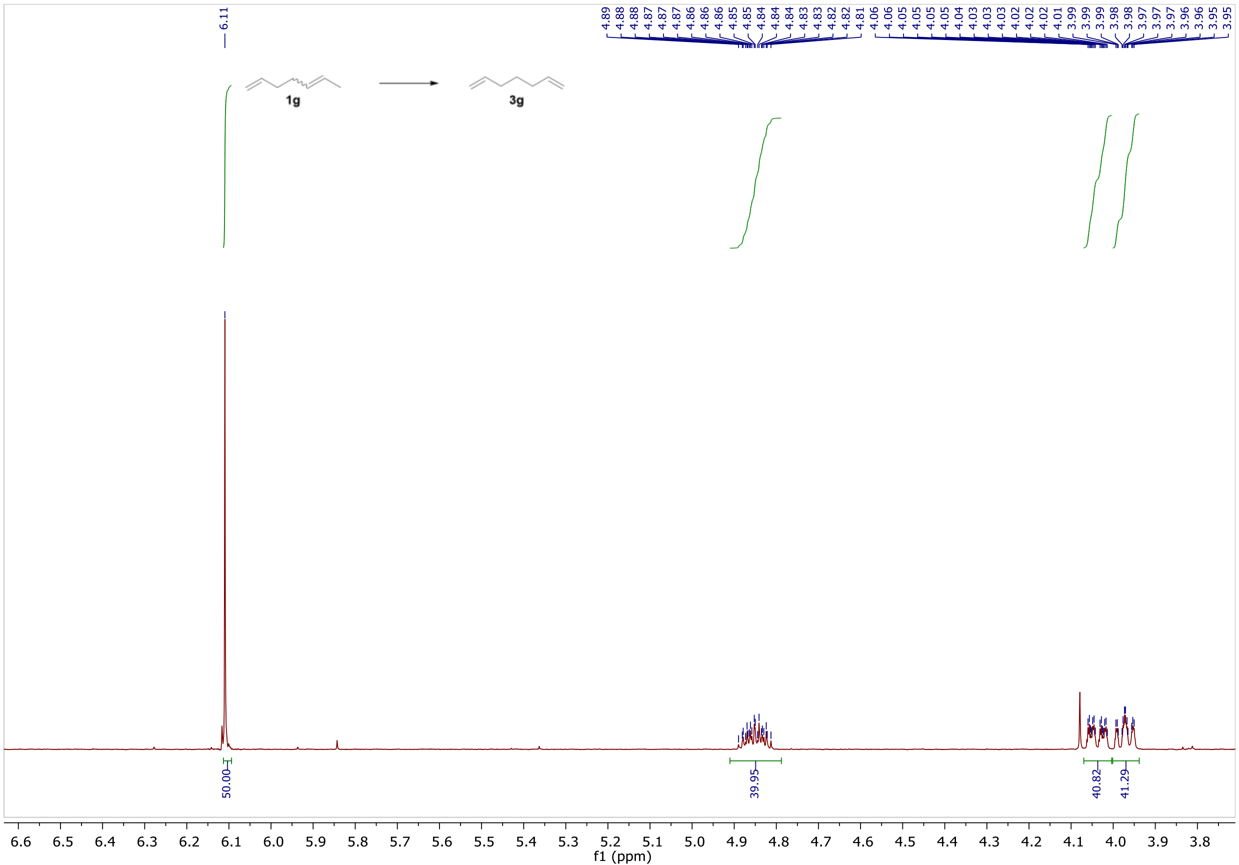
6.11
4.89
4.88
4.88
4.87
4.87
4.87
4.86
4.86
4.85
4.85
4.84
4.84
4.84
4.83
4.83
4.82
4.82
4.81
4.06
4.05
4.05
4.05
4.05
4.04
4.03
4.03
4.03
4.02
4.02
4.01
3.99
3.99
3.98
3.98
3.97
3.97
3.97
3.96
3.96
3.95
3.95
1g
3g
50.00
39.95
40.82
41.29
6.6
6.5
6.4
6.3
6.2
6.1
6.0
5.9
5.8
5.7
5.6
5.5
5.4
5.3
5.2
5.1
5.0
4.9
4.8
4.7
4.6
4.5
4.4
4.3
4.2
4.1
4.0
3.9
3.8
f1 (ppm)

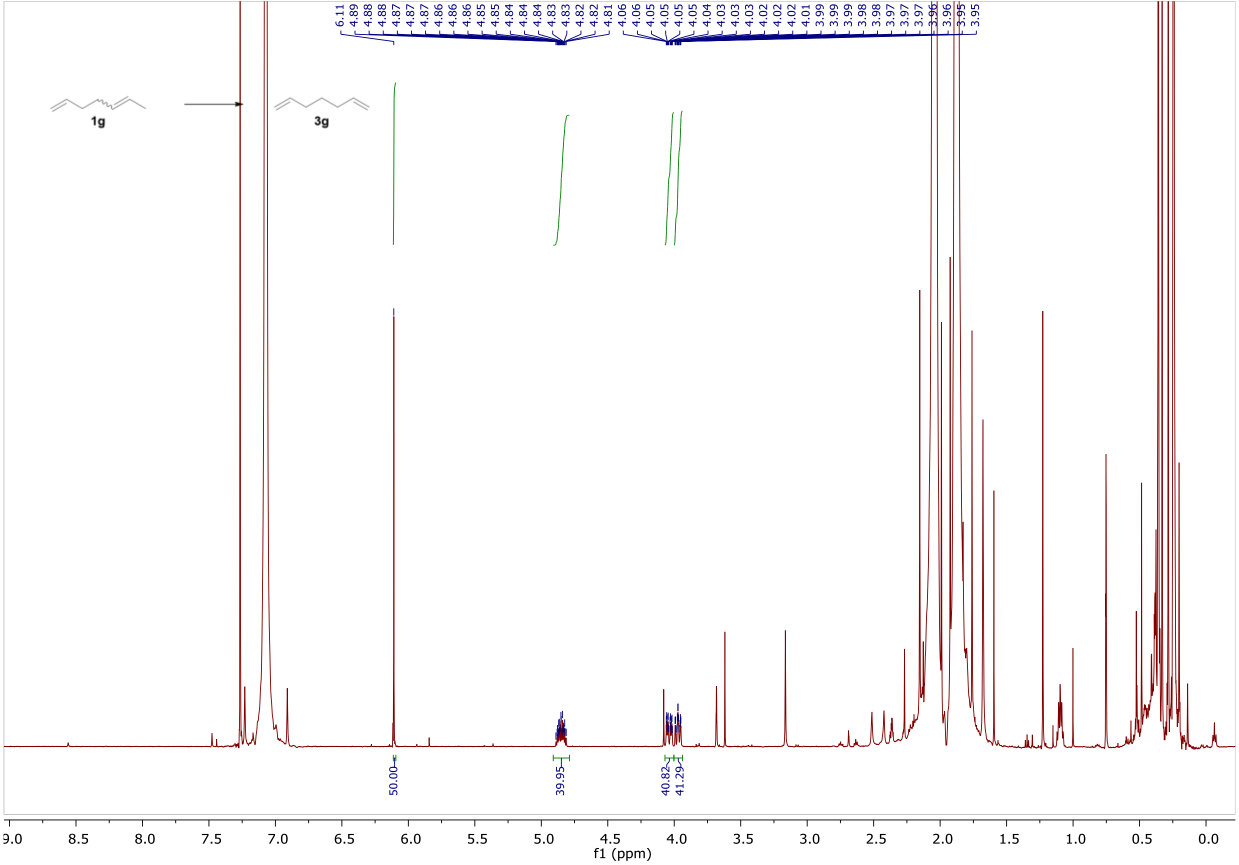
6.11
4.89
4.88
4.88
4.87
4.87
4.86
4.86
4.86
4.85
4.85
4.84
4.84
4.84
4.83
4.83
4.82
4.82
4.81
4.06
4.06
4.05
4.05
4.05
4.05
4.04
4.03
4.03
4.02
4.02
4.02
4.01
3.99
3.99
3.99
3.98
3.97
3.97
3.97
3.96
3.96
3.95
3.95
1g
3g
50.00
39.95
40.82
41.29
9.0
8.5
8.0
7.5
7.0
6.5
6.0
5.5
5.0
4.5
4.0
3.5
3.0
2.5
2.0
1.5
1.0
0.5
0.0
f1 (ppm)

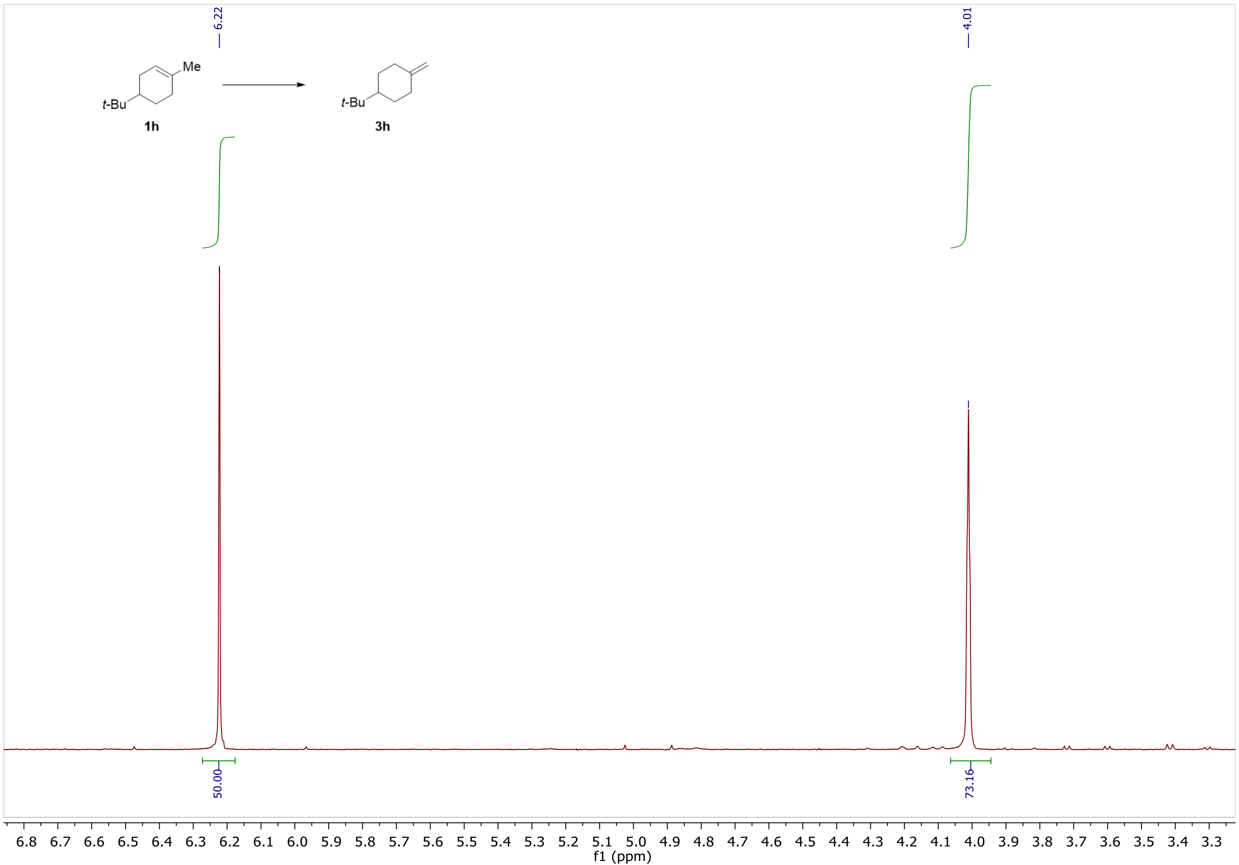
6.22
4.01
Me
t-Bu
1h
t-Bu
3h
50.00
73.16
6.8 6.7 6.6 6.5 6.4 6.3 6.2 6.1 6.0 5.9 5.8 5.7 5.6 5.5 5.4 5.3 5.2 5.1 5.0 4.9 4.8 4.7 4.6 4.5 4.4 4.3 4.2 4.1 4.0 3.9 3.8 3.7 3.6 3.5 3.4 3.3
f1 (ppm)

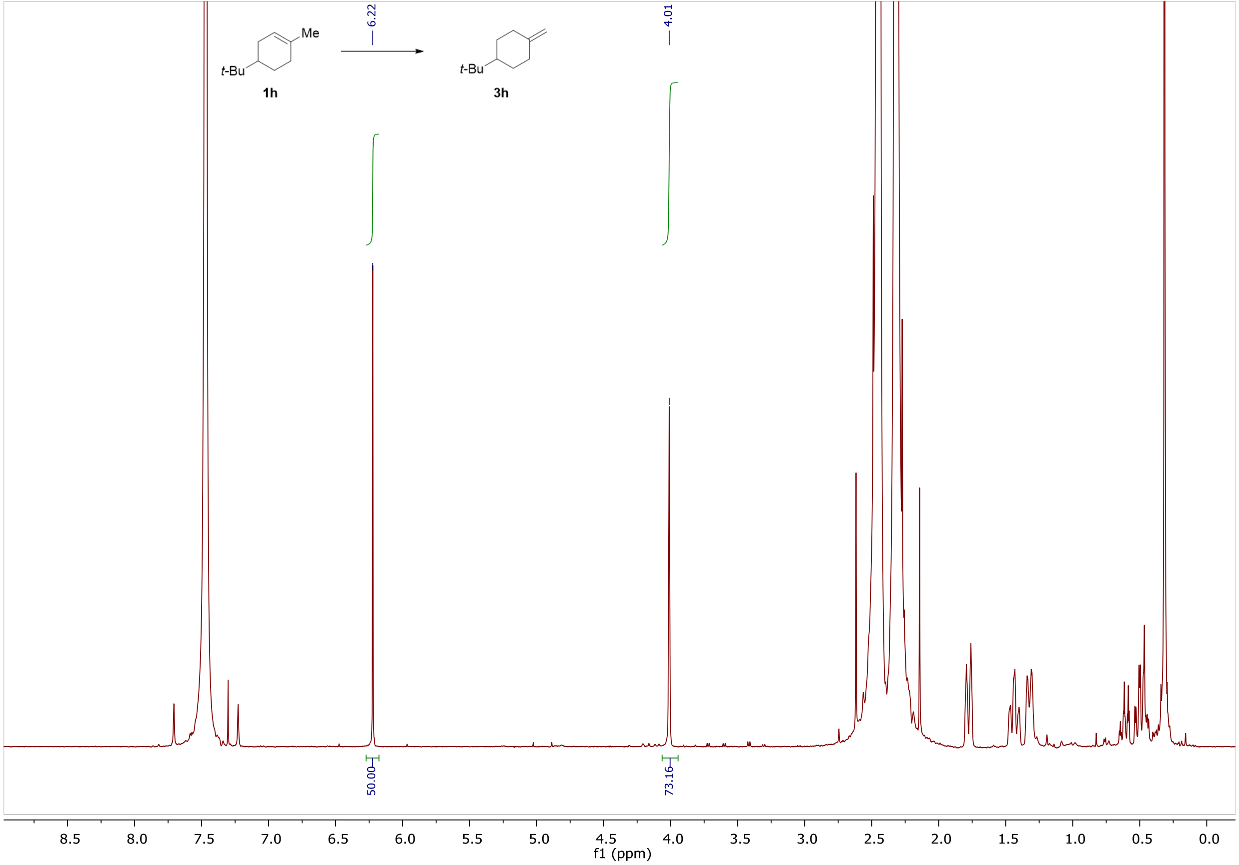
6.22
4.01
Me
t-Bu
1h
t-Bu
3h
50.00
73.16
8.5 8.0 7.5 7.0 6.5 6.0 5.5 5.0 4.5 4.0 3.5 3.0 2.5 2.0 1.5 1.0 0.5 0.0
f1 (ppm)

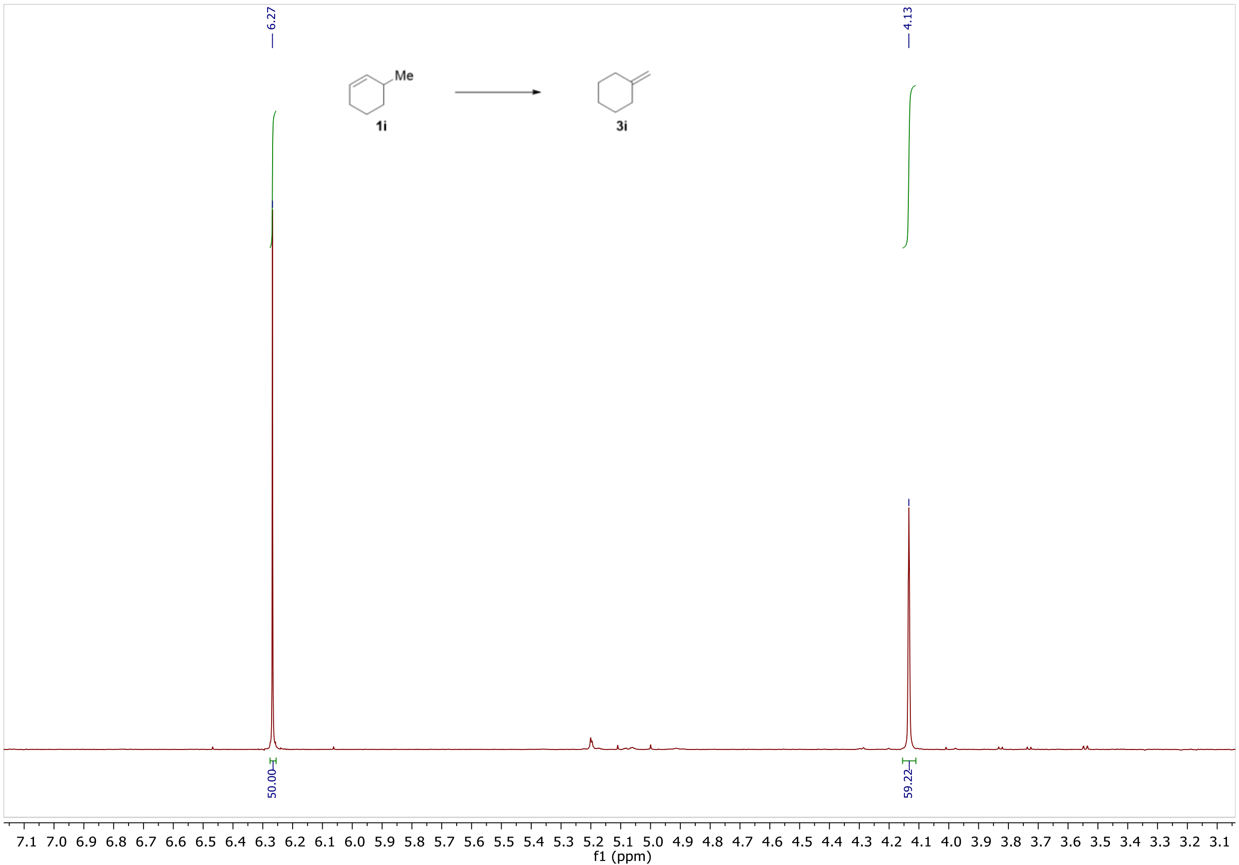

6.27
4.13
Me
1i
3i
50.00
59.22
7.1 7.0 6.9 6.8 6.7 6.6 6.5 6.4 6.3 6.2 6.1 6.0 5.9 5.8 5.7 5.6 5.5 5.4 5.3 5.2 5.1 5.0 4.9 4.8 4.7 4.6 4.5 4.4 4.3 4.2 4.1 4.0 3.9 3.8 3.7 3.6 3.5 3.4 3.3 3.2 3.1
f1 (ppm)

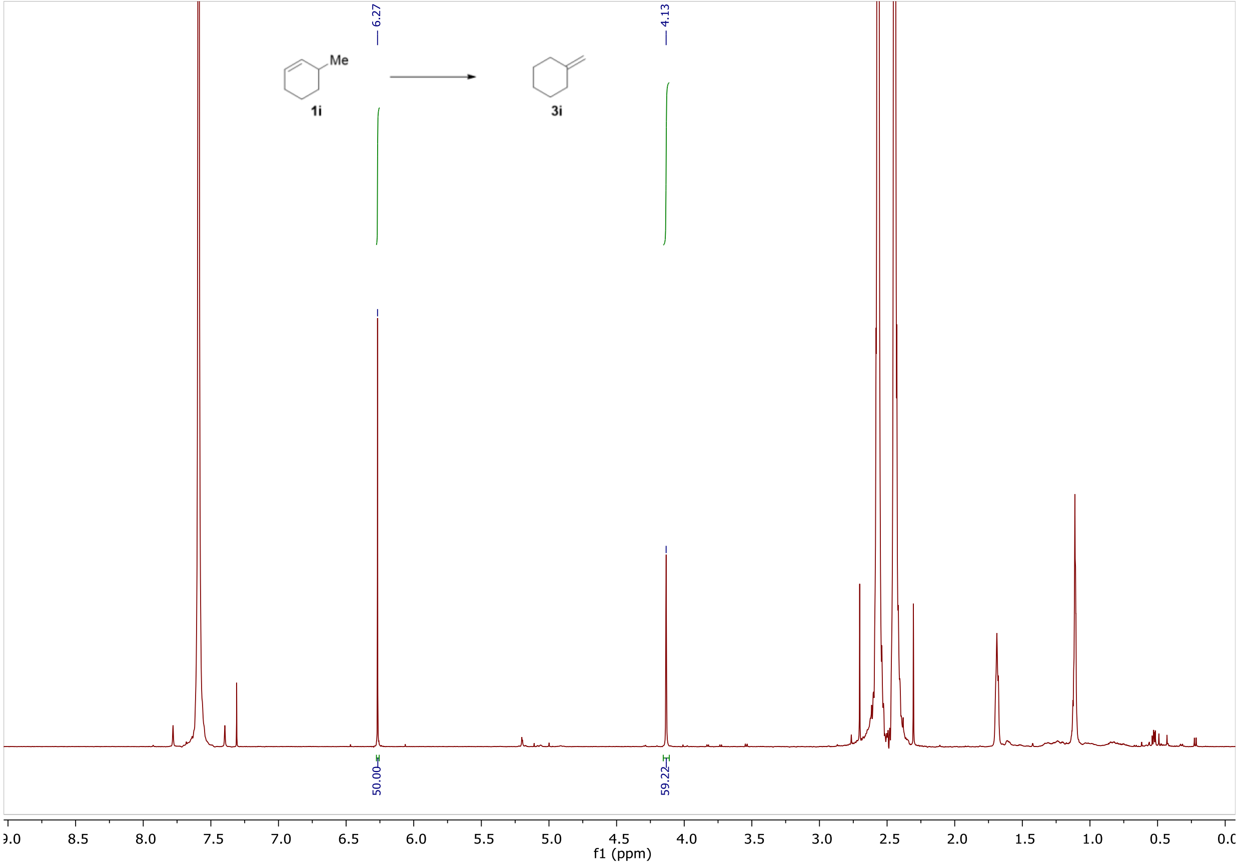

6.27
4.13
Me
1i
3i
50.00
59.22
9.0 8.5 8.0 7.5 7.0 6.5 6.0 5.5 5.0 4.5 4.0 3.5 3.0 2.5 2.0 1.5 1.0 0.5 0.0
f1 (ppm)

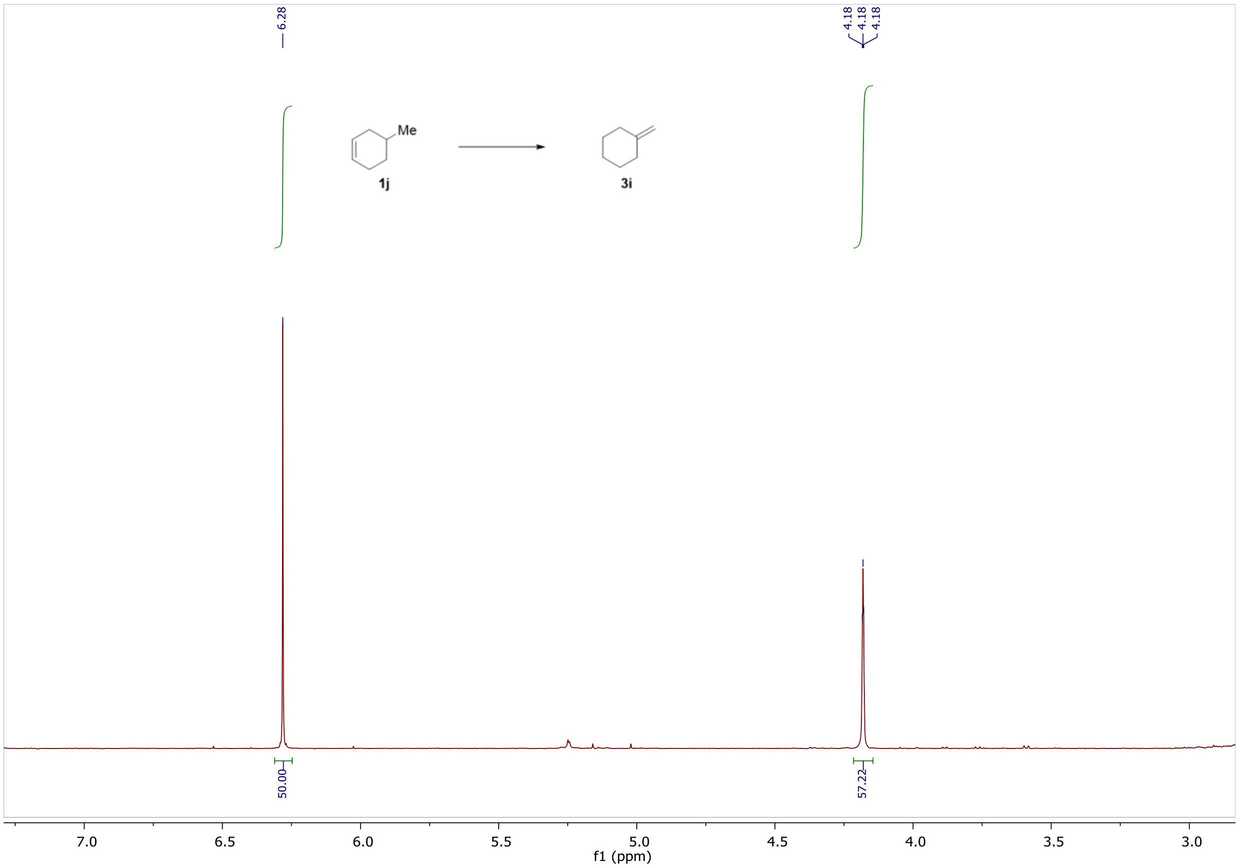
6.28
4.18
4.18
4.18
Me
1j
3i
50.00
57.22
7.0
6.5
6.0
5.5
5.0
4.5
4.0
3.5
3.0
f1 (ppm)

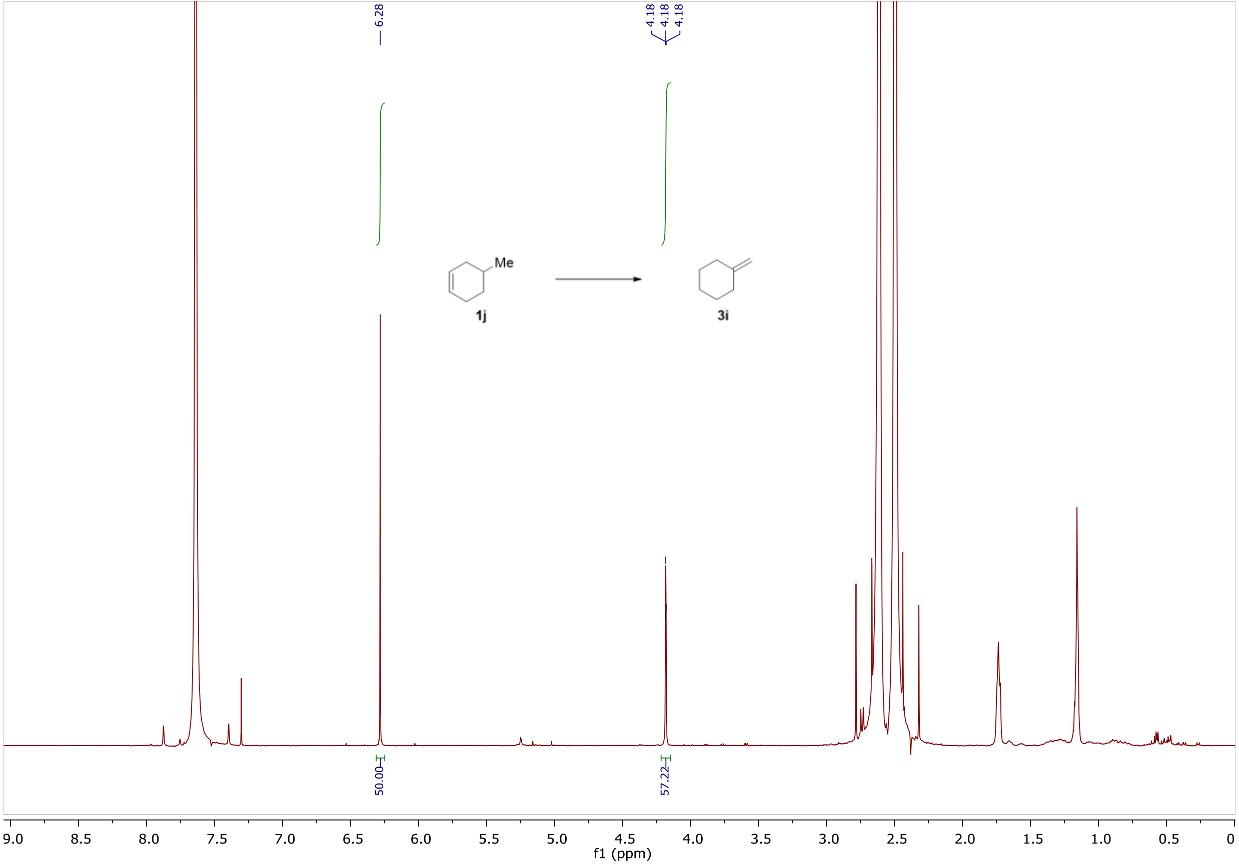
6.28
4.18
4.18
4.18
Me
1j
3i
50.00
57.22
9.0
8.5
8.0
7.5
7.0
6.5
6.0
5.5
5.0
4.5
4.0
3.5
3.0
2.5
2.0
1.5
1.0
0.5
0
f1 (ppm)

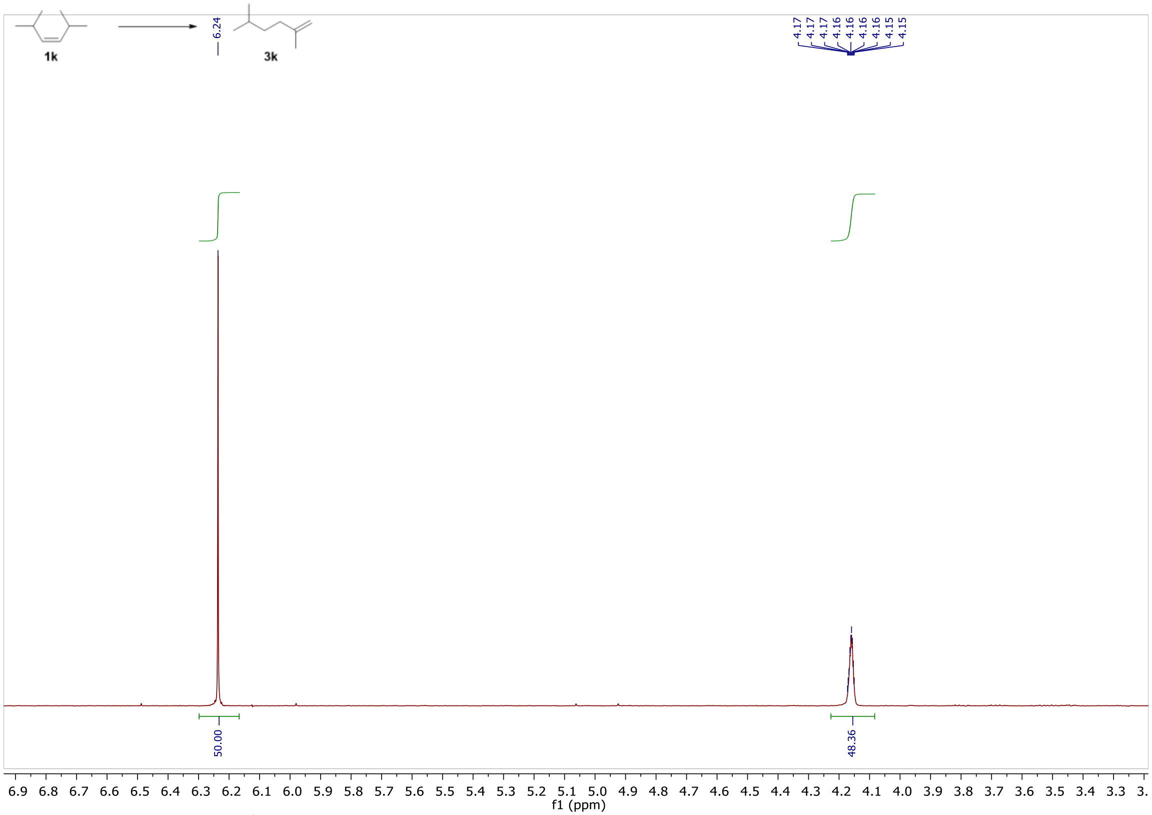
1k
3k
6.24
4.17
4.17
4.17
4.16
4.16
4.16
4.16
4.15
4.15
50.00
48.36
6.9 6.8 6.7 6.6 6.5 6.4 6.3 6.2 6.1 6.0 5.9 5.8 5.7 5.6 5.5 5.4 5.3 5.2 5.1 5.0 4.9 4.8 4.7 4.6 4.5 4.4 4.3 4.2 4.1 4.0 3.9 3.8 3.7 3.6 3.5 3.4 3.3 3.
f1 (ppm)

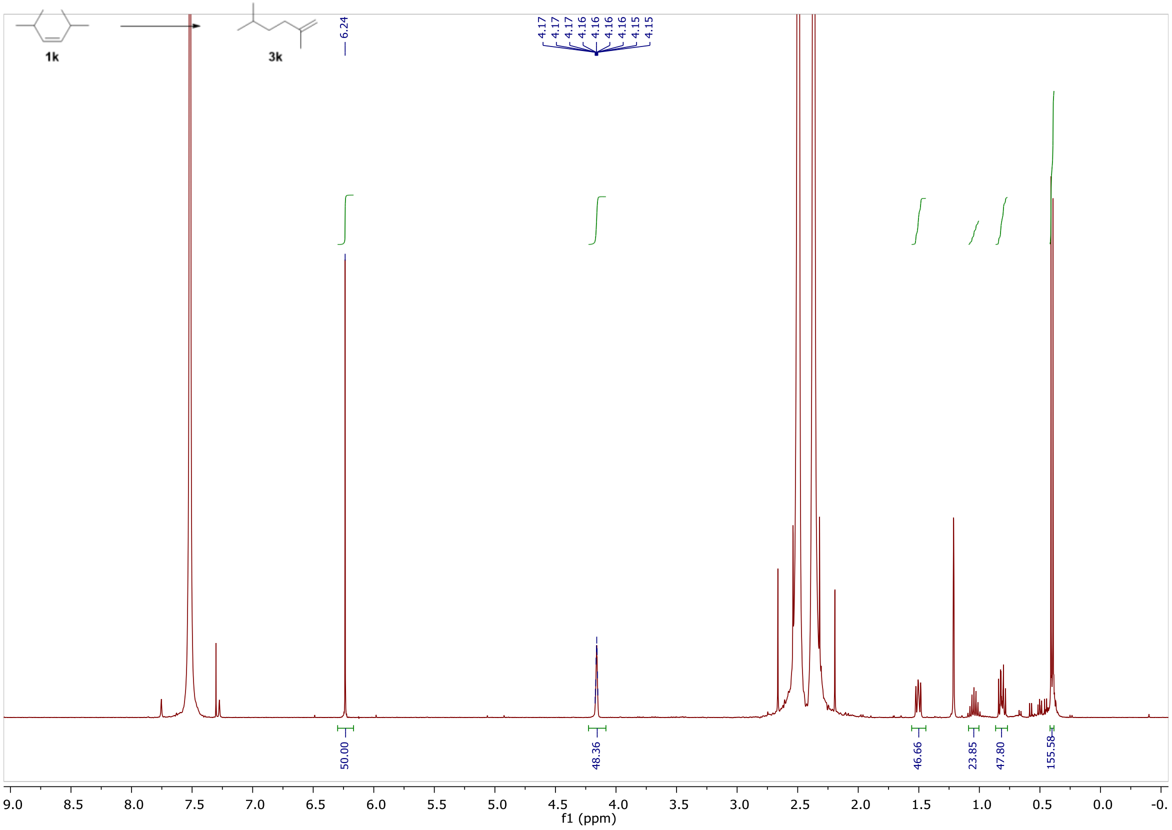
1k
3k
6.24
4.17
4.17
4.17
4.16
4.16
4.16
4.16
4.15
4.15
50.00
48.36
46.66
23.85
47.80
155.58
9.0 8.5 8.0 7.5 7.0 6.5 6.0 5.5 5.0 4.5 4.0 3.5 3.0 2.5 2.0 1.5 1.0 0.5 0.0 -0.
f1 (ppm)

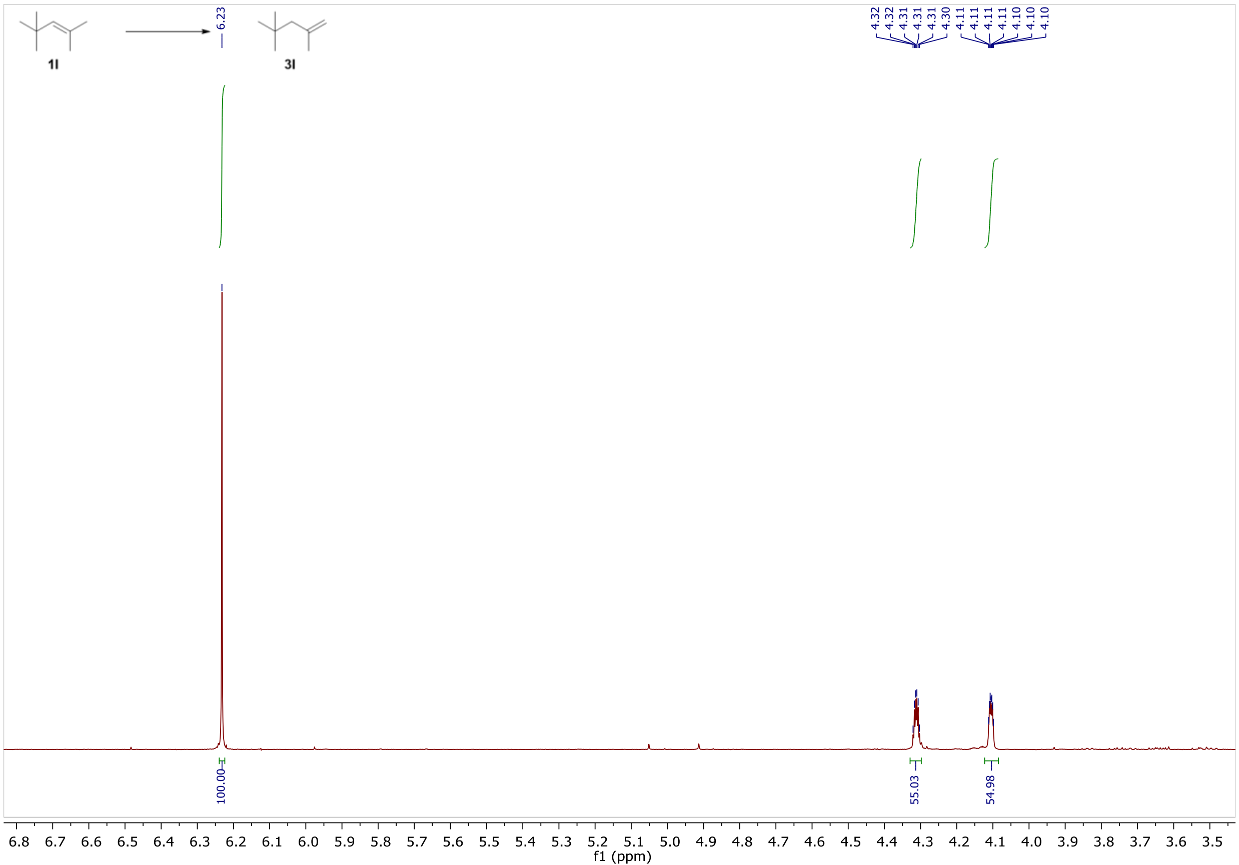
1l
3l
6.23
4.32
4.32
4.31
4.31
4.31
4.30
4.11
4.11
4.11
4.11
4.10
4.10
4.10
100.00
55.03
54.98
6.8
6.7
6.6
6.5
6.4
6.3
6.2
6.1
6.0
5.9
5.8
5.7
5.6
5.5
5.4
5.3
5.2
5.1
5.0
4.9
4.8
4.7
4.6
4.5
4.4
4.3
4.2
4.1
4.0
3.9
3.8
3.7
3.6
3.5
f1 (ppm)

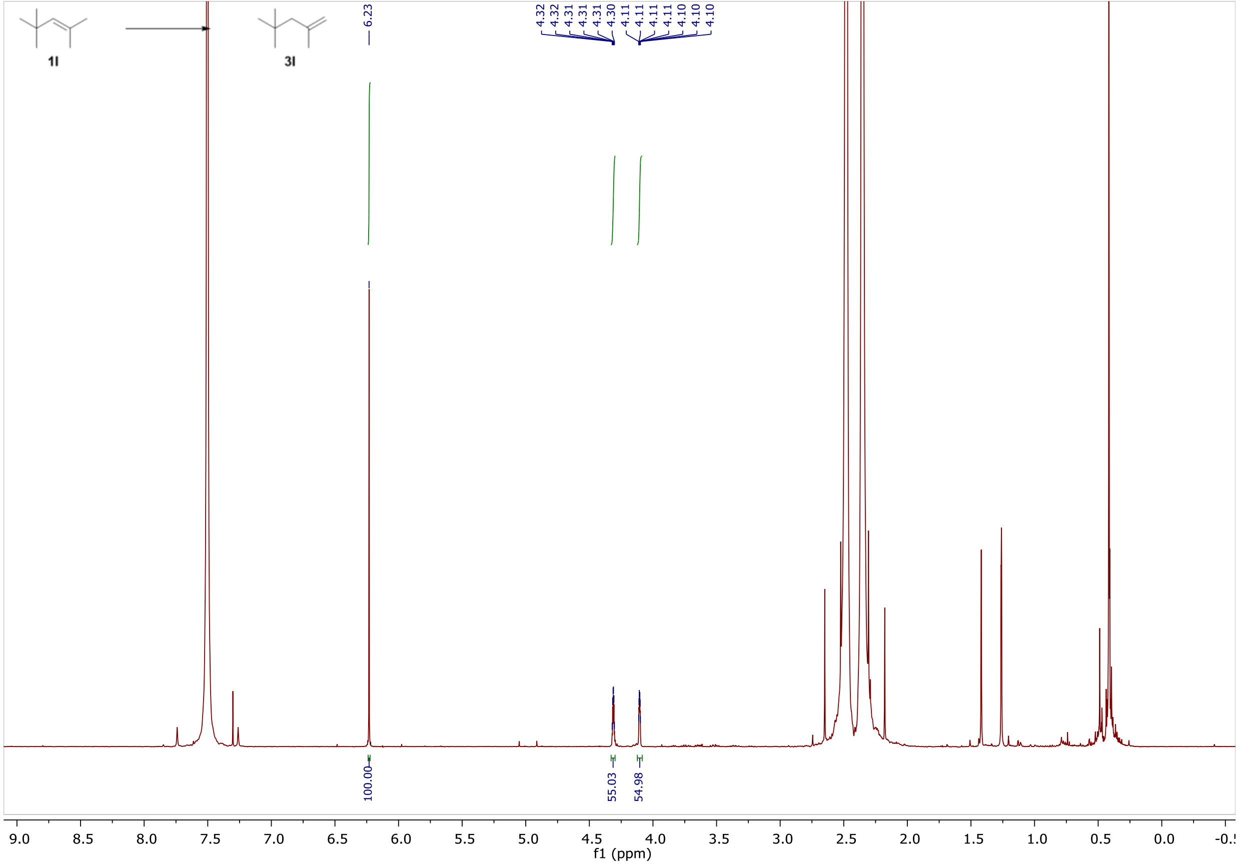
1l
3l
6.23
4.32
4.32
4.31
4.31
4.31
4.30
4.11
4.11
4.11
4.11
4.10
4.10
4.10
100.00
55.03
54.98
9.0
8.5
8.0
7.5
7.0
6.5
6.0
5.5
5.0
4.5
4.0
3.5
3.0
2.5
2.0
1.5
1.0
0.5
0.0
-0.5
f1 (ppm)

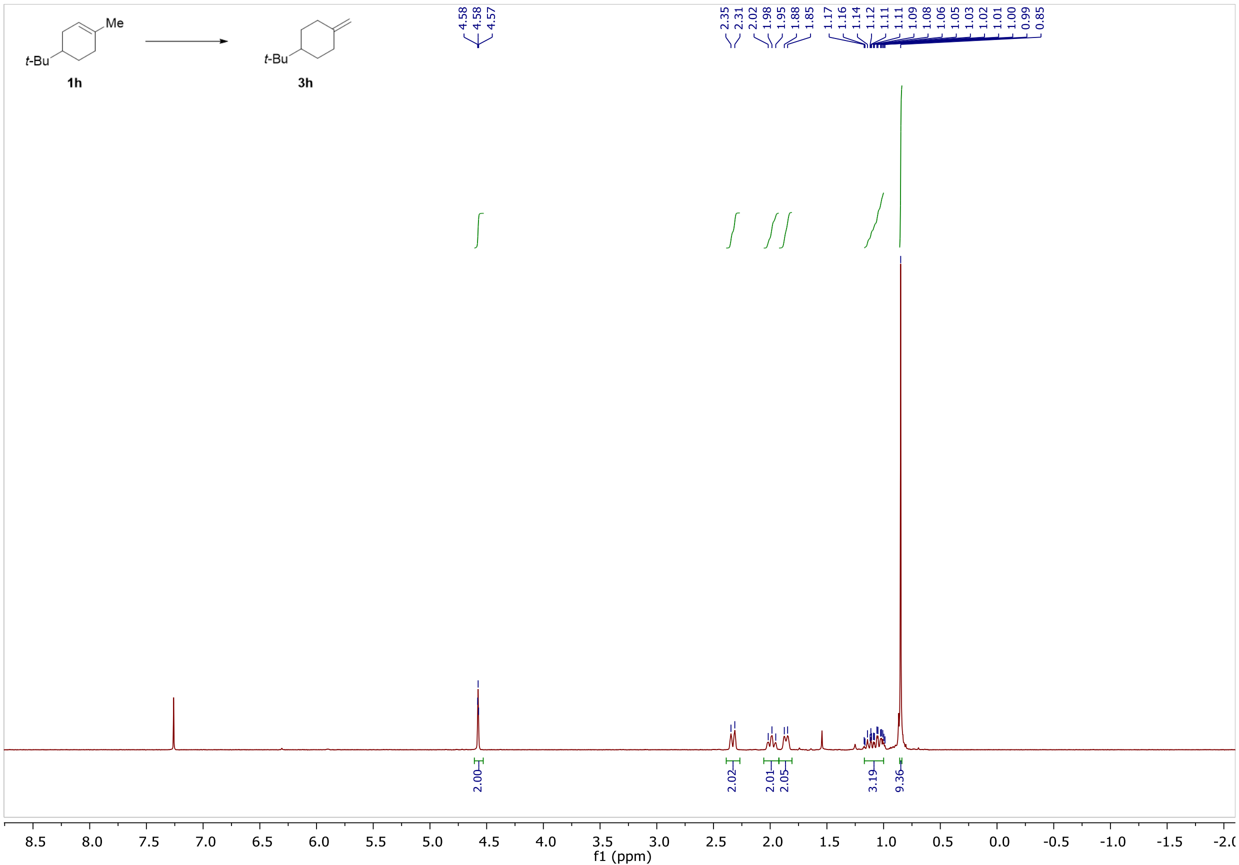
Me
t-Bu
1h
t-Bu
3h
4.58
4.58
4.57
2.35
2.31
2.02
1.98
1.95
1.88
1.85
1.17
1.16
1.14
1.12
1.11
1.11
1.09
1.08
1.06
1.05
1.03
1.02
1.01
1.00
0.99
0.85
2.00
2.02
2.01
2.05
3.19
9.36
8.5
8.0
7.5
7.0
6.5
6.0
5.5
5.0
4.5
4.0
3.5
3.0
2.5
2.0
1.5
1.0
0.5
0.0
-0.5
-1.0
-1.5
-2.0
f1 (ppm)

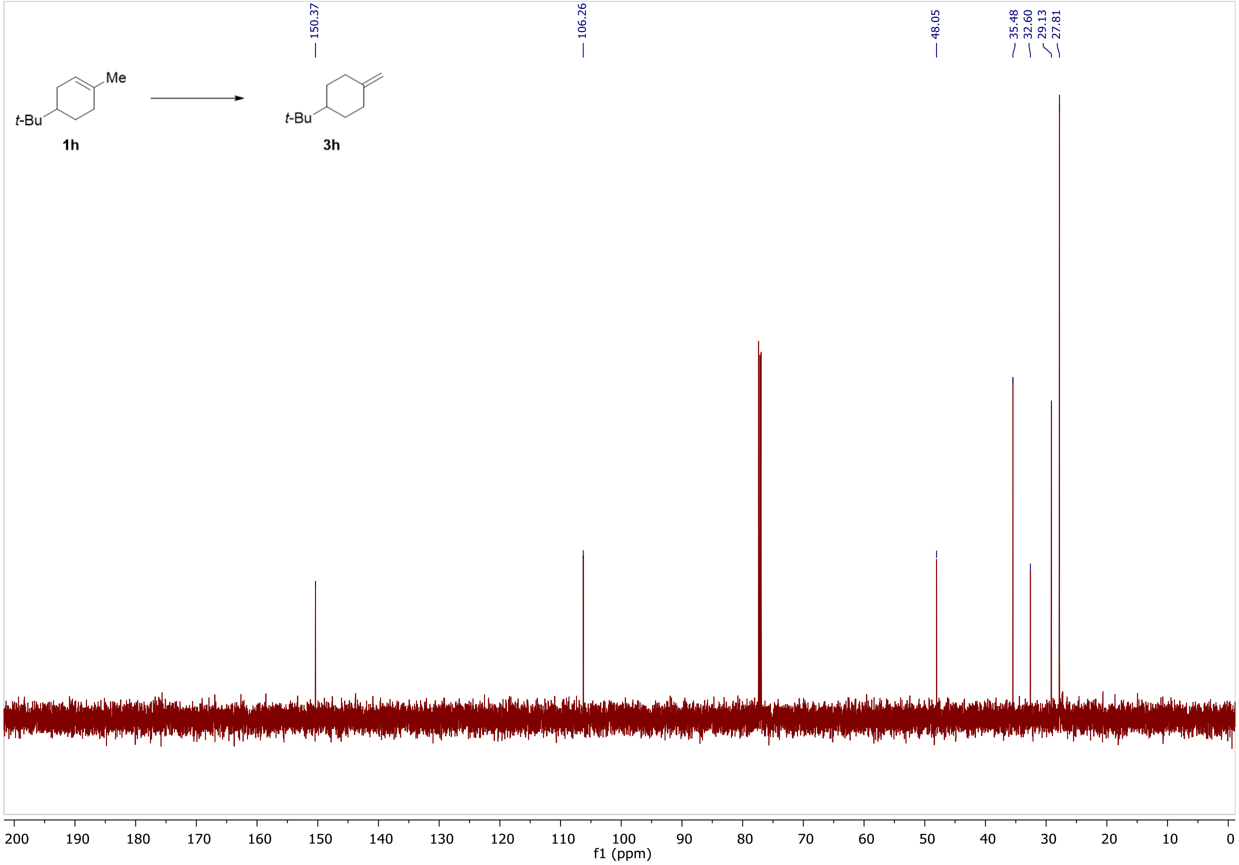
150.37
106.26
48.05
35.48
32.60
29.13
27.81
Me
t-Bu
1h
t-Bu
3h
200
190
180
170
160
150
140
130
120
110
100
90
80
70
60
50
40
30
20
10
0
f1 (ppm)

3.4 References

Parts of this chapter were reprinted with permission from:
"Contra-thermodynamic Olefin Isomerization by Chain-Walking Hydrofunctionalization and Formal Retro-hydrofunctionalization"
Hanna, S; Butcher, T. W.; Hartwig J. F. *Org. Lett.* **2019**, *21*, 7129–7133.

1. (a) Biswas, S.; Huang, Z.; Choliy, Y.; Wang, D. Y.; Brookhart, M.; Krogh-Jespersen, K.; Goldman, A. S. Olefin Isomerization by Iridium Pincer Catalysts. Experimental Evidence for an η^3-Allyl Pathway and an Unconventional Mechanism Predicted by DFT Calculations. *J. Am. Chem. Soc.* **2012**, *134*, 13276. (b) Larionov, E.; Li, H.; Mazet, C. Well-Defined Transition Metal Hydrides in Catalytic Isomerization. *Chem. Commun.* **2014**, *50*, 9816. (c) Crossley, S. W. M.; Barabé, F.; Shenvi, R. A. Simple, Chemoselective, Catalytic Olefin Isomerization. *J. Am. Chem. Soc.* **2014**, *136*, 16788.

2. (a) Harwood, L. M.; Julia, M. A Convenient Synthesis of (+)-β-Pinene from (+)-α-Pinene. *Synthesis* **1980**, *1980*, 456. (b) Min, Y.-F.; Zhang, B.-W.; Cao, Y. A New Synthesis of (-)-β-Pinene from (-)-α-Pinene. *Synthesis* **1982**, *1982*, 875. (c) Andrianome, M.; Häberle, K.; Delmond, B. Allyl-and benzylstannanes, new reagents in terpenic synthesis. *Tetrahedron* **1989**, *45*, 1079. (d) Eng, S. L.; Ricard, R.; Wan, C. S. K.; Weedon, A. C. Photochemical Deconjugation of α,β-Unsaturated Ketones. *J. Chem. Soc., Chem. Commun.* **1983**, 236. (e) Guignard, R. F.; Petit, L.; Zard, S. Z. A Method for the Net Contra-thermodynamic Isomerization of Cyclic Trisubstituted Alkenes. *Org. Lett.* **2013**, *15*, 4178.

3. (a) Brown, H. C.; Bhatt, M. V.; Munekata, T.; Zweifel, G. Organoboranes. VII. The Displacement Reaction with Organoboranes Derived from the Hydroboration of Cyclic and Bicyclic Olefins. Conversion of Endocyclic to Exocyclic Double Bonds. *J. Am. Chem. Soc.* **1967**, *89*, 567. (b) Brown, H. C.; Bhatt, M. V. Organoboranes. IV. The Displacement Reaction with Organoboranes Derived from the Hydroboration of Branched-Chain Olefins. A Contrathermodynamic Isomerization of Olefins. *J. Am. Chem. Soc.* **1966**, *88*, 1440.

4. (a) Sommer, H.; Juliá-Hernández, F.; Martin, R.; Marek, I. Walking Metals for Remote Functionalization. *ACS Cent. Sci.* **2018**, *4*, 153. (b) Juliá-Hernández, F.; Moragas, T.; Cornella, J.; Martin, R. Remote Carboxylation of Halogenated Aliphatic Hydrocarbons with Carbon Dioxide. *Nature* **2017**, *545*, 84.

5. (a) Saam, J.; Speier, J. The Addition of Silicon Hydrides to Olefinic Double Bonds. Part VI. Addition to Branched Olefins. *J. Am. Chem. Soc.* **1961**, *83*, 1351. (b) Bank, H. M.; Saam, J. C.; Speier, J. L. The Addition of Silicon Hydrides to Olefinic Double Bonds. IX. Addition of sym-Tetramethyldisiloxane to Hexene-1, -2, and -3. *J. Org. Chem.* **1964**, *29*, 792. (c) Benkeser, R. A.; Muench, W. C. The Addition Rates of Dichloro- and Trichlorosilane to 2-Pentene and 1-Octene. *J. Organomet. Chem.* **1980**, *184*, C3. (d) Yarosh, O. G.; Zhilitskaya, L. V.; Yarosh, N. K.; Albanov, A. I.; Voronkov, M. G. Hydrosilylation of Cyclohexene, 1-Methylcyclohexene, and Isopropylidenecyclohexane. *Russ. J. Gen. Chem.* **2004**, *74*, 1895.

6. (a) Edwards, D. R.; Crudden, C. M.; Yam, K. One-Pot Carbon Monoxide-Free Hydroformylation of Internal Olefins to Terminal Aldehydes. *Adv. Synth. Catal.* **2005**, *347*, 50. (b) Lata, C. J.; Crudden, C. M. Dramatic Effect of Lewis Acids on the Rhodium-Catalyzed Hydroboration of Olefins. *J. Am. Chem. Soc.* **2010**, *132*, 131. (c) Obligacion, J. V.; Chirik, P. J. Bis(imino)pyridine Cobalt-Catalyzed Alkene Isomerization–Hydroboration: A Strategy for Remote Hydrofunctionalization with Terminal Selectivity. *J. Am. Chem. Soc.* **2013**, *135*, 19107. (d) Palmer, W. N.; Diao, T.; Pappas, I.; Chirik, P. J. High-Activity Cobalt Catalysts for Alkene Hydroboration with Electronically Responsive Terpyridine and α-Diimine Ligands. *ACS Catal.* **2015**, *5*, 622. (e) Ogawa, T.; Ruddy, A. J.; Sydora, O. L.; Stradiotto, M.; Turculet, L. Cobalt- and Iron-Catalyzed Isomerization–Hydroboration of Branched Alkenes: Terminal Hydroboration with Pinacolborane and 1,3,2-Diazaborolanes. *Organometallics* **2017**, *36*, 417.

7. Arthur, P.; England, D. C.; Pratt, B. C.; Whitman, G. M. Addition of Hydrogen Cyanide to Unsaturated Compounds. *J. Am. Chem. Soc.* **1954**, *76*, 5364.

8. (a) van der Veen, L. A.; Kamer, P. C. J.; van Leeuwen, P. W. N. M. Hydroformylation of Internal Olefins to Linear Aldehydes with Novel Rhodium Catalysts. *Angew. Chem. Int. Ed.* **1999**, *38*, 336. (b) Yuki, Y.; Takahashi, K.; Tanaka, Y.; Nozaki, K. Tandem Isomerization/Hydroformylation/Hydrogenation of Internal Alkenes to *n*-Alcohols Using Rh/Ru Dual- or Ternary-Catalyst Systems. *J. Am. Chem. Soc.* **2013**, *135*, 17393. (c) Börner, M. V.-H.; Lutz, D.; Armin Isomerization–Hydroformylation Tandem Reactions. *ACS Catal.* **2014**, *4*, 1706.

9. (a) Jimenez Rodriguez, C.; Foster, D. F.; Eastham, G. R.; Cole-Hamilton, D. J. Highly Selective Formation of Linear Esters from Terminal and Internal Alkenes Catalysed by Palladium Complexes of Bis-(di-*tert*-Butylphosphinomethyl)benzene. *Chem. Commun.* **2004**, 1720. (b) Jiménez-Rodriguez, C.; Eastham, G. R.; Cole-

Hamilton, D. J. Dicarboxylic Acid Esters from the Carbonylation of Unsaturated Esters Under Mild Conditions. *Inorg. Chem. Commun.* **2005**, *8*, 878. (c) Mgaya, J. E.; Bartlett, S. A.; Mubofu, E. B.; Mgani, Q. A.; Slawin, A. M. Z.; Pogorzelec, P. J.; Cole-Hamilton, D. J. Synthesis of Bifunctional Monomers by the Palladium-Catalyzed Carbonylation of Cardanol and its Derivatives. *ChemCatChem* **2016**, *8*, 751. (d) Dong, K.; Fang, X.; Gülak, S.; Franke, R.; Spannenberg, A.; Neumann, H.; Jackstell, R.; Beller, M. Highly Active and Efficient Catalysts for Alkoxycarbonylation of Alkenes. *Nat. Commun.* **2017**, *8*, 14117.

10. (a) Fang, X.; Yu, P.; Morandi, B. Catalytic Reversible Alkene-Nitrile Interconversion Through Controllable Transfer Hydrocyanation. *Science* **2016**, *351*, 832. (b) Bhawal, B. N.; Morandi, B. Catalytic Transfer Functionalization through Shuttle Catalysis. *ACS Catal.* **2016**, *6*, 7528.

11. (a) Murphy, S. K.; Park, J.-W.; Cruz, F. A.; Dong, V. M. Rh-Catalyzed C–C Bond Cleavage by Transfer Hydroformylation. *Science* **2015**, *347*, 56. (b) Kusumoto, S.; Tatsuki, T.; Nozaki, K. The Retro-Hydroformylation Reaction. *Angew. Chem. Int. Ed.* **2015**, *54*, 8458.

12. (a) Oestreich, M. Transfer Hydrosilylation. *Angew. Chem. Int. Ed.* **2016**, *55*, 494. (b) Simonneau, A.; Oestreich, M. 3-Silylated Cyclohexa-1,4-dienes as Precursors for Gaseous Hydrosilanes: The $B(C_6F_5)_3$-Catalyzed Transfer Hydrosilylation of Alkenes. *Angew. Chem. Int. Ed.* **2013**, *52*, 11905. (c) Simonneau, A.; Friebel, J.; Oestreich, M. Salt-Free Preparation of Trimethylsilyl Ethers by $B(C_6F_5)_3$-Catalyzed Transfer Silylation by Using a Me_3SiH Surrogate. *Eur. J. Org. Chem.* **2014**, *2014*, 2077. (d) Oestreich, M.; Hermeke, J.; Mohr, J. A Unified Survey of Si–H and H–H Bond Activation Catalysed by Electron-Deficient Boranes. *Chem. Soc. Rev.* **2015**, *44*, 2202. (e) Keess, S.; Simonneau, A.; Oestreich, M. Direct and Transfer Hydrosilylation Reactions Catalyzed by Fully or Partially Fluorinated Triarylboranes: A Systematic Study. *Organometallics* **2015**, *34*, 790. (f) Simonneau, A.; Oestreich, M. Formal SiH_4 Chemistry Using Sable and Easy-to-Handle Surrogates. *Nat. Chem.* **2015**, *7*, 816. (g) Yuan, W.; Orecchia, P.; Oestreich, M. Cyclohexa-1,3-diene-based Dihydrogen and Hydrosilane Surrogates in $B(C_6F_5)_3$-Catalysed Transfer Processes. *Chem. Commun.* **2017**, *53*, 10390. (h) Orecchia, P.; Yuan, W.; Oestreich, M. Transfer Hydrocyanation of α- and α,β-Substituted Styrenes Catalyzed by Boron Lewis Acids. *Angew. Chem. Int. Ed.* **2019**, *58*, 3579. (i) Chen, W.; Walker, J. C. L.; Oestreich, M. Metal-Free Transfer Hydroiodination of C–C Multiple Bonds. *J. Am. Chem. Soc.* **2019**, *141*, 1135.

13. Tamao, K.; Yoshida, J.; Yamamoto, H.; Kakui, T.; Matsumoto, H.; Takahashi, M.; Kurita, A.; Murata, M.; Kumada, M. Organofluorosilicates in Organic Synthesis. 12. Preparation of Organopentafluorosilicates and their Cleavage Reactions by Halogens and *N*-Bromosuccinimide. Synthetic and Mechanistic Aspects. *Organometallics* **1982**, *1*, 355.

14. Fürstner, A.; Hannen, P. Platinum- and Gold-Catalyzed Rearrangement Reactions of Propargyl Acetates: Total Syntheses of (−)-α-Cubebene, (−)-Cubebol, Sesquicarene and Related Terpenes. *Chemistry – A European Journal* **2006**, *12*, 3006.

15. Lim, B.-Y.; Jung, B.-E.; Cho, C.-G. Ene-hydrazide from Enol Triflate for the Regioselective Fischer Indole Synthesis. *Organic Letters* **2014**, *16*, 4492.

16. Reid, W. B.; Watson, D. A. Synthesis of Trisubstituted Alkenyl Boronic Esters from Alkenes Using the Boryl-Heck Reaction. *Organic Letters* **2018**, *20*, 6832.

Chapter 4

Palladium-Catalyzed Oxidative Dehydrosilylation for Contra-Thermodynamic Olefin Isomerization

4.1 Introduction

Internal olefins are more thermodynamically stable than terminal olefins. Therefore, isomerizations of terminal olefins to internal olefins are exergonic, and many strategies to conduct such isomerizations have been reported.[1] However, strategies for the contra-thermodynamic isomerization of internal olefins to terminal olefins remain underdeveloped. Most strategies for contra-thermodynamic, positional isomerization of alkenes involve allylic functionalization followed by defunctionalization with allylic transposition;[2] however, these approaches enable translocation of a double bond by a maximum of only one carbon unit and require harsh reagents. Strategies for long-range, contra-thermodynamic olefin isomerizations, i.e., those that occur through two or more carbon units,[3] typically produce terminal alkenes in low yields and/or in low selectivities. A mild method for the contra-thermodynamic, long-range translocation of carbon-carbon double bonds could enable the valorization of mixtures of internal olefins to single isomers of terminal olefins, the late-stage derivatization of complex molecules containing internal olefins, and the installation of functional groups at sites that are remote from the initial position of the double bond.

A variety of transition-metal catalyzed, chain-walking hydrofunctionalizations could potentially be combined with dehydrofunctionalizations to enable such long-range, contra-thermodynamic olefin isomerizations.[4] We previously reported a one-pot process for the selective, long-range isomerization of internal olefins to terminal olefins involving platinum-catalyzed, chain-walking hydrosilylation of internal olefins with trichlorosilane followed by a formal, reagent-based retro-hydrosilylation of the resulting terminal alkylsilanes (eq 1).[5]

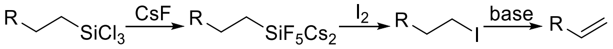

(1)

Platinum-catalyzed hydrosilylation occurs with high *n*:*iso* ratios, low loadings of catalyst, and without need for solvent, but the formal retro-hydrosilylation we developed comprises three uncatalyzed reactions: conversion of the terminal alkylsilane to a pentafluorosilicate, iodination of the silicate, and base-promoted elimination. This formal retro-hydrosilylation occurred in good yield, but each step required an excess of reagents. If any of these steps could be replaced by a catalytic process or, preferably, if multiple uncatalyzed steps could be combined in a single catalytic cycle, then the overall sequence would be more atom-efficient and operationally simple.

However, several factors make the development of a catalytic dehydrosilylation difficult (Scheme 1). Simple catalytic retro-hydrosilylation without coupling to additional exergonic processes is unlikely to occur because dehydrosilylation is substantially disfavored thermodynamically (Scheme 1A).[6] Even a catalytic transfer dehydrosilylation involving the microscopic reverse of hydrosilylation and addition of silane to a strained acceptor, e.g. norbornene, would be challenging because the oxidative addition of a C–Si bond that would occur to initiate the reverse of a Chalk-Harrod mechanism is an uncommon elementary step and because the oxidative addition of the β-C–H bond that would initiate the reverse of a modified Chalk-Harrod mechanism would be unlikely to occur selectively in the presence more accessible C–H bonds (Scheme 1B). Addition of a C–H bond other than the β-C–H bond would likely lead to dehydrogenation, rather than dehydrosilylation. Moreover, any retro-hydrosilylation applied to contra-thermodynamic olefin isomerization should occur under conditions that are irreversible and that lack a persistent hydride because equilibrating conditions and the presence of persistent metal-hydrides would likely lead to the isomerization of terminal olefins to internal olefins. Alternative pathways could involve cleavage of the C–Si bond by steps other than those in a microscopic reverse of hydrosilylation, but catalytic reactions that cleave unactivated alkyl–Si bonds under thermal conditions,[7] including transmetalations of alkylsilanes to enable cross-couplings,[8] are rare.

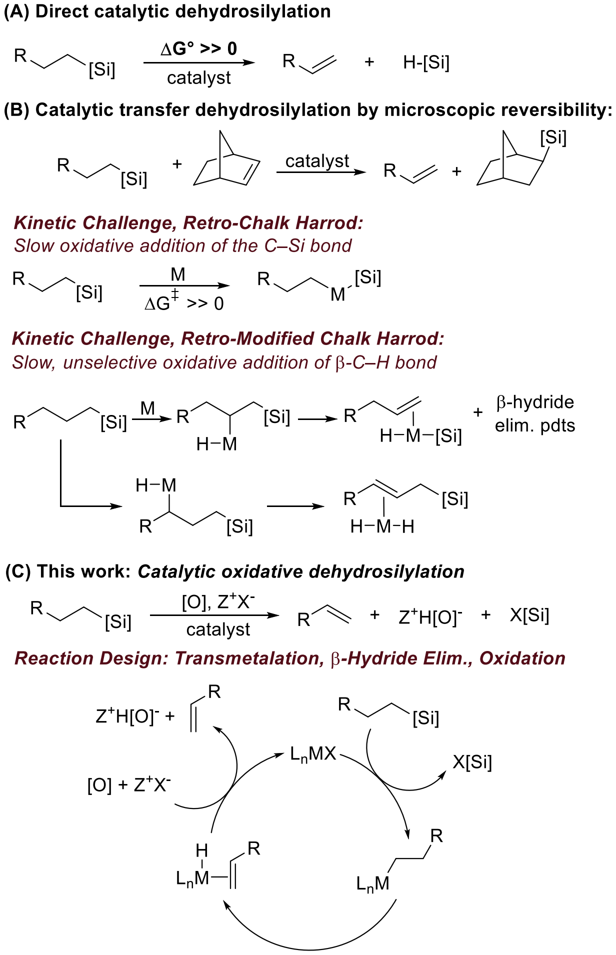
(A) Direct catalytic dehydrosilylation
ΔG° >> 0
catalyst
R
[Si]
H-[Si]
(B) Catalytic transfer dehydrosilylation by microscopic reversibility:
catalyst
Kinetic Challenge, Retro-Chalk Harrod:
Slow oxidative addition of the C–Si bond
M
ΔG‡ >> 0
Kinetic Challenge, Retro-Modified Chalk Harrod:
Slow, unselective oxidative addition of β-C–H bond
H–M
H–M–[Si]
β-hydride elim. pdts
H–M–H
(C) This work: Catalytic oxidative dehydrosilylation
[O], Z+X-
catalyst
Z+H[O]-
X[Si]
Reaction Design: Transmetalation, β-Hydride Elim., Oxidation
[O] + Z+X-
LnMX
LnM

Scheme 1. Challenges facing catalytic dehydrosilylation and design of a catalytic oxidative dehydrosilylation

To address these challenges, we envisioned an oxidative dehydrosilylation that draws analogies to oxidative dehydrogenation, by which endergonic alkane dehydrogenations are coupled with the exergonic reduction of O_2 to water.[9] In this case, the reaction design could involve transmetallation to cleave the C–Si bond, thereby creating more favorable kinetics if the oxidation step is fast.

We report the realization of such a process in the form of a palladium-catalyzed oxidative dehydrosilylation of primary alkylsilanes to form α-olefins with benzoquinone (BQ) as oxidant (Scheme 1C). This dehydrosilylation occurs in good yields with good selectivity for the 1-alkene and combines with chain-walking hydrosilylation to transform internal alkenes to terminal alkenes with translocation of the double bond through multiple carbon units. To develop a catalytic oxidative dehydrosilylation, we envisioned that the process could occur by the mechanism in Scheme 1C. Transmetalation of the alkylsilane to an electrophilic late transition-metal complex would generate an alkyl complex that could undergo β-hydride elimination to release the product and produce a metal hydride. This hydride could react with an oxidant to regenerate the starting electrophilic complex.[10]

4.2 Results and Discussion

To assess the viability of the proposed reaction, we conducted the oxidative dehydrosilylation of octadecyl trichlorosilane (**2a**) under the conditions shown in Table 1. A series of experiments varying the conditions of this reaction showed that alkylsilane **2a** reacts with benzoquinone and cesium fluoride in the presence of Pd_2dba_3 at 140 °C to form olefin **3b** in 67% yield (Table 1, entry 1). The reaction proceeded in 15 min; longer reaction times at this temperature did not significantly improve the yield (entry 2). Olefin **3b** formed in similar yields at 140 °C and 120 °C (entry 3). Olefin **3b** formed in much lower yields at 100 °C and 80 °C (entries 4-5), but these lower yields were simply due to slower rates. The yields of reactions at 100 °C and 80 °C were higher when the reaction was conducted for 20 h, rather than for 15 min (entries 6-7), and the yield of the reaction at 100 °C after 20 h was similar to that at 140 °C for 15 min (entry 6).

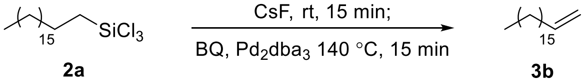

Entry	Deviation from Reaction Conditions	Yield[a]	terminal:internal[b]
1	none	67	83:17
2	20 h	68	79:21
3	120 °C	66	83:17
4	100 °C	17	n.d.[c]
5	80 °C	1	n.d.[c]
6	100 °C, 20 h	63	n.d.[c]
7	80 °C, 20 h	47	n.d.[c]
8	KF instead of CsF	0	n.d.[c]
9	TBAF instead of CsF	5	78:22
10	8 equiv CsF	66	82:18
11	6 equiv CsF	64	85:15
12	5 equiv CsF	58	n.d.[c]
13	4 equiv CsF	36	n.d.[c]
14	2 equiv BQ	62	82:18
15	3 mol% Pd_2dba_3	58	75:25
16	2 mol% Pd_2dba_3	54	75:25
17	1 mol% Pd_2dba_3	56	78:22
18	DMSO as solvent	1	n.d.[c]
19	THF as solvent	57	72:28
20	Toluene as solvent	41	73:27
21	$Pd(OAc)_2$ instead of Pd_2dba_3	58	81:19
22	600 μL dioxane	68	83:17

Conditions: silane (0.1 mmol), CsF (10 equiv), rt, 15 min, dioxane (100 μL); then BQ (3 equiv), Pd_2dba_3 (6 mol%), 140 °C, 15 min, dioxane (200 μL). [a]Determined by GC with hexadecane as an internal standard. [b]Determined by ^1H NMR spectroscopy. [c]Not determined.

Table 1. Catalytic dehydrosilylation of linear alkylsilanes

Olefin **3b** formed in low yields in the presence of fluoride sources other than CsF (entries 8-9). The yields and regioselectivities of the reaction were similar when the reaction was conducted with ten, eight, or six equivalents of CsF (entries 1, 10-11). Even with five equivalents of CsF, olefin **3b** formed in 58% yield (entry 12). However, olefin **3b** formed in low yields when the reaction was conducted with four or fewer equivalents of CsF (entry 13). The reaction with two equivalents of benzoquinone occurred in approximately the same yield as that with three equivalents (entry 14). Reactions conducted with catalyst loadings as low as 1 mol% occurred in yields and regioselectivities that were only slightly lower than those in entry 1 (entries 15-17).

Olefin **3b** formed in lower yields when the reaction was conducted in DMSO, THF, or toluene than when the reaction was conducted in dioxane (entries 18-20), and olefin **3b** formed in slightly lower yields when the reaction was conducted with $Pd(OAc)_2$ as the pre-catalyst rather than with Pd_2dba_3 as the pre-catalyst (entry 21). Finally, little change in yield was observed when the reaction was conducted under conditions that were more dilute than those in entry 1 (entry 22).

We also sought to determine whether our newly developed catalytic dehydrosilylation of linear alkylsilanes could be conducted on the crude product of a chain-walking hydrosilylation to enable a one-pot isomerization of internal olefins to terminal olefins.[4c-f,11] To do so, we reacted internal alkenes with varying geometries and with double bonds present at different positions along the chain with two equivalents of trichlorosilane in the presence of Speier's catalyst (0.1 mol%), evaporated the volatile materials, and subjected the crude reaction mixtures to conditions for dehydrosilylation.

The results in Table 2 show that this sequence leads to the conversion of 2-, 3-, and 4-alkenes, as well as deeply embedded alkenes, to the terminal 1-isomers. Specifically, internal octenes **1c**, **1d**, and **1e** underwent isomerization to 1-octene (olefin **3c**) in good yields. The results with this set of octenes also show that both (*E*) and (*Z*) alkenes undergo the olefin transfer process. Moreover, translocation of the double bond over seven positions occurred in yields similar to those for transfer over fewer positions. Specifically, *trans*-7-tetradecene (olefin **1f**) underwent isomerization to form 1-tetradecene (olefin **3f**) in good yield.

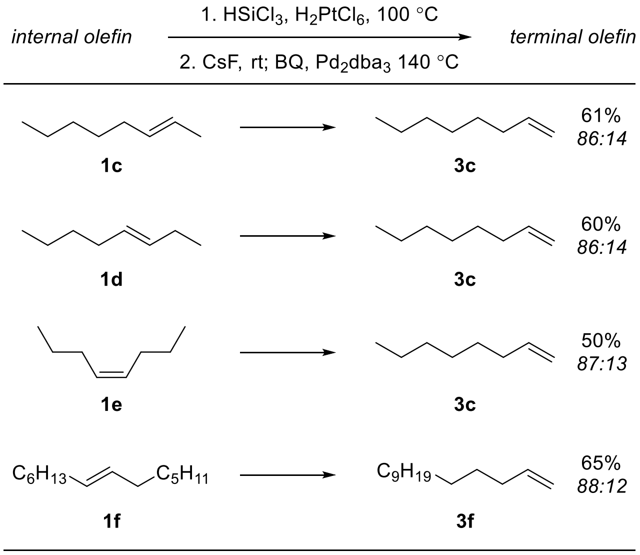

Step 1: Internal olefin (1 mmol), $HSiCl_3$ (2.5 equiv), H_2PtCl_6 (0.1 mol% in 2 μL isopropanol), 100 °C, 20 h, neat reaction, sealed vessel. Step 2: CsF (10 equiv), rt, 15 min, dioxane (1 mL), then BQ (3 equiv), Pd_2dba_3 (6 mol%), 140 °C, 12 h, dioxane (2 mL). Yields and regioselectivities were determined by ^1H NMR spectroscopy.

Table 2. One-pot contra-thermodynamic isomerizations of internal olefins to α-olefins

As a new class of reaction, this oxidative dehydrosilylation does have several limitations that must be addressed for broad applicability. For example, β-branched silanes underwent dehydrosilylation in low yields, presumably because the additional steric bulk at the β position inhibited transmetalation. One long-term goal is the isomerization of alkenes in natural products, such as terpenes, which contain trisubstituted alkenes bearing methyl substituents. Such alkenes would form β-branched silanes by chain-walking hydrosilylation. Thus, catalysts that undergo more rapid transmetalation would enable isomerization in such natural products, and the development of such catalysts is ongoing.

In addition, many common functional groups are incompatible with platinum-catalyzed chain-walking hydrosilylation with trichlorosilane because this silane is a powerful reducing agent, and Speier's catalyst is highly active. Thus, ketones and esters underwent reduction under the reaction conditions.[7f,12] Olefins bearing tertiary amines also did not undergo the reaction, forming precipitates immediately upon addition of trichlorosilane at room temperature. Thus, chain-walking hydrosilylations with silanes other than trichlorosilane and with catalysts enabling milder conditions are needed and are currently being sought.

Nonetheless, the catalytic dehydrosilylation we have developed has several advantages over the iodinative dehydrosilylation we reported recently.[5] The iodinative process occurs in two sequential steps (iodination and base-promoted elimination), while the catalytic dehydrosilylation reported here forms terminal olefins from alkylsilanes in a single step. In addition, the catalytic dehydrosilylation requires fewer equivalents of reagents than the iodinative process because the additional base-promoted elimination step of the iodinative process is not required. Further improvements to the atom efficiency of the new catalytic process are underway.

To elucidate the factors controlling the rate of the dehydrosilylation, preliminary mechanistic experiments connecting the identity of the silyl group to the rate of transmetalation were conducted (Scheme 2). Trialkoxysilane **2a'** did not undergo palladium-catalyzed dehydrosilylation, even in the presence of a fluoride activator. However, unactivated trifluoroalkylsilanes and unactivated pentafluoroalkylsilicates are known to undergo Hiyama couplings with aryl and vinyl electrophiles in the presence of fluoride activators.[8b-d] Trifluoroalkylsilanes are thought to form alkylpentafluorosilicates *in situ* prior to transmetalation and hexafluorosilicate salts after transmetalation.[8c] We have verified that trifluorooctadecylsilane (**2a''**), prepared from alkylsilane **2a**, undergoes dehydrosilylation under the reaction conditions in Table 1. Since the dehydrosilylation proceeds in low yields in the presence of a low number of equivalents of fluoride and gives no alkene in the absence of fluoride, alkylsilane **2a** likely undergoes nucleophilic substitution with fluoride to form a pentafluorosilicate prior to transmetalation. These data point to strongly nucleophilic silanes,[13] and silanes containing donating groups[8e] as potential reagents for the chain-walking hydrosilylation that would dovetail with catalytic dehydrosilylation to create an olefin isomerization with broader scope.

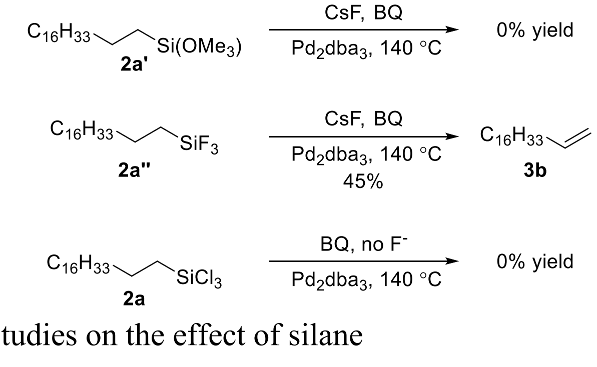

Scheme 2. Preliminary studies on the effect of silane

On the basis of these data, we propose the catalytic cycle in Scheme 3 in which a trichloroalkylsilane undergoes nucleophilic substitution with fluoride to form a pentafluorosilicate, transmetalation of this species to palladium, followed by β-hydride elimination, dissociation of alkene, and re-oxidation of palladium by benzoquinone to form the conjugate base of hydroquinone (HBQ^-) and to regenerate the active catalyst, although the precise fate of the reduced BQ is not known. The identity of the ancillary ligands and the X groups on palladium are unknown. However, given the high concentration of fluoride in the system, the X groups on palladium are likely fluorides.

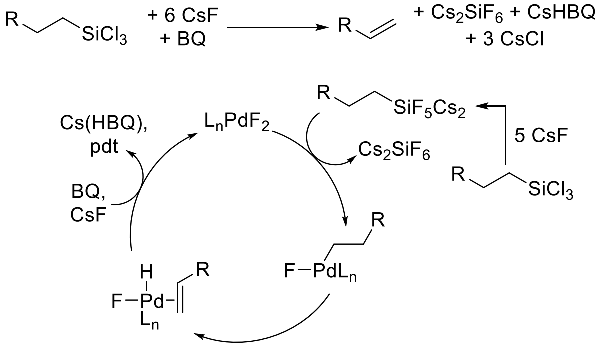
R
SiCl3
+ 6 CsF
+ BQ
R
+ Cs2SiF6 + CsHBQ
+ 3 CsCl
Cs(HBQ),
pdt
LnPdF2
R
SiF5Cs2
5 CsF
Cs2SiF6
R
SiCl3
BQ,
CsF
R
F−PdLn
H
R
F−Pd−
Ln

Scheme 3. Proposed catalytic cycle for the oxidative dehydrosilylation

4.3 Conclusion

In conclusion, we have developed the first catalytic dehydrosilylation of unactivated alkylsilanes and one of the few thermal reactions at an unactivated alkyl carbon-silicon bond besides oxidation to the alcohol.[7-8] This catalytic functionalization involving an Si–C bond, when conducted in tandem with chain-walking hydrosilylation, provides a method to convert internal olefins to terminal olefins, involving the transposition of the alkene unit through multiple carbon units, in good yields and selectivities. More detailed mechanistic studies and systems to expand the scope of the reaction are the subject of ongoing studies.

4.4 Experimental

4.4.1 General information

All air-sensitive manipulations were conducted under an inert atmosphere in a nitrogen-filled glovebox or by standard Schlenk techniques. Unless stated otherwise, reagents and solvents were purchased from commercial suppliers and used without further purification. All NMR spectra were recorded at the University of California, Berkeley NMR facility. Proton-NMR spectra were recorded on Bruker AVB-400, AVQ-400, AV-500, and AV-600 instruments with operating frequencies of 400, 400, 500, and 600 MHz, respectively, and Carbon-13 NMR spectra were recorded on a Bruker AV-600 instrument with a ^{13}C operating frequency of 151 MHz. Chemical shifts (δ) are reported in ppm, relative to those of residual solvent signals ($CDCl_3$ δ = 7.26 for ^{1}H NMR spectra and δ = 77.16 for ^{13}C NMR spectra). The following abbreviations were used in reporting NMR data: s, singlet; d, doublet; t, triplet; q, quartet; p, pentet; hept, heptet; m, multiplet. Crude reaction mixtures were analyzed by gas chromatography (GC) on an Agilent 7890 GC equipped with an HP-5 column (25 m x 0.20 mm x 0.33 µm film) and an FID detector. Quantitative analysis by GC was conducted with hexadecane as an internal standard.

4.5.2 Development of conditions for oxidative dehydrosilylation (Table 1)

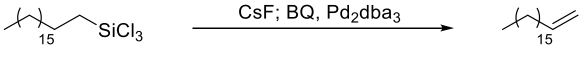

2a **3b**

In a nitrogen-filled glovebox, an oven-dried 4 mL vial was charged with CsF (152 mg, 1.0 mmol) and a solution of octadecyltrichlorosilane (39.4 μL, 0.1 mmol, 1 equiv) and hexadecane (29.3 μL, 0.1 mmol, 1 equiv) in *p*-dioxane (100 μL). The mixture was stirred at room temperature for 15 min. To this mixture were added *p*-dioxane (200 μL), benzoquinone (32.4 mg, 0.3 mmol, 3 equiv), and Pd_2dba_3 (5.5 mg, 0.006 mmol, 6 mol%). The mixture was stirred at 140 °C for 15 min, cooled to room temperature, treated with aqueous sodium hydroxide (750 μL), and diluted with diethyl ether (1 mL). The organic layer was filtered through a PTFE syringe filter and analyzed by gas chromatography. The regioselectivity of the reaction was determined by ^1H NMR spectroscopy in $CDCl_3$.

4.5.3 Procedure for contra-thermodynamic olefin isomerizations (Table 2)

Step 1: Chain-Walking Hydrosilylation

In a nitrogen-filled glove box, an oven-dried, heavy-walled Schlenk flask with a single opening (5–10 mL) and containing a magnetic stir bar was charged with internal olefin (1 mmol, 1 equiv) and 1.0 µL of a stock solution prepared by dissolving 100 mg $H_2PtCl_6{\bullet}6H_2O$ in 200 µL of isopropanol (~0.5 mg $H_2PtCl_6{\bullet}6H_2O$, 0.001 mmol, 0.1 mol%). The Schlenk flask was sealed with a Teflon plug, removed from the glove box, and cooled to 0 °C. Trichlorosilane (250 µL, 2.50 mmol, 2.50 equiv) was added to the reaction mixture under N_2, and the Schlenk flask was sealed and heated at 100 °C for 20 h. The reaction mixture was cooled to room temperature and subjected to high vacuum (<1 torr) for 30 minutes to remove excess $HSiCl_3$. The Schlenk flask was then backfilled with N_2 and transferred to a nitrogen-filled glove box.

Step 2: Palladium-Catalyzed Dehydrosilylation

In a nitrogen-filled glovebox, the Schlenk flask was charged with *p*-dioxane (1 mL) and CsF (1.52 g, 10.0 mmol, 10.0 equiv). The mixture was stirred at room temperature for 15 min. To the mixture were added *p*-dioxane (2 mL), benzoquinone (324 mg, 3.00 mmol, 3.00 equiv), and Pd_2dba_3 (54.9 mg, 0.0599 mmol, 6 mol%). The mixture was stirred at 140 °C for 12 h, cooled to room temperature, and diluted with $CDCl_3$ (1 mL). Trichloroethylene (90.0 µL, 1.00 mmol, 1.00 equiv), was added, and the mixture was stirred vigorously. The yield of the reaction was determined by ^1H NMR spectroscopy with trichloroethylene as an internal standard. To determine the regioselectivity of the reaction, an aliquot was filtered through a plug of silica, eluted with pentane, and analyzed by ^1H NMR spectroscopy.

4.5.4 ^{1}H NMR spectra (Table 2)

For each reaction in Table 2, two spectra were recorded. One spectrum was recorded of the crude reaction, and one was recorded after passing the reaction through a plug of silica gel.

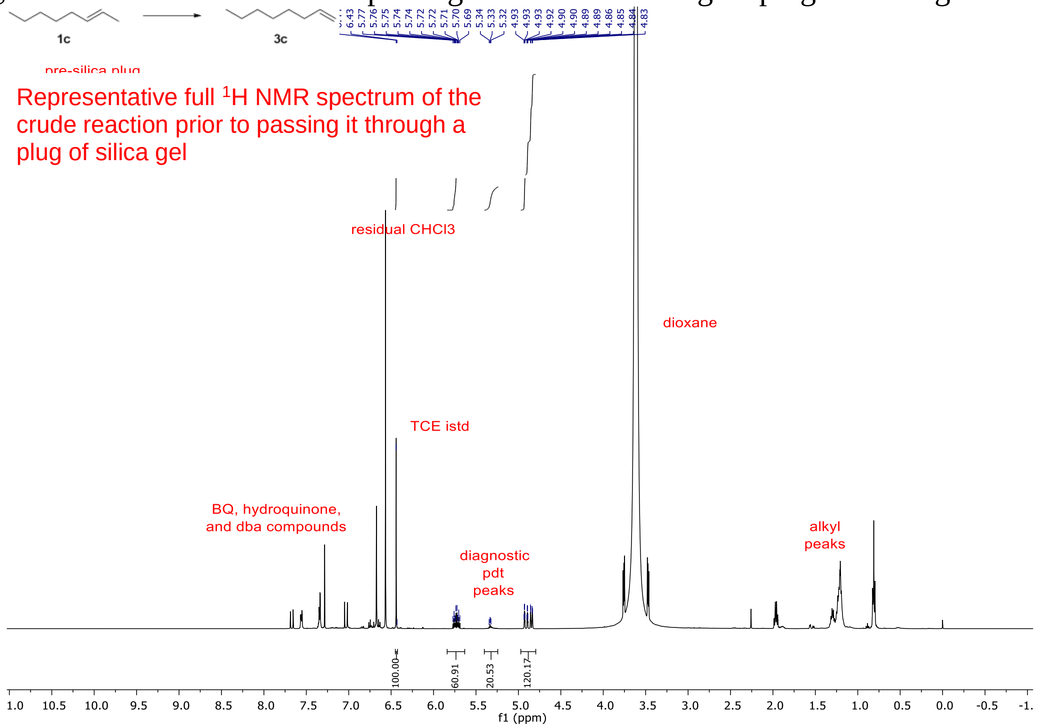

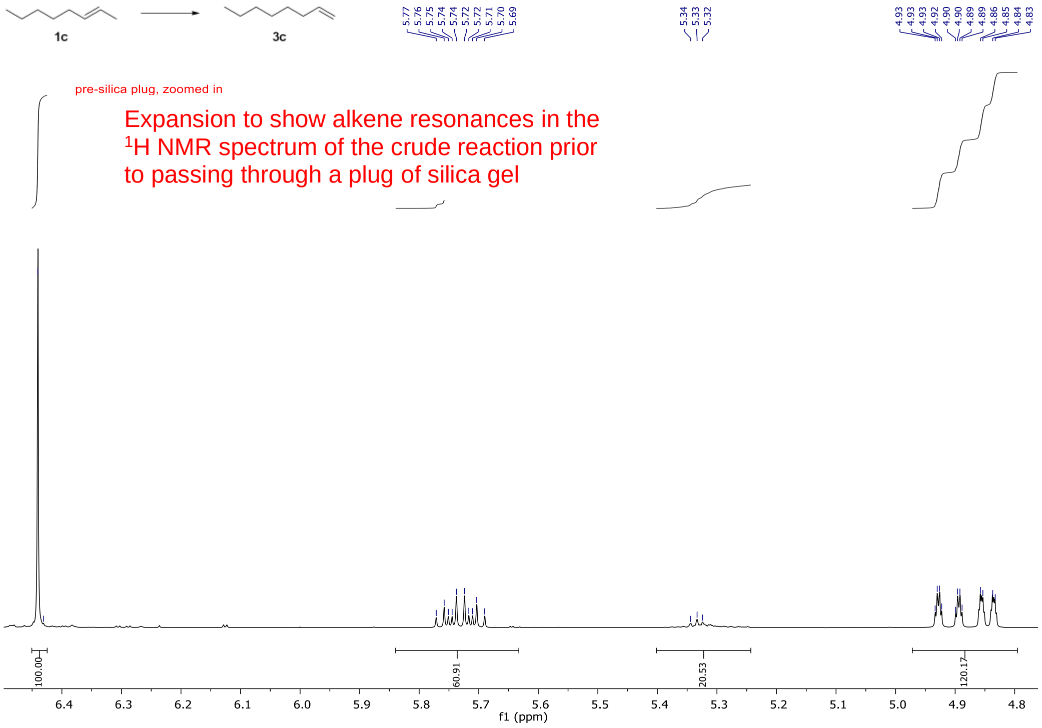

pre-silica plug, zoomed in

Expansion to show alkene resonances in the ^{1}H NMR spectrum of the crude reaction prior to passing through a plug of silica gel

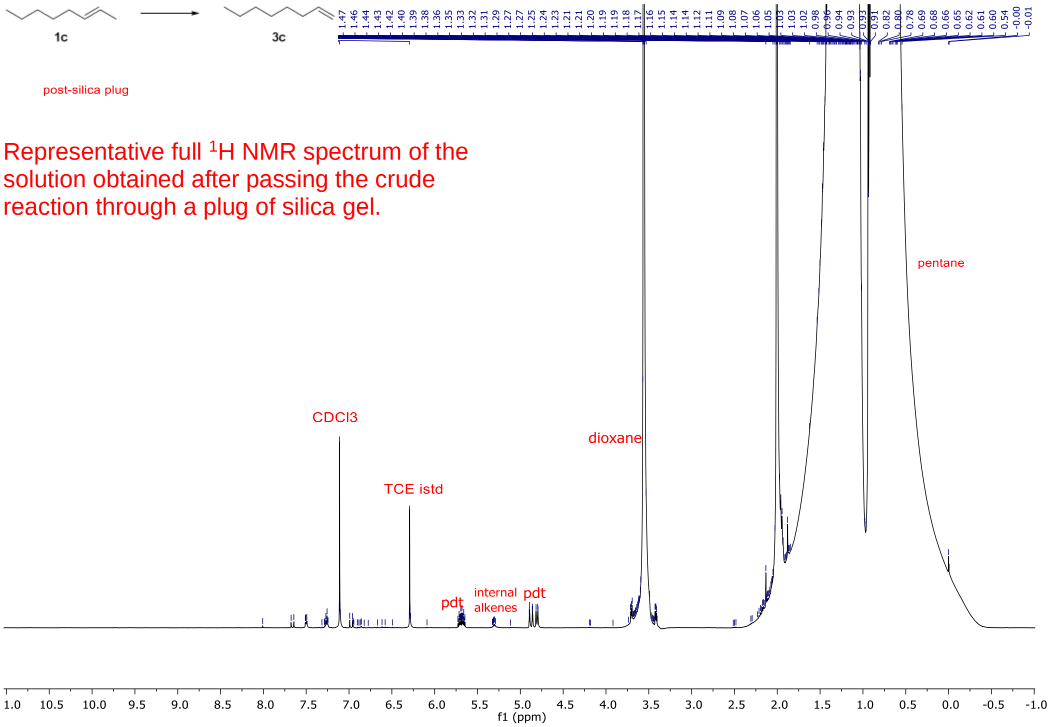

Representative full ^{1}H NMR spectrum of the solution obtained after passing the crude reaction through a plug of silica gel.

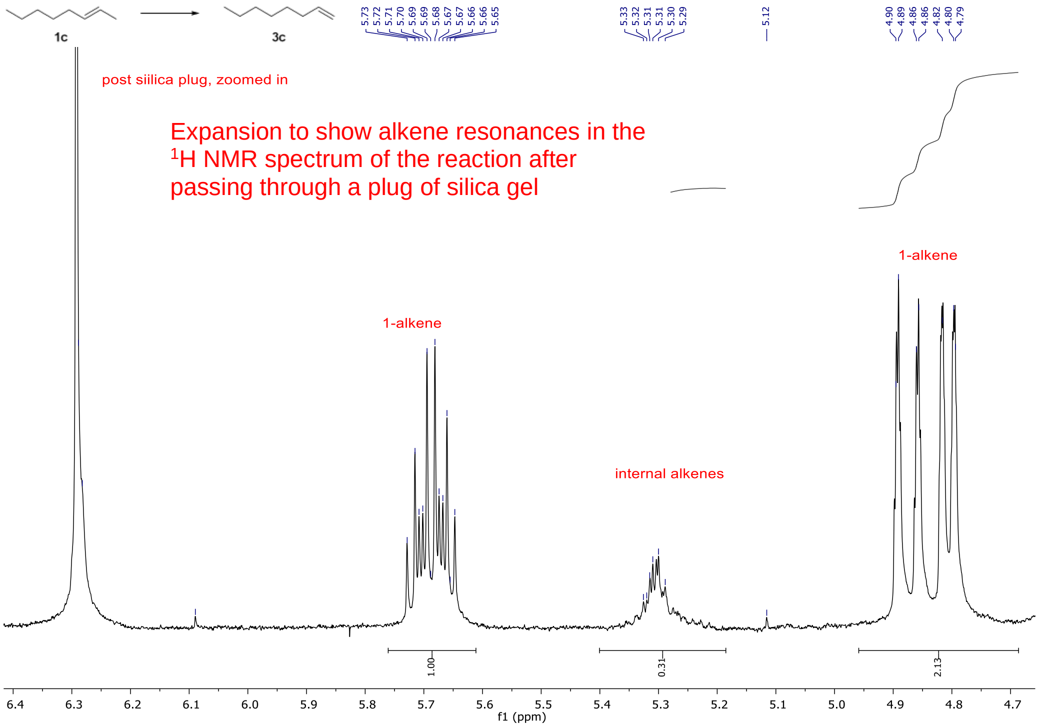

post siilica plug, zoomed in

Expansion to show alkene resonances in the ^{1}H NMR spectrum of the reaction after passing through a plug of silica gel

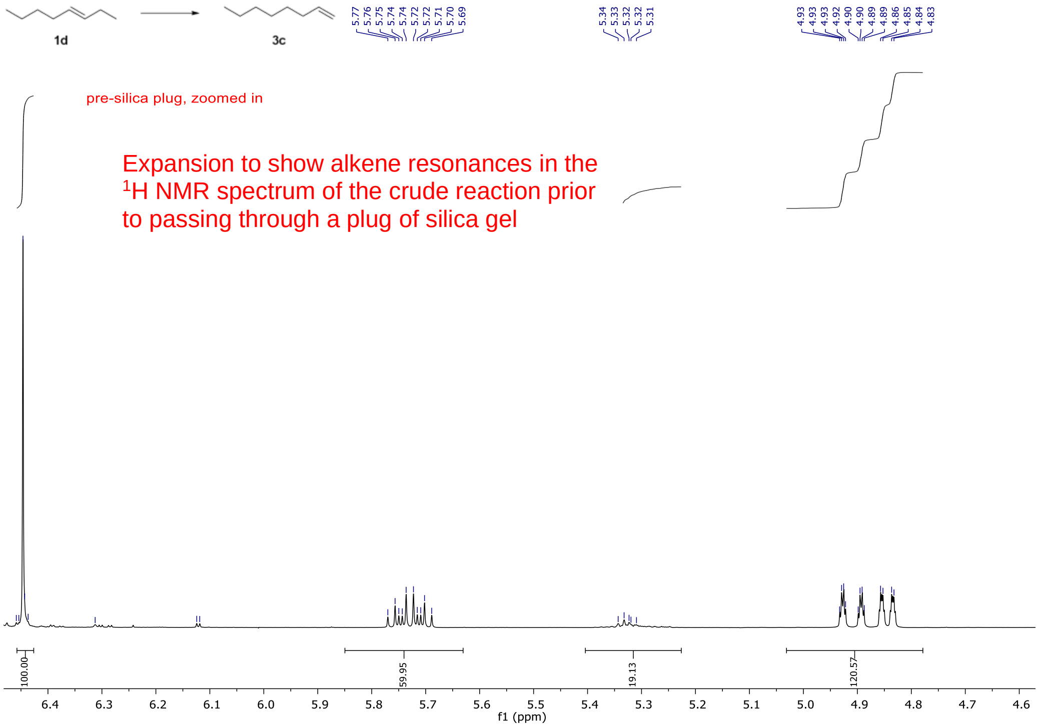

pre-silica plug, zoomed in

Expansion to show alkene resonances in the ^{1}H NMR spectrum of the crude reaction prior to passing through a plug of silica gel

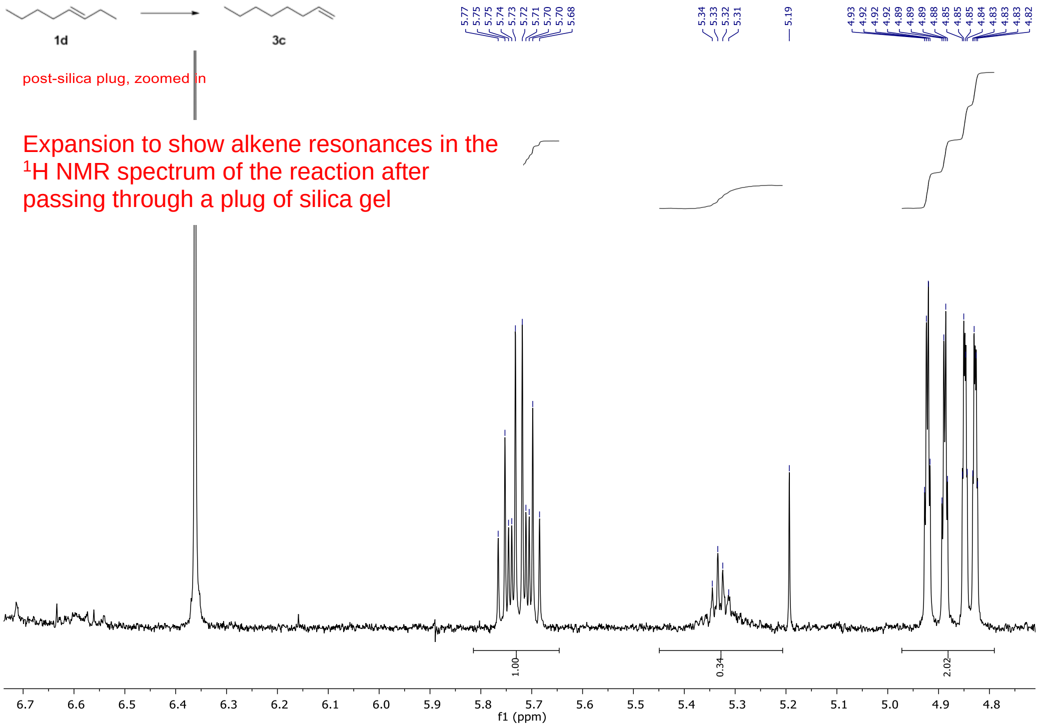

post-silica plug, zoomed in

Expansion to show alkene resonances in the ^{1}H NMR spectrum of the reaction after passing through a plug of silica gel

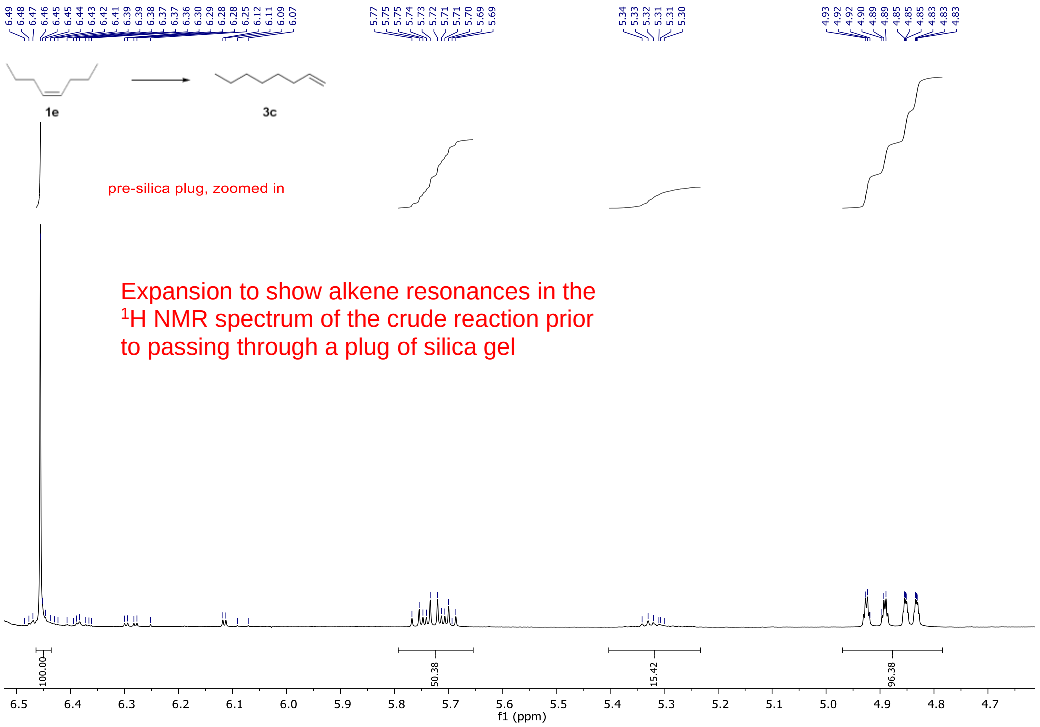

pre-silica plug, zoomed in

Expansion to show alkene resonances in the ^{1}H NMR spectrum of the crude reaction prior to passing through a plug of silica gel

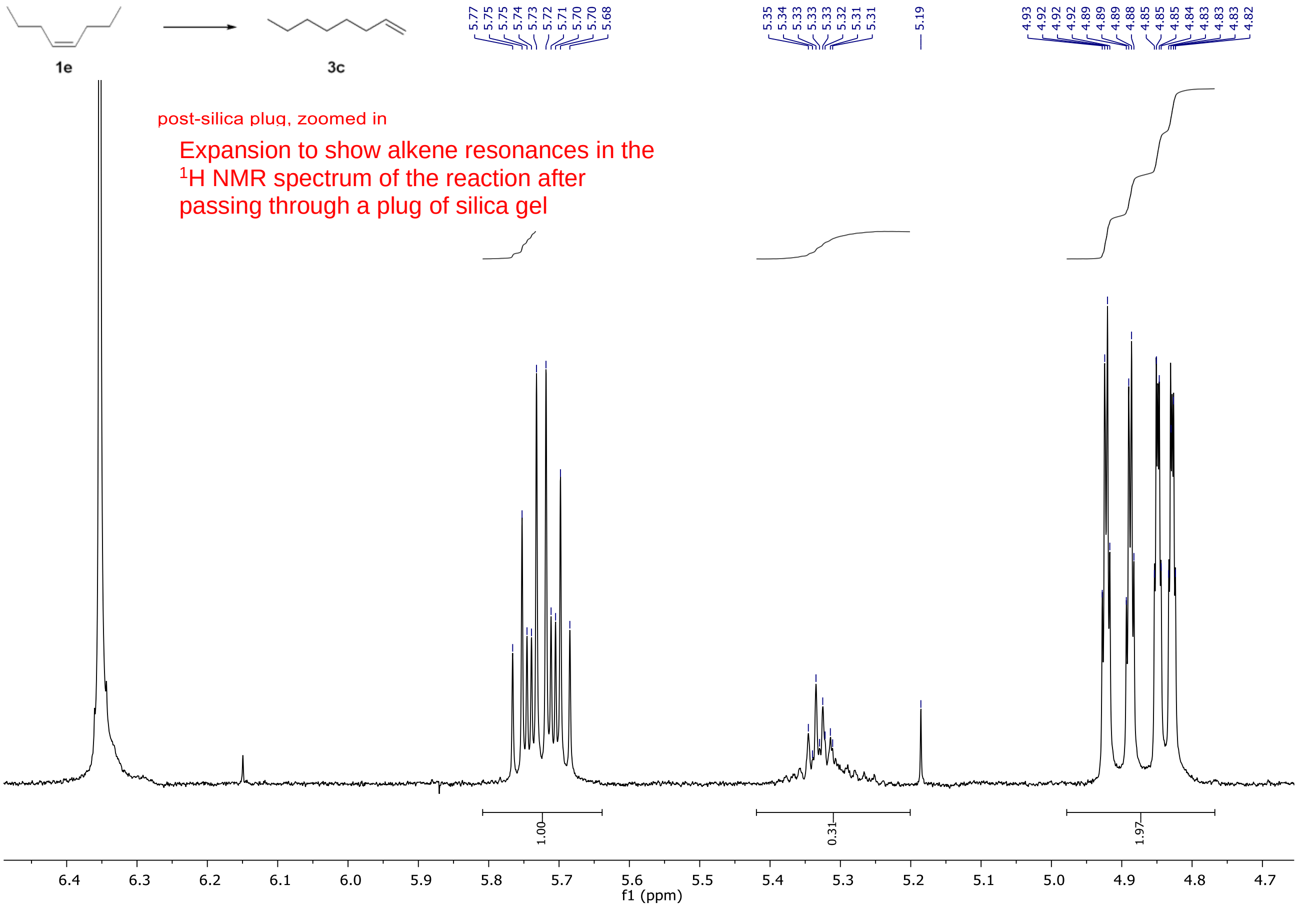
post-silica plug, zoomed in

Expansion to show alkene resonances in the ^{1}H NMR spectrum of the reaction after passing through a plug of silica gel

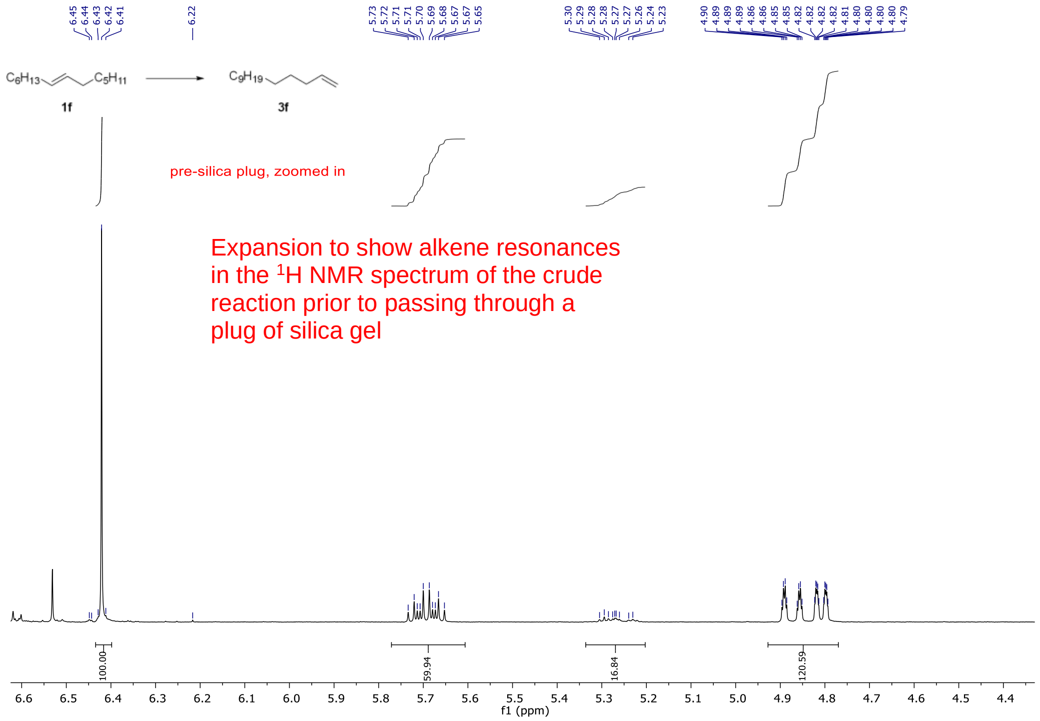

pre-silica plug, zoomed in

Expansion to show alkene resonances in the ^{1}H NMR spectrum of the crude reaction prior to passing through a plug of silica gel

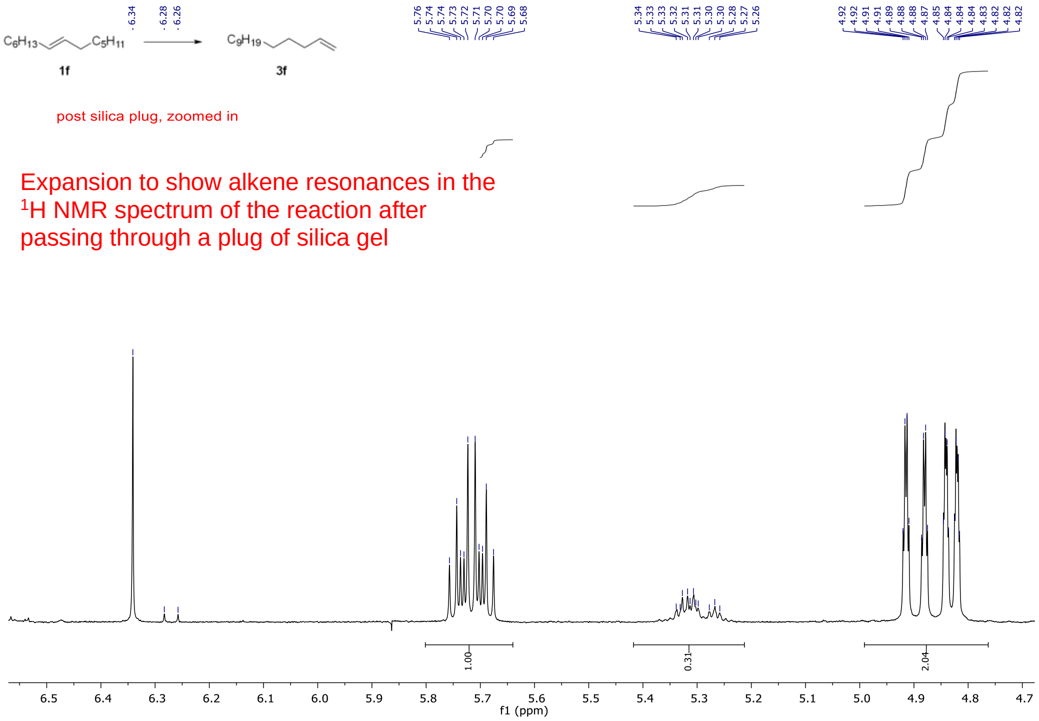

Expansion to show alkene resonances in the ^{1}H NMR spectrum of the reaction after passing through a plug of silica gel

4.4 References

Parts of this chapter were reprinted with permission from:

"Palladium-Catalyzed Oxidative Dehydrosilylation for Contra-Thermodynamic Olefin Isomerization"

Hanna, S.; Wills, T.; Butcher, T. W.; Hartwig, J. F. *ACS Catal.* **2020**, *10*, 8736–8741.

1. (a) Biswas, S.; Huang, Z.; Choliy, Y.; Wang, D. Y.; Brookhart, M.; Krogh-Jespersen, K.; Goldman, A. S. Olefin Isomerization by Iridium Pincer Catalysts. Experimental Evidence for an η^3-Allyl Pathway and an Unconventional Mechanism Predicted by DFT Calculations. *J. Am. Chem. Soc.* **2012**, *134*, 13276. (b) Larionov, E.; Li, H.; Mazet, C. Well-Defined Transition Metal Hydrides in Catalytic Isomerization. *Chem. Commun.* **2014**, *50*, 9816. (c) Crossley, S. W. M.; Barabé, F.; Shenvi, R. A. Simple, Chemoselective, Catalytic Olefin Isomerization. *J. Am. Chem. Soc.* **2014**, *136*, 16788. (d) Molloy, J. J.; Morack, T.; Gilmour, R. Positional and Geometrical Isomerisation of Alkenes: The Pinnacle of Atom Economy. *Angew. Chem. Int. Ed.* **2019**, *58*, 13654. (e) Zhang, S.; Bedi, D.; Cheng, L.; Unruh, D. K.; Li, G.; Findlater, M. Cobalt(II)-Catalyzed Stereoselective Olefin Isomerization: Facile Access to Acyclic Trisubstituted Alkenes. *J. Am. Chem. Soc.* **2020**, *142*, 8910.

2. (a) Harwood, L. M.; Julia, M. A Convenient Synthesis of (+)-β-Pinene from (+)-α-Pinene. *Synthesis* **1980**, *1980*, 456. (b) Min, Y.-F.; Zhang, B.-W.; Cao, Y. A New Synthesis of (-)-β-Pinene from (-)-α-Pinene. *Synthesis* **1982**, *1982*, 875. (c) Andrianome, M.; Häberle, K.; Delmond, B. Allyl-and benzylstannanes, new reagents in terpenic synthesis. *Tetrahedron* **1989**, *45*, 1079. (d) Eng, S. L.; Ricard, R.; Wan, C. S. K.; Weedon, A. C. Photochemical Deconjugation of α,β-Unsaturated Ketones. *J. Chem. Soc., Chem. Commun.* **1983**, 236. (e) Guignard, R. F.; Petit, L.; Zard, S. Z. A Method for the Net Contra-thermodynamic Isomerization of Cyclic Trisubstituted Alkenes. *Org. Lett.* **2013**, *15*, 4178.

3. (a) Brown, H. Isomerization of internal olefins to terminal olefins. US3173967A, 1965. (b) Brown, H. C.; Bhatt, M. V.; Munekata, T.; Zweifel, G. Organoboranes. VII. The Displacement Reaction with Organoboranes Derived from the Hydroboration of Cyclic and Bicyclic Olefins. Conversion of Endocyclic to Exocyclic Double Bonds. *J. Am. Chem. Soc.* **1967**, *89*, 567. (c) Brown, H. C.; Bhatt, M. V. Organoboranes. IV. The Displacement Reaction with Organoboranes Derived from the Hydroboration of Branched-Chain Olefins. A Contrathermodynamic Isomerization of Olefins. *J. Am. Chem. Soc.* **1966**, *88*, 1440. (d) Robert H. Allen, R. W. L., Andrew D. Overstreet Continuous Process for Preparing Aluminm 1-Alkyls and Linear 1-Olefins from Internal Olefins. US005274153A 1993. (e) de Klerk, A.; Hadebe, S. W.; Govender, J. R.; Jaganyi, D.; Mzinyati, A. B.; Robinson, R. S.; Xaba, N. Linear α-Olefins from Linear Internal Olefins by a Boron-Based Continuous Double-Bond Isomerization Process. *Ind. Eng. Chem. Res.* **2007**, *46*, 400.

4. (a) Sommer, H.; Juliá-Hernández, F.; Martin, R.; Marek, I. Walking Metals for Remote Functionalization. *ACS Cent. Sci.* **2018**, *4*, 153. (b) Juliá-Hernández, F.; Moragas, T.; Cornella, J.; Martin, R. Remote Carboxylation of Halogenated Aliphatic Hydrocarbons with Carbon Dioxide. *Nature* **2017**, *545*, 84. (c) Saam, J.; Speier, J. The Addition of Silicon Hydrides to Olefinic Double Bonds. Part VI. Addition to Branched Olefins. *J. Am. Chem. Soc.* **1961**, *83*, 1351. (d) Bank, H. M.; Saam, J. C.; Speier, J. L. The Addition of Silicon Hydrides to Olefinic Double Bonds. IX. Addition of sym-Tetramethyldisiloxane to Hexene-1, -2, and -3. *J. Org. Chem.* **1964**, *29*, 792. (e) Benkeser, R. A.; Muench, W. C. The Addition Rates of Dichloro- and Trichlorosilane to 2-Pentene and 1-Octene. *J. Organomet. Chem.* **1980**, *184*, C3. (f) Yarosh, O. G.; Zhilitskaya, L. V.; Yarosh, N. K.; Albanov, A. I.; Voronkov, M. G. Hydrosilylation of Cyclohexene, 1-Methylcyclohexene, and Isopropylidenecyclohexane. *Russ. J. Gen. Chem.* **2004**, *74*, 1895. (g) Edwards, D. R.; Crudden, C. M.; Yam, K. One-Pot Carbon Monoxide-Free Hydroformylation of Internal Olefins to Terminal Aldehydes. *Adv. Synth. Catal.* **2005**, *347*, 50. (h) Lata, C. J.; Crudden, C. M. Dramatic Effect of Lewis Acids on the Rhodium-Catalyzed Hydroboration of Olefins. *J. Am. Chem. Soc.* **2010**, *132*, 131. (i) Obligacion, J. V.; Chirik, P. J. Bis(imino)pyridine Cobalt-Catalyzed Alkene Isomerization–Hydroboration: A Strategy for Remote Hydrofunctionalization with Terminal Selectivity. *J. Am. Chem. Soc.* **2013**, *135*, 19107. (j) Palmer, W. N.; Diao, T.; Pappas, I.; Chirik, P. J. High-Activity Cobalt Catalysts for Alkene Hydroboration with Electronically Responsive Terpyridine and α-Diimine Ligands. *ACS Catal.* **2015**, *5*, 622. (k) Ogawa, T.; Ruddy, A. J.; Sydora, O. L.; Stradiotto, M.; Turculet, L. Cobalt- and Iron-Catalyzed Isomerization–Hydroboration of Branched Alkenes: Terminal Hydroboration with Pinacolborane and 1,3,2-Diazaborolanes. *Organometallics* **2017**, *36*, 417. (l) Arthur, P.; England, D. C.; Pratt, B. C.; Whitman, G. M. Addition of Hydrogen Cyanide to Unsaturated Compounds. *J. Am. Chem. Soc.* **1954**, *76*, 5364. (m) van der Veen, L. A.; Kamer, P. C. J.; van Leeuwen, P. W. N. M. Hydroformylation of Internal Olefins to Linear Aldehydes with Novel Rhodium Catalysts. *Angew. Chem. Int. Ed.* **1999**, *38*, 336. (n) Yuki, Y.; Takahashi, K.; Tanaka, Y.; Nozaki, K. Tandem Isomerization/Hydroformylation/Hydrogenation of Internal Alkenes to *n*-Alcohols Using Rh/Ru Dual- or Ternary-Catalyst Systems. *J. Am. Chem. Soc.* **2013**, *135*, 17393. (o) Börner, M. V.-H.; Lutz,

D.; Armin Isomerization–Hydroformylation Tandem Reactions. *ACS Catal.* **2014**, *4*, 1706. (p) Seayad, A.; Ahmed, M.; Klein, H.; Jackstell, R.; Gross, T.; Beller, M. Internal olefins to linear amines. *Science* **2002**, *297*, 1676. (q) Hanna, S.; Holder, J. C.; Hartwig, J. F. A Multicatalytic Approach to the Hydroaminomethylation of α-Olefins. *Angew. Chem. Int. Ed.* **2019**, *58*, 3368. (r) Jimenez Rodriguez, C.; Foster, D. F.; Eastham, G. R.; Cole-Hamilton, D. J. Highly Selective Formation of Linear Esters from Terminal and Internal Alkenes Catalysed by Palladium Complexes of Bis-(di-*tert*-Butylphosphinomethyl)benzene. *Chem. Commun.* **2004**, 1720. (s) Jiménez-Rodriguez, C.; Eastham, G. R.; Cole-Hamilton, D. J. Dicarboxylic Acid Esters from the Carbonylation of Unsaturated Esters Under Mild Conditions. *Inorg. Chem. Commun.* **2005**, *8*, 878. (t) Mgaya, J. E.; Bartlett, S. A.; Mubofu, E. B.; Mgani, Q. A.; Slawin, A. M. Z.; Pogorzelec, P. J.; Cole-Hamilton, D. J. Synthesis of Bifunctional Monomers by the Palladium-Catalyzed Carbonylation of Cardanol and its Derivatives. *ChemCatChem* **2016**, *8*, 751. (u) Dong, K.; Fang, X.; Gülak, S.; Franke, R.; Spannenberg, A.; Neumann, H.; Jackstell, R.; Beller, M. Highly Active and Efficient Catalysts for Alkoxycarbonylation of Alkenes. *Nat. Commun.* **2017**, *8*, 14117. (v) Fang, X.; Yu, P.; Morandi, B. Catalytic Reversible Alkene-Nitrile Interconversion Through Controllable Transfer Hydrocyanation. *Science* **2016**, *351*, 832. (w) Bhawal, B. N.; Morandi, B. Catalytic Transfer Functionalization through Shuttle Catalysis. *ACS Catal.* **2016**, *6*, 7528. (x) Bhawal, B. N.; Reisenbauer, J. C.; Ehinger, C.; Morandi, B. Overcoming Selectivity Issues in Reversible Catalysis: A Transfer Hydrocyanation Exhibiting High Kinetic Control. *J. Am. Chem. Soc.* **2020**, *142*, 10914. (y) Murphy, S. K.; Park, J.-W.; Cruz, F. A.; Dong, V. M. Rh-Catalyzed C–C Bond Cleavage by Transfer Hydroformylation. *Science* **2015**, *347*, 56. (z) Kusumoto, S.; Tatsuki, T.; Nozaki, K. The Retro-Hydroformylation Reaction. *Angew. Chem. Int. Ed.* **2015**, *54*, 8458. (aa) Cobley, C. J.; Klosin, J.; Qin, C.; Whiteker, G. T. Parallel Ligand Screening on Olefin Mixtures in Asymmetric Hydroformylation Reactions. *Org. Lett.* **2004**, *6*, 3277.

5. Hanna, S.; Butcher, T. W.; Hartwig, J. F. Contra-thermodynamic Olefin Isomerization by Chain-Walking Hydrofunctionalization and Formal Retro-hydrofunctionalization. *Org. Lett.* **2019**, *21*, 7129.

6. (a) Sakaki, S.; Mizoe, N.; Sugimoto, M. Theoretical Study of Platinum(0)-Catalyzed Hydrosilylation of Ethylene. Chalk−Harrod Mechanism or Modified Chalk−Harrod Mechanism. *Organometallics* **1998**, *17*, 2510. (b) Sakaki, S.; Takayama, T.; Sumimoto, M.; Sugimoto, M. Theoretical Study of the Cp$_2$Zr-Catalyzed Hydrosilylation of Ethylene. Reaction Mechanism Including New σ-Bond Activation. *J. Am. Chem. Soc.* **2004**, *126*, 3332.

7. (a) Wang, F.; Xu, P.; Cong, F.; Tang, P. Silver-mediated oxidative functionalization of alkylsilanes. *Chem. Sci.* **2018**, *9*, 8836. (b) Xu, P.; Wang, F.; Fan, G.; Xu, X.; Tang, P. Hypervalent Iodine(III)-Mediated Oxidative Fluorination of Alkylsilanes by Fluoride Ions. *Angew. Chem. Int. Ed.* **2017**, *56*, 1101. (c) Sakamoto, R.; Sakurai, S.; Maruoka, K. Bis(trialkylsilyl) peroxides as alkylating agents in the copper-catalyzed selective mono-*N*-alkylation of primary amides. *Chem. Commun.* **2017**, *53*, 6484. (d) Tamao, K.; Yoshida, J.; Yamamoto, H.; Kakui, T.; Matsumoto, H.; Takahashi, M.; Kurita, A.; Murata, M.; Kumada, M. Organofluorosilicates in organic synthesis. 12. Preparation of organopentafluorosilicates and their cleavage reactions by halogens and N-bromosuccinimide. Synthetic and mechanistic aspects. *Organometallics* **1982**, *1*, 355. (e) Yoshida, J.; Tamao, K.; Kumada, M.; Kawamura, T. Organofluorosilicates in organic synthesis. 10. Alkylation of tetracyanoethylene with organopentafluorosilicates: implication of one-electron-transfer mechanism. *J. Am. Chem. Soc.* **1980**, *102*, 3269. (f) Tamao, K.; Yoshida, J.; Takahashi, M.; Yamamoto, H.; Kakui, T.; Matsumoto, H.; Kurita, A.; Kumada, M. Organofluorosilicates in organic synthesis. 1. A novel general and practical method for anti-Markownikoff hydrohalogenation of olefins via organopentafluorosilicates derived from hydrosilylation products. *J. Am. Chem. Soc.* **1978**, *100*, 290.

8. (a) Francisco, F.; Carmen, N.; Miguel, Y. The Hiyama Cross-Coupling Reaction: New Discoveries. *Chem. Rec.* **2016**, *16*, 2521. (b) Schweizer, S. A.; Bach, T. Regioselective Pd(0)-Catalyzed Hiyama Cross-Coupling Reactions at Dihalo-Substituted Heterocycles. *Synlett* **2010**, *2010*, 81. (c) Hayao, M.; Satoshi, A.; Kazunori, H.; Yasuo, H.; Atsunori, M.; Tamejiro, H. Palladium-Catalyzed Cross-Coupling Reaction of Alkyltrifluorosilanes with Aryl Halides. *Bull. Chem. Soc. Jpn.* **1994**, *70*, 437. (d) Hatanaka, Y.; Hiyama, T. A wide range of organosilicon compounds couples with enol and aryl triflates in the presence of Pd catalyst and fluoride ion. *Tetrahedron Lett.* **1990**, *31*, 2719. (e) Waqar, R.; M., B. J. Catalytic Amide-Mediated Methyl Transfer from Silanes to Alkenes in Fujiwara–Moritani Oxidative Coupling. *Angew. Chem. Int. Ed.* **2008**, *47*, 4228.

9. (a) Kustov, L. M.; Kucherov, A. V.; Finashina, E. D. Oxidative dehydrogenation of C2–C4 alkanes into alkenes: Conventional catalytic systems and microwave catalysis. *Russ. J. Phys. Chem. A* **2013**, *87*, 345. (b) Sun, X.; Han, P.; Li, B.; Mao, S.; Liu, T.; Ali, S.; Lian, Z.; Su, D. Oxidative dehydrogenation reaction of short alkanes on nanostructured carbon catalysts: a computational account. *Chem. Commun.* **2018**, *54*, 864.

10. (a) Beccalli, E. M.; Broggini, G.; Martinelli, M.; Sottocornola, S. C−C, C−O, C−N Bond Formation on sp^2 Carbon by Pd(II)-Catalyzed Reactions Involving Oxidant Agents. *Chem. Rev.* **2007**, *107*, 5318. (b) Wang, D.; Weinstein, A. B.; White, P. B.; Stahl, S. S. Ligand-Promoted Palladium-Catalyzed Aerobic Oxidation Reactions. *Chem. Rev.* **2018**, *118*, 2636. (c) Brian V. Popp, S. S. S., *Palladium-Catalyzed Oxidation Reactions: Comparison of*

Benzoquinone and Molecular Oxygen as Stoichiometric Oxidants. Springer, Berlin, Heidelberg: Springer, Berlin, Heidelberg, 2006; p 253. (d) Porth, S.; Bats, J. W.; Trauner, D.; Giester, G.; Mulzer, J. Insight into the Mechanism of the Saegusa Oxidation: Isolation of a Novel Palladium(0)–Tetraolefin Complex. *Angew. Chem. Int. Ed.* **1999**, *38*, 2015.

11. (a) Schuster, C. H.; Diao, T.; Pappas, I.; Chirik, P. J. Bench-Stable, Substrate-Activated Cobalt Carboxylate Pre-Catalysts for Alkene Hydrosilylation with Tertiary Silanes. *ACS Catal.* **2016**, *6*, 2632. (b) Du, X.; Huang, Z. Advances in Base-Metal-Catalyzed Alkene Hydrosilylation. *ACS Catal.* **2017**, *7*, 1227. (c) Du, X.; Zhang, Y.; Peng, D.; Huang, Z. Base–Metal-Catalyzed Regiodivergent Alkene Hydrosilylations. *Angew. Chem. Int. Ed.* **2016**, *55*, 6671. (d) Jia, X.; Huang, Z. Conversion of alkanes to linear alkylsilanes using an iridium–iron-catalysed tandem dehydrogenation–isomerization–hydrosilylation. *Nat. Chem.* **2016**, *8*, 157. (e) Zuo, Z.; Zhang, L.; Leng, X.; Huang, Z. Iron-catalyzed asymmetric hydrosilylation of ketones. *Chem. Commun.* **2015**, *51*, 5073. (f) Obligacion, J. V.; Chirik, P. J. Earth-abundant transition metal catalysts for alkene hydrosilylation and hydroboration. *Nat. Rev. Chem.* **2018**, *2*, 15.

12. Trichlorosilane. In *Encyclopedia of Reagents for Organic Synthesis*, 2006.

13. Denmark, S. E.; Ambrosi, A. Why You Really Should Consider Using Palladium-Catalyzed Cross-Coupling of Silanols and Silanolates. *Organic Process Research & Development* **2015**, *19*, 982.

Chapter 5

Contra-Thermodynamic Olefin Isomerization by Chain-Walking Hydroboration and Dehydroboration

5.1 Introduction

Because internal olefins are more stable than terminal olefins, isomerizations of terminal olefins to internal olefins are exergonic and have been thoroughly investigated.[1] However, the reverse reaction, isomerization of an internal olefin to a terminal olefin, is endergonic and is much less explored than its exergonic counterpart. Typically, contra-thermodynamic, positional olefin isomerizations are conducted by allylic functionalization followed by defunctionalization with allylic transposition or by photodeconjugation.[2] These strategies enable translocation of a double bond, but by a maximum of one carbon unit and often require harsh conditions.

Only a small number of long-range (through at least two carbon units), contra-thermodynamic olefin isomerizations have been reported.[3] Typically, these reactions form terminal olefins in low yields, low selectivities, or both. Because long-range, contra-thermodynamic olefin isomerizations could enable the valorization of mixtures of internal olefins formed by catalytic cracking of heavy vacuum gasoil to constitutionally pure terminal olefins or the late-stage derivatization of complex molecules containing internal olefins to analogues containing terminal olefins for the remote installation of functional groups, our group has worked to develop mild contra-thermodynamic, long-range olefin isomerizations.

We have reported strategies for conducting long-range, contra-thermodynamic olefin isomerization through chain-walking hydrofunctionalization, followed by dehydrofunctionalization.[4] Selectivity for terminal olefins is achieved by identifying conditions for chain-walking hydrofunctionalization with high *n*:*iso* ratios. In theory, many systems for chain-walking hydrofunctionalization could be coupled to dehydrofunctionalizations to design long-range, contra-thermodynamic olefin isomerizations.[5] However, few dehydrofunctionalizations have been developed.[6]

In 2019, we published a one-pot process for the selective, long-range isomerization of internal olefins to terminal olefins by platinum-catalyzed, chain-walking hydrosilylation followed by a novel, formal dehydrosilylation (Scheme 1A).[4b] We improved upon this process in 2020 by developing a catalytic version of the formal dehydrosilylation (Scheme 1B).[4a] However, the substrate scope of each of these processes was limited due to the harsh conditions of the chain-walking hydrosilylation. Heteroatom-containing functional groups were not tolerated, and only hydrocarbons were competent substrates. In addition, large excesses of cesium fluoride and elevated temperatures were required to conduct both dehydrosilylation processes. Therefore, we sought to overcome these limitations by developing an isomerization sequence involving other chain-walking hydrofunctionalizations and dehydrofunctionalizations.

Conditions for chain-walking hydroboration are typically milder than those for chain-walking hydrosilylation with $HSiCl_3$ and Speier's catalyst. The chain-walking hydroboration of 4-octene to produce the pinacol ester of *n*-octylboronic acid was reported by Srebnik in 1996.[7] Since this seminal report, many advances in the field of chain-walking hydroboration have been made.[5g-k,7-8] We were particularly interested in several chain-walking hydroborations reported by Chirik (Scheme 1C),[5i,5j,9] because the catalysts for these reactions are capable of walking through methine units and because the hydroborations are conducted with pinacol boronic esters, which are particularly mild reagents.

Dehydroboration of boronic esters or acids is a rare reaction. Alkylboranes undergo acceptorless dehydroborations as well as transfer dehydroborations with olefins and aldehydes.[3a-c,10] However, alkylboranes are particularly reactive, and practical chain-walking hydroborations that produce terminal alkylboranes from internal olefins have not been reported. Therefore, we sought to develop a mild method for dehydroboration of alkylboronic esters. Meek and coworkers have reported a dehydroboration of β-alkoxy-*gem*-dipinacolato-alkyboronic esters involving palladium catalysis,[11] but a dehydroboration of unactivated alkylboronic esters has not been developed.

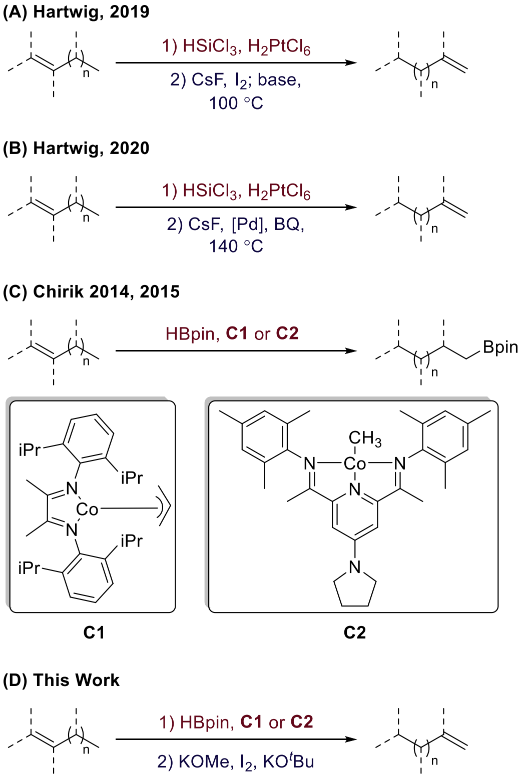

Scheme 1. Development of a long-range, contra-thermodynamic olefin isomerization through hydroboration and dehydroboration

We envisioned that alkylboronic esters could undergo dehydroboration through a sequence comprising the activation of the boronic ester with a nucleophile, iodination, and base-promoted elimination (Scheme 1D). Until recently, iodinations of unactivated alkylboronic esters had only been reported with organolithiates as activating reagents.[12] In the course of our studies, Renaud and co-workers reported a method for the radical bromination of unactivated alkylboronic esters with benzenesulfonyl bromide as the halogenating reagent.[12e] However, this reaction requires reagents, such as di-*tert*-butylhyponitrite, trimethylsilyl trifluoromethanesulfonate, methoxycatecholborane, and benzenesulfonyl bromide, and *S*-phenyl benzenethiosulfonate, that might be deactivated by reagents from the chain-walking hydroboration step or might interfere with the elimination step of the overall isomerization, and iodinations were not reported.

5.2 Results and discussion

We began the development of our isomerization by investigating the iodination of unactivated alkylboronic acid **2b** (Table 1). We sought to identify a mild, inexpensive nucleophile capable of activating boronic esters for the desired cascade. After surveying a variety of nucleophiles (Table 1, entries 1-13), we identified potassium methoxide as a suitable candidate. We found that alkyl iodide **3a** formed in lower yields when the reaction was conducted with commercial KOMe than when the reaction was conducted with KOMe prepared from free-flowing KH and anhydrous methanol (Table 1, entries 1-2, see SI for details) because commercial alkoxides often contain impurities, such as formate and water, that can decrease yields and selectivities of reactions.[13] Little or no product formed in the presence of various other oxygen (entries 4-9), nitrogen (entries 10-11), or hydride bases (entry 13). However, alkyl iodide **3a** formed in 78% yield in the presence of CsF.

When the reaction was conducted with oxidants other than iodine, alkyl iodide **3a** formed in lower yields (entries 15-16). We discovered that adding an aliquot of KO*t*Bu after the addition of I_2 further increased the yield of alkyl iodide **3a** (Table 1, entry 14) beyond that in entry 2 of Table 1. Temperature had little effect on the yield of alkyl iodide **3a** (Table 1, entries 17-20). Alkyl iodide **3a** formed in lower yields under more dilute conditions (Table 1, entry 21) than those in entry 14 of Table 1. Alkyl iodide **3a** formed in lower yields with greater equivalents of KOMe or of I_2 (Table 1, entries 23-24) than those in entry 14 of Table 1. A delicate balance of equivalents of these two reagents is likely required to ensure the formation of alkyl iodide **3a** in high yield due to the potential of iodine to oxidize potassium methoxide.

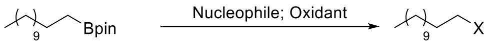

2a **3a**

Entry	Nucleophile	Oxidant	Temperature	Yield^{z}
1	KOMe^{a}	I_2	rt	50
2	KOMe^{b}	I_2	rt	86
3	KOMe + 18-c-6	I_2	rt	89
4	KO^{t}Bu	I_2	rt	29
5	KOEt	I_2	rt	15
6	NaOMe	I_2	rt	5
7	KOH	I_2	rt	3
8	Cs_2CO_3	I_2	rt	0
9	NaOAc	I_2	rt	0
10	$LiNH_2$	I_2	rt	8
11	KHMDS	I_2	rt	5
12	CsF	I_2	rt	78
13	KH	I_2	rt	0
14	KOMe^{b} + 1.0 equiv KO^{t}Bu^{c}	I_2	rt	93
15	KOMe^{b} + 1.0 equiv KO^{t}Bu^{c}	NIS	rt	37
16	KOMe^{b} + 1.0 equiv KO^{t}Bu^{c}	NBS	rt	0
17	KOMe^{b} + 1.0 equiv KO^{t}Bu^{c}	I_2	50	88
18	KOMe^{b} + 1.0 equiv KO^{t}Bu^{c}	I_2	65	85
19	KOMe^{b} + 1.0 equiv KO^{t}Bu^{c}	I_2	80	86
20	KOMe^{b} + 1.0 equiv KO^{t}Bu^{c}	I_2	100	77
21	KOMe^{b} + 1.0 equiv KO^{t}Bu$^{c, x}$	I_2	rt	81
22	KOMe^{b} + 1.0 equiv KO^{t}Bu$^{c, y}$	I_2	rt	63^{p}
23	KOMe^{b} + 1.0 equiv KO^{t}Bu$^{c, z}$	I_2	rt	12
24	KOMe^{b} + 1.0 equiv KO^{t}Bu$^{c, q}$	I_2	rt	16

Conditions: Nucleophile (2 equiv), THF (100 μL), 15 min, rt; Oxidant (2 equiv), THF (100 μL), 15 min, rt; [a]Commercial bottle; [b]Prepared form KH, see SI; [c]Entries 14-24: KO^{t}Bu (1 equiv), THF (100 μL), added 15 min after I_2, 15 min, rt, see SI for details; [x]At low concentration; [y]Long reaction time; [z]4.0 equiv KOMe; [p]Some olefin formed by elimination; [q]4.0 equiv I_2; [z]Determined by GC

Table 1. Iodination of boronic ester **2a**

Having identified conditions for the iodination of alkylboronic ester **2a**, we investigated the one-pot dehydroboration of alkylboronic ester **2a** to produce terminal olefin **4a** (Table 2). We conducted the elimination step with KO^{t}Bu as the base. The dehydroboration sequence was conducted with the elimination step at various temperatures and with various equivalents of KO^{t}Bu. We found that a minimum of 3 equivalents of KO^{t}Bu were required to conduct the elimination, possibly due to the presence of excess iodine after the completion of the iodination.

Regardless of the number of equivalents of KO^{t}Bu used, the elimination step could be conducted at room temperature.

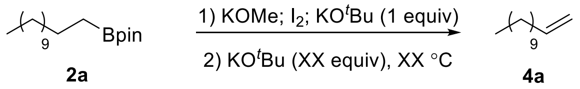
9
Bpin
1) KOMe; I$_2$; KO^{t}Bu (1 equiv)
2) KO^{t}Bu (XX equiv), XX °C
9
2a
4a

Entry	KO^{t}Bu (equiv)	Temp (°C)	Temperature	Yield
1	6	rt	rt	89
2	6	50	rt	94
3	6	65	rt	93
4	6	80	rt	84
5	5	rt	rt	90
6	5	50	rt	92
7	5	65	rt	87
8	5	80	rt	85
9	4	rt	rt	92
10	4	50	rt	91
11	4	65	rt	79
12	4	80	rt	87
13	3	rt	rt	91
14	3	50	rt	92
15	3	65	rt	91
16	3	80	rt	90
17	0	rt	50	91^a
18	0	50	65	91^a
19	0	65	80	92^a
20	0	80	100	92^a

Step 1: KOMe (2 equiv), THF (100 μL), 15 min, rt; I$_2$ (2 equiv), THF (100 μL), 15 min, rt; KO^{t}Bu (1 equiv), THF (100 μL); 15 min, rt. Step 2: KO*t*Bu, 22 h, THF (200 μL). ^{a}Yield of alkyl iodide.

Table 2. Iodination and elimination of boronic ester **2a**

We also conducted the iodination of *β*-branched alkylboronic ester **2b** to determine whether β branching inhibits the iodination process. We found that the iodination of alkylboronic ester **2b** occurred in lower yield than that of alkylboronic ester **2a**. However, repetition of the activation-iodination sequence significantly increased the yield. The combined yield of alkyl iodide **3b** and terminal olefin **4b** was 93% when the KOMe, I$_2$, and KO^{t}Bu were added portionwise over two iterations (Scheme 2). The iodinated product could subsequently undergo base-promoted elimination to product **3b** with excess KO^{t}Bu.

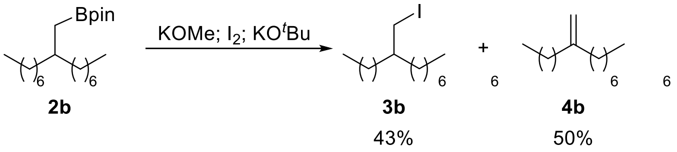

Conditions: KOMe (2 equiv), THF (100 μL), 5 min, rt; I$_2$ (1.5 equiv), THF (100 μL), 5 min, rt; KO^{t}Bu (1 equiv), 1 h; KOMe (2 equiv), THF (100 μL), 5 min, rt; I$_2$ (1.5 equiv), THF (100 μL), 5 min, rt; KO^{t}Bu (1 equiv), 1 h

Scheme 2. Iodination and elimination of boronic ester **2b**

We also sought to determine whether our newly developed catalytic dehydrosilylation of linear alkylsilanes could be conducted on the crude products of chain-walking hydroborations to enable one-pot, contra-thermodynamic, positional olefin isomerizations. Therefore, we conducted the dehydroboration of alkylboronic ester **2a** in the presence of various reagents used to conduct chain-walking hydroborations with catalysts **C1** and **C2** (Table 3). We found that HBpin and catalyst **C1** inhibit the dehydroboration process. Therefore, when conducting the dehydroboration portions of contra-thermodynamic olefin isomerizations, we added the KOMe, I_2, and KO^{t}Bu portionwise and in series over multiple iterations. As observed for the dehydroborations of pure β-branched boronic esters, the yields of dehydroborations conducted on the crude products of chain-walking hydroborations significantly increased upon adding the reagents portionwise in this fashion.

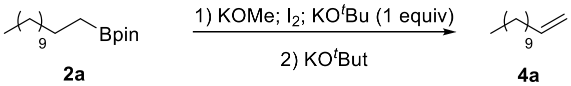

2a **4a**

Entry	deviation from conditions	Yield
1	none	90
2	added 0.1 equiv HBpin	86
3	added 0.5 equiv HBpin	67
4	added MTBE	85
5	added MTBE + 0.1 equiv HBPin	86
6	added MTBE + 0.5 equiv HBPin	64
7	added MTBE + **C1**	60
8	added MTBE + **C1** + 0.5 equiv HBpin	43

Step 1: KOMe (2 equiv), THF (100 mL), 15 min, rt; I_2 (2 equiv), THF (100 mL), 15 min, rt; KO^{t}Bu (1 equiv), THF (100 mL); 15 min, rt. Step 2: KO*t*Bu, 22 h, THF (200 mL). [a]Yield of alkyl iodide.

Table 3. Iodination and elimination of boronic ester 2b in the presence of components of hydroboration reaction

Having developed conditions for the dehydroboration of alkylboronic esters, we conducted one-pot, contra-thermodynamic isomerizations of internal olefins to terminal olefins by conducting chain-walking hydroboration and subsequent dehydroboration. We initially investigated olefin isomerizations in which catalyst **C1** was employed in the chain-walking hydroboration step (Scheme 3). We found that both hydrocarbon (olefins **1c**, **1d**, **1e**, and **1f**) and non-hydrocarbon (olefin **1g**) linear internal olefins reacted in good yields with excellent regioselectivities. Translocation of the double bond proceeded over as many as seven carbon units (olefin **1f**). Olefin **4f** was isolated cleanly in 68% yield. Olefin **4g** was also isolated in good yield and good selectivity for the terminal olefin.

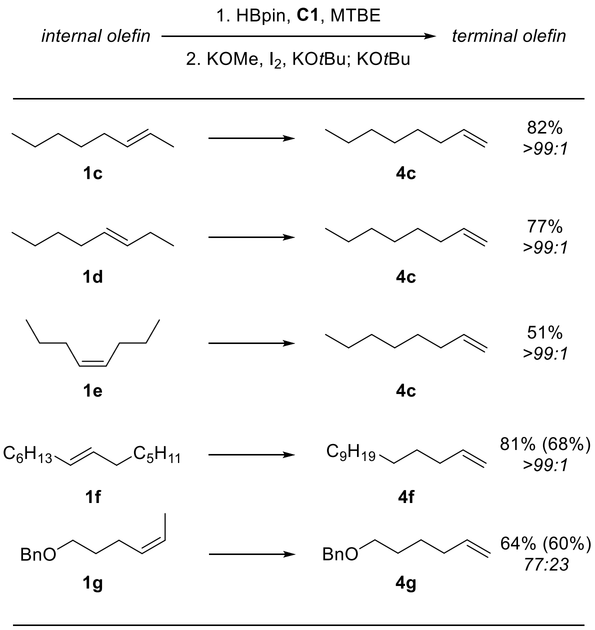

Step 1: Internal olefin (0.64 mmol), HBpin (1.05 equiv), **C1** (2 mol%), rt, 24 h, MTBE (640 μL). Step 2: KOMe (3 equiv), I_2 (3 equiv), KO^{t}Bu (1.5 equiv), portionwise, 3 iterations; KO^{t}Bu (5 equiv). Yields and regioselectivities were determined by ^{1}H NMR spectroscopy.

Scheme 3. Contra-thermodynamic olefin isomerizations in the presence of catalyst **C1**

To conduct contra-thermodynamic olefin isomerizations in the presence of additional functional groups and on branched internal olefins, we also investigated chain-walking hydroborations catalyzed by complex **C2**. Chirik initially developed catalyst **C2**,[5i] in which the cobalt pre-catalyst contains 16 valence electrons, for hydroboration of functionalized terminal olefins and branched internal olefins. Catalyst **C1** was subsequently determined to be more active than catalyst **C2**,[5j] but catalyst **C1** tolerates fewer functional groups than catalyst **C2**. The low functional-group tolerance of catalyst **C1** presumably originates from the conversion of the pre-catalyst to a highly unsaturated cobalt boryl species containing 14 valence electrons that is deactivated by heteroatoms containing Lewis basic sites, such as oxygen lone pairs. Chirik also found that internal olefins in 6-membered rings often did not undergo hydroborations catlayzed by complex **C1** because these olefins often reacted with the catalyst to form stable endocyclic π-allyl complexes.[5j]

Thus, to achieve the olefin migrations of trisubstituted alkenes and alkenes containing an acetal group, we used complex **C2** as the catalyst for the chain-walking hydroboration step (Scheme 4). Indeed, we found that the overall isomerization occurred with tri-substituted internal olefins (olefin **1h**), and we found that acetal groups were tolerated (olefin **1k**). We have also developed a route to catalyst **C2** in 5 steps in 22% overall yield, which is two fewer steps than are reported in the literature. This route can be conducted on relatively large scales, and 2.74 g of the cobalt-chloride precursor were obtained (see SI for details).

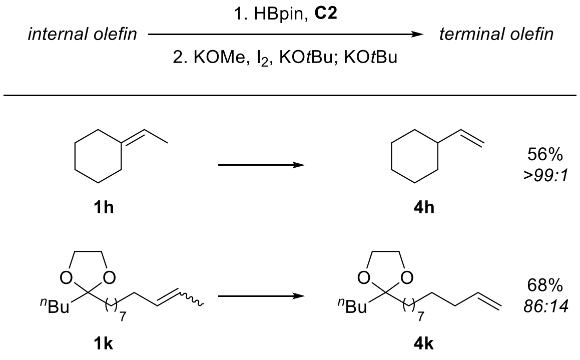

Step 1: Internal olefin (0.64 mmol), HBpin (1.05 equiv), **C2** (3-7 mol%), rt, 24 h. Step 2: KOMe (3-4 equiv), I_2 (3-4 equiv), KO^{t}Bu (1.5-2 equiv), portionwise, 3-4 iterations; KO^{t}Bu (5-6 equiv). Yields and regioselectivities were determined by ^{1}H NMR spectroscopy.

Scheme 4. Contra-thermodynamic olefin isomerizations in the presence of catalyst **C2**

5.3 Conclusion

In conclusion, we have developed a novel dehydroboration that was combined with chain-walking hydroboration to create a long-range, contra-thermodynamic isomerization of internal olefins to terminal olefins. The dehydroboration and the overall olefin isomerization proceed at room temperature with a mild reagent for hydrofunctionalization and do not require fluoride bases. The substrate scope of the overall isomerization was expanded, relative to that of previous isomerizations that involve chain-walking hydrofunctionalization, to include heteroatom-bearing internal olefins.

5.4 Experimental

5.4.1 General methods and materials

All air-sensitive manipulations were conducted under an inert atmosphere in nitrogen-filled or argon-filled gloveboxes or by standard Schlenk techniques. All reagents were purchased from commercial suppliers and used as received unless otherwise stated. Potassium methoxide was prepared as described below. Crude reaction mixtures were analyzed by gas chromatography (GC) on an Agilent 7890 GC equipped with an HP-5 column (25 m x 0.20 mm x 0.33 µm film) and an FID detector. Quantitative analysis by GC was conducted with dodecane as an internal standard. The products of catalytic reactions were purified by flash column chromatography with a Teledyne Isco CombiFlash® R_f system and RediSep R_f Gold™ columns. All NMR spectra were recorded at the University of California, Berkeley NMR facility. NMR spectra were recorded on Bruker AVB-400, AVQ-400, AV-500, and AV-600 instruments with operating frequencies of 400, 400, 500, and 600 MHz, respectively, and Carbon-13 NMR spectra were recorded on a Bruker AV-600 instrument with a ^{13}C operating frequency of 151 MHz. Chemical shifts (δ) are reported in ppm relative to those of residual solvent signals ($CDCl_3$ $\delta = 7.26$ for ^{1}H NMR spectra and $\delta = 77.16$ for ^{13}C NMR spectra).

5.4.2 Preparation of Potassium Methoxide

In an argon-filled glovebox, a commercial dispersion of potassium hydride in mineral oil was washed thoroughly with copious pentane and dried over a frit to yield pure, free-flowing potassium hydride powder. In the glovebox, an oven-dried round-bottom flask was charged with free-flowing potassium hydride (8.02 g, 200 mmol, 1 equiv) and anhydrous THF (100 mL). Anhydrous methanol (9.72 mL, 240 mmol, 1.2 equiv) was added dropwise at room temperature with stirring in the glovebox. The reaction was stirred at room temperature in the glovebox for 24 h, at which time bubbling had mostly ceased. The reaction mixture was filtered over a frit, washed with copious THF (~500 mL), washed with copious pentane (~500 mL), and dried under vacuum. This material was used in dehydroboration reactions without further purification.

5.4.3 Synthesis of Catalyst C1

[($^{\text{IPr}}$DI)CoCl$_2$] (S1)

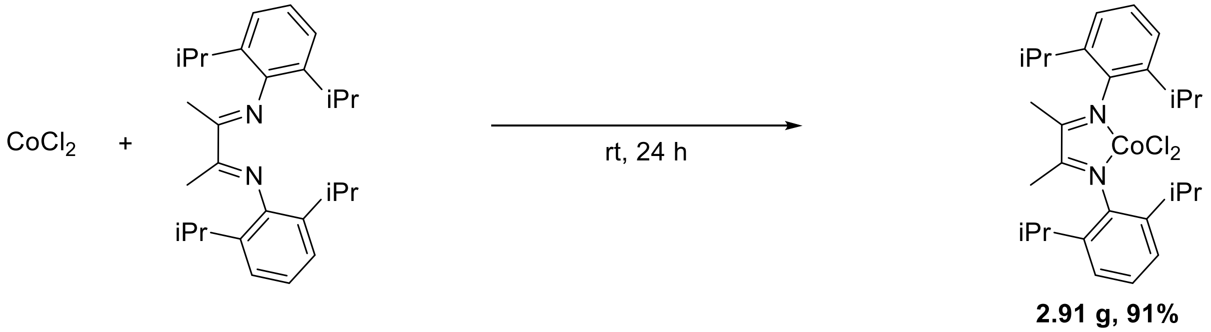

The following procedure was adapted from that of Thomas and coworkers.[14] In a nitrogen-filled glovebox, an oven-dried 500 mL round-bottom flask equipped with a stir bar was charged with (2*E*)-*N*-[(*E*)-(2,6-diisopropylphenylimino)butan-2-ylidene]-2,6-diisopropylbenzenamine (2.43 g, 6.00 mmol, 1 equiv, prepared according to the literature[14]), anhydrous cobalt dichloride (779 mg, 6.00 mmol, 1 equiv), and THF (90 mL). The reaction mixture was stirred at room temperature for 48 h and concentrated *in vacuo*. Diethyl ether (100 mL) was added. The resulting precipitate was collected by filtration and washed with diethyl ether (200 mL) to yield **S1** as a dark-green solid (2.91 g, 91% yield). The ^{1}H NMR spectrum matched that in the literature.[14]

[($^{\text{IPr}}$DI)CoCl]$_2$ (S2)

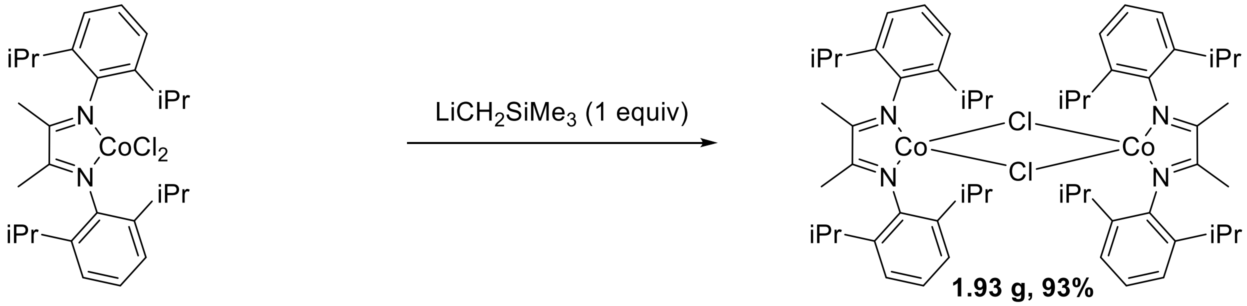

The following procedure was adapted from that of Chirik and coworkers.[5j] In a nitrogen-filled glovebox, a solution of [($^{\text{IPr}}$DI)CoCl$_2$] (**S1**, 2.15 g, 4.03 mmol, 1.00 equiv) in diethyl ether (60 mL) was prepared in a 250 mL round-bottom flask and cooled in a cold well in the drybox floor with a dry ice/acetone bath. A separate solution of LiCH$_2$SiMe$_3$ (4.0 mL, 1.0 M in pentane, 4.0 mmol, 1.0 equiv) in diethyl ether (30 mL) was chilled at -25 °C in a glovebox freezer and added dropwise with stirring over 40 min to the round-bottom flask containing the solution of [($^{\text{IPr}}$DI)CoCl$_2$]. Throughout the 40 min addition of LiCH$_2$SiMe$_3$, the round-bottom flask was kept in the cold well cooled with a dry ice/acetone bath. The round-bottom flask was removed from the cold well and stirred at room temperature for 1 h. The reaction mixture was filtered, and the filtrate was concentrated *in vacuo*. The residue was washed with several small aliquots of cold pentane (approximately 30 mL total) and collected on a frit to yield **S2** as a dark-green powder (1.87 g, 93% yield). This material is paramagnetic, and a ^{1}H NMR spectrum was not recorded. This material was converted to catalyst **C1** without further purification.

[($^{\text{IPr}}$DI)Co(η^3-C_3H_5)] (C1)

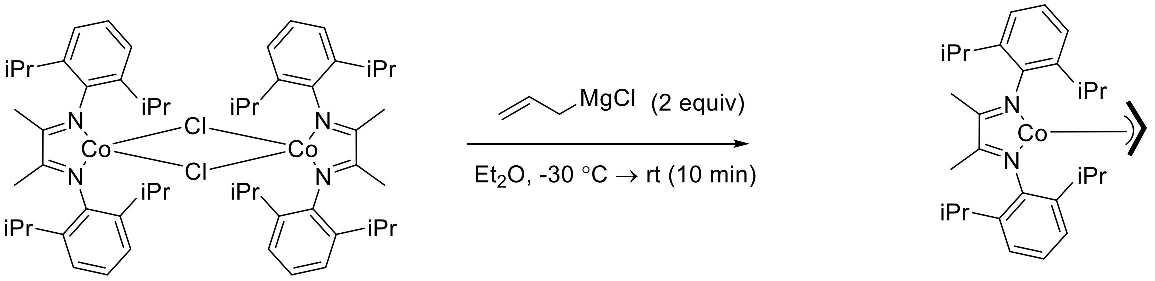

1.6 g, 85%

The following procedure was adapted from that of Chirik and coworkers.[5j] In a nitrogen-filled glovebox, a solution of [($^{\text{IPr}}$DI)CoCl]$_2$ (**S2**, 1.87 g, 1.87 mmol, 1.00 equiv) in diethyl ether (140 mL) was prepared in a 500 mL round-bottom flask and cooled in a cold well in the drybox floor with a dry ice/acetone bath. A solution of allylmagnesium chloride (1.87 mL, 2.0 M in THF, 3.74 mmol, 2.0 equiv) in diethyl ether (30 mL) was added dropwise with stirring over 15 min to the round-bottom flask containing the solution of [($^{\text{IPr}}$DI)CoCl$_2$]. Throughout the 15 min addition of allylmagnesium chloride, the round-bottom flask was kept in the cold well cooled with a dry ice/acetone bath. The round-bottom flask was removed from the cold well and stirred at room temperature for 80 min. The reaction mixture was filtered, and the filtrate was concentrated *in vacuo* to yield **C1** as a dark-blue-green solid (1.60 g, 85% yield). This material was used in catalytic reactions without further purification. The ^{1}H NMR spectrum matched that in the literature.[5j]

5.4.4 Synthesis of Catalyst C2

2,6-Dibromo-4-(1-pyrrolidinyl)-pyridine (S3)

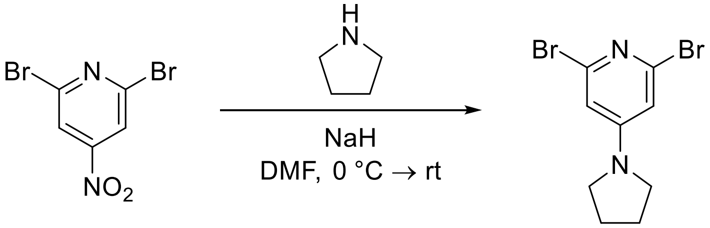

The following procedure was adapted from that of Kanbara and coworkers.[15]

In an argon-filled glovebox, pure, free-flowing sodium hydride (3.60 g, 150 mmol, 3.06 equiv, the commercial 60% dispersion in mineral oil was washed thoroughly with pentane to obtain the pure powder) and DMF (100 mL) were added to an oven-dried 500 mL round bottom flask. The flask was capped with a septum, removed from the glovebox, and cooled in an ice bath. A solution, prepared in the glovebox, of 2,6-dibromo-4-nitropyridine (13.8 g, 49.1 mmol, 1 equiv) in DMF (40 mL) was added dropwise with stirring at 0 °C under a flow of nitrogen. Pyrrolidine (4.20 mL, 49.9 mmol, 1.02 equiv) was added dropwise with stirring at 0 °C under a flow of nitrogen. The mixture was stirred at 0 °C for approximately 2 h before the ice melted. After the ice melted, the mixture was stirred for an additional 15 h at room temperature. The resulting mixture was cooled in the same ice bath and carefully quenched with water (40 mL) under a flow of nitrogen. An additional 200 mL of water was added, and the mixture was extracted into ethyl acetate (300 mL, 2x then 150 mL, 5x). Note: conducting the extraction with large solvent volumes was preferable to using smaller solvent volumes with salts and/or brine added to the aqueous layer because the latter method does not remove as much DMF as the former method. The combined extracts were concentrated *in vacuo* to a volume of approximately 500 mL, washed with brine (100 mL, 1x) to remove residual DMF, dried over sodium sulfate, and concentrated *in vacuo* to give a dark-red solid, which was recrystallized from hot ethyl acetate. Note: on smaller scales, recrystallization is unnecessary. The mother liquor was concentrated and purified by flash column chromatography on silica gel (~80 g silica, gradient elution: 5 → 20% ethyl acetate/hexane) to afford **S3** (8.87 g, 59% yield) as a pink, crystalline solid. The ^{1}H NMR spectrum matched that in the literature.[15]

2,6-Diacetyl-4-(1-pyrrolidinyl)-pyridine S4

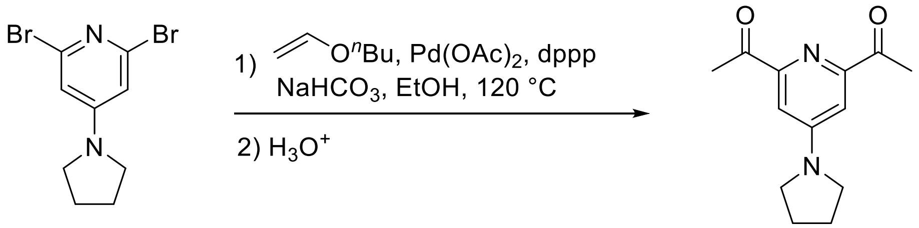

The following procedure was adapted from that of Kobata and coworkers.[16]

In a argon-filled glovebox (nitrogen-filled glovebox also acceptable), an oven-dried 120 mL pressure tube (selected due to buildup of CO_2 from $NaHCO_3$ and of ethanol vapor) was sequentially charged with dppp (441 mg, 1.07 mmol, 10.7 mol%), $Pd(OAc)_2$ (180 mg, 0.800 mmol, 8.00 mol%), thoroughly degassed ethanol (20 mL), 2,6-dibromo-4-(1-pyrrolidinyl)-pyridine (**S3**, 3.06 g, 10.0 mmol, 1.00 equiv), thoroughly degassed butyl vinyl ether (10.6 mL, 81.9 mmol, 8.19 equiv), and $NaHCO_3$ (5.04 g, 60.0 mmol, 6.00 equiv). The reaction mixture was heated at 120 °C for 24 h. The reaction was monitored by GCMS, with aliquots removed at room temperature inside an argon-filled glovebox. Upon completion of the reaction after 24 h (no starting material or mono-Heck products detected), the reaction mixture was filtered and washed with ethanol (140 mL). Aqueous HCl (6 M, 30 mL, 180 mmol, 18.0 equiv) was added to the filtrate, and the mixture was stirred at room temperature. The progress of the hydrolysis was monitored by GCMS. Upon completion of the reaction after 24 h, the reaction mixture was concentrated to a volume of approximately 70 mL. Sodium hydroxide (6 M, ~500 mL) was added until a pH of 13 was reached, and the reaction mixture was extracted into ethyl acetate (5x, 150 mL). The combined extracts were recrystallized from hot ethyl acetate (note: on smaller scales recrystallization is unnecessary), and the mother liquor was purified by flash column chromatography on silica gel (~60 g silica, gradient elution: 10 → 25% ethyl acetate/hexane) to afford **S4** (1.28 g, 55% yield) as a white solid. The ^{1}H NMR spectrum matched that in the literature.[16]

4-pyrr-$^{\mathrm{Mes}}$PDI (S5)

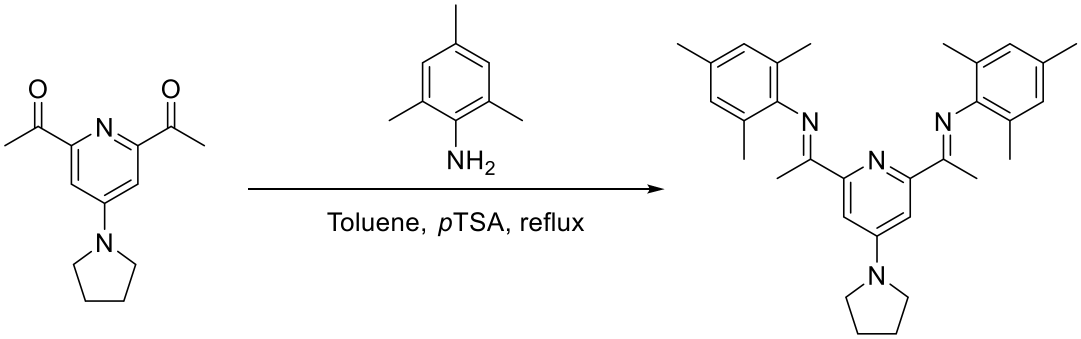

The following procedure was adapted from that of Chirik and coworkers.[5i]

In an argon-filled glovebox, 2,6-diacetyl-4-(1-pyrrolidinyl)-pyridine (**S4**, 1.28 g, 5.52 mmol, 1.00 equiv), toluene (65 mL, dry and degassed), 2,4,6-trimethylaniline (1.86 mL, 13.3 mmol, 2.40 equiv) and *p*-toluenesulfonic acid (7.4 mg, 0.039 mmol, 7.1 mol%) were added to an oven-dried 250 mL round-bottom flask. The flask was capped with a septum, removed from the glovebox, placed under a positive flow of nitrogen, fitted with a Dean-Stark apparatus, and heated at 130 °C for 48 h. The reaction was monitored by GCMS. The mixture was concentrated by rotary evaporation outside of the glovebox, and the resulting residue was brought back into the glovebox and washed with a minimal amount of anhydrous methanol (9 mL total, ~1 mL aliquots at a time) to yield **S5** (2.20 g, 85% yield) as a brown solid. The ^{1}H NMR spectrum matched that in the literature.[5i]

[(4-pyrr-^{Mes}PDI)CoCl$_2$] (S6)

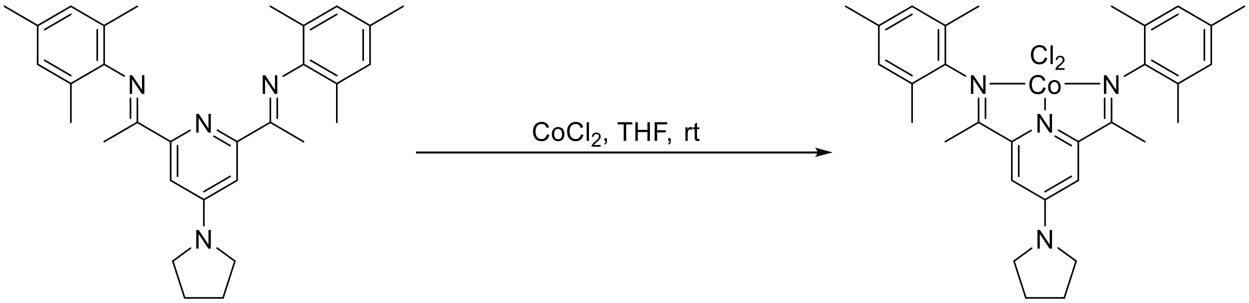

The following procedure was adapted from that of Chirik and coworkers.[5i]

In an argon-filled glovebox, 4-pyrr-^{Mes}PDI (**S5**, 2.20 g, 4.70 mmol, 1.00 equiv), THF (dry, degassed, 100 mL), and CoCl$_2$ (0.611 g, 4.70 mmol, 1.00 equiv) were added to an oven-dried 250 mL round-bottom flask and stirred at room temperature for 24 h. The reaction mixture was concentrated *in vacuo*, and the residue was washed with diethyl ether (~60 mL) to afford **S6** (2.74 g, 98% yield) as a bright, green powder. The ^{1}H NMR spectrum matched that in the literature.[5i]

[(4-pyrr-^{Mes}PDI)CoCH$_3$] (C2)

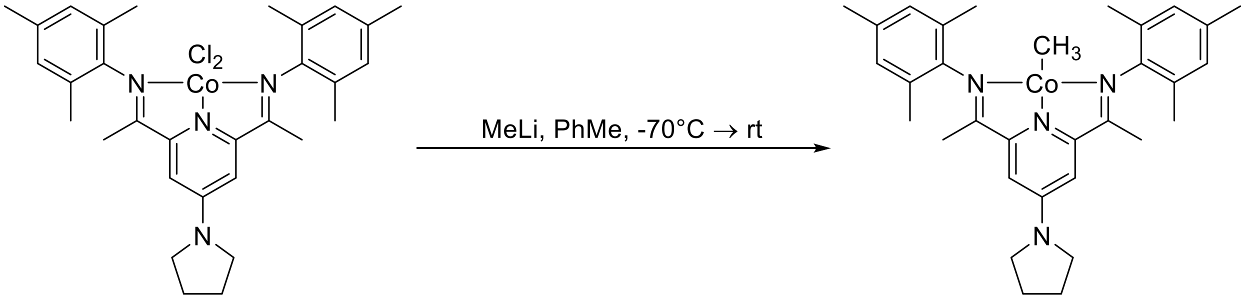

The following procedure was adapted from that of Chirik and coworkers.[5i]

In a nitrogen-filled glovebox, a solution of [(4-pyrr-^{Mes}PDI)CoCl$_2$] (**S6**, 500 mg, 0.838 mmol, 1.00 equiv) in dry, degassed toluene (30 mL) in a 100 mL round-bottom flask was cooled in a cold well with a dry ice/acetone bath. A solution of methyllithium (1.05 mL of a 1.6 M solution in Et$_2$O, 1.676 mmol, 2.00 equiv) additionally diluted with 3.0 mL diethyl ether was added dropwise with stirring while the flask was in the cold well. A color change from light green to blue-green was observed. The reaction mixture was stirred for 30 min in the cold well, removed from the cold well, stirred for 2.5 h at room temperature, filtered, and concentrated *in vacuo* to afford **C2** (370 mg, 82%). as a dark blue/purple solid. This material was used for catalytic reactions without further purification. The ^{1}H NMR spectrum matched that in the literature.[5i]

Overall yield: 59% × 55% × 85% × 98% × 82% = 22% over 5 steps

5.4.5 Synthesis of olefins

(*Z*)-((Hex-4-en-1-yloxy)methyl)benzene (1g)

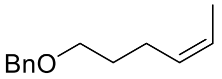

Olefin **1g** was synthesized according to the literature.[17]

Methyl dodec-10-enoate (S7)

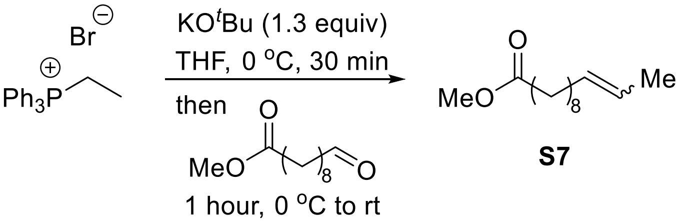

Under nitrogen, ethyl triphenylphosphonium bromide (4.83 g, 13.0 mmol, 1.3 equiv) was dissolved in dry THF (125 mL) in a flame-dried round-bottom flask and cooled to 0 °C. Potassium *tert*-butoxide (1.40 g 12.5 mmol, 1.25 equiv) was added in one portion. The solution immediately turned bright orange and was stirred at 0 °C for an additional 30 min. A solution of methyl 9-formylnonoate (2.00 g, 10 mmol, 1.00 equiv) in dry THF (10 mL) was added dropwise over 5 min at 0 °C, and the resulting canary yellow solution was stirred at 0 °C for an additional 45 minutes, at which point TLC confirmed complete consumption of starting material. The reaction mixture was diluted with diethyl ether (25 mL) and quenched by adding saturated NH_4Cl (50 mL). The organic layer was separated, and the aqueous layer was washed with diethyl ether (3 x 25 mL). The combined organic extracts were washed with brine, dried over Na_2SO_4, concentrated *in vacuo*, eluted through a 20 g silica plug with 5% EtOAc/hexanes, and concentrated *in vacuo* to afford **S7** as a colorless oil (1.95 g, 92%). The product was used without further purification. R_F = 0.50-0.56 in 6% EtOAc/hexanes.

N-Methoxy-*N*-methyldodec-10-enamide (S8)

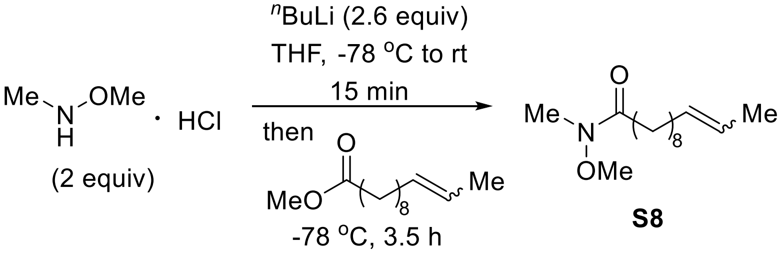

Under nitrogen, *N,O*-dimethylhydroxylamine hydrochloride (977 mg, 16.0 mmol, 2.00 equiv) was suspended in dry THF (9.50 mL) in a flame-dried round-bottom flask and cooled to -78 °C. *n*-Butyllithium (2.5 M in hexanes, 6.40 mL, 32.0 mmol, 2.60 equiv) was added dropwise with stirring to the suspension. The dry ice bath was removed, and the resulting pale-yellow solution was allowed to warm to room temperature for 15 minutes. The solution was cooled again to -78 °C, and a solution of methyl (E/Z)-dodec-10-enoate (**S7**, 1.70 g, 8.00 mmol, 1.00 equiv) in THF (5.00 mL) was added. The solution was stirred for 3.5 hours, diluted with diethyl ether (10 mL), and quenched with saturated NH_4Cl (10 mL). The organic layer was collected, and the aqueous phase was extracted into diethyl ether (3 x 25 mL). The combined organic extracts were washed with brine, dried over Na_2SO_4, concentrated *in vacuo*, and purified by flash column chromatography on silica gel (50 g silica 15-20% ethyl acetate/hexanes) to yield pure **S8** as a colorless oil (1.26 g, 65%). The product was used without further purification. R_F = 0.27 (20% EtOAc/hexanes).

Hexadec-14-en-5-one (S9)

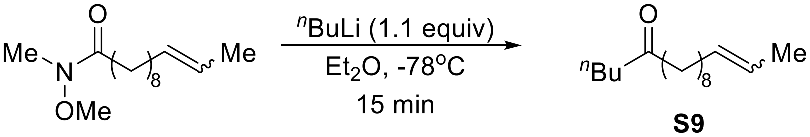

S9

Weinreb amide **S8** (483 mg, 2.00 mmol, 1.00 equiv) was dissolved in dry diethyl ether (15 mL) and cooled to -78 °C, and *n*-butyllithium (2.5 M in hexanes, 880 µL, 2.20 mmol, 1.10 equiv) was added dropwise with stirring. The starting material was consumed after 20 min, as indicated by TLC. The reaction was quenched with saturated NH_4Cl (10 mL). The organic layer was separated, and the aqueous layer extracted into diethyl ether (3 x 10 mL). The combined organic extracts were washed with brine, dried over Na_2SO_4, concentrated *in vacuo*, and purified by flash column chromatography (10 g silica, 10% ethyl acetate/hexanes) to afford pure **S9** as a colorless oil (468 mg, 98% yield). The product was used without further purification. R_F = 0.60 (10% EtOAc/hexanes).

2-Butyl-2-(undec-9-en-1-yl)-1,3-dioxolane (1k)

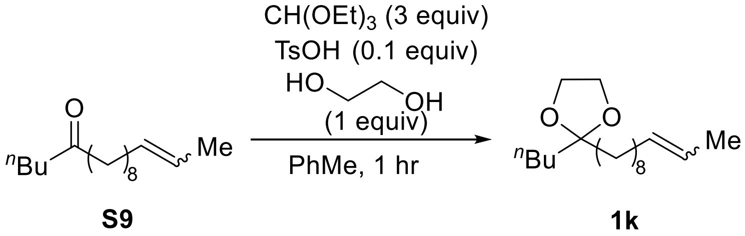

In a round-bottom flask, ketone **S9** (193.5, 0.812 mmol, 1.00 equiv) was dissolved in toluene (5 mL). TsOH·H_2O (20 mg, 0.1 equiv), ethylene glycol (45.4 µL, 0.812 mmol, 1.00 equiv), and triethyl orthoformate (582 µL, 2.44 mmol, 3.00 equiv) were added. The solution was stirred at room temperature for 1 hour, becoming orange-brown in color, and the solvent was removed at 40 °C with rotary evaporation (note: care was taken to avoid exposure of the product to water, which hydrolyzes the ketal). The reaction mixture was purified by flash column chromatography (dry loaded with 4 g basic alumina onto a 30 g silica column, eluted with 10% EtOAc/hexanes) to afford **4** as a pale-yellow oil (225 mg, 98.3% yield). The product was used without further purification. R_F = 0.60 (10% EtOAc/hexanes; the same as ketone **S9**).

5.4.6 General procedures for olefin isomerizations

Step 1: Hydroboration

In an argon-filled glovebox, olefin (dried over anhydrous $MgSO_4$ and sparged with argon for 30 minutes), solvent (640 μL), and HBpin (1.05 equiv) were added to an oven-dried 20 mL vial equipped with a stir bar. The hydroboration catalyst was then added as a solid with stirring (Note: deviations from this order of addition lead to lower yields. The hydroboration catalyst must be added after olefin and HBpin are already present in the reaction mixture). The reaction mixture was stirred at the specified temperature for the specified reaction time.

Step 2: Dehydroboration

In an argon-filled glovebox, potassium methoxide (0.640 mmol, prepared by above procedure) and THF (640 μL) were added to the reaction mixture, the reaction mixture was stirred for 5 min at room temperature, a solution of iodine (0.640 mmol) in THF (640 μL) was added, the reaction mixture was stirred for an additional 5 min at room temperature, a solution of potassium *tert*-butoxide (0.320 mmol) in THF (320 μL) was added, and the reaction was stirred for a third 5 minute period at room temperature. This procedure of sequentially adding KOMe and THF, a solution of I_2 in THF, and a solution of KO*t*Bu in THF was repeated 3-4 times, as specified for each reaction. After the addition of each reagent, the vial was shaken vigorously. Potassium *tert*-butoxide (5-6 equiv, as specified for each reaction) and THF (1280 μL) were added for the elimination, and the reaction was stirred at room temperature for 20 h at room temperature. The reaction mixture was diluted with $CDCl_3$ (15 mL, dropwise addition with rapid stirring), and trichloroethylene (57.5 μL, 0.640 mmol, 1.00 equiv) was added. The reaction mixture was vigorously shaken, an aliquot was filtered, and a crude ^1H NMR spectrum was recorded.

5.4.7 Isomerization of olefins

1-Octene (**1c** → **4c**)

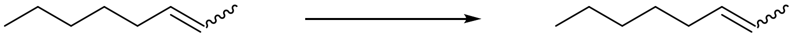

Prepared from 2-octene (mixture of *E* and *Z* isomers, 99.8 µL, 0.640 mmol) according to the general procedure with catalyst **C1** (6.5 mg, 2 mol%) as the hydroboration catalyst. The hydroboration was conducted at room temperature for 24 h. The iodination was conducted with 3 additions of KOMe, I_2, and KO(*t*-Bu) before the final elimination with 5 equiv KO(*t*-Bu).

^{1}H NMR Yield: 82%, no isomers detected

1-Octene (**1d** → **4c**)

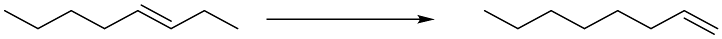

Prepared from (*E*)-3-octene (100.3 µL, 0.640 mmol) according to the general procedure with catalyst **C1** (6.5 mg, 2 mol%) as the hydroboration catalyst. The hydroboration was conducted at room temperature for 24 h. The iodination was conducted with 3 additions of KOMe, I_2, and KO(*t*-Bu) before the final elimination with 5 equiv KO(*t*-Bu).

^{1}H NMR Yield: 77%, no isomers detected

1-Octene (**1e** → **4c**)

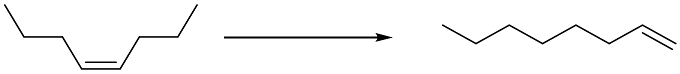

Prepared from *cis*-4-octene (99.9 µL, 0.640 mmol) according to the general procedure with catalyst **C1** (6.5 mg, 2 mol%) as the hydroboration catalyst. The hydroboration was conducted at room temperature for 24 h. The iodination was conducted with 3 additions of KOMe, I_2, and KO(*t*-Bu) before the final elimination with 5 equiv KO(*t*-Bu).

^{1}H NMR Yield: 51%, no isomers detected

1-Tetradecene (**1f** → **4f**)

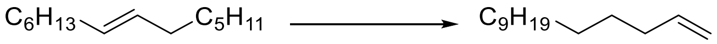

Prepared from *trans*-7-tetradecene (164.5 µL, 0.640 mmol) according to the general procedure with catalyst **C1** (6.5 mg, 2 mol%) as the hydroboration catalyst. The hydroboration was conducted at room temperature for 24 h. The iodination was conducted with 3 additions of KOMe, I_2, and KO(*t*-Bu) before the final elimination with 5 equiv KO(*t*-Bu).

^{1}H NMR Yield: 81%, no isomers detected

Isolation of Olefin **4f**: The NMR sample and crude reaction mixture were combined and carefully diluted with water (100 mL), and the resulting mixture was extracted with pentane (3 x 100 mL). The pentane layer was washed with 2 M sodium thiosulfate (3 x 100 mL) and brine (1 x 150 mL), dried over sodium sulfate, and carefully concentrated *in vacuo* to afford a pale-yellow liquid. Column chromatography on silica gel (60 g) with isocratic pentane followed by careful concentration *in vacuo* afforded pure 1-tetradecene as a clear oil (85.5 mg, 68% isolated yield). ^{1}H NMR (400 MHz, Chloroform-*d*) δ 5.86 (ddt, *J* = 16.9, 10.2, 6.7 Hz, 1H), 5.04 (dq, *J* = 17.1, 1.8 Hz, 1H), 4.97 (dq, *J* = 10.2, 1.4 Hz, 1H), 2.08 (tdd, *J* = 8.0, 6.1, 1.5 Hz, 2H), 1.30 (s, 17H), 0.92 (t, *J* = 6.8 Hz, 3H).

((Hex-5-en-1-yloxy)methyl)benzene (1g → 4g)

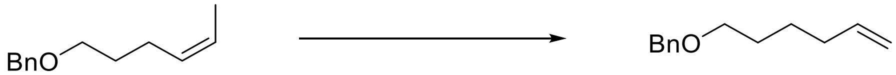

Prepared from (*Z*)-((hex-4-en-1-yloxy)methyl)benzene (85.8 μL, 0.640 mmol) according to the general procedure with catalyst **C1** (10.4 mg, 3 mol%) as the hydroboration catalyst. The hydroboration was conducted at room temperature for 72 h. The iodination was conducted with 3 additions of KOMe, I_2, and KO(*t*-Bu) before the final elimination with 5 equiv KO(*t*-Bu).

^{1}H NMR Yield: 64%, 77:23 terminal:internal

Isolation of Olefin **4g**: The NMR sample and crude reaction mixture were combined and carefully diluted with water (100 mL), and the resulting mixture was extracted with pentane (3 x 100 mL). The pentane layer was washed with 2 M sodium thiosulfate (3 x 100 mL) and brine (1 x 150 mL), dried over sodium sulfate, and carefully concentrated *in vacuo* to afford a pale-yellow liquid. Column chromatography on silica gel (60 g) with a gradient of 0 → 5% ether/pentane followed by careful concentration *in vacuo* afforded olefin XX as a clear oil (95.4 mg, 77:23 mixture of terminal:internal olefins, 60% yield of terminal olefin). ^{1}H NMR (400 MHz, Chloroform-*d*) δ 7.41 – 7.37 (m, 1H), 5.85 (ddt, *J* = 16.9, 10.2, 6.7 Hz, 0H), 5.05 (dq, *J* = 17.1, 1.7 Hz, 0H), 4.99 (ddt, *J* = 10.2, 2.2, 1.2 Hz, 0H), 4.55 (s, 0H), 3.60 – 3.48 (m, 1H), 2.17 – 2.06 (m, 0H), 1.80 – 1.59 (m, 1H).

Vinylcyclohexane (1h → 4h)

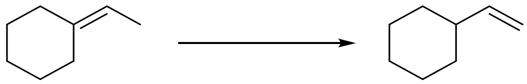

Prepared from ethylidene cyclohexane (85.8 μL, 0.640 mmol) according to the general procedure with catalyst **C2** (10.4 mg, 3 mol%) as the hydroboration catalyst. The hydroboration was conducted at room temperature for 24 h. The iodination was conducted with 4 additions of KOMe, I_2, and KO(*t*-Bu) before the final elimination with 6 equiv KO(*t*-Bu).

^{1}H NMR Yield: 56%, no isomers detected

2-Butyl-2-(undec-10-en-1-yl)-1,3-dioxolane (**1k** → **4k**)

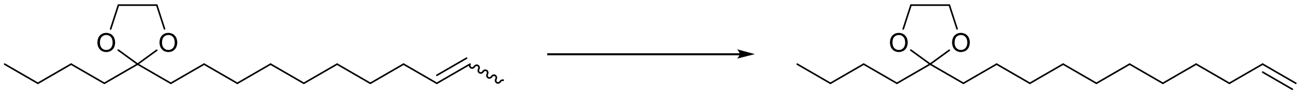

Prepared from 2-butyl-2-(undec-9-en-1-yl)-1,3-dioxolane (90.4 mg, 0.320 mmol) according to the general procedure with catalyst **C2** (12.1 mg, 7.0 mol%) as the hydroboration catalyst. The hydroboration was conducted at 50 °C for 96 h. The iodination was conducted with 3 additions of KOMe, I_2, and KO(*t*-Bu) before the final elimination with 5 equiv KO(*t*-Bu).

^{1}H NMR Yield: 68%, 86:14 terminal:internal

Isolation of Olefin **4k**: The NMR sample and crude reaction mixture were combined and carefully diluted with water (100 mL), and the resulting mixture was extracted with pentane (3 x 100 mL). The pentane layer was washed with 2 M sodium thiosulfate (3 x 100 mL) and brine (1 x 150 mL), dried over sodium sulfate, and carefully concentrated *in vacuo* to afford a pale-yellow liquid. Column chromatography on silica gel (60 g) with a gradient of 0 → 15% ether/pentane followed by careful concentration *in vacuo* afforded olefin **4k** as a yellow oil (62.3 mg, 86:14 mixture of terminal:internal olefins, 59% yield of terminal olefin). ^{1}H NMR (500 MHz, Chloroform-*d*) δ 4.99 (d, *J* = 17.1 Hz, 1H), 4.92 (d, *J* = 10.3 Hz, 1H), 3.92 (s, 5H), 2.03 (m, *J* = 7.2 Hz, 2H), 1.59 (dt, *J* = 11.9, 4.1 Hz, 5H), 1.40 – 1.24 (m, 26H), 0.89 (m, *J* = 5.6, 4.2 Hz, 5H).

5.4.8 NMR spectra of olefin isomerizations

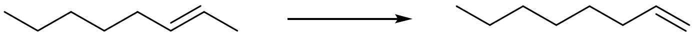

1c **4c**

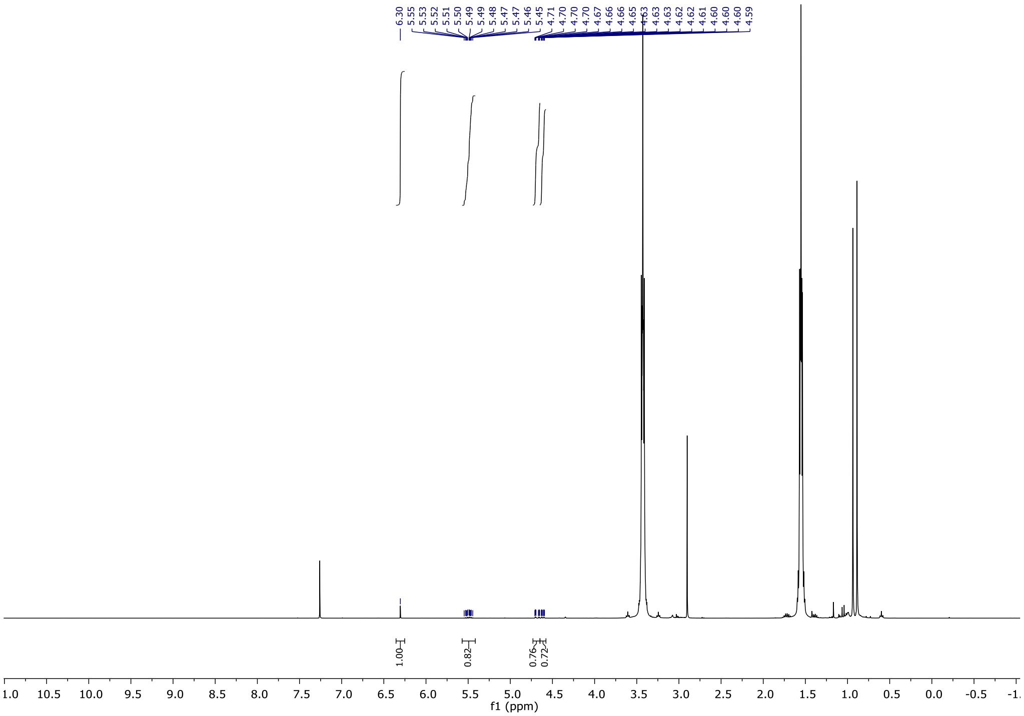

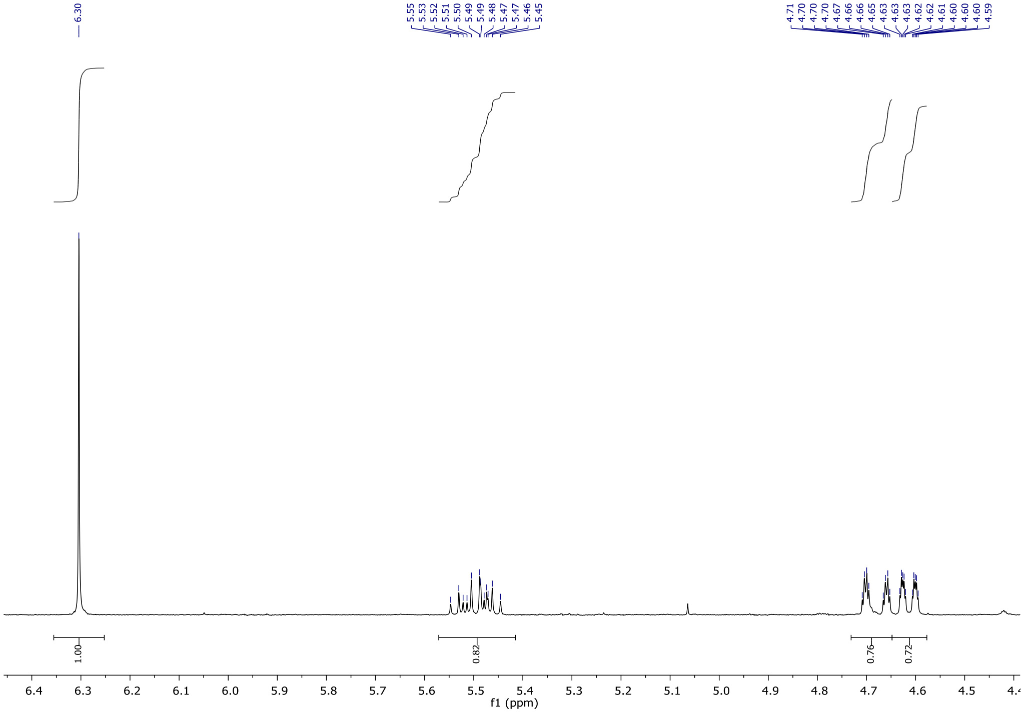

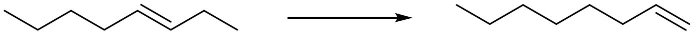

1d **4c**

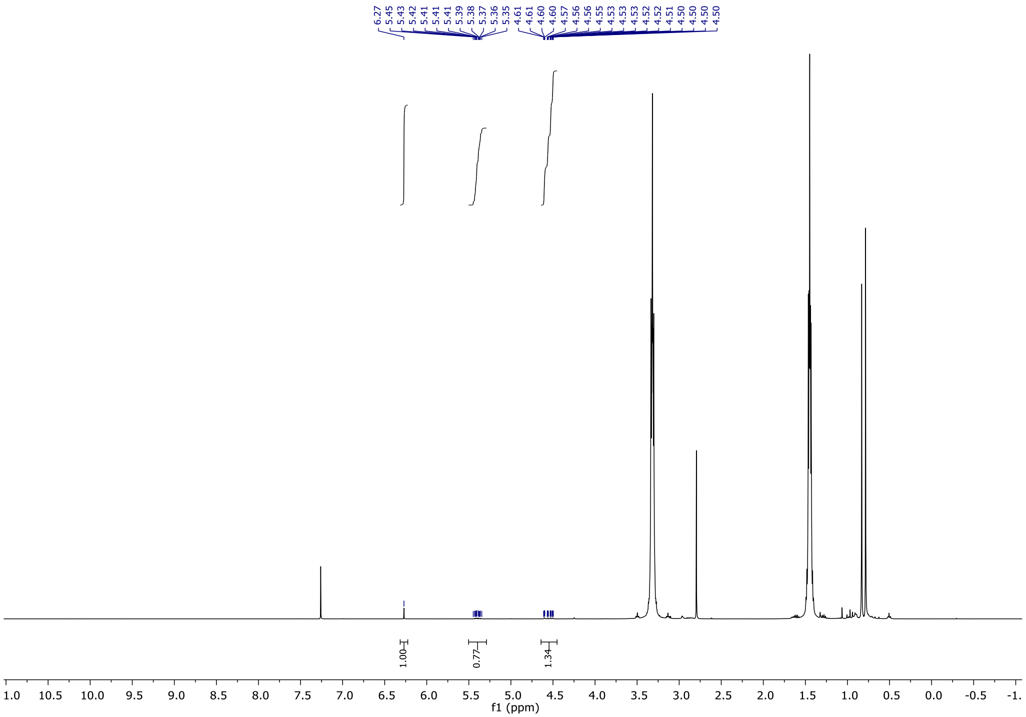
6.27
5.45
5.43
5.42
5.41
5.41
5.41
5.39
5.38
5.37
5.36
5.35
4.61
4.61
4.60
4.57
4.56
4.56
4.55
4.53
4.53
4.53
4.52
4.52
4.51
4.50
4.50
4.50
4.50
1.00
0.77
1.34
1.0 10.5 10.0 9.5 9.0 8.5 8.0 7.5 7.0 6.5 6.0 5.5 5.0 4.5 4.0 3.5 3.0 2.5 2.0 1.5 1.0 0.5 0.0 -0.5 -1.
f1 (ppm)

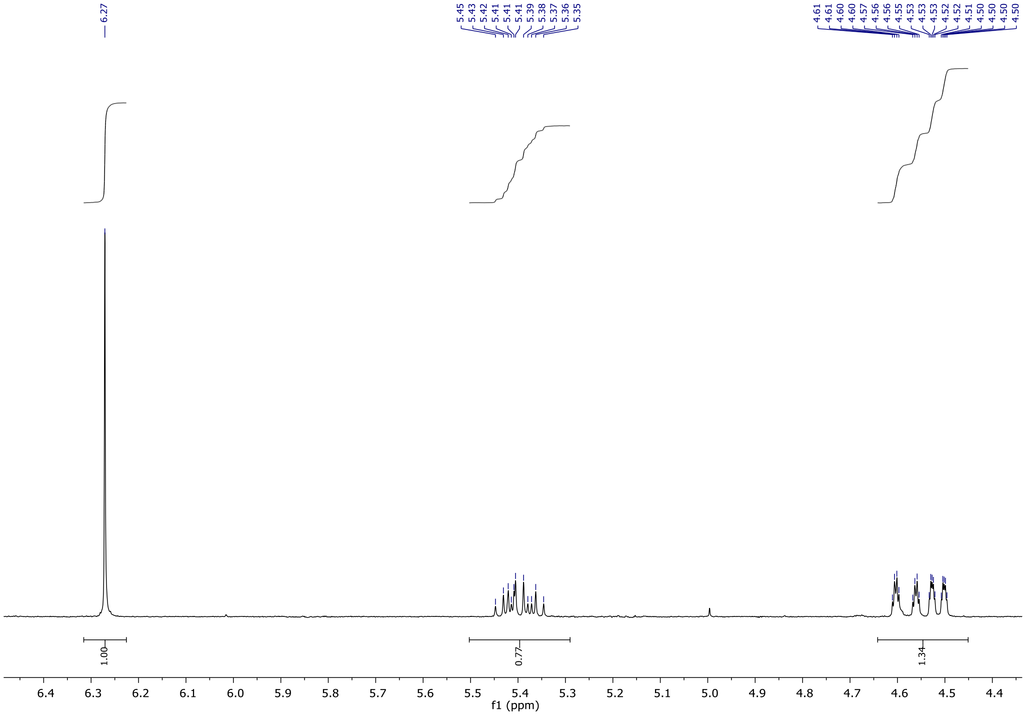
6.27
5.45
5.43
5.42
5.41
5.41
5.41
5.39
5.38
5.37
5.36
5.35
4.61
4.61
4.60
4.57
4.56
4.56
4.55
4.53
4.53
4.53
4.52
4.52
4.51
4.50
4.50
4.50
4.50
1.00
0.77
1.34
6.4 6.3 6.2 6.1 6.0 5.9 5.8 5.7 5.6 5.5 5.4 5.3 5.2 5.1 5.0 4.9 4.8 4.7 4.6 4.5 4.4
f1 (ppm)

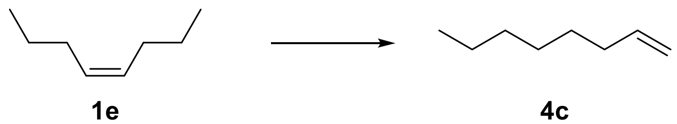

1e **4c**

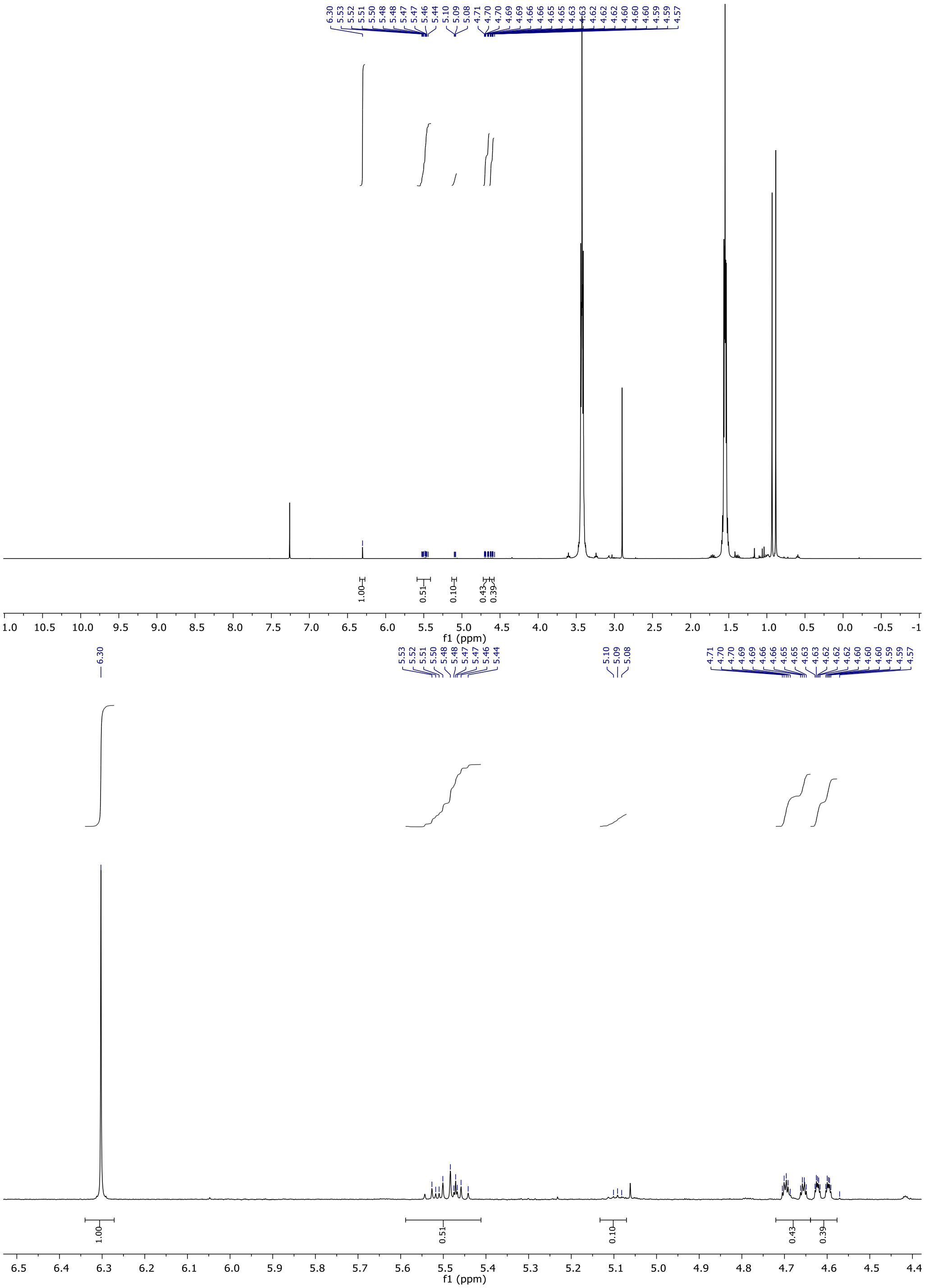
6.30
5.53
5.52
5.51
5.50
5.48
5.47
5.46
5.44
5.10
5.09
5.08
4.71
4.70
4.69
4.69
4.66
4.65
4.63
4.63
4.62
4.62
4.60
4.60
4.59
4.57
1.00
0.51
0.10
0.43
0.39
1.0
10.5
10.0
9.5
9.0
8.5
8.0
7.5
7.0
6.5
6.0
5.5
5.0
4.5
4.0
3.5
3.0
2.5
2.0
1.5
1.0
0.5
0.0
-0.5
-1
f1 (ppm)
6.5
6.4
6.3
6.2
6.1
6.0
5.9
5.8
5.7
5.6
5.5
5.4
5.3
5.2
5.1
5.0
4.9
4.8
4.7
4.6
4.5
4.4
f1 (ppm)

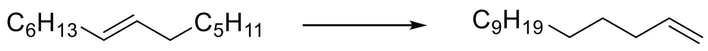
C6H13
C5H11
C9H19

1f

4f

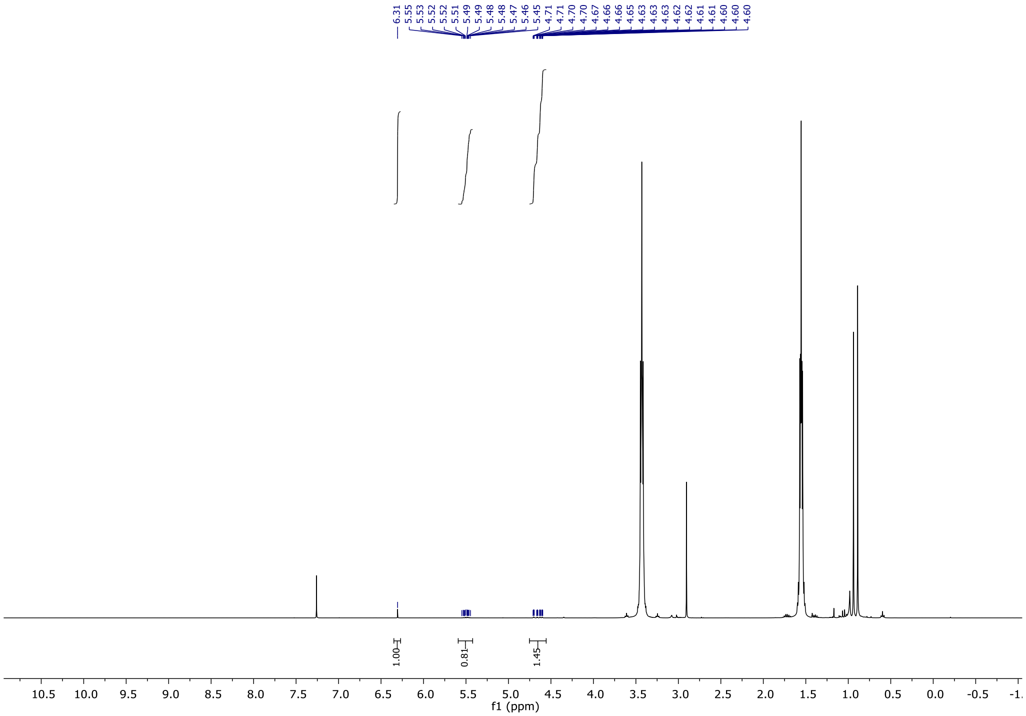
6.31
5.55
5.53
5.52
5.52
5.51
5.49
5.49
5.48
5.48
5.47
5.46
5.45
4.71
4.71
4.70
4.70
4.67
4.66
4.66
4.65
4.63
4.63
4.63
4.62
4.62
4.61
4.61
4.60
4.60
4.60
1.00
0.81
1.45
10.5
10.0
9.5
9.0
8.5
8.0
7.5
7.0
6.5
6.0
5.5
5.0
4.5
4.0
3.5
3.0
2.5
2.0
1.5
1.0
0.5
0.0
-0.5
f1 (ppm)

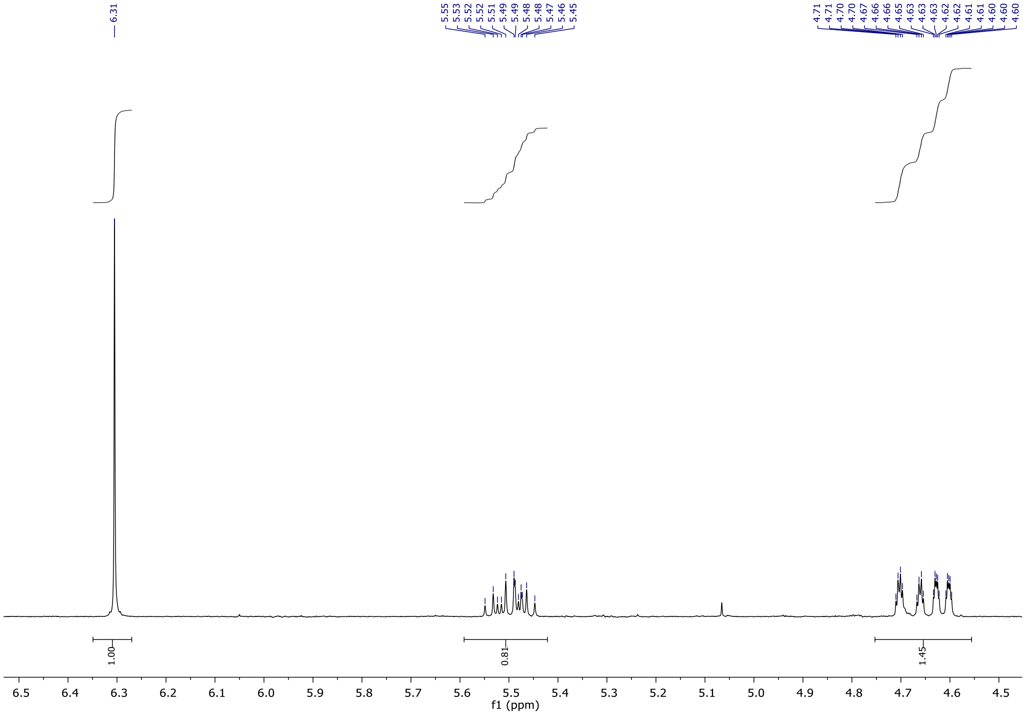
6.31
5.55
5.53
5.52
5.52
5.51
5.49
5.49
5.48
5.48
5.47
5.46
5.45
4.71
4.71
4.70
4.70
4.67
4.66
4.66
4.65
4.63
4.63
4.63
4.62
4.62
4.61
4.61
4.60
4.60
4.60
1.00
0.81
1.45
6.5
6.4
6.3
6.2
6.1
6.0
5.9
5.8
5.7
5.6
5.5
5.4
5.3
5.2
5.1
5.0
4.9
4.8
4.7
4.6
4.5
f1 (ppm)

Isolation of Olefin **4f**:

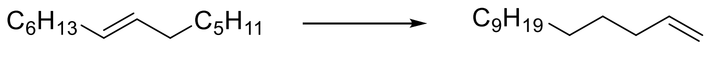

C_6H_{13}
C_5H_{11}
C_9H_{19}

1f **4f**

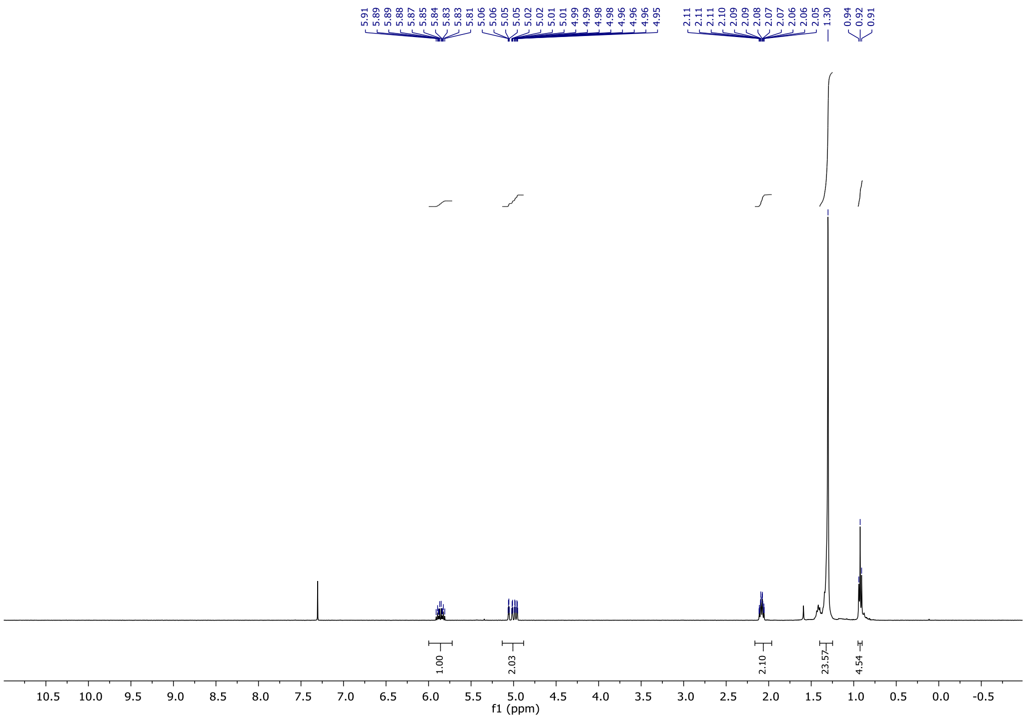

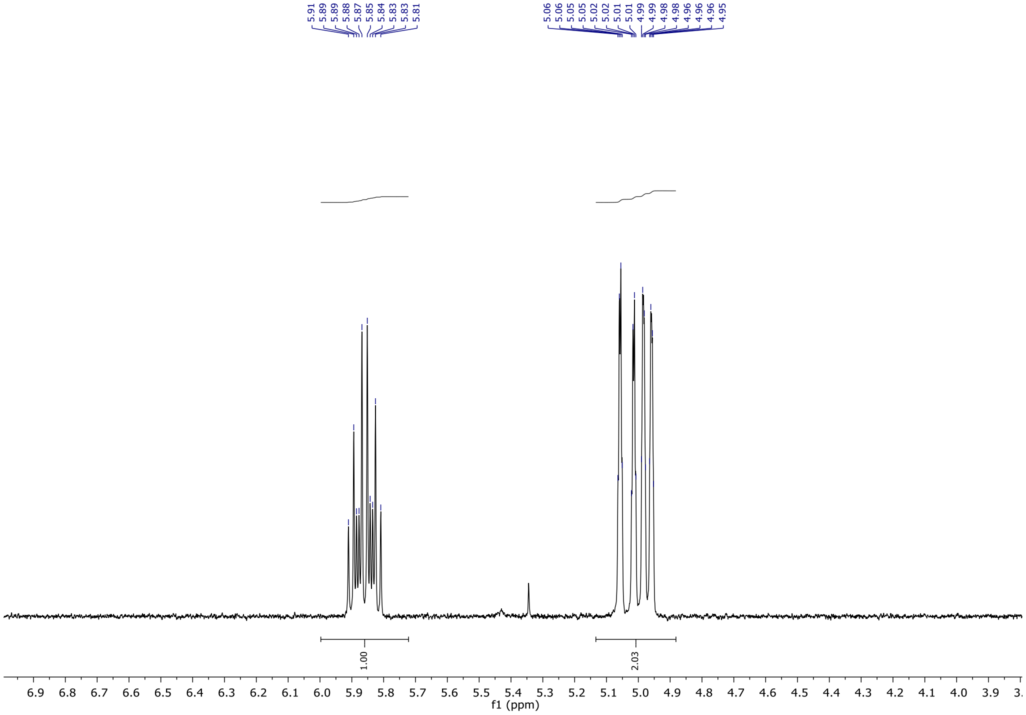

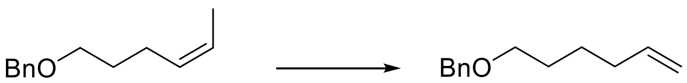
BnO
BnO

1g **4g**

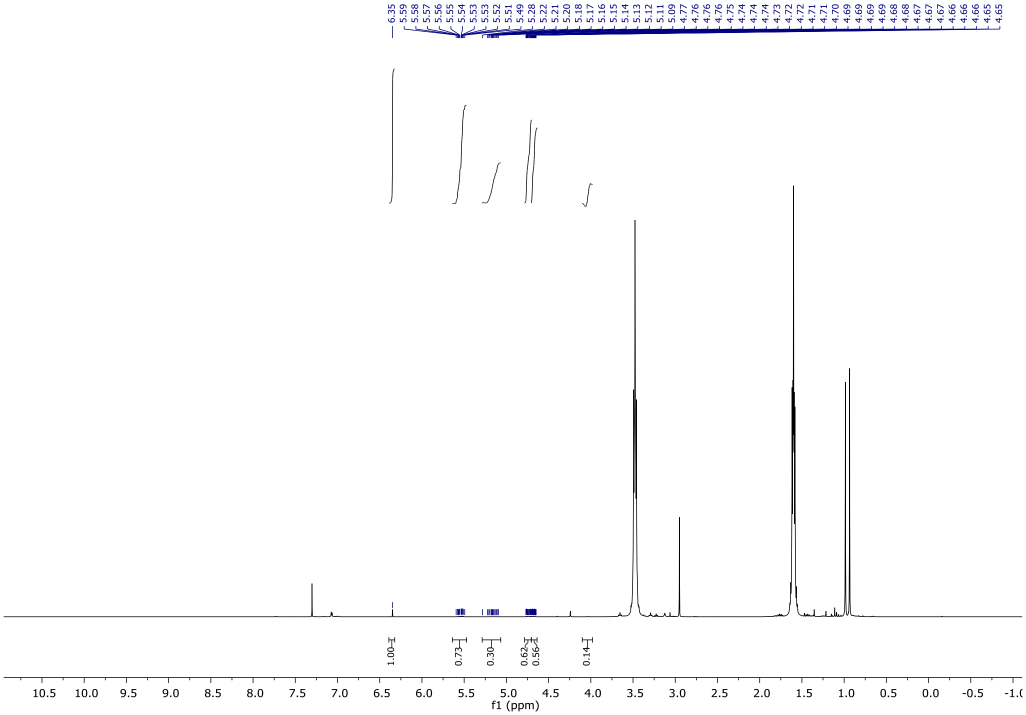
6.35
5.59 5.58 5.57 5.56 5.55 5.54 5.53 5.52 5.51 5.49 5.28 5.22 5.21 5.20 5.18 5.17 5.16 5.15 5.14 5.13 5.12 5.11 5.09 4.77 4.76 4.76 4.76 4.75 4.74 4.74 4.73 4.72 4.72 4.71 4.70 4.69 4.69 4.69 4.69 4.68 4.67 4.67 4.67 4.66 4.66 4.65 4.65
1.00
0.73
0.30
0.62
0.56
0.14
10.5 10.0 9.5 9.0 8.5 8.0 7.5 7.0 6.5 6.0 5.5 5.0 4.5 4.0 3.5 3.0 2.5 2.0 1.5 1.0 0.5 0.0 -0.5 -1.0
f1 (ppm)

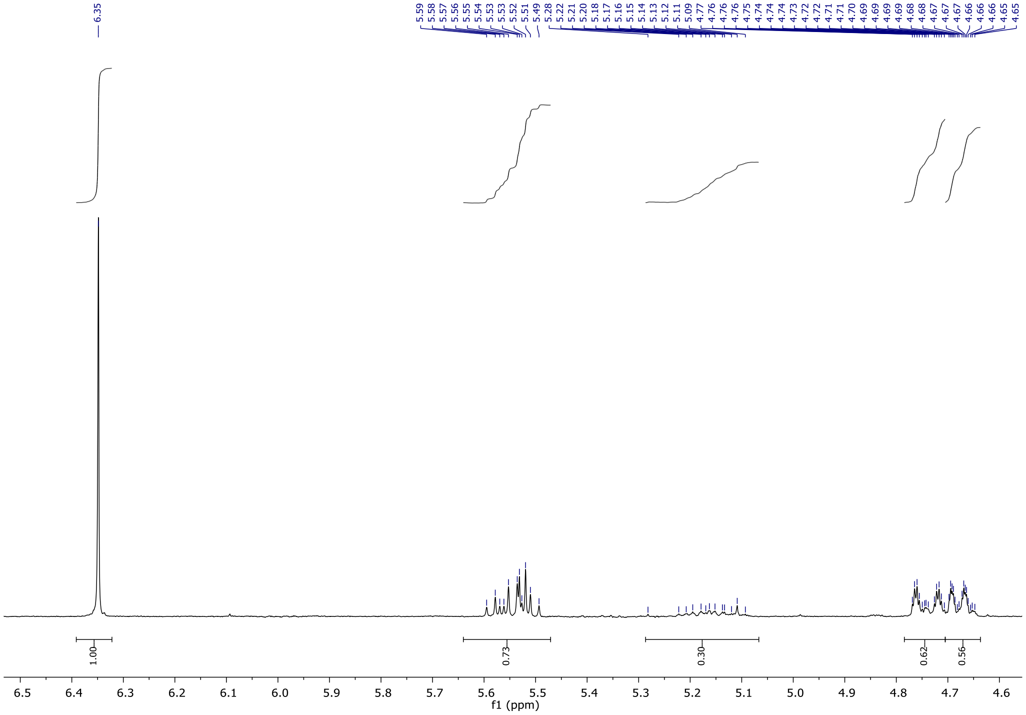
6.35
5.59 5.58 5.57 5.56 5.55 5.54 5.53 5.52 5.51 5.49 5.28 5.22 5.21 5.20 5.18 5.17 5.16 5.15 5.14 5.13 5.12 5.11 5.09 4.77 4.76 4.76 4.76 4.75 4.74 4.74 4.73 4.72 4.72 4.71 4.70 4.69 4.69 4.69 4.69 4.68 4.67 4.67 4.67 4.66 4.66 4.65 4.65
1.00
0.73
0.30
0.62
0.56
6.5 6.4 6.3 6.2 6.1 6.0 5.9 5.8 5.7 5.6 5.5 5.4 5.3 5.2 5.1 5.0 4.9 4.8 4.7 4.6
f1 (ppm)

Isolation of olefin **4g**

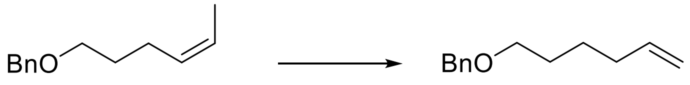

1g **4g**

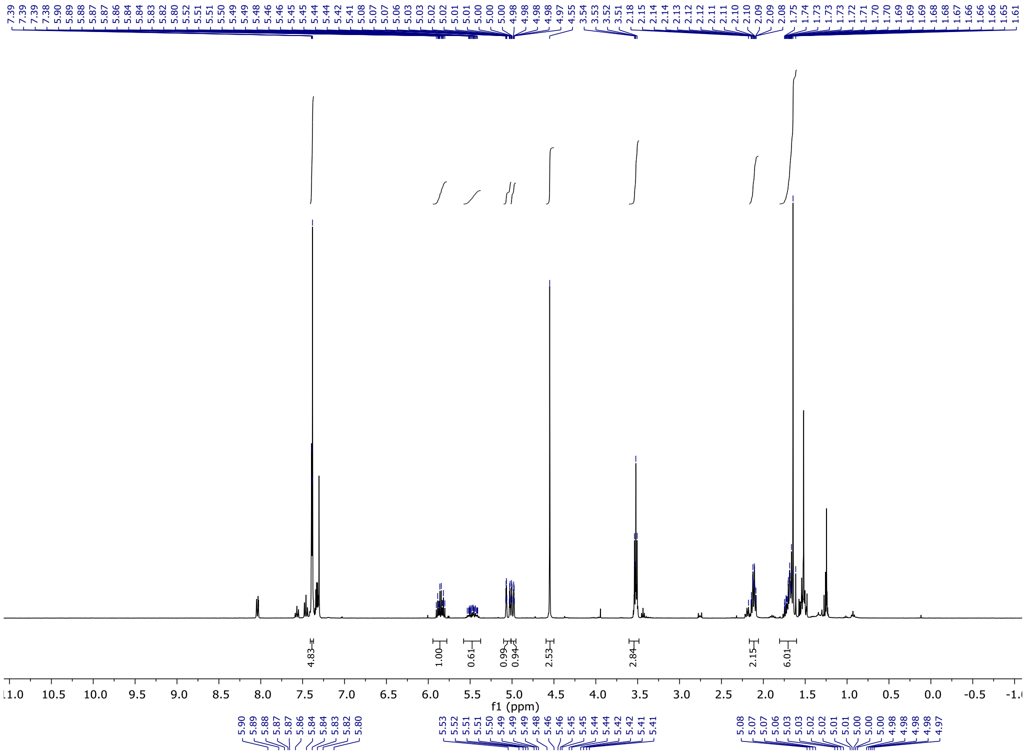

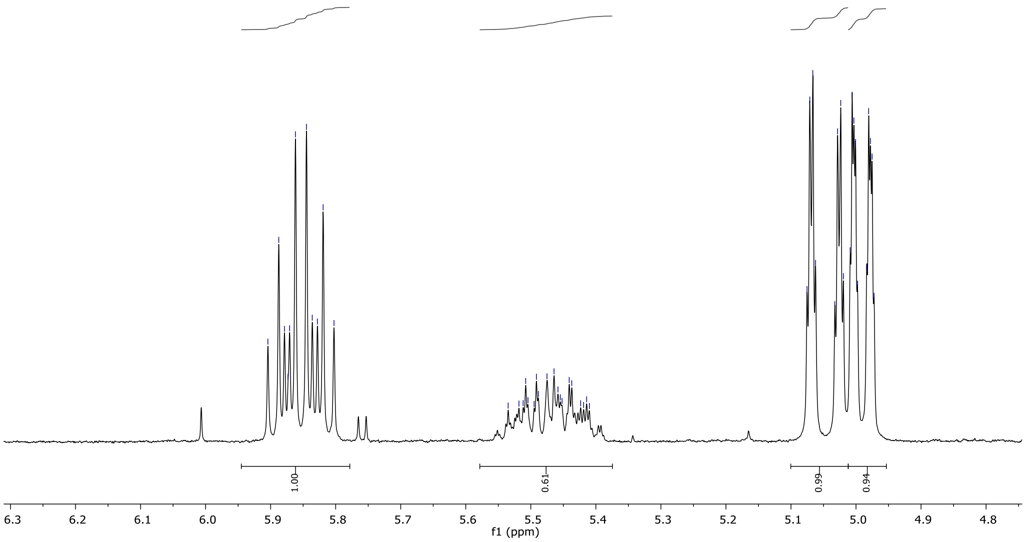

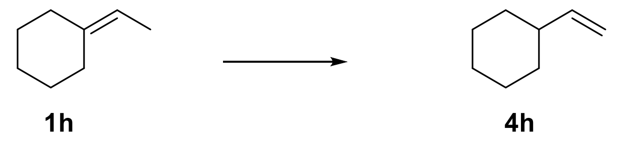
1h
4h

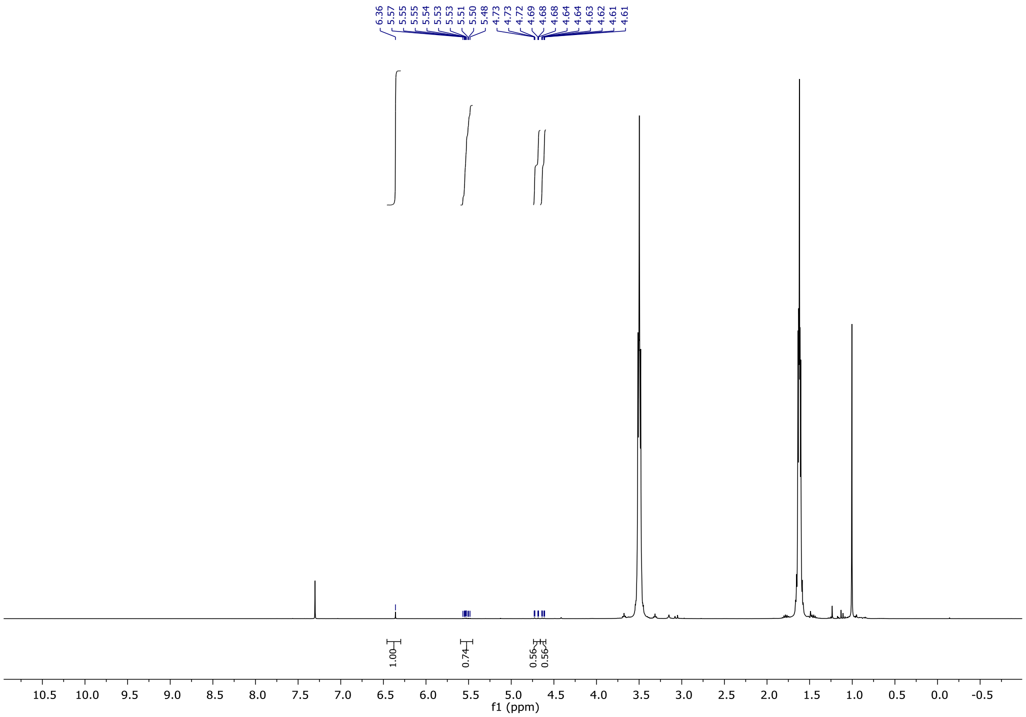
6.36
5.57
5.55
5.55
5.54
5.53
5.53
5.51
5.50
5.48
4.73
4.73
4.72
4.69
4.68
4.68
4.64
4.64
4.63
4.62
4.61
4.61
1.00
0.74
0.56
0.56
10.5
10.0
9.5
9.0
8.5
8.0
7.5
7.0
6.5
6.0
5.5
5.0
4.5
4.0
3.5
3.0
2.5
2.0
1.5
1.0
0.5
0.0
-0.5
f1 (ppm)

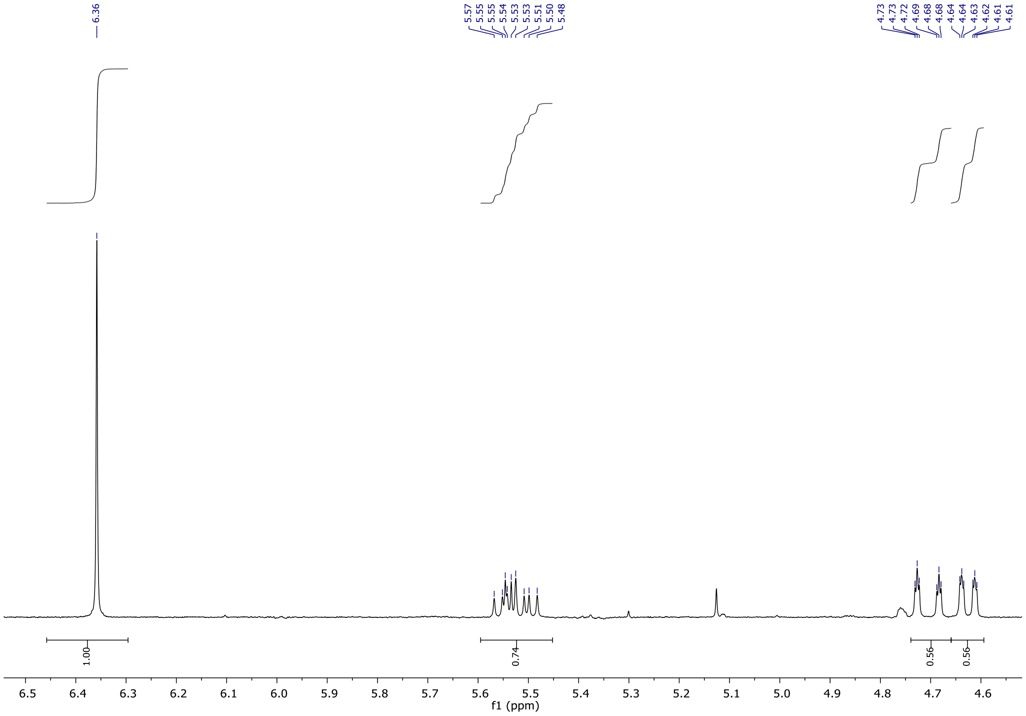
6.36
5.57
5.55
5.54
5.53
5.53
5.51
5.50
5.48
4.73
4.73
4.72
4.69
4.68
4.68
4.64
4.64
4.63
4.62
4.61
4.61
1.00
0.74
0.56
0.56
6.5
6.4
6.3
6.2
6.1
6.0
5.9
5.8
5.7
5.6
5.5
5.4
5.3
5.2
5.1
5.0
4.9
4.8
4.7
4.6
f1 (ppm)

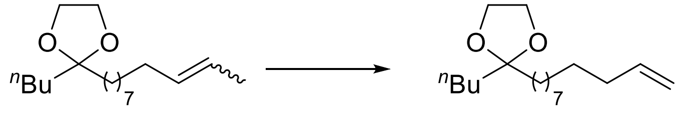

O
O
nBu
7
O
O
nBu
7

1k **4k**

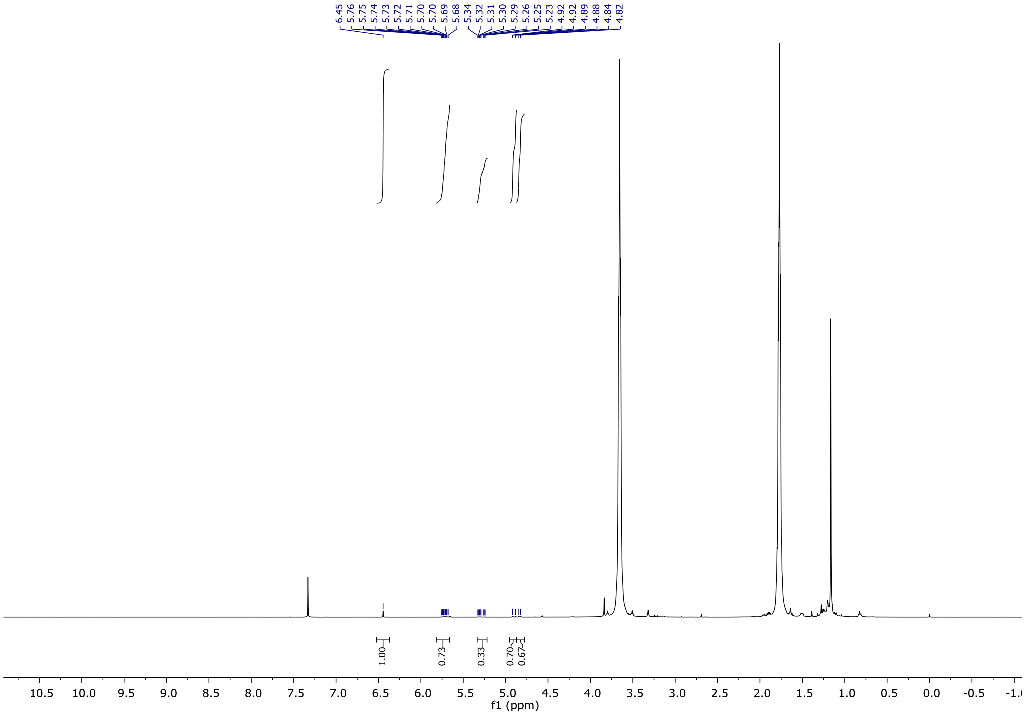

6.45
5.76
5.75
5.74
5.73
5.72
5.71
5.70
5.70
5.69
5.68
5.34
5.32
5.31
5.30
5.29
5.26
5.25
5.23
4.92
4.92
4.89
4.88
4.84
4.82
1.00
0.73
0.33
0.70
0.67
10.5
10.0
9.5
9.0
8.5
8.0
7.5
7.0
6.5
6.0
5.5
5.0
4.5
4.0
3.5
3.0
2.5
2.0
1.5
1.0
0.5
0.0
-0.5
-1.0
f1 (ppm)

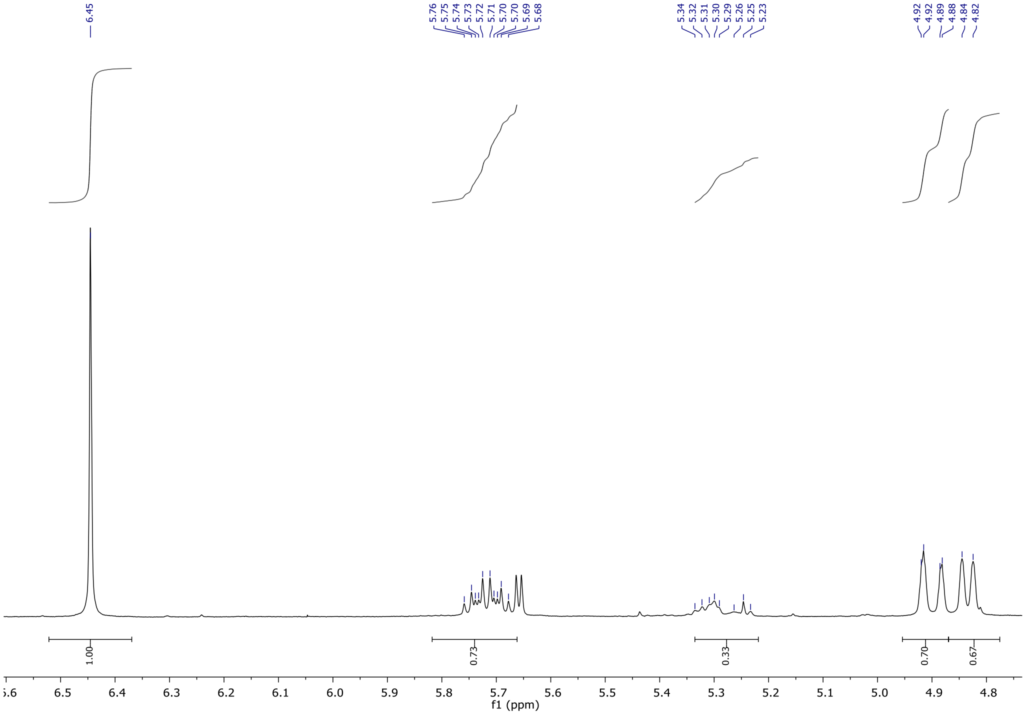

6.45
5.76
5.75
5.74
5.73
5.72
5.71
5.70
5.70
5.69
5.68
5.34
5.32
5.31
5.30
5.29
5.26
5.25
5.23
4.92
4.92
4.89
4.88
4.84
4.82
1.00
0.73
0.33
0.70
0.67
6.6
6.5
6.4
6.3
6.2
6.1
6.0
5.9
5.8
5.7
5.6
5.5
5.4
5.3
5.2
5.1
5.0
4.9
4.8
f1 (ppm)

Isolation of olefin **4k**:

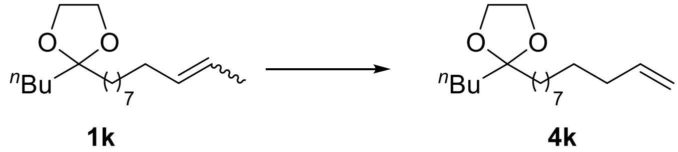

O
O
^{n}Bu
7
1k
O
O
^{n}Bu
7
4k

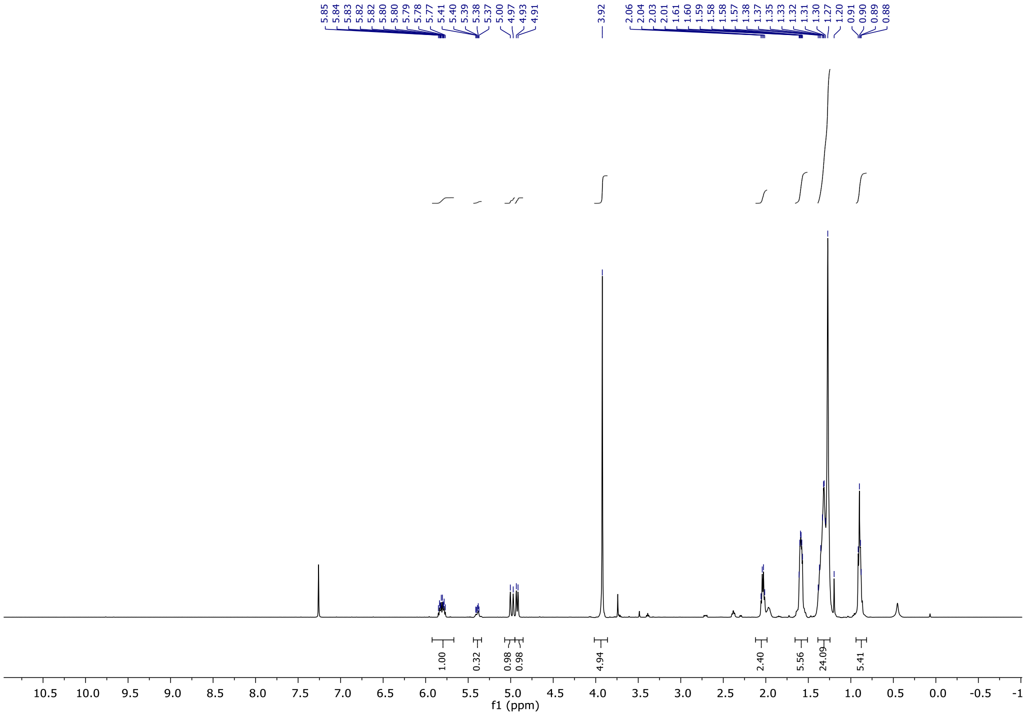

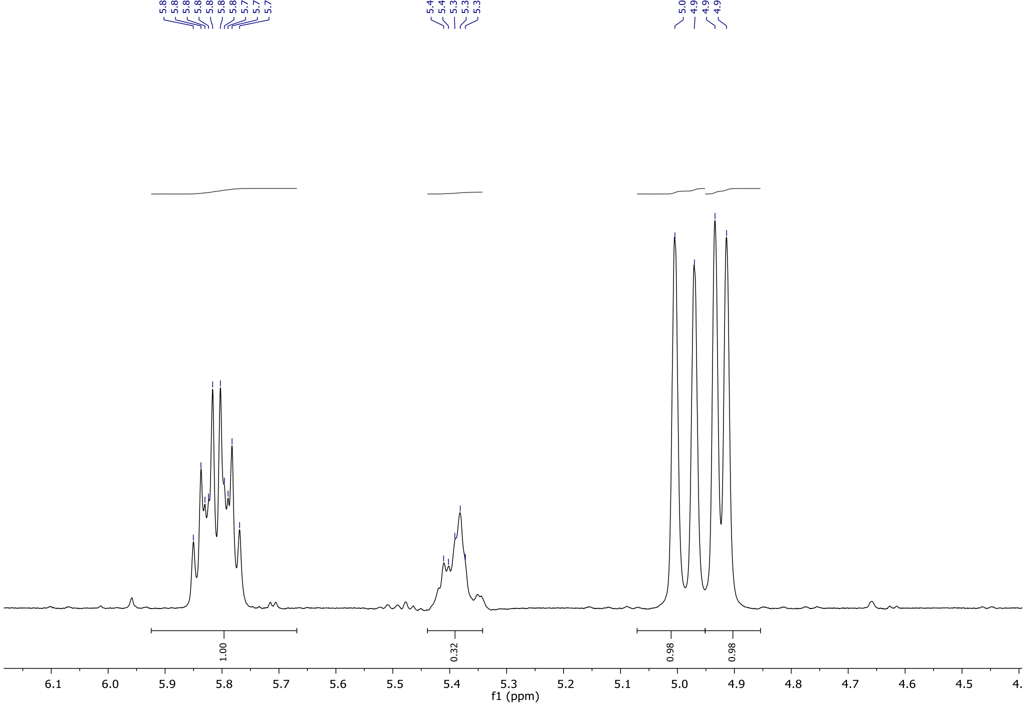

5.5 References

This work was conducted with Brandon Bloomer, Nico R. Ciccia, Dr. Trevor W. Butcher, and Professor John F. Hartwig.

1. (a) Biswas, S.; Huang, Z.; Choliy, Y.; Wang, D. Y.; Brookhart, M.; Krogh-Jespersen, K.; Goldman, A. S. Olefin Isomerization by Iridium Pincer Catalysts. Experimental Evidence for an η^3-Allyl Pathway and an Unconventional Mechanism Predicted by DFT Calculations. *J. Am. Chem. Soc.* **2012**, *134*, 13276. (b) Larionov, E.; Li, H.; Mazet, C. Well-Defined Transition Metal Hydrides in Catalytic Isomerization. *Chem. Commun.* **2014**, *50*, 9816. (c) Crossley, S. W. M.; Barabé, F.; Shenvi, R. A. Simple, Chemoselective, Catalytic Olefin Isomerization. *J. Am. Chem. Soc.* **2014**, *136*, 16788. (d) Molloy, J. J.; Morack, T.; Gilmour, R. Positional and Geometrical Isomerisation of Alkenes: The Pinnacle of Atom Economy. *Angew. Chem. Int. Ed.* **2019**, *58*, 13654. (e) Zhang, S.; Bedi, D.; Cheng, L.; Unruh, D. K.; Li, G.; Findlater, M. Cobalt(II)-Catalyzed Stereoselective Olefin Isomerization: Facile Access to Acyclic Trisubstituted Alkenes. *J. Am. Chem. Soc.* **2020**, *142*, 8910. (f) Scaringi, S.; Mazet, C. Kinetically Controlled Stereoselective Access to Branched 1,3-Dienes by Ru-Catalyzed Remote Conjugative Isomerization. *ACS Catal.* **2021**, 7970.

2. (a) Harwood, L. M.; Julia, M. A Convenient Synthesis of (+)-β-Pinene from (+)-α-Pinene. *Synthesis* **1980**, *1980*, 456. (b) Min, Y.-F.; Zhang, B.-W.; Cao, Y. A New Synthesis of (-)-β-Pinene from (-)-α-Pinene. *Synthesis* **1982**, *1982*, 875. (c) Andrianome, M.; Häberle, K.; Delmond, B. Allyl-and benzylstannanes, new reagents in terpenic synthesis. *Tetrahedron* **1989**, *45*, 1079. (d) Eng, S. L.; Ricard, R.; Wan, C. S. K.; Weedon, A. C. Photochemical Deconjugation of α,β-Unsaturated Ketones. *J. Chem. Soc., Chem. Commun.* **1983**, 236. (e) Guignard, R. F.; Petit, L.; Zard, S. Z. A Method for the Net Contra-thermodynamic Isomerization of Cyclic Trisubstituted Alkenes. *Org. Lett.* **2013**, *15*, 4178.

3. (a) Brown, H. Isomerization of internal olefins to terminal olefins. US3173967A, 1965. (b) Brown, H. C.; Bhatt, M. V.; Munekata, T.; Zweifel, G. Organoboranes. VII. The Displacement Reaction with Organoboranes Derived from the Hydroboration of Cyclic and Bicyclic Olefins. Conversion of Endocyclic to Exocyclic Double Bonds. *J. Am. Chem. Soc.* **1967**, *89*, 567. (c) Brown, H. C.; Bhatt, M. V. Organoboranes. IV. The Displacement Reaction with Organoboranes Derived from the Hydroboration of Branched-Chain Olefins. A Contrathermodynamic Isomerization of Olefins. *J. Am. Chem. Soc.* **1966**, *88*, 1440. (d) Robert H. Allen, R. W. L., Andrew D. Overstreet Continuous Process for Preparing Aluminm 1-Alkyls and Linear 1-Olefins from Internal Olefins. US005274153A 1993. (e) de Klerk, A.; Hadebe, S. W.; Govender, J. R.; Jaganyi, D.; Mzinyati, A. B.; Robinson, R. S.; Xaba, N. Linear α-Olefins from Linear Internal Olefins by a Boron-Based Continuous Double-Bond Isomerization Process. *Ind. Eng. Chem. Res.* **2007**, *46*, 400.

4. (a) Hanna, S.; Wills, T.; Butcher, T. W.; Hartwig, J. F. Palladium-Catalyzed Oxidative Dehydrosilylation for Contra-Thermodynamic Olefin Isomerization. *ACS Catal.* **2020**, *10*, 8736. (b) Hanna, S.; Butcher, T. W.; Hartwig, J. F. Contra-thermodynamic Olefin Isomerization by Chain-Walking Hydrofunctionalization and Formal Retro-hydrofunctionalization. *Org. Lett.* **2019**, *21*, 7129.

5. (a) Sommer, H.; Juliá-Hernández, F.; Martin, R.; Marek, I. Walking Metals for Remote Functionalization. *ACS Cent. Sci.* **2018**, *4*, 153. (b) Juliá-Hernández, F.; Moragas, T.; Cornella, J.; Martin, R. Remote Carboxylation of Halogenated Aliphatic Hydrocarbons with Carbon Dioxide. *Nature* **2017**, *545*, 84. (c) Saam, J.; Speier, J. The Addition of Silicon Hydrides to Olefinic Double Bonds. Part VI. Addition to Branched Olefins. *J. Am. Chem. Soc.* **1961**, *83*, 1351. (d) Bank, H. M.; Saam, J. C.; Speier, J. L. The Addition of Silicon Hydrides to Olefinic Double Bonds. IX. Addition of sym-Tetramethyldisiloxane to Hexene-1, -2, and -3. *J. Org. Chem.* **1964**, *29*, 792. (e) Benkeser, R. A.; Muench, W. C. The Addition Rates of Dichloro- and Trichlorosilane to 2-Pentene and 1-Octene. *J. Organomet. Chem.* **1980**, *184*, C3. (f) Yarosh, O. G.; Zhilitskaya, L. V.; Yarosh, N. K.; Albanov, A. I.; Voronkov, M. G. Hydrosilylation of Cyclohexene, 1-Methylcyclohexene, and Isopropylidenecyclohexane. *Russ. J. Gen. Chem.* **2004**, *74*, 1895. (g) Edwards, D. R.; Crudden, C. M.; Yam, K. One-Pot Carbon Monoxide-Free Hydroformylation of Internal Olefins to Terminal Aldehydes. *Adv. Synth. Catal.* **2005**, *347*, 50. (h) Lata, C. J.; Crudden, C. M. Dramatic Effect of Lewis Acids on the Rhodium-Catalyzed Hydroboration of Olefins. *J. Am. Chem. Soc.* **2010**, *132*, 131. (i) Obligacion, J. V.; Chirik, P. J. Bis(imino)pyridine Cobalt-Catalyzed Alkene Isomerization–Hydroboration: A Strategy for Remote Hydrofunctionalization with Terminal Selectivity. *J. Am. Chem. Soc.* **2013**, *135*, 19107. (j) Palmer, W. N.; Diao, T.; Pappas, I.; Chirik, P. J. High-Activity Cobalt Catalysts for Alkene Hydroboration with Electronically Responsive Terpyridine and α-Diimine Ligands. *ACS Catal.* **2015**, *5*, 622. (k) Ogawa, T.; Ruddy, A. J.; Sydora, O. L.; Stradiotto, M.; Turculet, L. Cobalt- and Iron-Catalyzed Isomerization–Hydroboration of Branched Alkenes: Terminal Hydroboration with Pinacolborane and 1,3,2-Diazaborolanes. *Organometallics* **2017**, *36*, 417. (l) Arthur, P.; England, D. C.; Pratt, B. C.; Whitman, G. M. Addition of Hydrogen Cyanide to Unsaturated Compounds. *J. Am. Chem. Soc.* **1954**, *76*, 5364. (m)

van der Veen, L. A.; Kamer, P. C. J.; van Leeuwen, P. W. N. M. Hydroformylation of Internal Olefins to Linear Aldehydes with Novel Rhodium Catalysts. *Angew. Chem. Int. Ed.* **1999**, *38*, 336. (n) Yuki, Y.; Takahashi, K.; Tanaka, Y.; Nozaki, K. Tandem Isomerization/Hydroformylation/Hydrogenation of Internal Alkenes to *n*-Alcohols Using Rh/Ru Dual- or Ternary-Catalyst Systems. *J. Am. Chem. Soc.* **2013**, *135*, 17393. (o) Börner, M. V.-H.; Lutz, D.; Armin Isomerization–Hydroformylation Tandem Reactions. *ACS Catal.* **2014**, *4*, 1706. (p) Seayad, A.; Ahmed, M.; Klein, H.; Jackstell, R.; Gross, T.; Beller, M. Internal olefins to linear amines. *Science* **2002**, *297*, 1676. (q) Hanna, S.; Holder, J. C.; Hartwig, J. F. A Multicatalytic Approach to the Hydroaminomethylation of α-Olefins. *Angew. Chem. Int. Ed.* **2019**, *58*, 3368. (r) Jimenez Rodriguez, C.; Foster, D. F.; Eastham, G. R.; Cole-Hamilton, D. J. Highly Selective Formation of Linear Esters from Terminal and Internal Alkenes Catalysed by Palladium Complexes of Bis-(di-*tert*-Butylphosphinomethyl)benzene. *Chem. Commun.* **2004**, 1720. (s) Jiménez-Rodriguez, C.; Eastham, G. R.; Cole-Hamilton, D. J. Dicarboxylic Acid Esters from the Carbonylation of Unsaturated Esters Under Mild Conditions. *Inorg. Chem. Commun.* **2005**, *8*, 878. (t) Mgaya, J. E.; Bartlett, S. A.; Mubofu, E. B.; Mgani, Q. A.; Slawin, A. M. Z.; Pogorzelec, P. J.; Cole-Hamilton, D. J. Synthesis of Bifunctional Monomers by the Palladium-Catalyzed Carbonylation of Cardanol and its Derivatives. *ChemCatChem* **2016**, *8*, 751. (u) Dong, K.; Fang, X.; Gülak, S.; Franke, R.; Spannenberg, A.; Neumann, H.; Jackstell, R.; Beller, M. Highly Active and Efficient Catalysts for Alkoxycarbonylation of Alkenes. *Nat. Commun.* **2017**, *8*, 14117. (v) Cobley, C. J.; Klosin, J.; Qin, C.; Whiteker, G. T. Parallel Ligand Screening on Olefin Mixtures in Asymmetric Hydroformylation Reactions. *Org. Lett.* **2004**, *6*, 3277.

6. (a) Kusumoto, S.; Tatsuki, T.; Nozaki, K. The Retro-Hydroformylation Reaction. *Angew. Chem. Int. Ed.* **2015**, *54*, 8458. (b) Fang, X.; Yu, P.; Morandi, B. Catalytic Reversible Alkene-Nitrile Interconversion Through Controllable Transfer Hydrocyanation. *Science* **2016**, *351*, 832. (c) Bhawal, B. N.; Morandi, B. Catalytic Transfer Functionalization through Shuttle Catalysis. *ACS Catal.* **2016**, *6*, 7528. (d) Bhawal, B. N.; Reisenbauer, J. C.; Ehinger, C.; Morandi, B. Overcoming Selectivity Issues in Reversible Catalysis: A Transfer Hydrocyanation Exhibiting High Kinetic Control. *J. Am. Chem. Soc.* **2020**, *142*, 10914. (e) Murphy, S. K.; Park, J.-W.; Cruz, F. A.; Dong, V. M. Rh-Catalyzed C–C Bond Cleavage by Transfer Hydroformylation. *Science* **2015**, *347*, 56.

7. (a) Pereira, S.; Srebnik, M. A study of hydroboration of alkenes and alkynes with pinacolborane catalyzed by transition metals. *Tetrahedron Lett.* **1996**, *37*, 3283. (b) Pereira, S.; Srebnik, M. Transition Metal-Catalyzed Hydroboration of and CCl_4 Addition to Alkenes. *J. Am. Chem. Soc.* **1996**, *118*, 909.

8. (a) Cipot, J.; McDonald, R.; Stradiotto, M. New bidentate cationic and zwitterionic relatives of Crabtree's hydrogenation catalyst. *Chem. Commun.* **2005**, 4932. (b) Cipot, J.; Vogels, C. M.; McDonald, R.; Westcott, S. A.; Stradiotto, M. Catalytic Alkene Hydroboration Mediated by Cationic and Formally Zwitterionic Rhodium(I) and Iridium(I) Derivatives of a P,N-Substituted Indene. *Organometallics* **2006**, *25*, 5965. (c) Ghebreyessus, K. Y.; Angelici, R. J. Isomerizing-Hydroboration of the Monounsaturated Fatty Acid Ester Methyl Oleate. *Organometallics* **2006**, *25*, 3040. (d) Scheuermann, M. L.; Johnson, E. J.; Chirik, P. J. Alkene Isomerization–Hydroboration Promoted by Phosphine-Ligated Cobalt Catalysts. *Org. Lett.* **2015**, *17*, 2716. (e) Léonard, N. G.; Palmer, W. N.; Friedfeld, M. R.; Bezdek, M. J.; Chirik, P. J. Remote, Diastereoselective Cobalt-Catalyzed Alkene Isomerization–Hydroboration: Access to Stereodefined 1,3-Difunctionalized Indanes. *ACS Catal.* **2019**, *9*, 9034. (f) Hu, M.; Ge, S. Versatile cobalt-catalyzed regioselective chain-walking double hydroboration of 1,n-dienes to access gem-bis(boryl)alkanes. *Nat. Commun.* **2020**, *11*, 765.

9. Obligacion, J. V.; Chirik, P. J. Earth-abundant transition metal catalysts for alkene hydrosilylation and hydroboration. *Nat. Rev. Chem.* **2018**, *2*, 15.

10. (a) Köster, R. Transformations of Organoboranes at Elevated Temperatures. *Angew. Chem., Int. Ed. Engl.* **1964**, *3*, 174. (b) Knights, E. F.; Brown, H. C. Cyclic hydroboration of 1,5-cyclooctadiene. A simple synthesis of 9-borabicyclo[3.3.1]nonane, an unusually stable dialkylborane. *J. Am. Chem. Soc.* **1968**, *90*, 5280. (c) Holliday, A. K.; Ottley, R. P. Reactions of trivinylborane with diboron tetrahalides: properties of some dihalogenoboryl(vinylboryl)ethanes. *J. Chem. Soc. A.* **1971**, 886. (d) Chiu, K.-W.; Negishi, E.-I.; S. Plante, M.; Silveria, A. An unusually facile dehydroboration of triorganoboranes formed by treatment of alkenyltrialkylborates with hydrochloric acid. *J. Organomet. Chem.* **1976**, *112*, C3. (e) Midland, M. M.; Tramontano, A.; Zderic, S. A. The reaction of B-alkyl-9-borabicyclo[3.3.1]nonanes with aldehydes and ketones. A facile elimination of the alkyl group by aldehydes. *J. Organomet. Chem.* **1978**, *156*, 203. (f) Midland, M. M.; Petre, J. E.; Zderic, S. A.; Kazubski, A. Thermal reactions of B-alkyl-9-borabicyclo[3.3.1]nonane (9-BBN). Evidence for unusually facile dehydroboration with B-pinanyl-9-BBN. *J. Am. Chem. Soc.* **1982**, *104*, 528. (g) Brown, H. C.; Joshi, N. N. Hydroboration of terpenes. 9. A simple improved procedure for upgrading the optical purity of commercially available alpha- and beta-pinenes. Conversion of (+)-alpha-pinene to (+)-beta-pinene via hydroboration-isomerization. *J. Org. Chem.* **1988**, *53*, 4059. (h) Laaziri, H.; Bromm, L. O.; Lhermitte, F.; Gschwind, R. M.; Knochel, P. A New Highly Stereoselective Rearrangement of Acyclic Tertiary Organoboranes: An Example of Highly Stereoselective Remote

C−H Activation. *J. Am. Chem. Soc.* **1999**, *121*, 6940. (i) Knochel, P.; Boudier, A.; Bromm, L. O.; Hupe, E.; Varela, J. A.; Rodriguez, A.; Koradin, C.; Bunlaksananusorn, T.; Laaziri, H.; Lhermitte, F. Selective transformations mediated by main-group organometallics. *Pure Appl. Chem.* **2000**, *72*, 1699. (j) Weliange, N. M.; McGuinness, D. S.; Patel, J. Thermal Dehydroboration: Experimental and Theoretical Studies of Olefin Elimination from Trialkylboranes and Its Relationship to Alkylborane Isomerization and Transalkylation. *Organometallics* **2014**, *33*, 4251. (k) Sakamoto, Y.; Amaya, T.; Suzuki, T.; Hirao, T. Palladium(II)-Catalyzed Dehydroboration via Generation of Boron Enolates. *Chem. Eur. J.* **2016**, *22*, 18686. (l) Cornils, B., Dehydroboration. In *Catalysis from A to Z* [Online] Wiley: 2020. https://onlinelibrary.wiley.com/doi/10.1002/9783527809080.cataz04896.

11. Murray, S. A.; Luc, E. C. M.; Meek, S. J. Synthesis of Alkenyl Boronates from Epoxides with Di-[B(pin)]-methane via Pd-Catalyzed Dehydroboration. *Org. Lett.* **2018**, *20*, 469.

12. (a) Larouche-Gauthier, R.; Elford, T. G.; Aggarwal, V. K. Ate Complexes of Secondary Boronic Esters as Chiral Organometallic-Type Nucleophiles for Asymmetric Synthesis. *J. Am. Chem. Soc.* **2011**, *133*, 16794. (b) Larsen, M. A.; Wilson, C. V.; Hartwig, J. F. Iridium-Catalyzed Borylation of Primary Benzylic C–H Bonds without a Directing Group: Scope, Mechanism, and Origins of Selectivity. *J. Am. Chem. Soc.* **2015**, *137*, 8633. (c) Fu, Z.; Hao, G.; Fu, Y.; He, D.; Tuo, X.; Guo, S.; Cai, H. Transition metal-free electrocatalytic halodeborylation of arylboronic acids with metal halides MX (X = I, Br) to synthesize aryl halides. *Organic Chemistry Frontiers* **2020**, *7*, 590. (d) Cai, Y.; Tan, D.; Zhang, Q.; Lv, W.; Li, Q.; Wang, H. Synthesis of difluoromethylated benzylborons via rhodium(I)-catalyzed fluorine-retainable hydroboration of gem-difluoroalkenes. *Chin. Chem. Lett.* **2021**, *32*, 417. (e) André-Joyaux, E.; Kuzovlev, A.; Tappin, N. D. C.; Renaud, P. A General Approach to Deboronative Radical Chain Reactions with Pinacol Alkylboronic Esters. *Angew. Chem. Int. Ed.* **2020**, *59*, 13859.

13. Wethman, R.; Derosa, J.; Tran, V. T.; Kang, T.; Apolinar, O.; Abraham, A.; Kleinmans, R.; Wisniewski, S. R.; Coombs, J. R.; Engle, K. M. An Under-Appreciated Source of Reproducibility Issues in Cross-Coupling: Solid-State Decomposition of Primary Sodium Alkoxides in Air. *ACS Catal.* **2021**, *11*, 502.

14. Docherty, J. H.; Peng, J.; Dominey, A. P.; Thomas, S. P. Activation and discovery of earth-abundant metal catalysts using sodium tert-butoxide. *Nat. Chem.* **2017**, *9*, 595.

15. Uchida, N.; Taketoshi, A.; Kuwabara, J.; Yamamoto, T.; Inoue, Y.; Watanabe, Y.; Kanbara, T. Synthesis, Characterization, and Catalytic Reactivity of a Highly Basic Macrotricyclic Aminopyridine. *Org. Lett.* **2010**, *12*, 5242.

16. Shuhei Kubota, M. K., Hideo Takaishi, Kenji Tsubata Method for producing diacetylpyridine derivative. JP2002212167A, 2001, 2004.

17. Harrison, T. J.; Ho, S.; Leighton, J. L. Toward More “Ideal” Polyketide Natural Product Synthesis: A Step-Economical Synthesis of Zincophorin Methyl Ester. *J. Am. Chem. Soc.* **2011**, *133*, 7308.

Chapter 6

Chemical Recycling of Polyethylene by Dehydrogenation and Isomerizing Ethenolysis

6.1 Introduction

Since the inception of the plastics industry in the 1950s, approximately 8.3 billion tonnes of plastic have been produced.[1] Plastic goods have since emerged as staples of the global economy and have improved living standards in developed countries. Approximately 380 million tonnes of plastics were produced in 2015, and production of plastic goods will only continue to rise as economies and populations grow. Inextricable from the production of plastic goods is the accumulation of plastics in ecosystems. The vast majority of plastic waste has accumulated in landfills, and between 4.8 and 12.7 million tonnes of plastics enter the world's oceans annually.[2] It is estimated that by 2050, approximately 12 billion tonnes of plastic will be present in landfills and oceans if current economic and policy trends continue.[1]

Approximately 9% of plastics produced since 1950 have been recycled, and approximately half of all plastics are designated for short-term use.[1] This disparity originates from the high cost of recycling single-use plastics, relative to that of sourcing virgin plastics from crude oil. Plastics that are recycled must first be collected, sorted, transported to a recycling facility, and washed. Mechanical downcycling of such waste involves further grinding and extrusion to form materials with physical properties that are inferior to those of virgin materials.[3]

Polyethylene (PE) is the largest single component of plastics waste (36% by mass).[1] Only 6.2% of linear low-density polyethylene (LLDPE) and low-density polyethylene (LDPE), and only 10.3% of high-density polyethylene (HDPE), are recycled. Several methods for chemical recycling of PE have been proposed. Thermal depolymerization of PE to ethylene is not economically viable because this reaction requires exceedingly high temperatures (Scheme 1A).[4] Thermal cracking[5] and catalytic cracking[6] of polyethylene produces complex, low-value mixtures of coke, gases, arenes, napthenes, and olefins (Scheme 1B). Nevertheless, Brightmark Energy has constructed a $260 million plant for the conversion of mixed polyolefins to naptha and diesel that will commence operations in early 2022.[7] Hydrocracking (Scheme 1C)[8] and alkane metathesis (Scheme 1D)[9] of PE produce light paraffins with good chemoselectivities, but the costs of conducting these reactions on PE waste far exceed those of recovering and refining crude oil to produce the same products. Distributions of liquid alkylarenes, and alkylnapthenes with average total carbon number = C_{34} and dispersity = 1.1 can be produced at moderate temperatures by tandem hydrogenolysis-aromatization (Scheme 1E).[10] However, the demand for these specialized compounds is much smaller than the amount of PE waste produced annually.

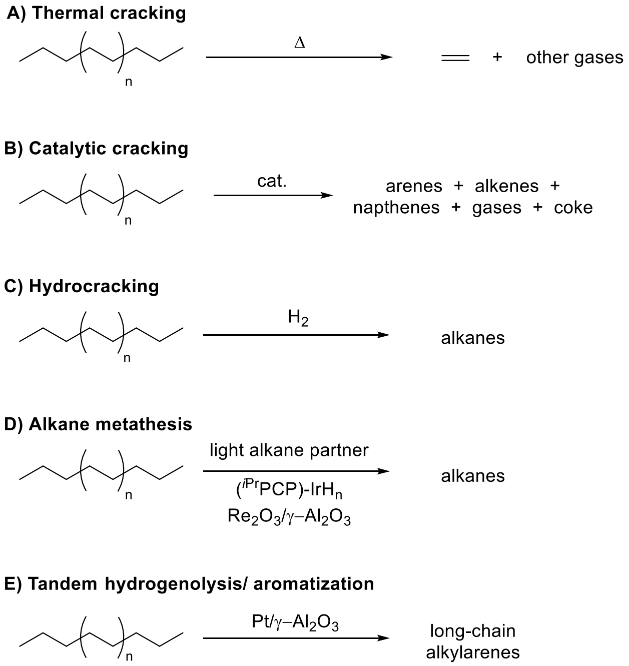
A) Thermal cracking
n
Δ
+ other gases
B) Catalytic cracking
n
cat.
arenes + alkenes +
napthenes + gases + coke
C) Hydrocracking
n
H2
alkanes
D) Alkane metathesis
n
light alkane partner
(iPrPCP)-IrHn
Re2O3/γ–Al2O3
alkanes
E) Tandem hydrogenolysis/ aromatization
n
Pt/γ–Al2O3
long-chain
alkylarenes

Scheme 1. Chemical recycling of polyethylene

For chemical recycling[3-6,8-11] to contribute significantly to the development of a closed-loop PE economy, the products should be valuable commodity chemicals for which demand approaches the supply of PE waste. Olefins are significantly more valuable than paraffins. A method for the selective and inexpensive production of olefins from polyethylene would provide a significant economic incentive for the recycling of polyethylene.

One olefin that could be produced from PE is propene. Approximately 98.2 tonnes of propene were produced in 2016.[12] Propene is mostly produced as a byproduct of steam cracking or fluid catalytic cracking; however, since the 1990s, propene has increasingly been produced "on-purpose" through methanol-to-olefins technology, propane dehydrogenation, and the conproportionation of butene and ethylene.[12] Propene can be used to produce polypropylene (PP) and many other commodity chemicals, such as isopropanol, acrylonitrile, propylene oxide, cumene, and acrylic acid.[12] Propene also readily undergoes disproportionation to ethylene, which can be used to recycle more polyethylene, and butenes, which can be used to manufacture commodity chemicals, sulfur-free gasoline, and polymers.[13]

Polyethylene is saturated, so olefins can be produced from polyethylene only by cleavage of either C–C or C–H bonds. To cleave C–C bonds, catalytic cracking can be conducted over acidic sites. [6,9b,13b] This reaction produces complex mixtures of olefins, naphthenes, aromatics, coke, and gases. To cleave C–H bonds, dehydrogenation can be conducted in the presence of homogeneous[14] or heterogeneous[15] catalysts. This reaction produces polymers with alkene sites.

While dehydrogenation does not directly convert polyethylene into small molecules, subsequent cleavage of the double bond could lead to the formation of smaller molecules. Double bonds can be cleaved oxidatively or through olefin metathesis, a reaction that involves the redistribution of the substituents about the double bonds of two olefins. If olefin metathesis of dehydrogenated polyethylene were conducted with a small olefin, such as ethylene, propylene, or butenes, the resulting cross metathesis products would have a significantly lower average molecular weight than the starting polymer. This reaction could constitute a first step towards unraveling the polymer into small-molecule commodity chemicals; however, no subsequent reactions that would significantly decrease average molecular weight would be expected to occur. If ethylene were selected as the cross-metathesis partner, the products of the initial cross metathesis would be long-chain α-olefins, which could undergo only degenerate metatheses.[9a,16]

In contrast, a combination of isomerization and metathesis with ethylene could form light alkenes. The isomerization of α-olefins to internal olefins is thermodynamically favorable.[17] The internal olefins that form from dehydrogenated PE after a combination of ethenolysis and isomerization could undergo subsequent, nondegenerate metatheses with ethylene to produce propene and other short α-olefins, and this sequence could repeat to fully unravel the long-chain alkene, which was generated from polyethylene, to propene (Scheme 2).

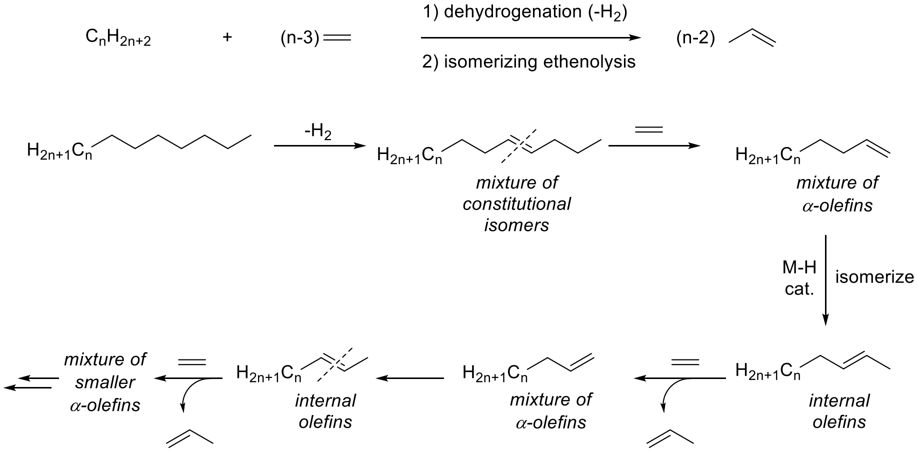
C_nH_{2n+2}
+
(n-3)
1) dehydrogenation (-H_2)
2) isomerizing ethenolysis
(n-2)
$H_{2n+1}C_n$
-H_2
mixture of constitutional isomers
mixture of α-olefins
M-H cat.
isomerize
internal olefins
mixture of α-olefins
internal olefins
mixture of smaller α-olefins

Scheme 2. Reaction design for conversion of polyethylene to propene

The tandem-orthogonal, i.e., simultaneous integration of, ethenolysis and olefin isomerization is known as isomerizing ethenolysis;[18] this transformation has been applied to the synthesis of styrenes from allylbenzenes[18f] and to the conversion of fatty-acid esters to defined distributions of olefin products (Scheme 3).[18e] If isomerizing ethenolysis could be conducted at the alkene sites formed after dehydrogenation of polyethylene, then the polymer would be unraveled to propene. We report the realization of this strategy for the chemical recycling of polyethylene by the combination of dehydrogenation and isomerizing ethenolysis to form propene as the sole product of the depolymerization process (Scheme 2). Propene is easily separated from the liquid phase and results from selective isomerization of 1-alkenes to 2-alkenes due to faster rates for metathesis than further isomerization. Overall, this use of polyethylene as a source of methylene units shows a new way to convert this polymer to a valuable commodity chemical.

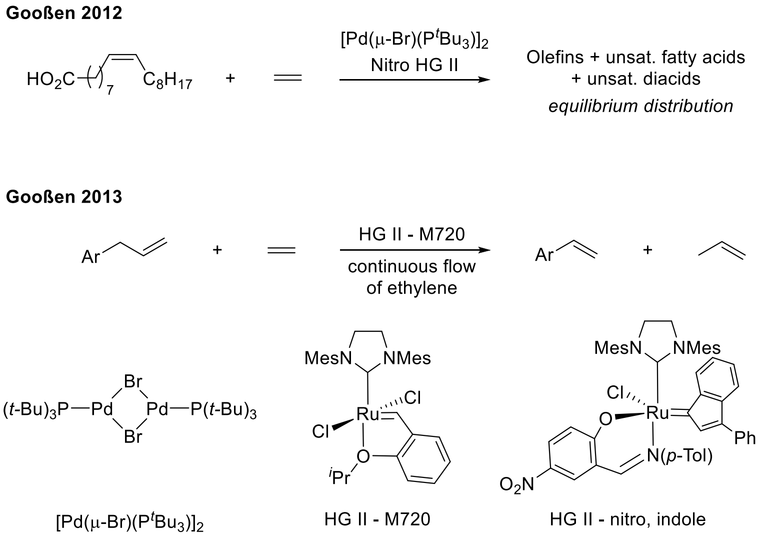
Gooßen 2012
$HO_2C-(\,)_7-CH=CH-C_8H_{17}$
+
$[Pd(\mu\text{-}Br)(P^tBu_3)]_2$
Nitro HG II
Olefins + unsat. fatty acids
+ unsat. diacids
equilibrium distribution
Gooßen 2013
Ar
+
HG II - M720
continuous flow
of ethylene
Ar
+
$(t\text{-}Bu)_3P$
Br
Pd
Pd
$P(t\text{-}Bu)_3$
Br
MesN
NMes
Cl
Ru
Cl
O
^iPr
MesN
NMes
Cl
O
Ru
Ph
N(p-Tol)
O_2N
$[Pd(\mu\text{-}Br)(P^tBu_3)]_2$
HG II - M720
HG II - nitro, indole

Scheme 3. Selected examples of isomerizing ethenolysis

6.2 Results and discussion

To initiate the envisioned cascade of isomerizing ethenolysis to form propene from an alkene generated from polyethylene, we first needed to identify processes to form alkenes from polyethylene. To do so, we conducted three types of dehydrogenations: transfer dehydrogenations at low temperatures in the presence of homogeneous catalysts, acceptorless dehydrogenations at high temperatures in the presence of heterogeneous catalysts, and multi-step, net dehydrogenations by a combination of iodination and base-promoted elimination. The dehydrogenation of LDPE to a polymer containing 4.4% double bonds in the presence of an iridium-pincer catalyst was reported by Goldman in 2004 (Scheme 4).[14a-c] However, all homogeneous dehydrogenations we have conducted thus far have not produced alkenes from polyethylene. No triplet resonance for an alkene unit within polyethylene has been observed from reaction of these catalyst with norbornene and LDPE. More experiments are needed to investigate this mode of dehydrogenation.

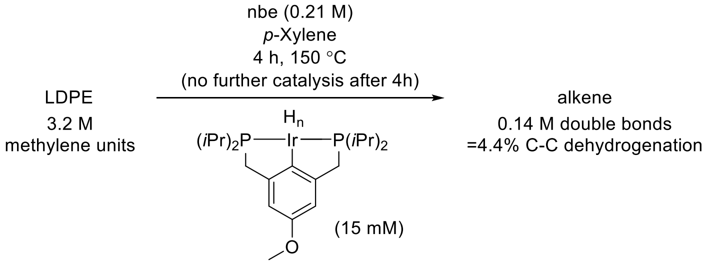
nbe (0.21 M)
p-Xylene
4 h, 150 °C
(no further catalysis after 4h)
LDPE
3.2 M
methylene units
H_n
$(iPr)_2P$
Ir
$P(iPr)_2$
O
(15 mM)
alkene
0.14 M double bonds
=4.4% C-C dehydrogenation

Scheme 4. Dehydrogenation of LDPE with homogeneous catalysts

An alternative method for dehydrogenation involves the direct extrusion of H_2 at high temperatures (acceptorless dehydrogenation) over heterogeneous catalysts. Medium-length *n*-paraffins are commonly dehydrogenated by UOP's Oleflex process, which relies on Pt/Sn catalysts.[15a,15b] We dehydrogenated LDPE (M_n = 2,657 g/mol) over a heterogeneous, Oleflex-type $Pt/Sn/Al_2O_3$ catalyst (20 wt% catalyst, relative to PE) at 330 °C under a flow of argon for 21 h, resulting in a polymer containing 0.20% monoene double bonds (Scheme 5). These double bonds were identified by the presence of two triplets in the ^1H NMR spectrum corresponding to the *cis* and *trans* isomers in a 2:1 ratio.

$$\underset{(M_n = 2657)}{\text{LDPE}} \xrightarrow[\text{flow of Ar, 350 °C}]{\text{Pt/Sn (5-20 wt\%)}} \text{Dehydrogenated PE up to 0.2\% olefinic protons, } ^1\text{H NMR}$$

Scheme 5. Dehydrogenation of LDPE over an Oleflex-type Pt/Sn catalyst

In addition to transfer dehydrogenations and acceptorless dehydrogenations, we conducted a net dehydrogenation of HDPE by a one-pot iodination of the polyethylene C-H bonds and base-promoted elimination (Scheme 6). The iodination step was conducted with I_2 and NaO^{t}Bu, and the base-promoted elimination step was conducted with NaO^{t}Bu.[19] The dehydrogenated polymer from iodination and elimination contained 0.59% monoene internal olefinic protons by ^{1}H NMR spectroscopy. Again, these double bonds were identified by the presence of two triplets in the ^{1}H NMR spectrum, in this case in a 4:1 ratio. In addition, 0.18% terminal olefinic protons were detected by ^{1}H NMR spectroscopy.

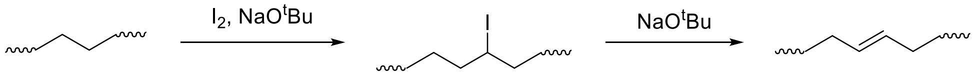

Scheme 6. Iodination and elimination of PE

In addition to dehydrogenation, catalytic cracking at high temperatures in oxygen-free atmospheres is known to produce olefins from paraffins. We sought to crack HDPE to olefins by heating a mixture of HDPE and the same Pt/Sn/Al_2O_3 catalyst at higher temperatures than were used for dehydrogenation. This mixture was heated at 450 °C for 2 h and filtered to yield a mixture consisting mostly of olefins and arenes (Scheme 7). By ^{1}H NMR spectroscopy, this mixture contained 2.0% olefin protons (0.27% terminal olefin protons and 1.73% internal olefin protons) and a smaller 0.38% of arene protons. The arene-olefin mixture is waxy and is readily soluble in chloroform at room temperature.

$$\underset{(M_n = 30{,}029)}{\text{HDPE}} \xrightarrow[\text{sealed tube, under Ar, 450 °C}]{\text{Pt/Sn (5 wt\%)}} \text{Olefins 1.7\% olefinic protons, } ^1\text{H NMR} + \text{Arenes 0.4\% aromatic protons, } ^1\text{H NMR}$$

Scheme 7. Catalytic cracking of HDPE over a Pt/Sn catalyst

Having established methods for the installation of olefinic units into polyethylene by dehydrogenation or catalytic cracking, we investigated conditions for the isomerizing ethenolysis of the resulting material. A long-chain α-olefin would result from ethenolysis of the internal alkenes in these materials. Thus, we conducted a proof-of-concept study by testing catalysts for the isomerizing ethenolysis of the model α-olefin 1-octadecene. The M720 second-generation Hoveyda-Grubbs catalyst and [Pd(μ-Br)(P^{t}Bu$_3$)]$_2$ are known to be active, selective, and mutually compatible catalysts for ethenolysis and isomerization, respectively. Indeed, the reaction of 1-octadecene with the M720 Hoveyda-Grubbs catalyst (HG II) as the metathesis catalyst (6 mol%) and [Pd(P^{t}Bu$_3$)(μ-Br)]$_2$ as the isomerization catalyst (2 mol%) at 60 °C for 24 h formed propene in 72% yield.[20] Butenes formed in only 6% yield (Scheme 8).

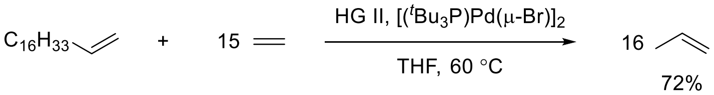

Scheme 8. Isomerizing ethenolysis of octadecene

Having developed conditions for the dehydrogenation and isomerizing ethenolysis steps separately, we sought to use the dehydrogenated PE containing internal alkenes directly in an isomerizing ethenolysis to assess the potential to form propene from ethylene and either LDPE or HDPE (Scheme 9). LDPE that was dehydrogenated over Pt/Sn/Al_2O_3 under the conditions in Scheme 5 was subjected to conditions for isomerizing ethenolysis (50.0 mg polymer, 25 bar ethylene, 1 mL THF, 60 °C), but with higher loadings of catalysts (80 wt% metathesis catalyst, 60 wt% isomerization catalyst), than were used for octadecene. Under these conditions, propene formed in 32% yield, and butenes formed in 8% yield (Scheme 9).

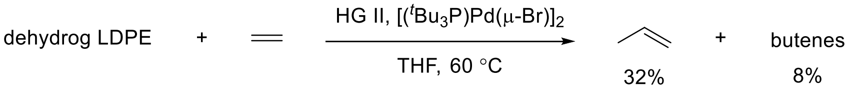

Scheme 9. Isomerizing ethenolyses of LDPE and HDPE dehydrogenated over Pt/Sn/Al_2O_3

While the dehydrogenated polymer from iodination and elimination of HDPE contained 0.59% olefinic protons by ^{1}H NMR spectroscopy, isomerizing ethenolysis of this polymer produced propene in only 1% yield and butenes in 48% yield. The concomitant formation of relatively large quantities of butenes and virtually no propene in this experiment led us to consider two hypotheses. First, we considered that the product distribution could result from fast isomerization, relative to ethenolysis; however, the product distribution did not change in the presence of higher loadings of metathesis catalyst.

Second, we hypothesized that the polymer resulting from iodination-elimination of HDPE contained compounds that poisoned the catalysts for isomerizing ethenolysis and that the butenes formed by dimerization of ethylene. This hypothesis was supported by the results of a control experiment in which a 450 mL vessel of ethylene at 25 bar was allowed to react with the isomerization and metathesis catalysts in THF without any dehydrogenated polymer or smaller exogenously added alkene. Under these conditions, a significant amount of butenes and a small amount of propene formed. The amounts of butenes and propene that formed were equivalent to the amounts that would from if 0.1 mmol of alkene were converted to butenes in 99% yield and to propene 8% yield. This result suggests that most butenes that form under the conditions of isomerizing ethenolysis originate from ethylene dimerization, and a small amount of propene that forms under the conditions of isomerizing ethenolysis originates from ethylene dimerization followed by disproportionation.

To improve the isomerizing ethenolysis step, we are currently investigating the effects of altering the pressure of ethylene, altering the identities of the catalysts, and altering solvents and temperatures to promote solubility. We are also investigating the effects of various reaction parameters on the yields and selectivities of dehydrogenation and cracking of HDPE and LDPE. In addition to isomerizing ethenolysis, we are interested in developing a method for isomerizing propenolysis of dehydrogenated polymers. By such a method, the propene produced from chemical recycling of PE could be used to convert a second batch of PE to butene. This butene could react with an additional equivalent of ethylene to produce propene, which could be used to recycle subsequent batches and thereby create a closed-loop PE economy. In addition, we are interested in conducting isomerizing ethenolyses and propenolyses of dehydrogenated polymers other than polyethylene, such as polypropylene, polystyrene, and polyvinylchloride (Scheme 10).

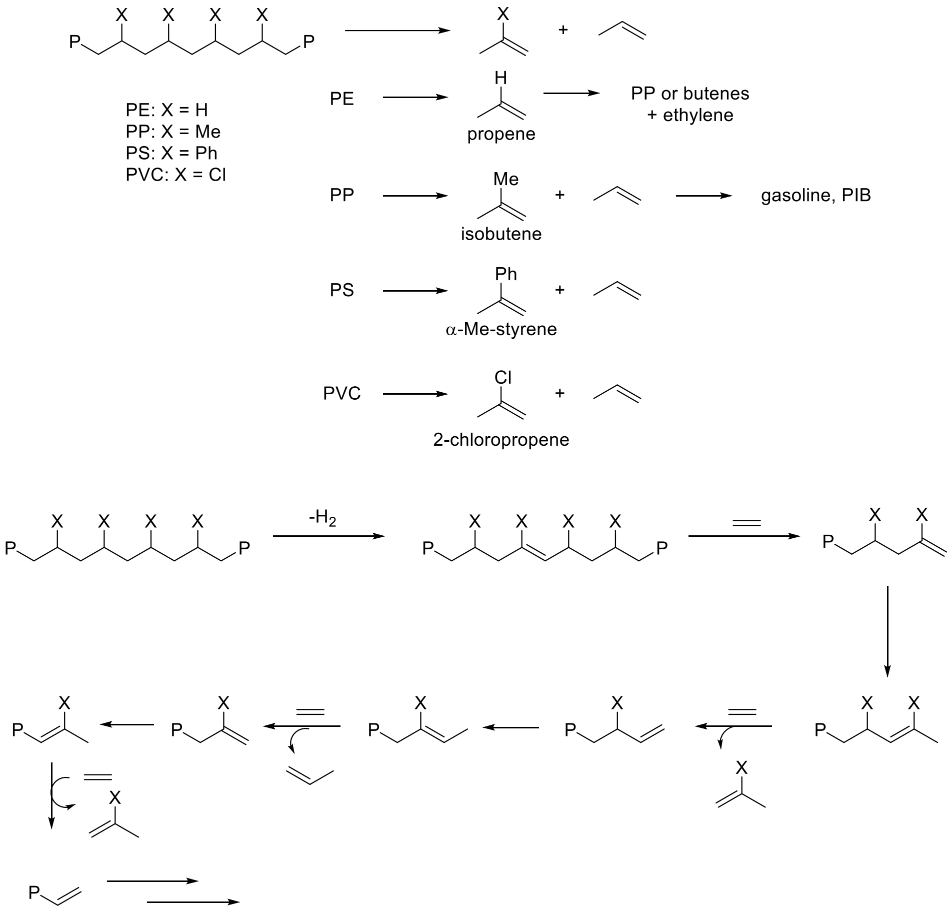
X
P
PE: X = H
PP: X = Me
PS: X = Ph
PVC: X = Cl
+
PE
H
propene
PP or butenes
+ ethylene
PP
Me
isobutene
gasoline, PIB
PS
Ph
α-Me-styrene
PVC
Cl
2-chloropropene
-H2

Scheme10. Application of isomerizing ethenolysis to polymers other than PE

6.3 Conclusion

Dehydrogenation followed by isomerizing ethenolysis is a promising method for the chemical recycling of polyethylene to propene. We have converted polyethylene to olefins by cracking and by dehydrogenation, and we have converted these olefins to propene by a combination of alkene isomerization and ethenolysis in a process called isomerizing ethenolysis. Up to 33% yield of propene was obtained from dehydrogenated LDPE and up to 72% yield of propene was obtained from octadecene.

6.4 Experimental

6.4.1 General methods and materials

All air-sensitive manipulations were conducted under an inert atmosphere in nitrogen-filled or argon-filled gloveboxes or by standard Schlenk techniques under nitrogen or argon. All reagents were purchased from commercial suppliers and used as received unless otherwise stated. HDPE (M_n = 30029) and LDPE (M_n = 2657) were purchased from Sigma Aldrich and knife milled to 2 mm particles. The headspaces of crude reaction mixtures were analyzed by gas chromatography (GC) on an Agilent 7820A GC system equipped with a GASPRO column (30 m x 0.320 mm, part number 113-4332) and an FID detector. Quantitative analysis of headspaces by GC was conducted with methane as an internal standard. The liquid phases of crude reaction mixtures were analyzed by gas chromatography (GC) on an Agilent 7890 GC equipped with an HP-5 column (25 m x 0.20 mm x 0.33 µm film) and an FID detector. Flash column chromatography was conducted with a Teledyne Isco CombiFlash® R_f system and RediSep R_f Gold™ columns. All NMR spectra were recorded at the University of California, Berkeley NMR facility. NMR spectra were recorded on Bruker AVB-400, AVQ-400, AV-500, and AV-600 instruments with operating frequencies of 400, 400, 500, and 600 MHz, respectively, and Carbon-13 NMR spectra were recorded on a Bruker AV-600 instrument with a ^{13}C operating frequency of 151 MHz. Chemical shifts (δ) are reported in ppm relative to those of residual solvent signals ($CDCl_3$ $\delta = 7.26$ for ^{1}H NMR spectra and $\delta = 77.16$ for ^{13}C NMR spectra; 1,1,2,2-Tetrachloroethane-d_2 $\delta = 6.0$ for ^{1}H NMR spectra).

6.4.2 Dehydrogenations

6.4.2.1 Synthesis of $Pt/Sn/Al_2O_3$ catalyst

The $Pt/Sn\text{-}Al_2O_3$ catalyst was prepared using $\gamma\text{-}Al_2O_3$ as a support with introduction of Pt and Sn species via impregnation using $Pt(H_3O)_2Cl_6\cdot nH_2O$ as the Pt precursor and $SnCl_2\cdot 2H_2O$ as the Sn precursor. $Pt(H_3O)_2Cl_6\cdot nH_2O$ (114 mg) and $SnCl_2\cdot 2H_2O$ (173 mg) were added to deionized water (20 g) and stirred with a magneton for 1 h. $\gamma\text{-}Al_2O_3$ (2 g) was added. The resulting slurry was dried at room temperature and then further dried at 353 K under a flow of nitrogen for 3 h. The powder mixture was then ground for 30 min, calcined at 520 °C for 8 h in static air, and reduced under a flow of hydrogen diluted with helium (10% H_2, flow rate of 100 mL/min) at 470 °C.

6.4.2.2 Acceptorless dehydrogenation of LDPE over $Pt/Sn/Al_2O_3$

In an argon-filled glovebox, a 25 mL stainless steel Parr autoclave fitted with a quartz liner was charged with LDPE (100 mg, M_n = 2657 g/mol) and $Pt/Sn/Al_2O_3$ catalyst (20 mg). The Parr autoclave was sealed and removed from the glovebox. The reaction mixture was stirred. Hydrogen was flowed through the autoclave for 30 min at 350 °C, and argon was flowed through the autoclave for 24 h at 350 °C. The resulting mixture was characterized by NMR in 1,1,2,2-tetrachloroethane at 100 °C and used in isomerizing ethenolyses without further purification.

6.4.2.3 Net dehydrogenation of HDPE through iodination and elimination

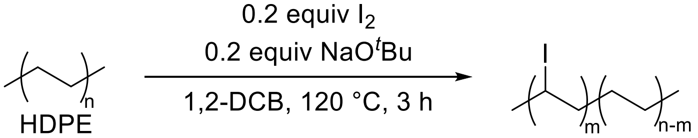

The iodination of high-density polyethylene (HDPE) was performed following a modified literature precedent.[19] In flame-dried 100 mL round-bottom flask, HDPE (1.1 g, 39.3 mmol, 1 equiv) was dissolved in 1,2-dichlorobenzene (50 mL) at 120 °C and then cooled to room temperature. Iodine (1.81 g, 7.13 mmol, 0.2 equiv) and 731 mg NaO*t*Bu (7.6 mmol, 0.2 equiv) were added to the reaction mixture. The reaction mixture was stirred at 120 °C for 3 hours. The reaction mixture was then cooled to room temperature and quenched with a saturated solution of aqueous $Na_2S_2O_3$ (150 mL). The resulting solid was filtered and dried under vacuum. A portion of the purified polymer (ca. 10 mg) was dissolved in $C_2D_2Cl_4$ (0.5 mL) in an NMR tube at 120 °C, and NMR spectra of the sample were recorded at 100 °C.

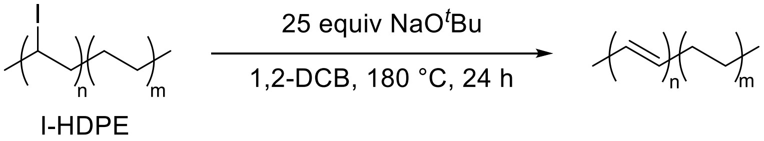

In a flame-dried 200 mL pressure vessel, iodinated high-density polyethylene (1.1 g, 0.82% iodide, 0.322 mmol iodide) was dissolved in 1,2-dichlorobenzene (50 mL) at 120 °C and cooled to room temperature. Sodium *tert*-butoxide (793 mg, 8.25 mmol, 25 equiv) was added, and the reaction was stirred at 180 °C for 24 hours. The reaction mixture was cooled to room temperature, quenched with 1 M aqueous HCl (~10 mL, until bubbling ceased), and poured into cold MeOH (200 mL). The resulting solid was filtered and dried under vacuum. A portion of the purified polymer (ca. 10 mg) was dissolved in $C_2D_2Cl_4$ (0.5 mL) in an NMR tube at 120 °C, and NMR spectra of the sample were recorded at 100 °C.

6.4.2.3 NMR Spectra of LDPE dehydrogenated over Pt/Sn/Al_2O_3

Full spectrum:

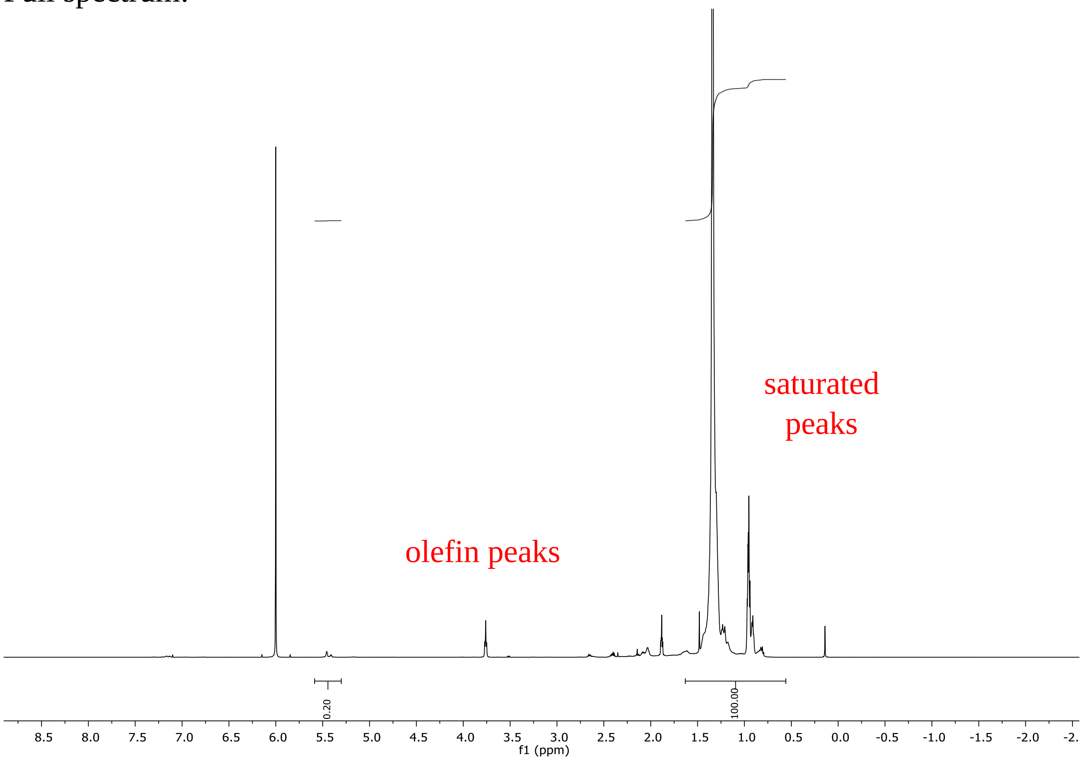

Olefin region:

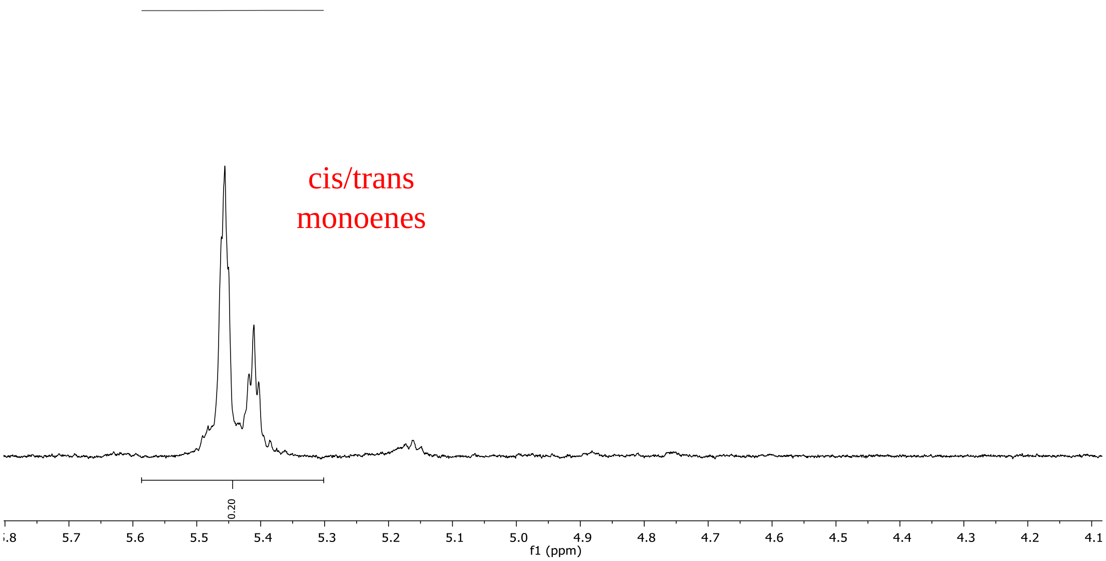

6.4.2.4 NMR Spectra of HDPE subjected to iodination/elimination

Full spectrum:

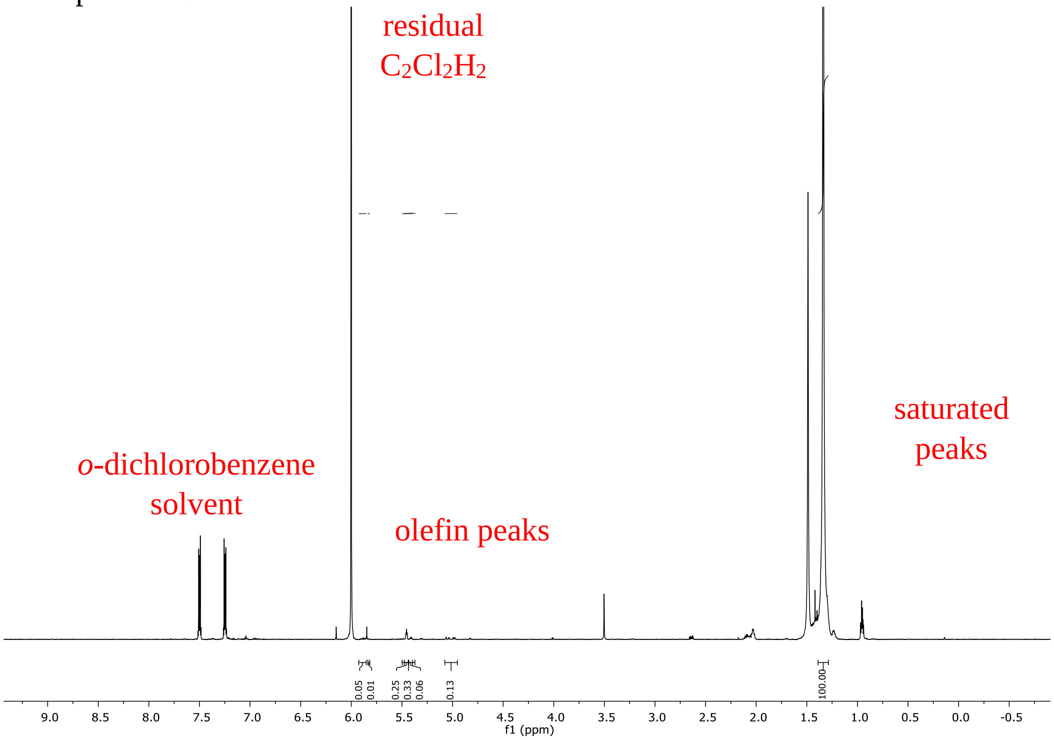

Olefin region:

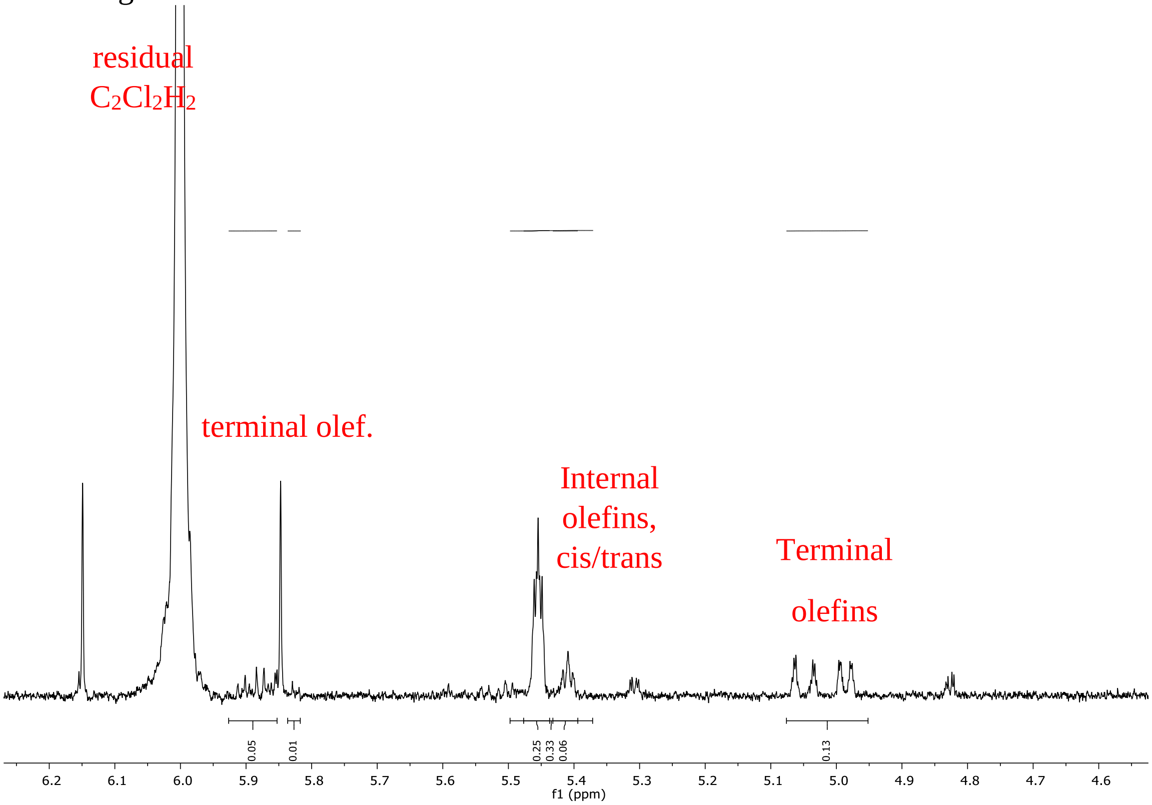

6.4.2.5 NMR Spectra of HDPE subjected to conditions for catalytic cracking

Full spectrum:

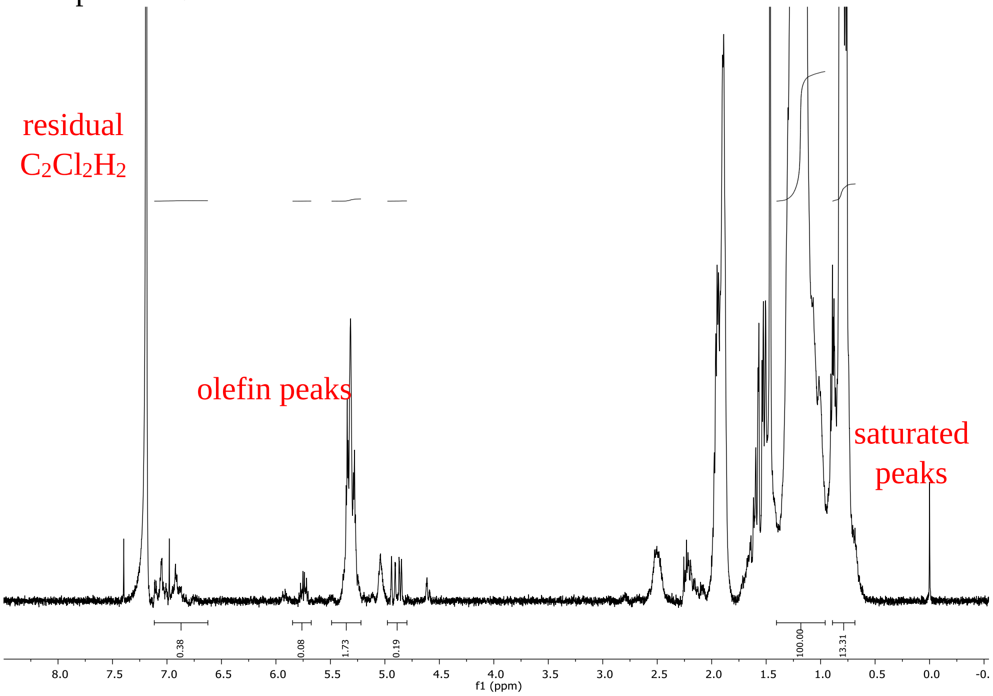

Arene/olefin region:

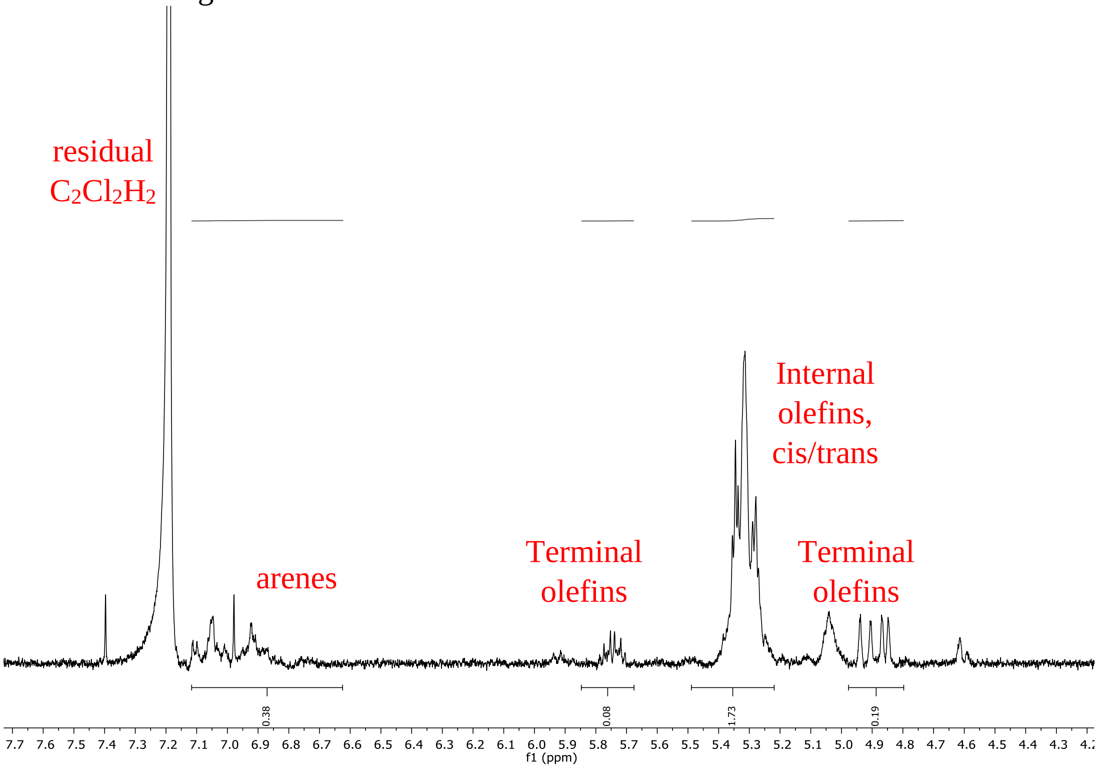

6.4.3 Isomerizing ethenolyses

6.4.3.1 Procedure for isomerizing ethenolysis of octadecene

A 25 mL stainless steel Parr autoclave equipped with a borosilicate or quartz liner (note: the reaction can also be conducted in a borosilicate test tube within a 450 mL stainless steel Parr autoclave) was charged with M720 Hoveyda Grubbs II catalyst (18.8 mg, 0.0300 mmol, 6 mol%), $[Pd(\mu\text{-}Br)(P^tBu_3)]_2$ (11.7 mg, 0.0150 mmol, 3 mol%), THF (1 mL), and octadecene (160 µL, 0.500 mmol, 1.00 equiv). The autoclave was charged at room temperature with a mixture of methane and ethylene (1:1, 50.0 bar) and heated for 24 h at 60 °C. The reaction mixture was vented at 60 °C into a 10 mL round-bottom flask fitted with a vent needle. A 40 µL aliquot of the gas in this round-bottom flask was manually injected onto an Agilent 7820A GC system equipped with a GASPRO column (30 m x 0.320 mm, part number 113-4332) and an FID detector. The yield of propene relative to octadecene was computed with the ideal gas law. The following equation was used to compute the yield of propene from octadecene. The temperature used in the ideal gas law equation was the temperature at which the bomb was charged with methane, which was always room temperature. The volume used in the ideal gas law equation was the volume of the Parr autoclave. The pressure of CH_4 used in the equation was 25 bar, because the bomb was charged with 50 bar of a 1:1 CH_4:C_2H_6 mixture. The response factor for propene: methane was approximated to be 3.0. The stoichiometric coefficients for octadecene, ethylene, and propene in the reaction are 1, 15, and 16, respectively. In the equation below, $A_{propene}$ and A_{CH4} are the areas of propene and methane in the gas chromatogram.

$$\text{yield} = 100\% * \frac{mol\ C3}{mol\ starting\ alkene} * \frac{1\ mol\ SM}{16\ mol\ C3\ (stoichiometric\ coef)}$$

$$= 100\% * \frac{mol\ CH_4\ istd * \left(\frac{A_{propene}}{A_{CH_4}}\right) * \left(\frac{1}{response\ factor}\right)}{mol\ starting\ alkene} * \frac{1\ mol\ SM}{16\ mol\ propene\ (stoich\ coef)}$$

$$= 100\% * \frac{\frac{P_{CH_4} V_{bomb}}{RT_{charge}} * \left(\frac{A_{propene}}{A_{CH_4}}\right) * \left(\frac{1}{3}\right)}{mol\ starting\ alkene} * \frac{1\ mol\ SM}{16\ mol\ propene}$$

6.4.3.2 Procedure for isomerizing ethenolyses of dehydrogenated LDPE & HDPE

A 25 mL stainless steel Parr autoclave equipped with a borosilicate or quartz liner (note: the reaction can also be conducted in a borosilicate test tube within a 450 mL stainless steel Parr autoclave) was charged with M720 Hoveyda Grubbs II catalyst (40.0 mg, 80 wt%), $[Pd(\mu\text{-}Br)(P^tBu_3)]_2$ (30.0 mg, 60 wt%), THF (1 mL), and dehydrogenated HDPE or LDPE (50 mg, 1.00 equiv). The autoclave was charged at room temperature with a mixture of methane and ethylene (1:1, 50.0 bar) and heated for 24 h at 60 °C. The reaction mixture was vented at 60 °C into a 10 mL round-bottom flask fitted with a vent needle. A 40 µL aliquot of the gas in this round-bottom flask was manually injected onto an Agilent 7820A GC system equipped with a GASPRO column (30 m x 0.320 mm, part number 113-4332) and an FID detector. The yield of propene relative to methylene units was computed with the ideal gas law.

The following equation was used to compute the yield of propene from polyethylene. The yield was calculated relative to the methylene units in polyethylene. The temperature used in the ideal gas law equation was the temperature at which the bomb was charged with methane, which was always room temperature. The volume used in the ideal gas law equation was the volume of the Parr autoclave. The pressure of CH_4 used in the equation was 25 bar, because the bomb was charged with 50 bar of a 1:1 CH_4:C_2H_6 mixture. The response factor for propene: methane was approximated to be 3.0. The stoichiometric coefficients for C_nH_{2n+2} polymer, ethylene, and propene in the reaction are 1, (n-3), and (n-2), respectively. The molecular weight of the polymer was approximated as 14.02688*n g/mol, where n is the number of carbon atoms in the polymer and 14.02688 is the weight of one methylene unit. The values of (n-2) and n, where n is the number of carbon atoms in the polymer, were assumed to be approximately equal. In the equation below, $A_{propene}$ and A_{CH4} are the areas of propene and methane in the gas chromatogram.

$$\text{yield} = 100\% * \frac{mol\ propene}{mol\ C_nH_{2n}\ polymer} * \frac{1\ mol\ C_nH_{2n}\ polymer}{(n-2)\ mol\ C3\ (stoich\ coef)}$$

$$= 100\% * \frac{mol\ CH_4\ istd * \left(\frac{A_{propene}}{A_{CH_4}}\right) * \left(\frac{1}{response\ factor}\right)}{mass\ C_nH_{2n+2}\ polymer * \frac{1\ mol\ C_nH_{2n+2}\ polym.}{14.02688n\ g\ C_nH_{2n+2}}} * \frac{1\ mol\ C_nH_{2n+2}}{(n-2)\ mol\ propene}$$

$$= 100\% * \frac{\frac{P_{CH_4}V_{bomb}}{RT_{charge}} * \left(\frac{A_{propene}}{A_{CH_4}}\right) * \left(\frac{1}{3}\right)}{mass\ C_nH_{2n+2}\ polymer * \frac{1\ mol\ C_nH_{2n+2}\ polym.}{14.02688 * n\ g\ C_nH_{2n+2}}} * \frac{1\ mol\ C_nH_{2n+2}}{(n-2)\ mol\ propene\ (stoich\ coef)}$$

$$= 100\% * \frac{P_{CH_4}V_{bomb}}{RT_{charge}} * \left(\frac{A_{propene}}{A_{CH_4}}\right) * \left(\frac{1}{3}\right) * \frac{1}{mass\ C_nH_{2n+2}} * \frac{14.02688 * n\ g\ C_nH_{2n+2}}{1\ mol\ C_nH_{2n+2}} * \frac{1\ mol\ C_nH_{2n+2}}{(n-2)\ mol\ propene}$$

$$= 100\% * \frac{P_{CH_4}V_{bomb}}{RT_{charge}} * \left(\frac{A_{propene}}{A_{CH_4}}\right) * \left(\frac{1}{3}\right) * \frac{1}{mass\ C_nH_{2n+2}\ polymer} * 14.02688$$

6.5 References

This work was conducted with Richard J. Conk, Dr. Liang Qi, Nico R. Ciccia, Brandon Bloomer, Dr. Ji Su, Jake Shi, Professor Alex Bell, and Professor John F. Hartwig.

1. Geyer, R.; Jambeck, J. R.; Law, K. L. Production, use, and fate of all plastics ever made. *Sci. Adv.* **2017**, *3*, e1700782.

2. Jambeck, J. R.; Geyer, R.; Wilcox, C.; Siegler, T. R.; Perryman, M.; Andrady, A.; Narayan, R.; Law, K. L. Plastic waste inputs from land into the ocean. *Science* **2015**, *347*, 768.

3. Rahimi, A.; García, J. M. Chemical recycling of waste plastics for new materials production. *Nat. Rev. Chem.* **2017**, *1*, 0046.

4. Vollmer, I.; Jenks, M. J. F.; Roelands, M. C. P.; White, R. J.; van Harmelen, T.; de Wild, P.; van der Laan, G. P.; Meirer, F.; Keurentjes, J. T. F.; Weckhuysen, B. M. Beyond Mechanical Recycling: Giving New Life to Plastic Waste. *Angew. Chem. Int. Ed.* **2020**, *59*, 15402.

5. Della Zassa, M.; Favero, M.; Canu, P. Two-steps selective thermal depolymerization of polyethylene. 1: Feasibility and effect of devolatilization heating policy. *J. Anal. Appl. Pyrolysis* **2010**, *87*, 248.

6. (a) Adams, C. J.; Earle, M. J.; Seddon, K. R. Catalytic cracking reactions of polyethylene to light alkanes in ionic liquids. *Green Chem.* **2000**, *2*, 21. (b) Ajibola, A. A.; Omoleye, J. A.; Efeovbokhan, V. E. Catalytic cracking of polyethylene plastic waste using synthesised zeolite Y from Nigerian kaolin deposit. *Appl. Petrochem. Res.* **2018**, *8*, 211.

7. Tullo, A. H., Plastic has a problem; is chemical recycling the solution? *Chemical & Engineering News* October 6, 2019, 2019.

8. (a) Ding, W.; Liang, J.; Anderson, L. L. Hydrocracking and Hydroisomerization of High-Density Polyethylene and Waste Plastic over Zeolite and Silica−Alumina-Supported Ni and Ni−Mo Sulfides. *Energy Fuels* **1997**, *11*, 1219. (b) Dufaud, V.; Basset, J.-M. Catalytic Hydrogenolysis at Low Temperature and Pressure of Polyethylene and Polypropylene to Diesels or Lower Alkanes by a Zirconium Hydride Supported on Silica-Alumina: A Step Toward Polyolefin Degradation by the Microscopic Reverse of Ziegler–Natta Polymerization. *Angew. Chem. Int. Ed.* **1998**, *37*, 806.

9. (a) Jia, X.; Qin, C.; Friedberger, T.; Guan, Z.; Huang, Z. Efficient and selective degradation of polyethylenes into liquid fuels and waxes under mild conditions. *Sci. Adv.* **2016**, *2*, e1501591. (b) Ellis, L. D.; Orski, S. V.; Kenlaw, G. A.; Norman, A. G.; Beers, K. L.; Román-Leshkov, Y.; Beckham, G. T. Tandem Heterogeneous Catalysis for Polyethylene Depolymerization via an Olefin-Intermediate Process. *ACS Sustain. Chem. Eng.* **2021**, *9*, 623.

10. Zhang, F.; Zeng, M.; Yappert, R. D.; Sun, J.; Lee, Y.-H.; LaPointe, A. M.; Peters, B.; Abu-Omar, M. M.; Scott, S. L. Polyethylene upcycling to long-chain alkylaromatics by tandem hydrogenolysis/aromatization. *Science* **2020**, *370*, 437.

11. (a) García, J. M. Catalyst: Design Challenges for the Future of Plastics Recycling. *Chem* **2016**, *1*, 813. (b) Monsigny, L.; Berthet, J.-C.; Cantat, T. Depolymerization of Waste Plastics to Monomers and Chemicals Using a Hydrosilylation Strategy Facilitated by Brookhart's Iridium(III) Catalyst. *ACS Sustain. Chem. Eng.* **2018**, *6*, 10481. (c) Celik, G.; Kennedy, R. M.; Hackler, R. A.; Ferrandon, M.; Tennakoon, A.; Patnaik, S.; LaPointe, A. M.; Ammal, S. C.; Heyden, A.; Perras, F. A.; Pruski, M.; Scott, S. L.; Poeppelmeier, K. R.; Sadow, A. D.; Delferro, M. Upcycling Single-Use Polyethylene into High-Quality Liquid Products. *ACS Cent. Sci.* **2019**, *5*, 1795. (d) Kots, P. A.; Liu, S.; Vance, B. C.; Wang, C.; Sheehan, J. D.; Vlachos, D. G. Polypropylene Plastic Waste Conversion to Lubricants over Ru/TiO2 Catalysts. *ACS Catal.* **2021**, 8104.

12. Zimmermann, H., Propene. In *Ullmann's Encyclopedia of Industrial Chemistry*, 2013; pp 00.

13. (a) Geilen, F. M. A.; Stochniol, G.; Peitz, S.; Schulte-Koerne, E., Butenes. In *Ullmann's Encyclopedia of Industrial Chemistry*, 2014; pp 1. (b) Primo, A.; Garcia, H. Zeolites as catalysts in oil refining. *Chem. Soc. Rev.* **2014**, *43*, 7548.

14. (a) Stefanovskaya, N. N.; Gavrilenko, I. F.; Markevich, I. N.; Shmonina, V. L.; Tinyakova, E. I.; Dolgoplosk, B. A. Formation of polyconjugated systems by dehydrogenation of polymers by quinones. *Bull. Acad. Sci. USSR, Div. Chem. Sci.* **1967**, *16*, 2254. (b) Ray, A.; Zhu, K.; Kissin, Y. V.; Cherian, A. E.; Coates, G. W.; Goldman, A. S. Dehydrogenation of aliphatic polyolefins catalyzed by pincer-ligated iridium complexes. *Chem. Commun.* **2005**, 3388. (c) Angela Rouleau, C. M. J. Dehydrogenation Of Polyethylene Catalyzed by Dihydrido Iridium PCP Pincer Complexes. University of Hawaii Manoa, 2004. (d) Shada, A. D. R.; Miller, A. J. M.; Emge, T. J.; Goldman, A. S. Catalytic Dehydrogenation of Alkanes by PCP–Pincer Iridium Complexes Using Proton and Electron Acceptors. *ACS Catal.* **2021**, *11*, 3009. (e) Huang, Z.; Rolfe, E.; Carson, E. C.; Brookhart, M.; Goldman, A. S.; El-Khalafy, S. H.; MacArthur, A. H. R. Efficient Heterogeneous Dual Catalyst Systems for Alkane Metathesis.

Adv. Synth. Catal. **2010**, *352*, 125. (f) Choi, J.; MacArthur, A. H. R.; Brookhart, M.; Goldman, A. S. Dehydrogenation and Related Reactions Catalyzed by Iridium Pincer Complexes. *Chem. Rev.* **2011**, *111*, 1761. (g) Zhu, K.; Achord, P. D.; Zhang, X.; Krogh-Jespersen, K.; Goldman, A. S. Highly Effective Pincer-Ligated Iridium Catalysts for Alkane Dehydrogenation. DFT Calculations of Relevant Thermodynamic, Kinetic, and Spectroscopic Properties. *J. Am. Chem. Soc.* **2004**, *126*, 13044. (h) Chowdhury, A. D.; Julis, J.; Grabow, K.; Hannebauer, B.; Bentrup, U.; Adam, M.; Franke, R.; Jackstell, R.; Beller, M. Photocatalytic Acceptorless Alkane Dehydrogenation: Scope, Mechanism, and Conquering Deactivation with Carbon Dioxide. *ChemSusChem* **2015**, *8*, 323. (i) Kumar, A.; Zhou, T.; Emge, T. J.; Mironov, O.; Saxton, R. J.; Krogh-Jespersen, K.; Goldman, A. S. Dehydrogenation of n-Alkanes by Solid-Phase Molecular Pincer-Iridium Catalysts. High Yields of α-Olefin Product. *J. Am. Chem. Soc.* **2015**, *137*, 9894. (j) Chianese, A. R.; Drance, M. J.; Jensen, K. H.; McCollom, S. P.; Yusufova, N.; Shaner, S. E.; Shopov, D. Y.; Tendler, J. A. Acceptorless Alkane Dehydrogenation Catalyzed by Iridium CCC-Pincer Complexes. *Organometallics* **2014**, *33*, 457. (k) Fang, H.; Liu, G.; Huang, Z., Chapter 18 - Pincer Iridium and Ruthenium Complexes for Alkane Dehydrogenation. In *Pincer Compounds*, Morales-Morales, D., Ed. Elsevier: 2018; pp 383. (l) Liu, F.; S. Goldman, A. Efficient thermochemical alkane dehydrogenation and isomerization catalyzed by an iridium pincer complex. *Chem. Commun.* **1999**, 655. (m) Sattler, J. J. H. B.; Ruiz-Martinez, J.; Santillan-Jimenez, E.; Weckhuysen, B. M. Catalytic Dehydrogenation of Light Alkanes on Metals and Metal Oxides. *Chem. Rev.* **2014**, *114*, 10613. (n) Das, K.; Kumar, A., Chapter One - Alkane dehydrogenation reactions catalyzed by pincer-metal complexes. In *Adv. Organomet. Chem.*, Pérez, P. J., Ed. Academic Press: 2019; Vol. 72, pp 1. (o) Punji, B.; Emge, T. J.; Goldman, A. S. A Highly Stable Adamantyl-Substituted Pincer-Ligated Iridium Catalyst for Alkane Dehydrogenation. *Organometallics* **2010**, *29*, 2702. (p) Kumar, A.; Bhatti, T. M.; Goldman, A. S. Dehydrogenation of Alkanes and Aliphatic Groups by Pincer-Ligated Metal Complexes. *Chem. Rev.* **2017**, *117*, 12357.

15. (a) He, S.; Wang, B.; Dai, X.; Sun, C.; Bai, Z.; Wang, X.; Guo, Q. Industrial development of long chain paraffin (*n*-C_{100}–C_{130}) dehydrogenation catalysts and the deactivation characterization. *Chem. Eng. J.* **2015**, *275*, 298. (b) He, S.; Krishnamurthy, K. R.; Seshan, K., Dehydrogenation of long chain n-paraffins to olefins – a perspective. In *Catalysis: Volume 29*, The Royal Society of Chemistry: 2017; Vol. 29, pp 282. (c) Nakaya, Y.; Miyazaki, M.; Yamazoe, S.; Shimizu, K.-i.; Furukawa, S. Active, Selective, and Durable Catalyst for Alkane Dehydrogenation Based on a Well-Designed Trimetallic Alloy. *ACS Catal.* **2020**, 5163. (d) Siri, G. J.; Casella, M. L.; Santori, G. F.; Ferretti, O. A. Tin/Platinum on Alumina as Catalyst for Dehydrogenation of Isobutane. Influence of the Preparation Procedure and of the Addition of Lithium on the Catalytic Properties. *Ind. Eng. Chem.* **1997**, *36*, 4821. (e) Abdulrhman S. Al-Awadi, S. M. A.-Z., Ahmed Mohamed El-Toni, and; Abasaeed, A. E. Dehydrogenation of Ethane to Ethylene by CO_2 over Highly Dispersed Cr on Large-Pore Mesoporous Silica Catalysts. *Catalysts* **2020**, *10*, 97. (f) He, S.; Castello, D.; Krishnamurthy, K. R.; Al-Fatesh, A. S.; Winkelman, J. G. M.; Seshan, K.; Fakeeha, A. H.; Kersten, S. R. A.; Heeres, H. J. Kinetics of long chain n-paraffin dehydrogenation over a commercial Pt-Sn-K-Mg/γ-Al2O3 catalyst: Model studies using n-dodecane. *Appl. Catal., A* **2019**, *579*, 130.

16. (a) Haibach, M. C.; Kundu, S.; Brookhart, M.; Goldman, A. S. Alkane Metathesis by Tandem Alkane-Dehydrogenation–Olefin-Metathesis Catalysis and Related Chemistry. *Acc. Chem. Res.* **2012**, *45*, 947. (b) Goldman, A. S.; Roy, A. H.; Huang, Z.; Ahuja, R.; Schinski, W.; Brookhart, M. Catalytic Alkane Metathesis by Tandem Alkane Dehydrogenation-Olefin Metathesis. *Science* **2006**, *312*, 257.

17. (a) Larsen, C. R.; Grotjahn, D. B. Stereoselective Alkene Isomerization over One Position. *J. Am. Chem. Soc.* **2012**, *134*, 10357. (b) Scaringi, S.; Mazet, C. Kinetically Controlled Stereoselective Access to Branched 1,3-Dienes by Ru-Catalyzed Remote Conjugative Isomerization. *ACS Catal.* **2021**, 7970. (c) Zhang, S.; Bedi, D.; Cheng, L.; Unruh, D. K.; Li, G.; Findlater, M. Cobalt(II)-Catalyzed Stereoselective Olefin Isomerization: Facile Access to Acyclic Trisubstituted Alkenes. *J. Am. Chem. Soc.* **2020**, *142*, 8910. (d) Ren, W.; Sun, F.; Chu, J.; Shi, Y. A Pd-Catalyzed Site-Controlled Isomerization of Terminal Olefins. *Org. Lett.* **2020**, *22*, 1868. (e) Crossley, S. W. M.; Barabé, F.; Shenvi, R. A. Simple, Chemoselective, Catalytic Olefin Isomerization. *J. Am. Chem. Soc.* **2014**, *136*, 16788. (f) Larionov, E.; Li, H.; Mazet, C. Well-Defined Transition Metal Hydrides in Catalytic Isomerization. *Chem. Commun.* **2014**, *50*, 9816. (g) Molloy, J. J.; Morack, T.; Gilmour, R. Positional and Geometrical Isomerisation of Alkenes: The Pinnacle of Atom Economy. *Angew. Chem. Int. Ed.* **2019**, *58*, 13654. (h) Liu, X.; Li, B.; Liu, Q. Base-Metal-Catalyzed Olefin Isomerization Reactions. *Synthesis* **2019**, *51*, 1293. (i) Kapat, A.; Sperger, T.; Guven, S.; Schoenebeck, F. Olefins through intramolecular radical relocation. *Science* **2019**, *363*, 391. (j) Kochi, T.; Kanno, S.; Kakiuchi, F. Nondissociative chain walking as a strategy in catalytic organic synthesis. *Tetrahedron Lett.* **2019**, *60*, 150938. (k) Biswas, S.; Huang, Z.; Choliy, Y.; Wang, D. Y.; Brookhart, M.; Krogh-Jespersen, K.; Goldman, A. S. Olefin Isomerization by Iridium Pincer Catalysts. Experimental Evidence for an η^3-Allyl Pathway and an Unconventional Mechanism Predicted by DFT Calculations. *J. Am. Chem. Soc.* **2012**, *134*, 13276. (l) Hanna, S.; Wills, T.; Butcher, T. W.; Hartwig, J. F. Palladium-Catalyzed Oxidative Dehydrosilylation for Contra-Thermodynamic Olefin Isomerization. *ACS Catal.* **2020**, *10*, 8736. (m) Hanna, S.; Butcher, T. W.; Hartwig, J. F.

Contra-thermodynamic Olefin Isomerization by Chain-Walking Hydrofunctionalization and Formal Retro-hydrofunctionalization. *Org. Lett.* **2019**, *21*, 7129.

18. (a) Gartside, R. J. Process for the production of linear alpha olefins and ethylene. US6727396B2, 2004. (b) Bala Ramachandran, S. C., Robert J. Gartside, Shane Kleindienst, Wolfgang Ruettinger, Saeed Alerasool Olefin isomerization and metathesis catalyst. US 2010/0056839 A1, 2009. (c) Flook, M. M.; Jiang, A. J.; Schrock, R. R.; Müller, P.; Hoveyda, A. H. Z-Selective Olefin Metathesis Processes Catalyzed by a Molybdenum Hexaisopropylterphenoxide Monopyrrolide Complex. *J. Am. Chem. Soc.* **2009**, *131*, 7962. (d) Consorti, C. S.; Aydos, G. L. P.; Dupont, J. Tandem isomerisation–metathesis catalytic processes of linear olefins in ionic liquid biphasic system. *Chem. Commun.* **2010**, *46*, 9058. (e) Ohlmann, D. M.; Tschauder, N.; Stockis, J.-P.; Gooßen, K.; Dierker, M.; Gooßen, L. J. Isomerizing Olefin Metathesis as a Strategy To Access Defined Distributions of Unsaturated Compounds from Fatty Acids. *J. Am. Chem. Soc.* **2012**, *134*, 13716. (f) Baader, S.; Ohlmann, D. M.; Gooßen, L. J. Isomerizing Ethenolysis as an Efficient Strategy for Styrene Synthesis. *Chem. Eur. J.* **2013**, *19*, 9807. (g) Dobereiner, G. E.; Erdogan, G.; Larsen, C. R.; Grotjahn, D. B.; Schrock, R. R. A One-Pot Tandem Olefin Isomerization/Metathesis-Coupling (ISOMET) Reaction. *ACS Catal.* **2014**, *4*, 3069. (h) Hulea, V. Direct transformation of butenes or ethylene into propylene by cascade catalytic reactions. *Catal. Sci. Technol.* **2019**, *9*, 4466. (i) Pollini, J.; Pankau, W. M.; Gooßen, L. J. Isomerizing Olefin Metathesis. *Chem. Eur. J.* **2019**, *25*, 7416. (j) De, S.; Sivendran, N.; Maity, B.; Pirkl, N.; Koley, D.; Gooßen, L. J. Dinuclear PdI Catalysts in Equilibrium Isomerizations: Mechanistic Understanding, in Silico Casting, and Catalyst Development. *ACS Catal.* **2020**, *10*, 4517.

19. Montoro, R.; Wirth, T. Direct Iodination of Alkanes. *Org. Lett.* **2003**, *5*, 4729.

20. (a) Thomas, R. M.; Keitz, B. K.; Champagne, T. M.; Grubbs, R. H. Highly Selective Ruthenium Metathesis Catalysts for Ethenolysis. *J. Am. Chem. Soc.* **2011**, *133*, 7490. (b) Marx, V. M.; Sullivan, A. H.; Melaimi, M.; Virgil, S. C.; Keitz, B. K.; Weinberger, D. S.; Bertrand, G.; Grubbs, R. H. Cyclic Alkyl Amino Carbene (CAAC) Ruthenium Complexes as Remarkably Active Catalysts for Ethenolysis. *Angew. Chem. Int. Ed.* **2015**, *54*, 1919. (c) Bidange, J.; Fischmeister, C.; Bruneau, C. Ethenolysis: A Green Catalytic Tool to Cleave Carbon–Carbon Double Bonds. *Chem. Eur. J.* **2016**, *22*, 12226.